

# Steel Framing Strategies for Highly Skewed Bridges to Reduce/Eliminate Distortion near Skewed Supports

**FDOT Contract No. BDK80 977-21**

**Final Report**

May 2014

Jawad H. Gull, Florida International University

Atorod Azizinamini, Ph.D., P.E., Florida International University

## **DISCLAIMER**

The opinions, findings, and conclusions expressed in this publication are those of the authors and not necessarily those of the State of Florida Department of Transportation

# CONVERSION TABLES

Approximate conversion to SI Units

| Symbol                              | When you know               | Multiply by              | To find                     | Symbol            |
|-------------------------------------|-----------------------------|--------------------------|-----------------------------|-------------------|
| <b>Length</b>                       |                             |                          |                             |                   |
| <b>in</b>                           | inches                      | 25.4                     | millimeters                 | mm                |
| <b>ft</b>                           | feet                        | 0.305                    | meters                      | m                 |
| <b>yd</b>                           | yards                       | 0.914                    | meters                      | m                 |
| <b>mi</b>                           | miles                       | 1.61                     | kilometers                  | km                |
| <b>Area</b>                         |                             |                          |                             |                   |
| <b>in<sup>2</sup></b>               | square inches               | 645.2                    | square millimeters          | mm <sup>2</sup>   |
| <b>ft<sup>2</sup></b>               | square feet                 | 0.093                    | square meters               | m <sup>2</sup>    |
| <b>yd<sup>2</sup></b>               | square yard                 | 0.836                    | square meters               | m <sup>2</sup>    |
| <b>ac</b>                           | acres                       | 0.405                    | hectares                    | ha                |
| <b>mi<sup>2</sup></b>               | square miles                | 2.59                     | square kilometers           | km <sup>2</sup>   |
| <b>Volume</b>                       |                             |                          |                             |                   |
| <b>fl oz</b>                        | fluid ounces                | 29.57                    | milliliters                 | mL                |
| <b>gal</b>                          | gallons                     | 3.785                    | liters                      | L                 |
| <b>ft<sup>3</sup></b>               | cubic feet                  | 0.028                    | cubic meters                | m <sup>3</sup>    |
| <b>yd<sup>3</sup></b>               | cubic yards                 | 0.765                    | cubic meters                | m <sup>3</sup>    |
| <b>Mass</b>                         |                             |                          |                             |                   |
| <b>oz</b>                           | ounces                      | 28.35                    | grams                       | g                 |
| <b>lb</b>                           | pounds                      | 0.454                    | kilograms                   | kg                |
| <b>T</b>                            | short tons (2000 lb)        | 0.907                    | megagrams (or "metric ton") | Mg (or "t")       |
| <b>Temperature</b>                  |                             |                          |                             |                   |
| <b>°F</b>                           | Fahrenheit                  | 5 (F-32)/9 or (F-32)/1.8 | Celsius                     | °C                |
| <b>Illumination</b>                 |                             |                          |                             |                   |
| <b>fc</b>                           | foot-candles                | 10.76                    | lux                         | lx                |
| <b>fl</b>                           | foot-Lamberts               | 3.426                    | candela/m <sup>2</sup>      | cd/m <sup>2</sup> |
| <b>Force and Pressure or Stress</b> |                             |                          |                             |                   |
| <b>lbf</b>                          | pound force                 | 4.45                     | newtons                     | N                 |
| <b>lbf/in<sup>2</sup></b>           | pound force per square inch | 6.89                     | kilopascals                 | kPa               |

## Approximate conversion to US Customary Units

| Symbol                              | When you know               | Multiply by | To find                     | Symbol              |
|-------------------------------------|-----------------------------|-------------|-----------------------------|---------------------|
| <b>Length</b>                       |                             |             |                             |                     |
| mm                                  | millimeters                 | 0.039       | inches                      | in                  |
| m                                   | meters                      | 3.28        | feet                        | ft                  |
| m                                   | meters                      | 1.09        | yards                       | yd                  |
| km                                  | kilometers                  | 0.621       | miles                       | mi                  |
| <b>Area</b>                         |                             |             |                             |                     |
| mm <sup>2</sup>                     | square millimeters          | 0.0016      | square inches               | in <sup>2</sup>     |
| m <sup>2</sup>                      | square meters               | 10.764      | square feet                 | ft <sup>2</sup>     |
| m <sup>2</sup>                      | square meters               | 1.195       | square yards                | yd <sup>2</sup>     |
| ha                                  | hectares                    | 2.47        | acres                       | ac                  |
| km <sup>2</sup>                     | square kilometers           | 0.386       | square miles                | mi <sup>2</sup>     |
| <b>Volume</b>                       |                             |             |                             |                     |
| mL                                  | milliliters                 | 0.034       | fluid ounces                | fl oz               |
| L                                   | liters                      | 0.264       | gallons                     | gal                 |
| m <sup>3</sup>                      | cubic meters                | 35.314      | cubic feet                  | ft <sup>3</sup>     |
| m <sup>3</sup>                      | cubic meters                | 1.307       | cubic yards                 | yd <sup>3</sup>     |
| <b>Mass</b>                         |                             |             |                             |                     |
| g                                   | grams                       | 0.035       | ounces                      | oz                  |
| kg                                  | kilograms                   | 2.202       | pounds                      | lb                  |
| Mg (or "t")                         | megagrams (or "metric ton") | 1.103       | short tons (2000 lb)        | T                   |
| <b>Temperature</b>                  |                             |             |                             |                     |
| °C                                  | Celsius                     | 1.8C+32     | Fahrenheit                  | °F                  |
| <b>Illumination</b>                 |                             |             |                             |                     |
| lx                                  | lux                         | 0.0929      | foot-candles                | fc                  |
| cd/m <sup>2</sup>                   | candela/m <sup>2</sup>      | 0.2919      | foot-Lamberts               | fl                  |
| <b>Force and Pressure or Stress</b> |                             |             |                             |                     |
| N                                   | newtons                     | 0.225       | pound force                 | lbf                 |
| kN                                  | Kilonewtons                 | 0.225       | kilopound                   | kip                 |
| kPa                                 | kilopascals                 | 0.000145    | kilopound per square inch   | ksi                 |
| kPa                                 | kilopascals                 | 0.145       | pound force per square inch | lbf/in <sup>2</sup> |

# TECHNICAL REPORT DOCUMENTATION PAGE

|   |  |   |           |
|---|--|---|-----------|
| 1. Report No.   | 2. Government Accession No.                          | 3. Recipient's Catalog No.  |           |
| 4. Title and Subtitle<br>Steel Framing Strategies for Highly Skewed Bridges to Reduce/Eliminate Distortion near Skewed Supports   |  | 5. Report Date<br>May 2014  |           |
|   |  | 6. Performing Organization Code   |           |
| 7. Author(s)<br>Jawad H. Gull, Atorod Azizinamini (PI)  |  | 8. Performing Organization Report No.                                       |           |
| 9. Performing Organization Name and Address<br>Florida International University, Miami<br>University Park, Room P.C. 539<br>Miami, FL 33199-0000<br>USA   |  | 10. Work Unit No. (TRAIS)   |           |
|   |  | 11. Contract or Grant No.<br>BDK80-977-21                                   |           |
| 12. Sponsoring Agency Name and Address<br>Florida Department of Transportation<br>605 Suwannee Street<br>Tallahassee, FL 32399<br>USA   |  | 13. Type of Report and Period Covered<br>Final Report<br>Jun. 2011-May 2014 |           |
|   |  | 14. Sponsoring Agency Code  |           |
| 15. Supplementary Notes   |  |   |           |
| 16. Abstract<br><p>Different problems in straight skewed steel I-girder bridges are often associated with the methods used for detailing the cross-frames. Use of theoretical terms to describe these detailing methods and absence of complete and simplified design approach has led to disputes between stakeholders, costly repairs, and delays in construction.</p> <p>The objectives of this research were introduction of simplified terminologies to describe detailing methods, identification of structural responses affected by the detailing methods and recommendation of methods of analysis to evaluate these responses, development of methods to estimate fit-up forces and practices to reduce them, and finally development of design provisions for the skewed bridges.</p> <p>Two terminologies, erected fit and final fit, are introduced to describe the detailing methods in order to be consistent with field practice. The components of the structural responses affected by the detailing method are identified and are referred to as lack-of-fit effects. It has been shown that lack-of-fit effects for the final fit detailing method at steel dead load stage are equal and opposite to the lack-of-fit effect for the erected fit detailing method at total dead load stage. It is recommended to use improved 2D grid analysis to calculate the lack-of-fit effects for the erected fit and final fit detailing methods. The fit-up forces required to attach the cross-frames during the erection can be estimated from improved 2D grid analysis. 3D erection simulation has shown that erecting the cross-frames starting from the middle of a bay and going toward the ends reduces the maximum fit-up force. Finally, recommendations were made on the method of calculating the cambers, and a flow chart was developed for each detailing method to facilitate the selection of the detailing method and carrying out the necessary design checks.</p> |  |   |           |
| 17. Key Word<br>Skew bridges, Steel frames, Distortion (Structures), Bridge design, Steel bridges, Recommendations, Florida   |  | 18. Distribution Statement<br>No restrictions.                              |           |
| 19. Security Classif. (of this report)<br>Unclassified  | 20. Security Classif. (of this page)<br>Unclassified | 21. No. of Pages<br>172   | 22. Price |

## **ACKNOWLEDGEMENTS**

The authors would like to thank Florida Department of Transportation (FDOT) and Project Manager Dennis Golabek.

## EXECUTIVE SUMMARY

Construction of highly skewed steel bridges often faces significant challenges due the effects of the skewed support on the framing of the bridge. The girders in a skew bridge have a tendency to twist or layover at different loading stages during the construction, depending on the detailing option selected for the cross-frames that provide bracing to the steel girders. The consequence of this behavior is that decisions must be regarding at which stage the girder web should be plumb and that entails selection of a detailing option used for cross-frames before the fabrication of steel framing. Each of these different options has certain advantages during different stages of construction. Problems have been investigated in the past to identify some of the issues related to behavior of straight and skewed steel bridges. These studies provided some of the elements that were needed to develop comprehensive and coherent design, fabrication, and construction approaches for straight and skewed steel bridges. However, sufficient knowledge is lacking for a complete, simplified, and coherent approach. Further, the use of theoretical terms and lack of identification of important structural responses have added to the complexity of the problem, which can result in miscommunication between designers, fabricators, and contractors, thereby leading to field delays and subsequent litigation.

The main objective of this project was to simplify the design and construction of steel bridges with skewed supports by introducing a complete and coherent design approach. The focus of the project was on straight bridges; however, the knowledge gained through the research presented here also explains horizontally curved girder systems. The objective was achieved with recommendations with respect to three important areas: 1) the introduction of simplified terminologies that are consistent with field practices; 2) the identification of important structural responses and recommended methods of analyses for obtaining these responses; and 3) the development of a flow chart that can help designers to choose the appropriate detailing of the cross-frames for straight skewed I-girder bridges.

Two methods of detailing, design and construction were introduced for straight skewed I-girder bridges. These methods namely, the erected fit and the final fit, identify the construction stages during which the girder webs are plumb. These methods also indicate the options used for detailing the cross-frames. The component of different structural responses of straight skewed steel I-girder bridges affected by the erected fit and the final fit at different construction stages of skewed bridges are identified and are referred to as the lack-of-fit effects. Project results indicated that the lack-of-fit effects for the final fit detailing method at the steel dead load stage are equal and opposite to the lack-of-fit effects for the final

fit detailing method at the total dead load stage for straight skewed steel I-girder bridges. As a result of this conclusion, simplified methods can be used to estimate the lack-of-fit effects for different detailing methods. This report also provides simplified methods of calculating the fit-up forces required to attach the cross-frames between their connections to girders to erect the steel frame of the bridge. Analysis on limited number of bridges has shown that sequence of erecting the cross-frames can have impact the maximum fit-up force required the erection of skew bridge. It has been found that erecting the cross-frames starting from the middle of a bay and moving toward the ends reduce maximum fit-up force and might alleviate some of the fit-up problems. Discussion of different important issues affected by the detailing methods provides the elements required for the development of complete and comprehensive design provisions for the skewed bridges. The design provisions include the recommendation on calculation of camber for different detailing methods. The recommendation on camber calculation was verified by numerical analysis and supported by the mechanisms understood as part of this research. Finally, a flow chart was developed for each detailing method to facilitate the selection of the detailing method and carrying out the necessary design checks.

# TABLE OF CONTENTS

|  |             |
|--|-------------|
| <b>DISCLAIMER</b> .....  | <b>ii</b>   |
| <b>CONVERSION TABLES</b> .....   | <b>iii</b>  |
| <b>TECHNICAL REPORT DOCUMENTATION PAGE</b> .....   | <b>v</b>    |
| <b>ACKNOWLEDGEMENTS</b> .....  | <b>vi</b>   |
| <b>EXECUTIVE SUMMARY</b> .....   | <b>vii</b>  |
| <b>LIST OF TABLES</b> .....  | <b>xii</b>  |
| <b>LIST OF FIGURES</b> .....   | <b>xiii</b> |
| <b>Chapter 1 INTRODUCTION</b> .....  | <b>1</b>    |
| 1.1 Background.....  | 1           |
| 1.2 Twist in Skew Bridge.....  | 1           |
| 1.3 Bridge Industry Perception .....   | 3           |
| 1.4 Problem Statement.....   | 3           |
| 1.5 Objectives .....   | 4           |
| 1.6 Organization of the Report.....  | 4           |
| <b>Chapter 2 COMPARISON OF ERECTED FIT AND FINAL FIT DETAILING METHODS</b> .....             | <b>6</b>    |
| 2.1 Existing and Proposed Terminologies .....  | 7           |
| 2.2 Fabrication for Different Detailing Methods .....  | 9           |
| 2.3 Numerical Analysis for Different Detailing Methods .....                                 | 11          |
| 2.4 Structural Responses of the Skewed Bridges Affected By Different Detailing Methods ..... | 12          |
| 2.4.1 Description of Structures Used for Comparison of Different Detailing Methods .....     | 12          |
| 2.4.2 Layovers.....  | 14          |
| 2.4.3 Deflections .....  | 16          |
| 2.4.4 Reactions.....   | 19          |
| 2.4.5 Flange Lateral Bending Stress ( $f_l$ ) .....  | 22          |
| 2.4.6 Cross-frame Forces .....   | 23          |
| 2.5 Discussion of the Results .....  | 24          |
| 2.6 Summary and Conclusions .....  | 26          |
| <b>Chapter 3 METHODS OF ANALYSIS FOR DIFFERENT DETAILING METHODS</b> .....                   | <b>28</b>   |
| 3.1 Erected Fit Detailing Method.....  | 28          |
| 3.1.1 Methods of Analysis .....  | 28          |
| 3.1.2 Comparison of Different Methods of Analysis.....                                       | 30          |
| 3.2 Final Fit Detailing Method.....  | 40          |
| 3.2.1 Methods of Analysis .....  | 40          |
| 3.2.2 Comparison of Different Methods of Analysis.....                                       | 47          |
| 3.3 SUMMARY AND CONCLUSIONS .....  | 50          |
| <b>Chapter 4 FIT-UP FORCES</b> .....   | <b>51</b>   |
| 4.1 Introduction.....  | 51          |
| 4.1.1 Lack-of-fit in Skewed Bridges.....   | 52          |
| 4.1.2 Fit-Up Forces .....  | 53          |
| 4.2 Proposed Methods of Calculating Fit-Up Forces.....                                       | 54          |
| 4.2.1 Cross-frame Forces Method.....   | 55          |
| 4.2.2 3D Erection Simulation Method .....  | 56          |
| 4.2.3 Discussion and Comparison of Fit-Up Forces .....                                       | 58          |
| 4.3 Effect of Different Practices on Fit-Up Forces .....                                     | 61          |
| 4.3.1 Different erection sequences.....  | 61          |
| 4.3.2 Distance of the First Intermediate Cross-frame from Support.....                       | 64          |

|   |            |
|---|------------|
| 4.4 Summary and Conclusions .....   | 65         |
| <b>Chapter 5 DESIGN PROVISIONS .....</b>  | <b>66</b>  |
| 5.1 Recommendation on Calculation Of Cambers .....                                | 66         |
| 5.1.1 Verification of Recommendation Using Numerical Models .....                 | 67         |
| 5.1.2 Summary and Discussion on Numerical Analysis.....                           | 74         |
| 5.2 Structural Responses of The Skewed Bridges Affected By Detailing Methods..... | 75         |
| 5.3 Other Considerations .....  | 78         |
| 5.4 Parametric Studies .....  | 79         |
| 5.4.1 Effect of Cross-frame Stiffness.....  | 79         |
| 5.4.2 Effect of Distance of the First Intermediate Cross-frame from Support ..... | 80         |
| 5.4.3 Effect of Cross-frame Orientation .....                                     | 85         |
| 5.5 Cross-frame Configuration .....   | 86         |
| 5.6 Flow Chart for Design .....   | 89         |
| 5.7 Summary and Conclusions .....   | 90         |
| <b>Chapter 6 CONCLUSIONS AND RECOMMENDATIONS.....</b>                             | <b>92</b>  |
| <b>References.....</b>  | <b>94</b>  |
| <b>Appendix A: Description of Bridges .....</b>                                   | <b>96</b>  |
| <b>Appendix B: Comparison of Detailing Methods.....</b>                           | <b>99</b>  |
| B.1 Concrete Dead Load Deflections .....  | 99         |
| B.1.1 Bridge A.....   | 99         |
| B.1.2 Bridge B.....   | 100        |
| B.1.3 Bridge C.....   | 101        |
| B.1.4 Bridge B2.....  | 102        |
| B.2 Layovers.....   | 103        |
| B.2.1 Bridge A.....   | 103        |
| B.2.2 Bridge B.....   | 104        |
| B.2.3 Bridge C.....   | 105        |
| B.2.4 Bridge B2.....  | 106        |
| B.3 Flange Lateral Bending Stress .....   | 107        |
| B.3.1 Bridge A.....   | 107        |
| B.3.2 Bridge B.....   | 108        |
| B.3.3 Bridge C.....   | 109        |
| B.3.4 Bridge B2.....  | 110        |
| B.4 Reactions.....  | 111        |
| B.4.1 Bridge A.....   | 111        |
| B.4.2 Bridge B.....   | 111        |
| B.4.3 Bridge C.....   | 112        |
| B.4.4 Bridge B2.....  | 112        |
| B.5 Cross-frame Forces .....  | 114        |
| B.5.1 Bridge A.....   | 114        |
| B.5.2 Bridge B.....   | 115        |
| B.5.3 Bridge C.....   | 116        |
| B.5.4 Bridge B2.....  | 117        |
| <b>Appendix C: Methods of Analysis: Erected Fit .....</b>                         | <b>118</b> |
| C.1 Concrete Dead Load Deflections .....  | 118        |
| C.1.1 Bridge A.....   | 118        |
| C.1.2 Bridge B.....   | 119        |
| C.1.3 Bridge C.....   | 120        |

|   |            |
|---|------------|
| C.2 Layovers.....   | 121        |
| C.2.1 Bridge A.....   | 121        |
| C.2.2 Bridge B.....   | 122        |
| C.2.3 Bridge C.....   | 123        |
| C.3 Flange Lateral Bending Stress .....                         | 124        |
| C.3.1 Bridge A.....   | 124        |
| C.3.2 Bridge B.....   | 125        |
| C.3.3 Bridge C.....   | 126        |
| C.4 Reactions.....  | 127        |
| C.4.1 Bridge A.....   | 127        |
| C.4.2 Bridge B.....   | 127        |
| C.4.3 Bridge C.....   | 128        |
| C.5 Cross-frame Forces .....                                    | 129        |
| C.5.1 Bridge A.....   | 129        |
| C.5.2 Bridge B.....   | 130        |
| C.5.3 Bridge C.....   | 131        |
| <b>Appendix D: Methods of Analysis: Final Fit.....</b>          | <b>132</b> |
| D.1 Change in Elevation Due to Lack of Fit .....                | 132        |
| D.1.1 Bridge C.....   | 132        |
| D.2 Layovers.....   | 133        |
| D.2.1 Bridge C.....   | 133        |
| D.3 Flange Lateral Bending Stress .....                         | 134        |
| D.3.1 Bridge C.....   | 134        |
| D.4 Change in Reactions .....                                   | 135        |
| D.4.1 Bridge C.....   | 135        |
| D.5 Cross-frame Forces .....                                    | 136        |
| D.5.1 Bridge C.....   | 136        |
| <b>Appendix E: Examples.....</b>                                | <b>137</b> |
| E.1 Calculation of Initial Strains .....                        | 137        |
| E.1.1 Intermediate Cross-frame.....                             | 138        |
| E.1.2 End cross-frame .....                                     | 141        |
| E.2 Calculation of $J_{eq}$ for Improved 2D Grid Analysis ..... | 144        |
| E.3 Calculation of Responses from 2D Grid Analysis.....         | 148        |
| E.3.1 Layovers.....   | 148        |
| E.3.2 Cross-frame Forces .....                                  | 149        |
| E.3.3 Flange Lateral Bending Stress .....                       | 151        |

## LIST OF TABLES

|   |    |
|---|----|
| Table 4.1: Absolute Maximum fit-up force from different methods .....                   | 61 |
| Table 4.2: Absolute Maximum fit-up force from different erection sequences .....        | 64 |
| Table 5.1: Method of calculation of camber for different detailing methods .....        | 67 |
| Table 5.2: Summary of camber analysis .....   | 75 |
| Table 5.3: Structural issues related to Erected fit and Final fit detailing method..... | 77 |
| Table 5.4: Summary of effect area of cross-frame members on cross-frame forces .....    | 80 |

## LIST OF FIGURES

|   |    |
|---|----|
| Figure 1.1: Main sources of twist in straight skew bridges .....  | 2  |
| Figure 2.1: Erected fit and final fit detailing methods .....   | 9  |
| Figure 2.2: Differential camber in a skew bridge .....  | 10 |
| Figure 2.3: Options for the erected fit detailing.....  | 11 |
| Figure 2.4: Framing plans and girder sizes of the Bridge A.....   | 13 |
| Figure 2.5: Framing plans and girder sizes of the Bridge B .....  | 13 |
| Figure 2.6: Framing plans and girder sizes of the Bridge C .....  | 14 |
| Figure 2.7: Layovers in Girder 1 of Bridge A for different detailing methods at different loading stages of construction .....                                      | 16 |
| Figure 2.8: Deflection in Girder 5 of Bridge A for different detailing methods at different loading stages of construction .....                                    | 17 |
| Figure 2.9: Component of deflection due lack-of-fit in Girder 5 of Bridge A for different detailing methods at different loading stages of construction .....       | 18 |
| Figure 2.10: Reactions of Bridge A for different detailing methods at different loading stages of construction.....   | 20 |
| Figure 2.11: Component of reaction due to lack-of-fit ( $R_{Y2}$ ) for Bridge A for different detailing methods at different loading stages of construction .....   | 21 |
| Figure 2.12: Flange lateral bending stress in top flange of Girder 1 of Bridge A for different detailing methods at different loading stages of construction .....  | 23 |
| Figure 2.13: Cross-frame forces in top chord of cross-frames in Bay 7 of Bridge A for different detailing methods at different loading stages of construction ..... | 24 |
| Figure 2.14: Equal and opposite lack-of-fit .....   | 26 |
| Figure 3.1: Comparison of layovers calculated by different analysis method for Girder 8 of Bridge A .   | 31 |
| Figure 3.2: Comparison of layovers calculated by different analysis method for Girder 8 of Bridge B..   | 32 |
| Figure 3.3: Comparison of $D_{Y2}$ calculated by different analysis method for Bridge A for erected fit at the TDL stage.....                                       | 34 |
| Figure 3.4: Comparison of $D_{Y2}$ calculated by different analysis method for Bridge B for erected fit at the TDL stage.....                                       | 34 |
| Figure 3.5: Comparison of $R_{Y2}$ calculated by different analysis method for Bridge A for erected fit at the TDL stage.....                                       | 36 |

|  |    |
|--|----|
| Figure 3.6: Comparison of $R_{Y2}$ calculated by different analysis method for Bridge B for erected fit at the TDL stage.....                                  | 36 |
| Figure 3.7: Comparison of flange lateral bending stress calculated by different analysis method in Girder 8 of Bridge A for erected fit at the TDL stage.....  | 38 |
| Figure 3.8: Comparison of flange lateral bending stress calculated by different analysis methods in Girder 4 of Bridge B for erected fit at the TDL stage..... | 38 |
| Figure 3.9: Comparison of cross-frame forces calculated by different analysis method for Bridge A for erected fit at the TDL stage.....                        | 39 |
| Figure 3.10: Comparison of cross-frame forces calculated by different analysis method for Bridge B for erected fit at the TDL stage.....                       | 40 |
| Figure 3.11: Configurations to calculate initial strain in the cross-frames that are perpendicular to girder web.....  | 43 |
| Figure 3.12: Configurations to calculate initial strain in the cross-frames that are parallel to skew.....   | 44 |
| Figure 3.13: Application of concrete dead load on girders after killing cross-frame elements.....  | 46 |
| Figure 3.14: Removal of concrete dead load from girders after making cross-frame elements alive.....   | 46 |
| Figure 3.15: Comparison of layovers calculated by different analysis methods—final fit at the SDL stage.....   | 47 |
| Figure 3.16: Comparison of component of deflection due to lack-of-fit ( $D_{Y2}$ ) calculated by different analysis methods.....                               | 48 |
| Figure 3.17: Comparison of change in reactions due to lack-of-fit ( $R_{Y2}$ ) calculated by different analysis method for Bridge A.....                       | 48 |
| Figure 3.18: Comparison of flange lateral bending stress calculated by different analysis methods.....   | 49 |
| Figure 3.19: Comparison of cross-frame forces calculated by different analysis methods.....  | 49 |
| Figure 4.1: Final fit detailing methods.....   | 51 |
| Figure 4.2: Differential camber in a skew bridge.....  | 53 |
| Figure 4.3: Fit-up forces required to attach the cross-frames to the girders.....  | 54 |
| Figure 4.4: Fit-up forces by resolving cross-frame forces at connection points.....  | 56 |
| Figure 4.5: Steps followed to calculate fit-up forces in erection simulation.....  | 57 |
| Figure 4.6: Geometry of Girder 4 of Bridge C after completion of erection.....   | 58 |
| Figure 4.7: Lateral fit-up forces applied to Girder 3 of Bridge C for erecting cross-frames in Bay 3.....  | 59 |
| Figure 4.8: Vertical fit-up forces applied to Girder 3 of Bridge C for erecting cross-frames in Bay 3....  | 60 |
| Figure 4.9: Erection sequences for attaching cross-frames to girders in final fit detailing method.....  | 62 |

|  |    |
|--|----|
| Figure 4.10: Fit-up force at the top of Girder 8 of Bridge A for erecting the cross-frames in Bay 8.....   | 63 |
| Figure 5.1: Framing plans and girder sizes of the Bridge A .....   | 68 |
| Figure 5.2: Framing plans and girder sizes of the Bridge B .....   | 69 |
| Figure 5.3: Framing plans and girder sizes of the Bridge C .....   | 69 |
| Figure 5.4: Verification of camber recommendation for the erected fit detailing method-Bridge A Girder 1.....  | 71 |
| Figure 5.5: Verification of camber recommendation for the final fit detailing method-Bridge A Girder 1 .....   | 72 |
| Figure 5.6: Verification of camber recommendation for the erected fit detailing method-Bridge B Girder 1.....  | 72 |
| Figure 5.7: Verification of camber recommendation for the final fit detailing method-Bridge B Girder 1 .....   | 73 |
| Figure 5.8: Verification of camber recommendation for the erected fit detailing method-Bridge C Girder 1.....  | 73 |
| Figure 5.9: Verification of camber recommendation for the final fit detailing method-Bridge C Girder 1 .....   | 74 |
| Figure 5.10: Effect of reducing the area of cross member on cross-frame forces in Bridge A for erected fit at the TDL stage .....  | 80 |
| Figure 5.11: Framing planes to study effects of location of first intermediate cross-frame from the support in bridge A .....  | 81 |
| Figure 5.12: Variation of structural responses by changing location of first intermediate cross-frame from the support in bridge A with erected fit detailing under TDL..... | 82 |
| Figure 5.13: Framing planes to study effects of location of first intermediate cross-frame from the support in a continuous bridge.....                                      | 83 |
| Figure 5.14: Variation of cross-frame forces by changing location of first intermediate cross-frame from the support for erected fit at the TDL stage .....                  | 84 |
| Figure 5.15: Variation of reactions by changing location of first intermediate cross-frame from the support for erected fit at the TDL stage .....                           | 84 |
| Figure 5.16: Different cross-frame orientations.....   | 85 |
| Figure 5.17: Layover for different cross-frame orientations for erected fit at the TDL stage .....   | 86 |
| Figure 5.18: Conventional and lean-on bracing line.....  | 87 |
| Figure 5.19: A skew bridge with lean-on bracing system .....   | 87 |

|  |     |
|--|-----|
| Figure 5.20: Lean-on bracing system in 19 <sup>th</sup> street Bridge.....   | 88  |
| Figure 5.21: Flow chart to guide designer to deal with skew bridges .....  | 90  |
| Figure A.1: Framing plans and girder sizes of the Bridge A .....   | 96  |
| Figure A.2: Framing plans and girder sizes of the Bridge B .....   | 97  |
| Figure A.3: Framing plans and girder sizes of the Bridge C .....   | 97  |
| Figure A.4: Framing plans and girder sizes of the Bridge B2 .....  | 98  |
| Figure B.1: Concrete dead load (CDL) deflection in Girder 1 of Bridge A .....  | 99  |
| Figure B.2: Concrete dead load (CDL) deflection in Girder 5 of Bridge A .....  | 99  |
| Figure B.3: Concrete dead load (CDL) deflection in Girder 1 of Bridge B .....  | 100 |
| Figure B.4: Concrete dead load (CDL) deflection in Girder 5 of Bridge B .....  | 100 |
| Figure B.5: Concrete dead load (CDL) deflection in Girder 1 of Bridge C .....  | 101 |
| Figure B.6: Concrete dead load (CDL) deflection in Girder 2 of Bridge C .....  | 101 |
| Figure B.7: Deflection in Girder 1 of Bridge B2 for different detailing methods at different loading stages of construction.....                                   | 102 |
| Figure B.8: Component of deflection due lack-of-fit in Girder 1 of Bridge B2 for different detailing methods at different loading stages of construction .....     | 102 |
| Figure B.9: Layovers in Girder 1 of Bridge A for different detailing methods at different loading stages of construction .....                                     | 103 |
| Figure B.10: Layovers in Girder 5 of Bridge A for different detailing methods at different loading stages of construction .....                                    | 103 |
| Figure B.11: Layovers in Girder 1 of Bridge B for different detailing methods at different loading stages of construction .....                                    | 104 |
| Figure B.12: Layovers in Girder 5 of Bridge B for different detailing methods at different loading stages of construction .....                                    | 104 |
| Figure B.13: Layovers in Girder 1 of Bridge C for different detailing methods at different loading stages of construction .....                                    | 105 |
| Figure B.14: Layovers in Girder 2 of Bridge C for different detailing methods at different loading stages of construction .....                                    | 105 |
| Figure B.15: Layovers in Girder1 of Bridge B2 for different detailing methods at different loading stages of construction .....                                    | 106 |
| Figure B.16: Flange lateral bending stress in top flange of Girder 1 of Bridge A for different detailing methods at different loading stages of construction ..... | 107 |

|   |     |
|---|-----|
| Figure B.17: Flange lateral bending stress in top flange of Girder 5 of Bridge A for different detailing methods at different loading stages of construction .....  | 107 |
| Figure B.18: Flange lateral bending stress in top flange of Girder 1 of Bridge B for different detailing methods at different loading stages of construction .....  | 108 |
| Figure B.19: Flange lateral bending stress in top flange of Girder 5 of Bridge B for different detailing methods at different loading stages of construction .....  | 108 |
| Figure B.20: Flange lateral bending stress in top flange of Girder 1 of Bridge C for different detailing methods at different loading stages of construction .....  | 109 |
| Figure B.21: Flange lateral bending stress in top flange of Girder 2 of Bridge C for different detailing methods at different loading stages of construction .....  | 109 |
| Figure B.22: Flange lateral bending stress in top flange of Girder 5 of Bridge B2 for different detailing methods at different loading stages of construction ..... | 110 |
| Figure B.23: Reactions of Bridge A for different detailing methods at different loading stages of construction.....   | 111 |
| Figure B.24: Reactions of Bridge B for different detailing methods at different loading stages of construction.....   | 111 |
| Figure B.25: Reactions of Bridge C for different detailing methods at different loading stages of construction.....   | 112 |
| Figure B.26: Reactions of Bridge B2 for different detailing methods at different loading stages of construction.....  | 112 |
| Figure B.27: Component of reaction due to lack-of-fit ( $R_{Y2}$ ) for Bridge B2 for different detailing methods at different loading stages of construction .....  | 113 |
| Figure B.28: Cross-frame forces in top chord of cross-frames in Bay 1 of Bridge A for different detailing methods at different loading stages of construction ..... | 114 |
| Figure B.29: Cross-frame forces in top chord of cross-frames in Bay 4 of Bridge A for different detailing methods at different loading stages of construction ..... | 114 |
| Figure B.30: Cross-frame forces in top chord of cross-frames in Bay 1 of Bridge B for different detailing methods at different loading stages of construction ..... | 115 |
| Figure B.31: Cross-frame forces in top chord of cross-frames in Bay 4 of Bridge B for different detailing methods at different loading stages of construction ..... | 115 |
| Figure B.32: Cross-frame forces in top chord of cross-frames in Bay 1 of Bridge C for different detailing methods at different loading stages of construction ..... | 116 |

|  |     |
|--|-----|
| Figure B.33: Cross-frame forces in top chord of cross-frames in Bay 2 of Bridge C for different detailing methods at different loading stages of construction .....  | 116 |
| Figure B.34: Cross-frame forces in top chord of cross-frames in Bay 5 of Bridge B2 for different detailing methods at different loading stages of construction ..... | 117 |
| Figure C.1: Concrete dead load (CDL) deflection in Girder 1 of Bridge A by different methods of analysis.....  | 118 |
| Figure C.2: Concrete dead load (CDL) deflection in Girder 5 of Bridge A by different methods of analysis.....  | 118 |
| Figure C.3: Concrete dead load (CDL) deflection in Girder 1 of Bridge B by different methods of analysis.....  | 119 |
| Figure C.4: Concrete dead load (CDL) deflection in Girder 5 of Bridge B by different methods of analysis.....  | 119 |
| Figure C.5: Concrete dead load (CDL) deflection in Girder 1 of Bridge C by different methods of analysis.....  | 120 |
| Figure C.6: Concrete dead load (CDL) deflection in Girder 1 of Bridge C by different methods of analysis.....  | 120 |
| Figure C.7: Comparison of layovers calculated by different analysis method for Girder 1 of Bridge A  | 121 |
| Figure C.8: Comparison of layovers calculated by different analysis method for Girder 5 of Bridge A  | 121 |
| Figure C.9: Comparison of layovers calculated by different analysis method for Girder 1 of Bridge B  | 122 |
| Figure C.10: Comparison of layovers calculated by different analysis method for Girder 5 of Bridge B .....   | 122 |
| Figure C.11: Comparison of layovers calculated by different analysis method for Girder 1 of Bridge C .....   | 123 |
| Figure C.12: Comparison of layovers calculated by different analysis method for Girder 2 of Bridge C .....   | 123 |
| Figure C.13: Comparison of flange lateral bending stress calculated by different analysis method in Girder 1 of Bridge A for erected fit at the TDL stage .....      | 124 |
| Figure C.14: Comparison of flange lateral bending stress calculated by different analysis method in Girder 5 of Bridge A for erected fit at the TDL stage .....      | 124 |
| Figure C.15: Comparison of flange lateral bending stress calculated by different analysis method in Girder 1 of Bridge B for erected fit at the TDL stage.....       | 125 |

|  |     |
|--|-----|
| Figure C.16: Comparison of flange lateral bending stress calculated by different analysis method in Girder 4 of Bridge B for erected fit at the TDL stage..... | 125 |
| Figure C.17: Comparison of flange lateral bending stress calculated by different analysis method in Girder 1 of Bridge C for erected fit at the TDL stage..... | 126 |
| Figure C.18: Comparison of flange lateral bending stress calculated by different analysis method in Girder 2 of Bridge C for erected fit at the TDL stage..... | 126 |
| Figure C.19: Comparison of vertical reactions calculated by different analysis method for Bridge A for erected fit at the TDL stage.....                       | 127 |
| Figure C.20: Comparison of vertical reactions calculated by different analysis method for Bridge B for erected fit at the TDL stage.....                       | 127 |
| Figure C.21: Comparison of vertical reactions calculated by different analysis method for Bridge C for erected fit at the TDL stage.....                       | 128 |
| Figure C.22: Comparison of cross-frame forces calculated by different analysis method for Bridge A for erected fit at the TDL stage.....                       | 129 |
| Figure C.23: Comparison of cross-frame forces calculated by different analysis method for Bridge A for erected fit at the TDL stage.....                       | 129 |
| Figure C.24: Comparison of cross-frame forces calculated by different analysis method for Bridge B for erected fit at the TDL stage.....                       | 130 |
| Figure C.25: Comparison of cross-frame forces calculated by different analysis method for Bridge B for erected fit at the TDL stage.....                       | 130 |
| Figure C.26: Comparison of cross-frame forces calculated by different analysis method for Bridge C for erected fit at the TDL stage.....                       | 131 |
| Figure C.27: Comparison of cross-frame forces calculated by different analysis method for Bridge C for erected fit at the TDL stage.....                       | 131 |
| Figure D.1: Change in elevation due to lack of fit calculated by different analysis method for Bridge C for final fit at the SDL stage .....                   | 132 |
| Figure D.2: Change in elevation due to lack of fit calculated by different analysis method for Bridge C for final fit at the SDL stage .....                   | 132 |
| Figure D.3: Comparison of layovers obtained by different analysis method for Bridge C for final fit at the SDL stage.....                                      | 133 |
| Figure D.4: Comparison of layovers obtained by different analysis method for Bridge C for final fit at the SDL stage.....                                      | 133 |

|   |     |
|---|-----|
| Figure D.5: Comparison of flange lateral bending stress obtained by different analysis method for Bridge C for final fit at the SDL stage ..... | 134 |
| Figure D.6: Comparison of flange lateral bending stress obtained by different analysis method for Bridge C for final fit at the SDL stage ..... | 134 |
| Figure D.7: Comparison of vertical reaction obtained by different analysis method for Bridge C for final fit at the SDL stage .....             | 135 |
| Figure D.8: Comparison of cross frame forces obtained by different analysis method for Bridge C for final fit at the SDL stage .....            | 136 |
| Figure D.9: Comparison of cross frame forces obtained by different analysis method for Bridge C for final fit at the SDL stage .....            | 136 |

# **Chapter 1 INTRODUCTION**

## **1.1 Background**

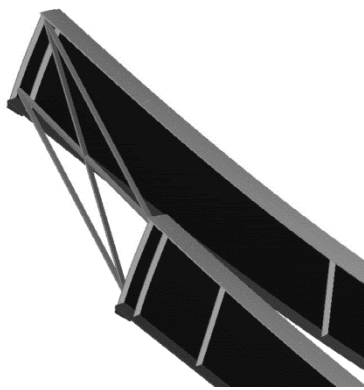
Steel I-girder bridges are frequently used in applications where the bridge site necessitates complex geometrical configurations. Predicting the girder deformations are often complicated by uncertainties in the girder support conditions as well as the interaction between the girders and the bracing. The behavior of horizontally curved as well as straight girders with skewed supports can be difficult to predict. Some of the difficulties are due to the simplified grid models that are used to predict the behavior; however, even with three-dimensional models, the behavior is highly dependent on the modeling assumptions.

The bridge owner generally desires to have a bridge with a uniform concrete deck thickness in which the girders are properly supported on the bearings at the piers and abutments. However, deformations during construction can result in distorted girder geometries at the supports that can also have a significant impact on the profile of the bridge deck and may also impact the performance of the bearings that allow the bridge to expand and contract due to temperature changes. Although curved girders have twist at the supports due to the torsional loads that arise from the geometry, straight bridges with skewed supports also can have significant support twist that distorts the girder geometry. For skew angles larger than 20 degrees, the AASHTO Specifications [1] require intermediate cross-frames to be oriented perpendicular to the longitudinal axis of the girders; however, the braces at the supports are typically parallel to the skew angle. The support rotation in skewed girders is related to the in-plane rotation of the girders and the skewed orientation of the cross-frame or diaphragms at the supports. Because the skewed braces have components directed along both the longitudinal and transverse directions, the girders experience a twist that is proportional to the magnitude of the in-plane rotation. Although the magnitude of the twist at the support can be predicted during design, the actual deformations in the field are dependent on several factors such as the rotational stiffness of the bearing and the staging of the concrete deck placement.

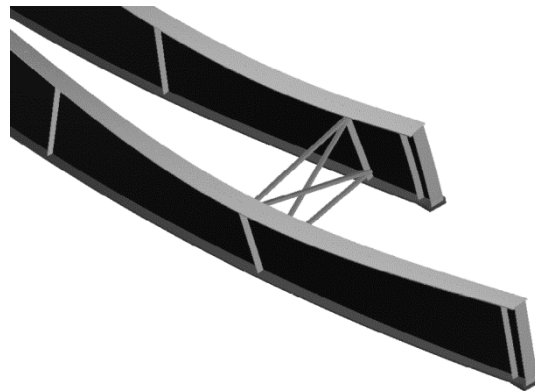
## **1.2 Twist in Skew Bridge**

One of the contributing factors for excessive girder twist in systems with skewed supports is the relatively low torsional stiffness of the steel I shapes during construction. There are two main sources of girder twist in straight skewed I-girder bridges: 1) twist induced by the skewed cross-frame line at the

supports and 2) twist induced by the differential girder deflection that occurs at the two ends of cross-frames located at intermediate locations along the bridge length. Figure 1.1 shows the two different cross-frame orientations that can contribute to the girder twist. Figure 1.1a depicts a cross-frame located at an exterior support of a skewed girder system. Flexure in the girders from gravity loads results in major axis bending that causes ends of the girders to rotate. Cross-frames attached to these ends rotate about their own axis that is parallel to skewed supports because warping stiffness of the cross-frames is very high compared to torsional stiffness of the girders. This cross-frame rotation has a component parallel to longitudinal axis of the girders resulting in twist of the girders. Figure 1.1b shows an intermediate cross-frame that connects to two adjacent skewed girders at different locations along the length of the individual girders. As the girder deflect from the applied dead load the two ends of the cross-frame experience a differential vertical displacement that leads to torsional deformations in the girders. Previous studies have resulted in analytical expressions for both the twist caused by rotation of the cross-frame at bearing line and the twist caused by differential deflection by assuming the cross-frames to be rigid [2].



(a) Twist due to rotation of cross-frames at bearing lines



(b) Twist due to differential deflection

**Figure 1.1: Main sources of twist in straight skew bridges**

### 1.3 Bridge Industry Perception

Communications has been made with the designers, fabricators and erectors to understand their perception of the problems in skewed bridge.

The designers are interested in the answer to following questions.

- What structural response are affected by different detailing methods
- What is the level of analysis required for the erection and detailing of skew bridges
- How construction of skewed bridges can be accommodated in design procedure
- How to estimate the fit-up forces required during the erection of skewed bridges

The fabricator have shown concern about the following issues

- Miscommunications can result in slowdown, stops, unnecessary extra work, back charges, poor/disastrous erection problems, litigation
- Must clearly specify which “plumb” condition is required
- Fabricators do not know/cannot control the accuracy of the design deflections
- AASHTO requires the owner to state the intended erected condition. If the contract dictates the condition, fabricators/detailer will work to it.
- Behavior of bearings in skewed bridges needs special attention.

The main message delivered was that: there is a need for complete comprehensive design procedure that takes into account the fabrication, detailing, and erection of the skew bridges.

### 1.4 Problem Statement

The AASHTO LRFD Bridge Design Specifications require that when skew angle exceeds, 20 degrees, the cross-frames to be normal to girder webs. As a result, as indicated in Figure 1.1, the cross-frames are connected to adjacent girders with different deflections. This differential deflection, coupled with relative in-plane stiffness of cross-frames and the rotational stiffness of the girder at the connection locations, result in twisting of the girder along the length and at the supports. The twisting of the girder results in number of disadvantages, which includes: field fit-up, built-in residual stresses, additional lateral loads, increased lateral bending of compression flanges, complex camber analysis and difficulties

properly screeding the bridge deck and more complex analysis to account for the variety of framing configurations.

## 1.5 Objectives

The main objective of this project was to comprehend the effect of skew in steel bridges and develop a set of recommendations for FDOT with respect to analysis, design and detailing of highly skewed steel bridges (I-shaped). Additional objectives of the project are:

- a) Review recommendations from previous investigations
- b) Determining the analysis, design and analysis issues requiring attention
- c) Examining the advantages and disadvantages of various framing schemes to resolve issues related to highly skewed steel girder bridges
- d) Develop preferred framing plans for various conditions
- e) Consider needs of various stakeholders and incorporate them in the final recommendations.

The focus of the project will be on skewed straight steel bridges using I-shaped girders.

## 1.6 Organization of the Report

The report is organized in six chapters. Chapter 2 starts by describing the twist caused in skew bridges due to differential deflection and bearing line rotation. Different terminologies used for different detailing method in the past are explained. Simplified terminologies that are erected fit and the final fit are proposed for describing the detailing methods for straight skewed steel bridges. Different design and analysis issues requiring attention are identified from literature review. 3D Finite Element Method (FEM) analyses were carried out on different straight skewed bridges to identify different structural responses affected by the detailing methods. These responses or component of these responses are defined as lack-of-fit effects. These lack-of-fit effects include girder layovers, cross-frame forces, flange lateral bending stress, component of vertical deflection due to lack-of-fit, and component of vertical reaction due to lack-of-fit. This chapter compares the lack-of-fit effects for the erected fit and the final fit detailing methods at the steel dead load (SDL) and total dead load (TDL) stages. The final conclusion of this chapter is that lack-of-fit effects for the final fit detailing method at the SDL stage are equal and opposite to the lack-of-fit effects for the erected fit detailing method at the TDL stage.

Chapter 3 discusses different methods of analysis that can be used to evaluate the lack-of-fit effects discussed in chapter 2. Separate methods of analysis are compared for erected and final fit detailing methods. For the erected fit detailing method 1D line girder analysis, traditional 2D grid analysis, improved 2D grid analysis and 3D FEM analysis are compared. For the final fit detailing method reversing improved 2D grid analysis, 3D FEM using initial strains, and 3D FEM using dead and live cross-frames are compared. This chapter concludes that improved 2D grid analysis can be used for both erected and final fit detailing methods to estimate lack-of-fit effects. Further, 3D FEM analysis with dead and live cross-frames is a very simple 3D FEM analysis that does not require tedious calculation of initial strains and give almost the same results as method of initial strains.

Chapter 4 discusses an important erection issue related to final fit detailing method. In final fit detailing method cross-frame are detailed in such a way that they do not fit between their connections to girder during erection. Therefore the girders are required to moved and twisted in order to make connections between cross-frames and girders. The forces required for moving or twisting the girders are referred as fit-up forces. Methods of calculation of these forces are provided in this chapter. These methods include 3D erection simulation and 2D grid analysis. In 3D erection simulation cross-frames are erected one by one and change in stiffness and geometry of the structure was taken into consideration. Further different erections sequences can be followed for erecting the cross-frames in these erections simulations. In 2D grid analysis, cross-frame forces are used to estimate the maximum fit-up forces. This chapter concludes that improved 2D grid analysis can be used to estimate the maximum fit-up force required during erection of a particular bridge. Further erecting the cross-frame starting from the middle of a bay toward the ends of the bay may alleviate the fit-up problems.

Chapter 2, 3 and 4 provide the elements required for developing a complete comprehensive design provisions. These provisions are proposed in Chapter 5. Chapter 5 recommends way of calculating camber for different detailing methods. These recommendations are verified by carrying out numerical analyses. The ultimate choice of detailing method is left to designer, however, a flow chart is provided for each detailing method to facilitate the design. Flow charts require flange lateral bending stress to be checked for both detailing methods to satisfy the AASHTO requirements. For the final fit detailing method, fit-up forces are also required to be estimated and communicator to contractor/erector. The procedure for estimation of fit-up force is provided in chapter 4.

Chapter 6 describes the conclusion of overall research.

## **Chapter 2      COMPARISON OF ERECTED FIT AND FINAL FIT DETAILING METHODS**

Earlier studies have reported a number of problems in straight skewed steel bridges both during girder erection and placement of the concrete bridge deck. These problems include, excessive twist of the girders, uplift at the support locations, development of flange lateral bending stresses, and difficulty fitting the cross-frames during erection [2, 3, 4, 5, 6]. These problems are generally associated with the detailing method used for the girders and cross-frames. Detailing terminologies that are commonly used for steel bridges with skewed supports include no load fit (NLF), steel dead load fit (SDLF), total dead load fit (TDLF), consistent detailing, and inconsistent detailing [2, 3, 4, 7, 8]. These terminologies generally refer to the plumb condition of the web at a particular loading stage (NLF, SDLF, and TDLF) or refer to the fact that girder and cross-frame might be detailed for the web to be plumb at different load stages (inconsistent detailing) or the same load stages (consistent detailing). The use of these terminologies have contributed to miscommunication between individuals in the bridge industry and have further led to the belief that skewed steel bridges are difficult to detail, design and construct.

Further different detailing methods have been investigated in the past to identify and compare structural responses affected by the detailing methods. However, for TDLF detailing method 2D grid analysis cambers or 3D FEM cambers calculated from the deflection of girders attached with cross-frames under total dead load were used to simulate lack-of-fit effects [2, 3, 4]. It has been shown that use of these cambers to simulate lack-of-fit effects is wrong and line girder analysis cambers should be used to simulate lack-of-fit effects for the final fit detailing method.

The objectives of this chapter are:

- To introduce of simplified terminologies consistent with field practices.
- To identify of structural responses affected by different detailing methods.
- To compare of different detailing methods for straight skewed I girder bridges.

## 2.1 Existing and Proposed Terminologies

The girder webs in straight skewed bridges can be detailed to be plumb at one of the different construction loading stages. As noted earlier, there are generally three stages that are used to reference when the girder webs are plumb: 1) the No Load (NL) stage, 2) the steel dead load (SDL) stage, or 3) the total dead load (TDL) stage [9]. The term consistent detailing is used to describe the case in which both the girders and the cross-frames to be detailed so that the webs are plumb at the same stage. The girders are often fabricated to be plumb at the NL stage; however, cross-frames can be fabricated for web plumb at either NL or SDL or TDL stage. The term inconsistent detailing would be used to describe the situation where the girder webs are detailed to be plumb in one stage (usually the NL stage) and the cross-frames are detailed for the web to be plumb at a different stage (i.e. the SDL or TDL stages). Another set of terminologies, No Load Fit (NLF), steel dead load Fit (SDLF), and total dead load (TDLF), is also used to describe above three scenarios. When the NLF method is employed, the cross-frames are fabricated for the web to be plumb at the NL stage. As the name implies, both the girder and cross-frame are detailed to fit when the girder rests on the ground, blocked-up in its fabricated NL geometry including any vertical curve and camber in the girders. However, once dead load is applied the girder experiences twist due to bearing line rotation and differential deflection as explained earlier. When the SDLF method is employed, the cross-frames are fabricated for the web to be plumb at the SDL stage. In this scenario, both the girders and cross-frames are detailed to fit when the girders are erected and supported at the bearing lines (SDL stage). Similarly when the TDLF method is employed, the cross-frames are fabricated for the web to be plumb at the TDL stage. In this scenario, both the girders and cross-frames are detailed to fit when the girders are supported at the bearing lines under total construction dead load.

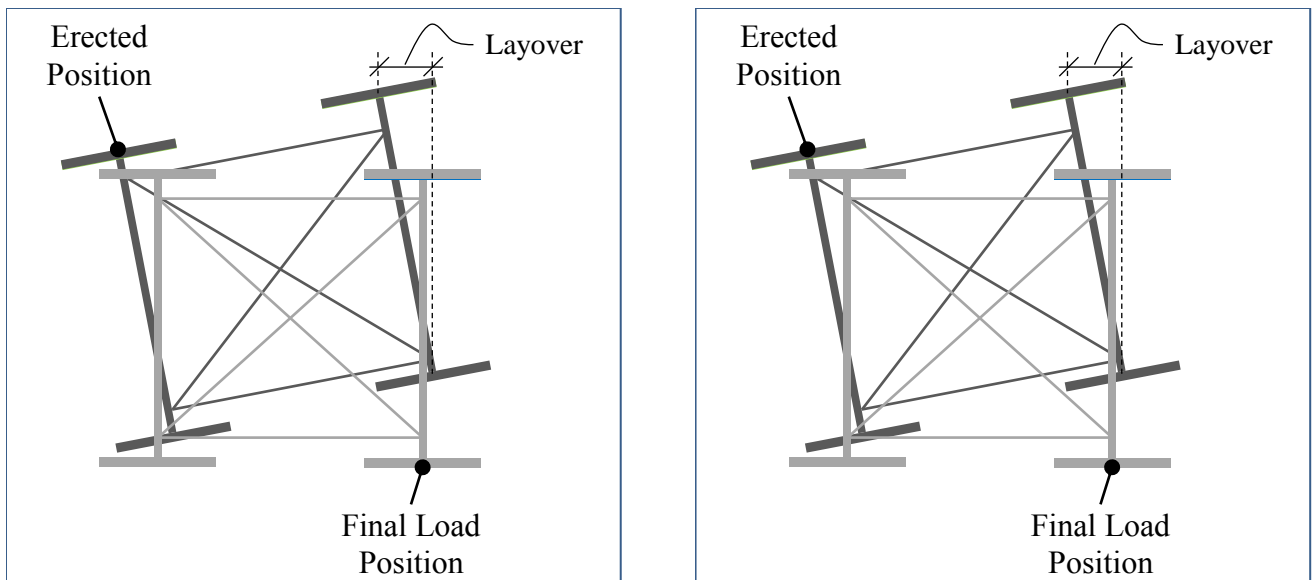
The cross-frames will generally be the easiest to install in the SDLF case as the cross-frames are typically installed as the girders are erected and the girders will have ideally deflected to the SDL condition, which matches the detail condition of the cross-frames. If the NLF scenario is used, significant force may be necessary to fit the girders and cross-frames when the construction is unshored or partially shored. If the TDLF scenario is used, significant force may be necessary to fit the girders and cross-frames, since at the time of the steel erection, the girders have not yet been deflected by the dead load from the concrete deck. As an example, consider the TDLF case in which the girders and cross-frames have been detailed for web plumbness under full construction dead load. Since the girder webs will not be plumb during steel erection, the girders will need to be twisted to install the cross-

frames. The amount of force necessary to fit the cross-frames is highly dependent on the bridge geometry. The force required to twist the girders to have web out of plumb is henceforth referred as the fit-up force.

The terms NLF, SDLF, and TDLF are generally idealized stages that may not actually occur in common practice. For example, in typical steel bridge fabrication, using bolted field splices, the girders are fabricated for the NLF (i.e. laydown). During erection, holding cranes or temporary supports may be necessary to fit-up of the main girder. Therefore, this stage is usually somewhere between the NL stage and SDL stage at the start of erection and gets close to SDL stage near the completion of erection. As a result, the development of simplified terminologies that are consistent with the erection practices is desirable.

To reduce miscommunication, in this chapter the detailing terminologies erected fit (EF) and final fit (FF) are introduced in lieu of NLF, SDLF, TDLF, consistent detailing, and inconsistent detailing.

In the erected fit detailing method, the cross-frames are detailed to fit between the girders at erection or the SDL stage as shown in Figure 2.1a. These cross-frames do not fit between the girders after the deck is cast or the TDL stage as shown in Figure 2.1a. In the final fit detailing method, the cross-frames are detailed to fit between the girders after deck is casted or TDL stage as shown in Figure 2.1b. These cross-frames do not fit between the girders at erection or SDL stage as shown in Figure 2.1b.



(a) Erected fit detailing method

(b) Final fit detailing method

**Figure 2.1: Erected fit and final fit detailing methods**

## 2.2 Fabrication for Different Detailing Methods

The erected fit detailing method can be achieved in two ways:

1. Change the lengths of cross-frame members, or
2. Change the location of connection of points; i.e., change the bolt hole locations on the stiffeners.

Since the cross-frames in skewed bridges are typically perpendicular to the girder web, the braces connect the two adjacent girders at different elevations due to camber and cross-slope. The difference in elevation of girders due to cross-slope remains same at different loading stages and therefore does not contribute to lack-of-fit effects. However, the difference in elevations of girders due to camber does contribute to lack-of-fit effects as illustrated in Figure 2.2, which depicts the camber diagrams for three girders of a skewed bridge. The figure shows some of the detailing complexities that the differential camber produces with respect to cross-frame detailing.

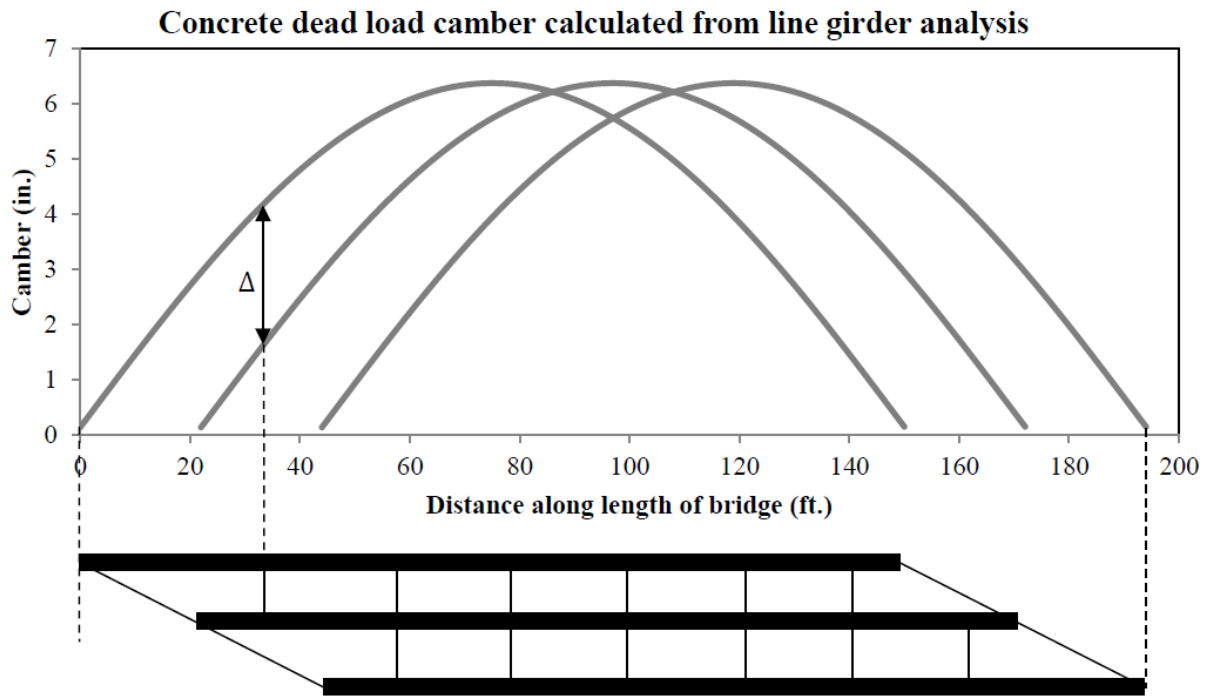
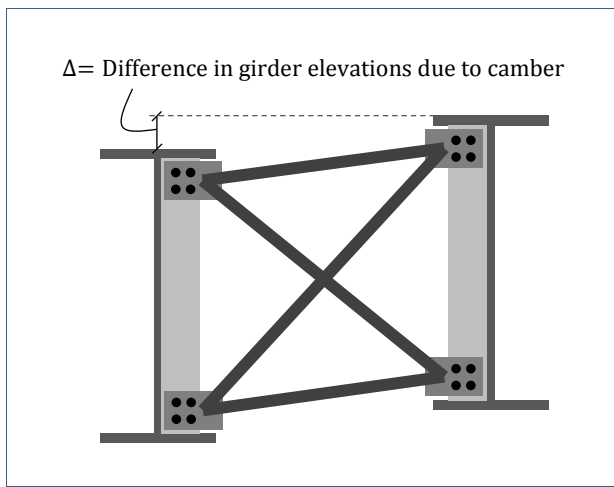
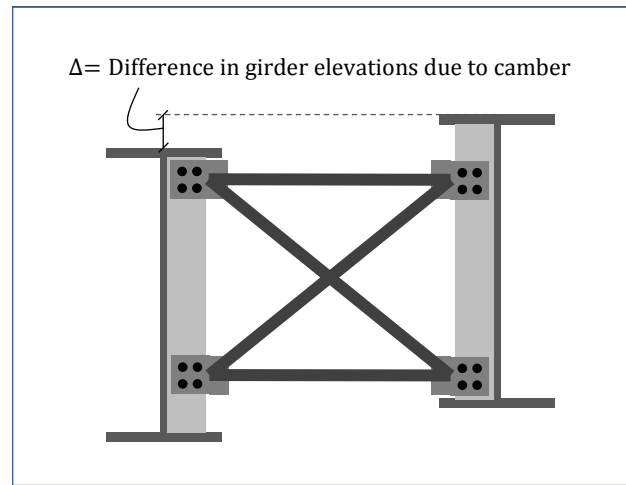


**Figure 2.2: Differential camber in a skew bridge**

There are two approaches to fit the cross-frame to account for differential camber: a) varying member lengths for each cross-frame, or b) adjusting the connection points of the cross-frames (see Figure 2.3). It should be noted that the difference in elevation of girders due to cross-slope is built into the cross-frames regardless of the detailing methods used for the bridge.



(a) Change lengths of cross-frame members



(b) Change location of connection of points

**Figure 2.3: Options for the erected fit detailing**

### 2.3 Numerical Analysis for Different Detailing Methods

During conduct of research, numerous three-dimensional analyses were carried out using ANSYS [10]. Three-dimensional finite element method (3D FEM) analyses can be used with different levels of modeling techniques. For example, in a 3D FEM, the flanges can be modeled using either beam elements or shell elements with or without bearing pads. Results presented in this chapter were from 3D FEM models with flanges modeled by shell elements. These models also include bearing pads that were modeled by solid elements with modulus of elasticity of 10 ksi. ANSYS [10] was used for 3D FEM analysis. The term isolated girder analysis (IGA) used in this chapter refers to a 3D FEM analysis of bridge girders without attaching cross-frames.

3D FEM analysis for the erected fit detailing method can be accomplished by applying SDL on girders without attaching the cross-frames. Once SDL was applied, cross-frames were attached to the girders followed by application of concrete dead load (CDL).

3D FEM analysis for the final fit detailing method could be carried out in two different ways. The first approach uses imposing initial strains in cross-frame members. The use of 3D FEM analysis using the initial strain approach [2] requires a) building the entire model (cross-frame and girders attached), b) imposing initial strain in the cross-frame members to simulate the lack-of-fit of cross-frames between

the girders at the SDL stage (initial strains were calculated from the camber diagram see chapter 3 for details), and c) applying the load simulating the wet concrete weight. The second approach relies on applying concrete dead load, followed by activating the cross-frame members, followed by removing concrete dead load. Detail of this approach is provided in chapter 3. The results presented in this chapter were obtained from initial strain approach.

## **2.4 Structural Responses of the Skewed Bridges Affected By Different Detailing Methods**

This section discusses various structural responses of steel bridges that are affected by lack-of-fit of cross-frame between girders including layovers, deflections, reactions, flange lateral bending stress, and cross-frame forces. Component of these structural responses affected by lack-of-fit henceforth shall be called lack-of-fit effects. These lack-of-fit effects appear after attaching the cross-frames to girders at a loading stage at which cross-frames do not fit between the girders. Therefore these effects appear at the TDL stage for the erected fit detailing method and SDL stage for the final fit detailing method.

In the discussions to follow, three bridges are used to compare for the final fit and erected fit detailing methods. The next section first describes these three bridges, and then discusses lack-of-fit effects in these bridges.

### **2.4.1 Description of Structures Used for Comparison of Different Detailing Methods**

Three straight skewed, simply supported I-girder bridges, having different levels of skew, are selected for consideration in this study. All three bridges have their girders and cross-frames designed with Grade 50 steel having a modulus of elasticity of 29,000 ksi.

**Bridge A** is an extreme case of straight skew bridges and was used to show extreme skew effects in previous studies [2, 3, 4]. It has 300 ft. long by 144 in. deep girders simply supported on 70.4° skewed supports. The girders are braced with X-type cross-frames containing L6 x 6 x 1 angles. The bridge uses staggered cross-frames at spacing of 22 ft. between 9 girders at 9.25 ft. c/c spacing. Framing planes and sizes of the web and flanges of the bridges studied are shown in Figure 2.4.

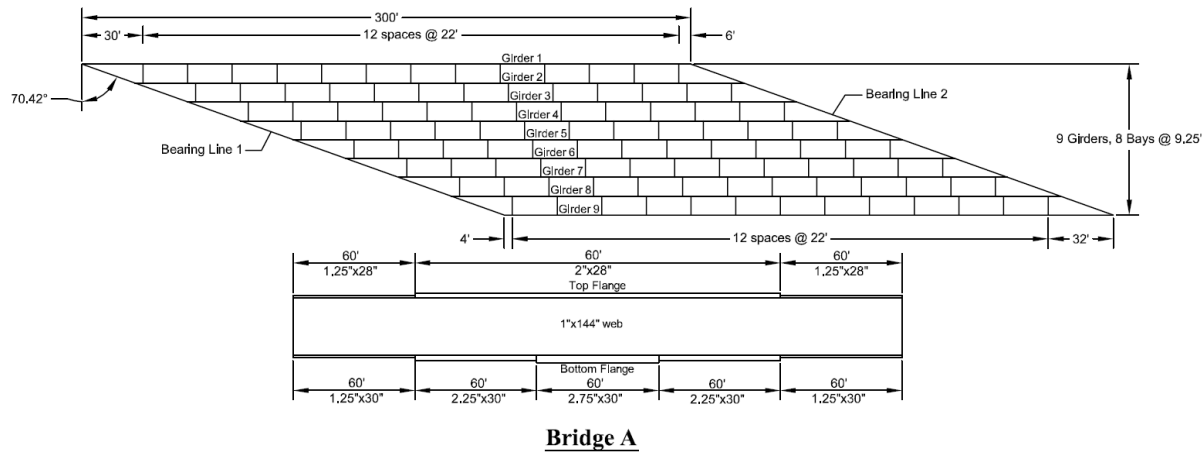


**Figure 2.4: Framing plans and girder sizes of the Bridge A**

**Bridge B** is another highly skewed bridge, however skewed effect in Bridge B is smaller compared to Bridge A. Bridge B has 266 ft long by 120.5 in. deep girders simply supported on 62.6° skewed supports. The girders of the Bridge B are braced with X-type cross-frames containing L6 x 6 x 1/2 angles. The bridge uses cross-frames at spacing of 16 ft between eight girders at 7.26 ft c/c spacing. Framing planes and sizes of the web and flanges of the bridges studied are shown in Figure 2.5.

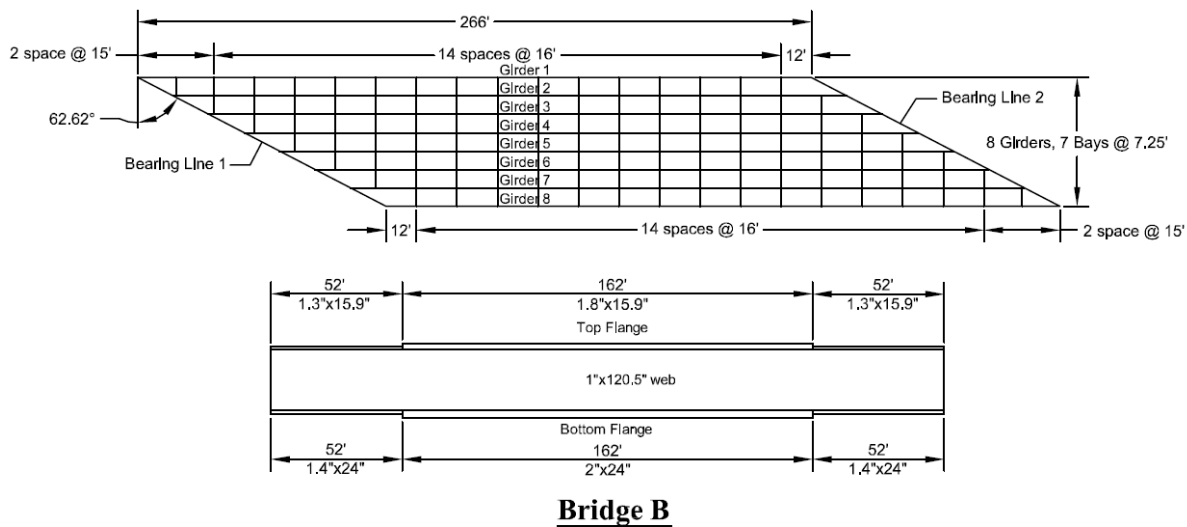


**Figure 2.5: Framing plans and girder sizes of the Bridge B**

**Bridge C** has 150 ft long by 56.1 in. deep girders simply supported on 62.6° skewed supports. The girders of the Bridge C are braced with X-type cross-frames containing L6 x 3 1/2 x 5/16 angles. The bridge uses cross-frames at spacing of 21 ft between four girders at 8ft c/c spacing. Framing planes and sizes of the web and flanges of the bridges studied are shown in Figure 2.6.

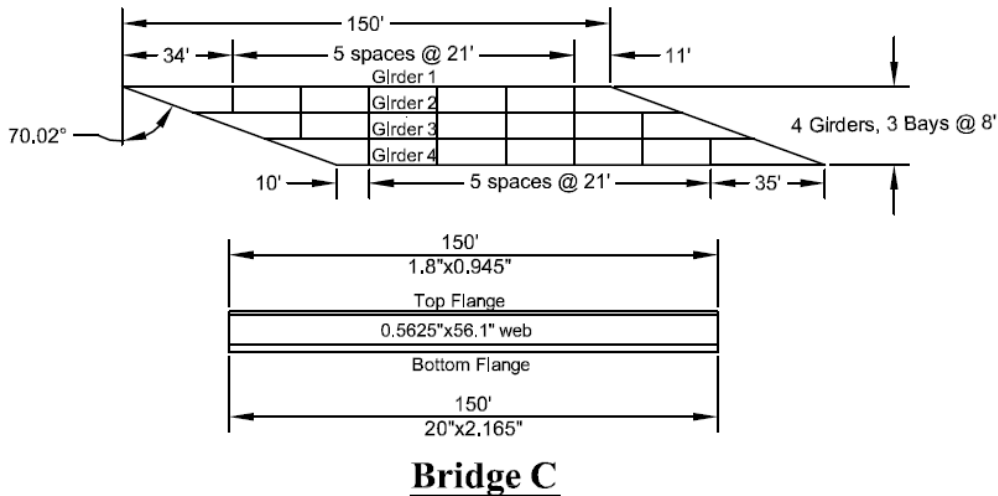


**Figure 2.6: Framing plans and girder sizes of the Bridge C**

### 2.4.2 Layovers

Layover is defined as lateral displacement from center of top flange to center of bottom flange at any particular section of the girder. As long as the load levels are less than a small fraction of the critical elastic buckling load at the factored strength load levels, layovers are not of any structural consequence, i.e., do not have any significant impact on the strength of the structural system. The NCHRP 725 report [4] recommends when the factored loads under the appropriate strength load combinations are less than approximately 10 % of the estimated elastic buckling load level, global second-order amplification can be neglected in the strength checks. In addition, AASHTO [1] Article 6.10.1.6 currently allows the engineer to neglect local amplification of flange lateral bending stresses between cross-frame locations when the factored loads are less than 15 % of the estimated elastic lateral-torsional buckling load for a given girder unbraced length. Both of the limits are based on judgment. If these limits are satisfied at factored load levels, or if they are not satisfied but second-order amplification is addressed in the

calculation of the factored strength load requirements, then the impact of any dead load layovers on the strength of the system is negligible.

However, it is recommended that the layovers should be calculated at the relevant loading stages of the construction and be communicated to the parties involved (i.e., owner, fabricators, contractors, and erector) in construction of skewed bridges. In the case of erected fit, the layovers appear after casting of the deck. In the case of final fit, the layovers appear at the SDL stage after attaching the cross-frames to girders.

Layovers along the length of Girder 1 of Bridge A are obtained from 3D FEM analysis for different detailing methods at different loading stages of construction, as shown in Figure 2.7. The following observations can be noted by inspecting the data presented in Figure 2.7:

For the final fit detailing method,

- Layovers are zero at the TDL stage because for the final fit detailing method cross-frames are fabricated to fit between the girders and there is no lack-of-fit between the cross-frames and girders.
- Layovers are NOT zero at the SDL stage because for the final fit detailing method cross-frame do not fit between the girders at the SDL stage.

The reverse is true for the erected fit detailing method. In addition, the layovers for the final fit at the SDL stage are equal and opposite to the layovers for the erected fit at the TDL stage. Similar observations were observed for other bridges analyzed as part of this study.

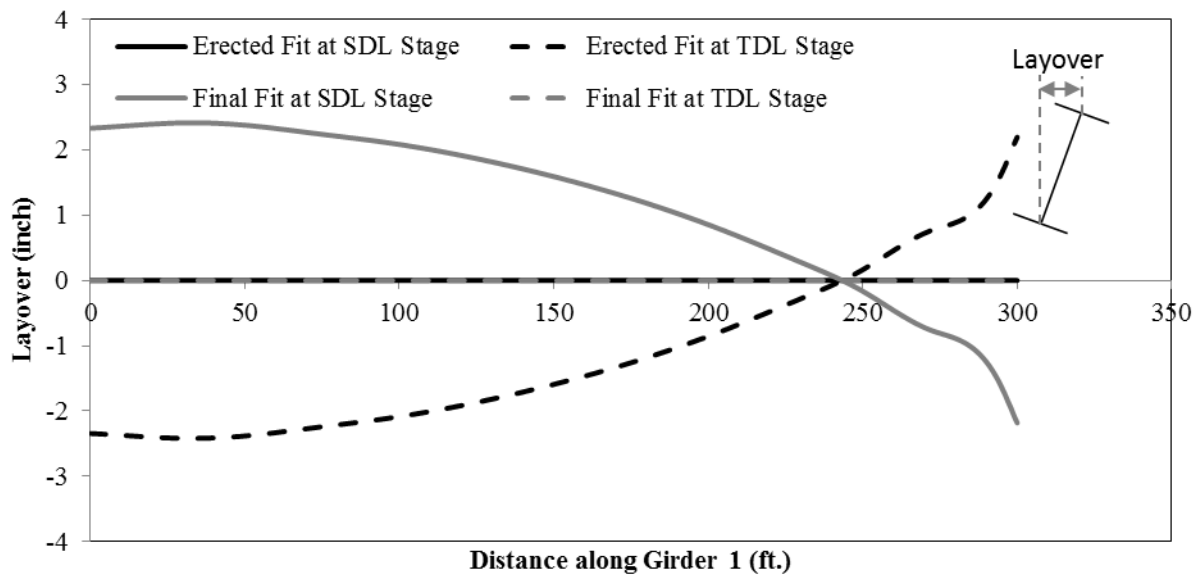


**Figure 2.7: Layovers in Girder 1 of Bridge A for different detailing methods at different loading stages of construction**

### 2.4.3 Deflections

In straight skew I-girder bridges, the deflections of the girders are affected by the lack-of-fit of the cross-frames between girders. These lack-of-fit deflections might be temporary or permanent depending on the method of detailing. Therefore, it is important to calculate the deflection using the correct method of analysis and camber the girders accordingly.

The deflections for Bridge A are obtained from the 3D FEM analysis for different detailing methods at different loading stages of construction, as shown in Figure 2.8. The following observations could be noticed by inspecting data presented in Figure 2.8:

- For the final fit detailing method, deflection is not affected by lack-of-fit at the TDL stage and can be estimated by line girder analysis.
- The deflections are affected by lack-of-fit for the final fit detailing method at the SDL stage.

The reverse is true for the erected fit detailing method

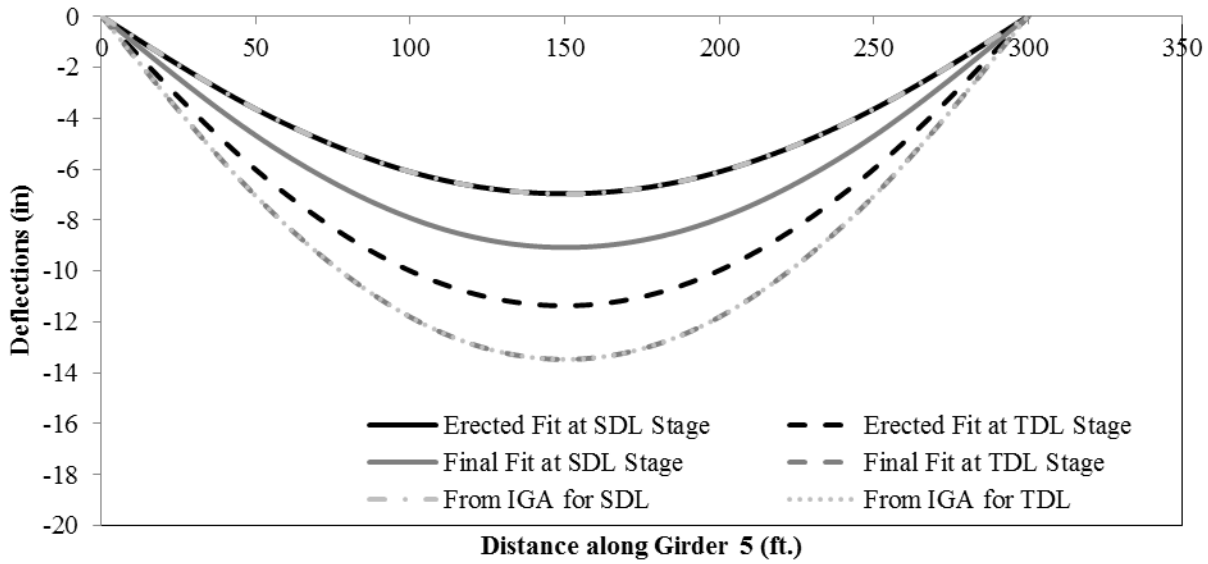


**Figure 2.8: Deflection in Girder 5 of Bridge A for different detailing methods at different loading stages of construction**

Deflections at a particular loading stage consists of two components as shown by the following equation

$$\text{Deflection} = D_{Y1} + D_{Y2} \tag{Eq. (2.1)}$$

$D_{Y1}$  is the component of deflection from dead load and can be estimated from isolated girder analysis (IGA) without attaching the cross-frames

$D_{Y2}$  is the component of deflection due to lack-of-fit and can be estimated by rearranging Eq. (2.1) as follows

$$D_{Y2} = \text{Deflection} - D_{Y1}$$

The component of deflection due to lack-of-fit ( $D_{Y2}$ ) was obtained for different detailing methods at different loading stages and plotted in Figure 2.9.

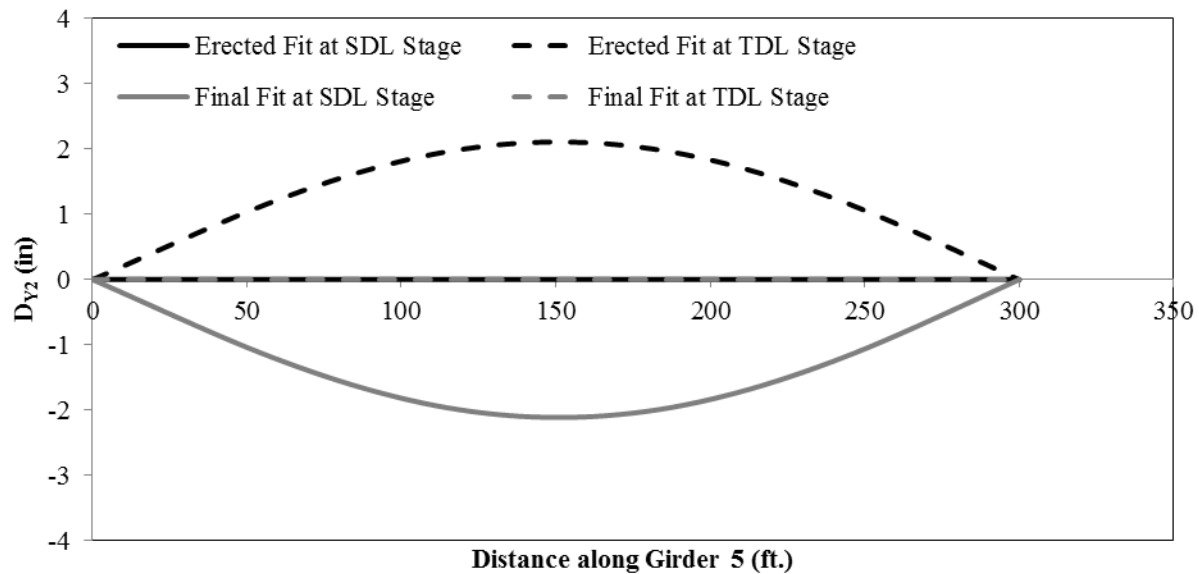


**Figure 2.9: Component of deflection due lack-of-fit in Girder 5 of Bridge A for different detailing methods at different loading stages of construction**

The following observations could be noticed by inspecting the data presented in Figure 2.9:

- For the final fit detailing method,
  - $D_{Y2}$  is zero at the TDL stage because for the final fit detailing method cross-frames are fabricated to fit between the girders and there is no lack-of-fit between the cross-frames and girders
  - $D_{Y2}$  is NOT zero at the SDL stage because for the final fit detailing method cross-frame do not fit between the girders at the SDL stage.

For the erected fit detailing method, the reverse is true. Also notice that  $D_{Y2}$  for the final fit at the SDL stage is equal and opposite to  $D_{Y2}$  for the erected fit at the TDL stage. Similar observations were made for other bridges analyzed as part of this study.

#### 2.4.4 Reactions

In straight skew I-girder bridges, the girders can have negative reactions resulting in lifting of girders from support after the erection is complete or after the casting of concrete deck, depending on the detailing method used. Therefore it is important to check reactions for straight skew bridges in order to know the chances of lift up.

The reactions for Bridge A are obtained from the 3D FEM analysis for different detailing methods at different loading stages of construction as shown in Figure 2.10. The following observations could be noticed by inspecting data presented in Figure 2.10:

- For the final fit detailing method, distribution of reactions is not affected by lack-of-fit at the TDL stage. This is because for the final fit detailing method cross-frame are fabricated to fit between the girders at the TDL stage. These reactions can be estimated by line girder analysis.
- The distribution of reactions is affected by lack-of-fit for the final fit detailing method at the SDL stage.
- For the erected fit detailing method, the cross-frames are fabricated to fit between the girders at the SDL stage and do not fit between the girders at the TDL stage. Due this lack-of-fit for the erected fit detailing method at the TDL stage, additional reactions are generated that change the distribution of the reactions at this stage.
- Similarly, for the erected fit detailing method at the SDL stage reactions are not affected by lack-of-fit and can be estimated by line girder analysis.

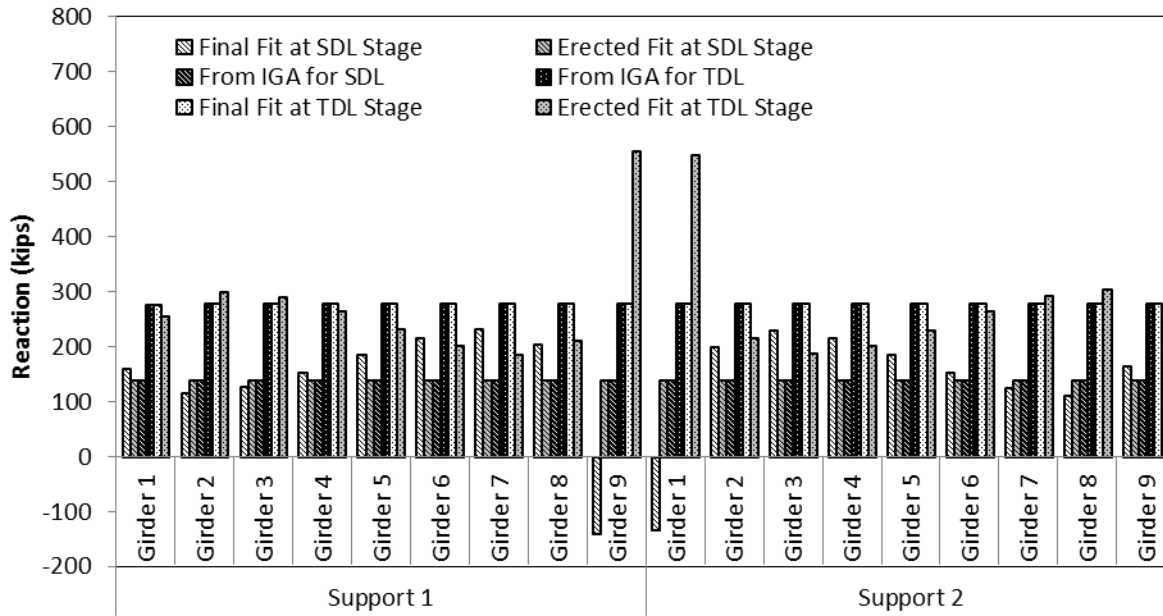


**Figure 2.10: Reactions of Bridge A for different detailing methods at different loading stages of construction**

For Bridge A negative reactions can be seen at obtuse corners of the bridge (Support 1 of Girder 9 and Support 2 of Girder 1) for the final fit detailing method at the SDL stage. However, the SDL stage is a transient stage in construction of skew bridges therefore; such negative reactions causing the girder to lift up from the support are temporary and are not problematic. The girders will be seated on the supports once concrete deck is placed, as shown in Figure 2.10 for the final fit detailing method at the TDL stage—all the reactions are positive and uniform. Therefore, one only need check for uplift at the TDL stage when the erected fit detailing method is used, since any negative reaction at the TDL stage will be permanent.

Reactions at a particular loading stage consists of two components as shown by the following equation

$$\text{Reaction} = R_{Y1} + R_{Y2}$$

Eq. (2.2)

$R_{Y1}$  is component of reaction from dead load and can be estimated from IGA without attaching the cross-frames.

$R_{Y2}$  is the component of reaction due to lack-of-fit and can be estimated by rearranging Eq. (2.2) as follows

$$R_{Y2} = \text{Reaction} - R_{Y1}$$

The component of reaction due to lack-of-fit ( $R_{Y1}$ ) was obtained for different detailing methods at different loading stages and plotted in Figure 2.11.

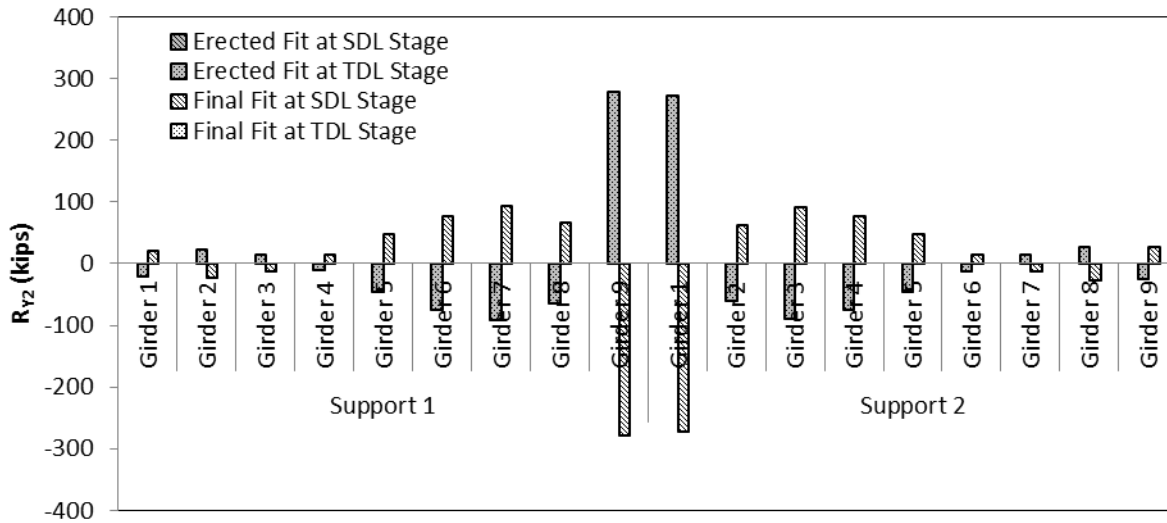


**Figure 2.11: Component of reaction due to lack-of-fit ( $R_{Y2}$ ) for Bridge A for different detailing methods at different loading stages of construction**

Following observations could be noticed by inspecting data presented in Figure 2.11:

- For the final fit detailing method,
  - o  $R_{Y2}$  is zero at the TDL stage because for the final fit detailing method cross-frames are fabricated to fit between the girders and there is no lack-of-fit between the cross-frames and girders
  - o  $R_{Y2}$  is NOT zero at the SDL stage because for the final fit detailing method cross-frame do not fit between the girders at the SDL stage.

The reverse is true for the erected fit detailing method. Also notice that  $R_{Y2}$  for the final fit at the SDL stage is equal and opposite to  $R_{Y2}$  for the erected fit at the TDL stage. Similar observations were observed for other bridges analyzed as part of this study.

#### 2.4.5 Flange Lateral Bending Stress ( $f_l$ )

Flange lateral bending stress,  $f_l$ , needs to be checked for both erected fit and final fit detailing method in order to meet the AASHTO requirements.

The  $f_l$  in girders of Bridge A was obtained from the 3D FEM analysis for different detailing methods at different loading stages of construction and is shown in Figure 2.12. The following observations can be noted by inspecting the data presented in Figure 2.12:

- For the final fit detailing method,  $f_l$  is close to zero at the TDL stage. This is because for the final fit detailing method, the cross-frames are fabricated to fit between the girders at the TDL stage. Therefore, these cross-frames do not apply any lateral load on girders at the TDL stage. The lateral loads applied by the cross-frames to the flanges due to lack-of-fit at the SDL stage are the main reason for  $f_l$  in skewed bridge.
- At the SDL stage,  $f_l$  generally will have a significant magnitude when final fit detailing is used.
- For the erected fit detailing method, the cross-frames are fabricated to fit between the girders at the SDL stage and do not fit between the girders at the TDL stage. Therefore the corresponding cross-frame forces act on the bridge girders at the TDL stage and result in  $f_l$  at the TDL stage.
- At the SDL stage,  $f_l$  is close to zero for the erected fit detailing method.
- It can be noted that  $f_l$  for the erected fit detailing method at the TDL stage is almost equal and opposite to the  $f_l$  for the final fit detailing method at the SDL stage.

Similar observations were made for other bridges analyzed as part of this study.

Flange major axis bending stress,  $f_b$ , is higher at the TDL stage compared to  $f_b$  at the SDL stage for both of the detailing methods. The  $f_l$  for the final fit detailing method can be less critical compared to  $f_l$  for the erected fit detailing method as it appears when  $f_b$  is relatively low. However, if wind loads are significant then  $f_l$  final fit detailing method can be more critical compared to  $f_l$  for the erected fit detailing method.

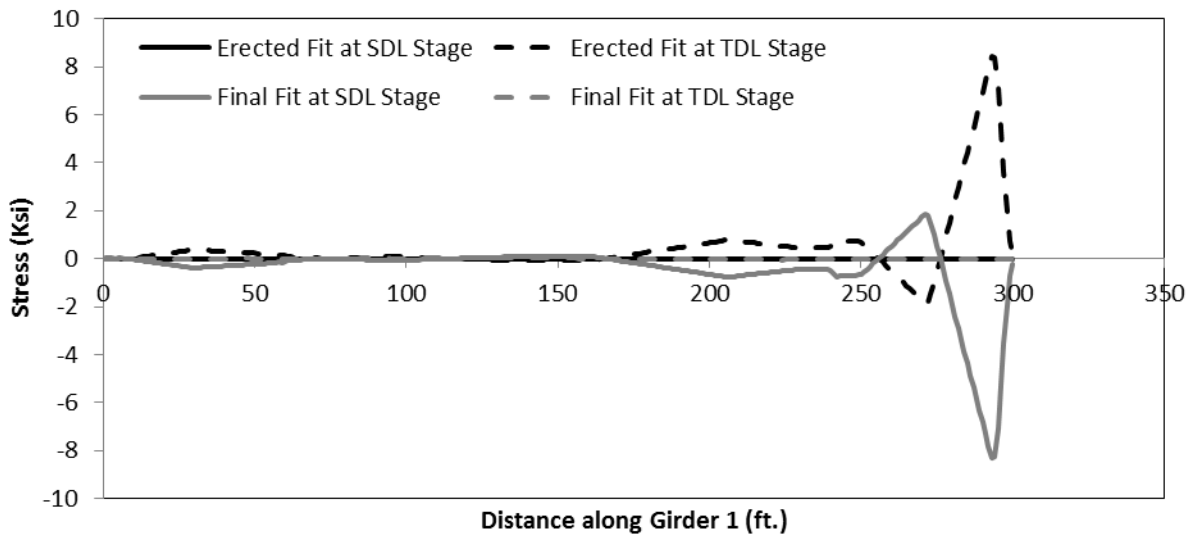


**Figure 2.12: Flange lateral bending stress in top flange of Girder 1 of Bridge A for different detailing methods at different loading stages of construction**

#### 2.4.6 Cross-frame Forces

In general the cross-frame forces for the erected fit at the TDL stage are equal and opposite to the cross-frame forces for the final fit at the SDL stage. It should be noted that skewed steel bridges have been constructed successfully for many years, and to the authors' knowledge there have been no reported field problems with cross-frame forces.

Forces in top chord members of cross-frames in Bay 7 of Bridge A are obtained from the 3D FEM analysis for different detailing methods at different loading stages of construction as shown in Figure 2.13. The following observations can be noted by inspecting the data presented in Figure 2.13:

- For the final fit detailing method, cross-frame forces are very small at the TDL stage. This behavior is because of the fact that for the final fit detailing method, the cross-frames are fabricated to fit between the girders at the TDL stage. Therefore these cross-frames do not develop forces.
- For the erected fit detailing method, cross-frames are fabricated to fit between the girders at the SDL stage and do not fit between the girders at the TDL stage. Therefore, these cross-frames develop significant forces at the TDL stage.

- At the SDL stage, the cross-frame forces are zero for the erected fit detailing method and are significant for the final fit detailing method.

Similar observations were made for other bridges analyzed as part of this study.

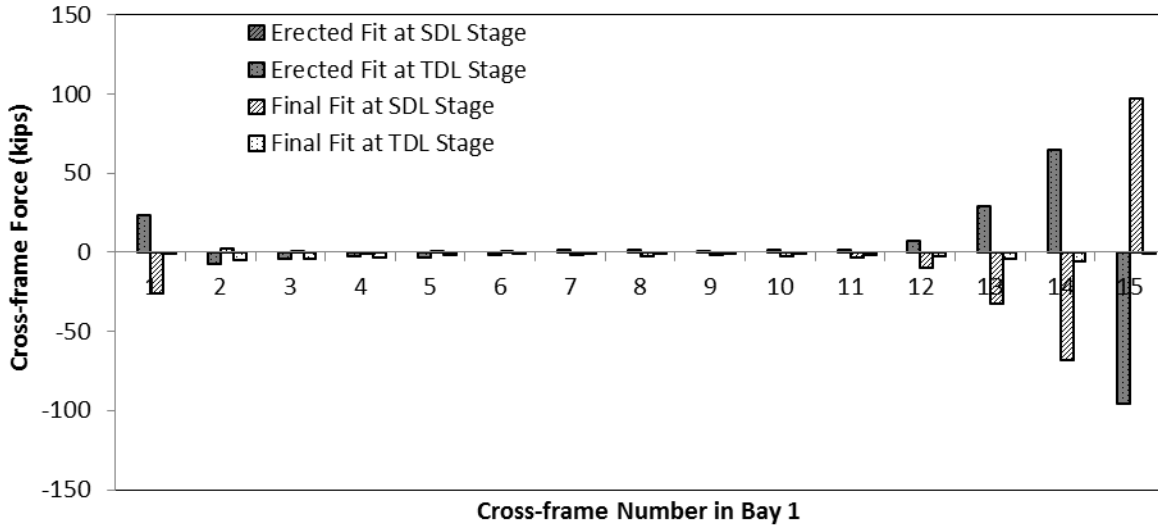


**Figure 2.13: Cross-frame forces in top chord of cross-frames in Bay 7 of Bridge A for different detailing methods at different loading stages of construction**

## 2.5 Discussion of the Results

The comparison of the erected fit and the final fit presented above shows that lack-of-fit effects for the final fit detailing method at the SDL stage are equal and opposite to the lack-of-fit effects for the erected fit detailing method at the TDL stage

This observation can be explained in part by Figure 2.14 assuming in-plane stiffness of cross-frames to be very large compared to torsional stiffness of the girders.

Before explaining the equal and opposite lack-of-fit shown in Figure 2.14, the following two facts are worth noting:

1. Cross-frames for the final fit detailing method are different from cross-frames for the erected fit detailing method. Regardless of these small differences in lengths of cross-frame members in

different detailing methods, the assumption that in-plane stiffness of cross-frames is very large compared to torsional stiffness of the girders stands correct.

2. In a static analysis of the bridge framing under the dead loads, girders with or without attaching cross-frames cannot deflect by lateral torsional buckling.

Keeping the above two facts in mind, Figure 2.14 shows the erected fit and final fit detailing method at different loading stages. For the erected fit detailing method the cross-frames fit between the girders at the SDL stage as shown in Figure 2.14a. However, if the concrete dead load is applied without attaching the cross-frames to one of the girders; the girders get deflected following a line or isolated girder deflections and assume a configuration shown in Figure 2.14b. Notice that the distance between cross-frames and their connection points ( $\Delta$ ) shown in Figure 2.14b is from application of concrete dead load on line or isolated girders. For the final detailing method the cross-frames are detailed to fit between the girders at the TDL stage as shown in Figure 2.14d. However, if the concrete dead load is removed without attaching the cross-frames to one of the girders, the girders get deflected following a line or isolated girder deflections and assume a configuration shown in Figure 2.14c. Notice that the distance between cross-frames and their connection points ( $\Delta$ ) shown in Figure 2.14c is from removal of concrete dead load on line or isolated girders.

Since for both the erected fit and final fit  $\Delta$  is from line or isolated girder analysis, it can be stated that  $\Delta$  at the TDL for the erected fit detailing method is equal and opposite to  $\Delta$  at the SDL stage for the final fit detailing method.

Lack-of-fit effects appear for the erected fit detailing at the TDL stage and final fit detailing method at the SDL stage only when the cross-frames are connected to the girders. Given the equal and opposite distances between cross-frames and their connection points for these detailing methods at these loading stages, the lack-of-fit effects are equal and opposite for these detailing methods at these loading stages.

It is important to note that the lack-of-fit effects also include a component of vertical deflection. For example if the concrete dead load is applied to girders after attaching the cross-frames, detailed with erected fit, the deflection of girders include a component from the lack-of-fit. Therefore, these deflections should not be used to simulate lack-of-fit effects for the final fit detailing method. Using these deflections to simulate lack-of-fit effects in final fit detailing method shall be equivalent to

considering the lack-of-fit effect twice in the final fit detailing method and shall result in erroneous responses shown in [2, 3, 4] for the final fit detailing method.

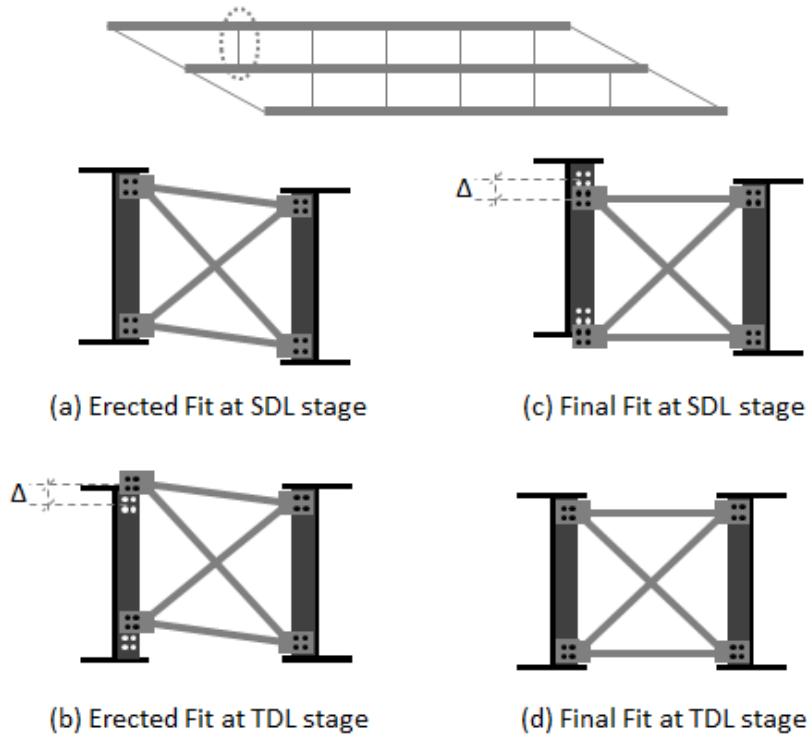


**Figure 2.14: Equal and opposite lack-of-fit**

## 2.6 Summary and Conclusions

This chapter provides summary of structural responses affected by different detailing methods in skewed and straight steel girder bridges. Included are simple terminologies that are bound to reduce the miss communications that is present between owner, designer, fabricator, erector and contractor. Two detailing methods, erected and final fit are used.

The main conclusion of this chapter is that lack-of-fit effects for the final fit detailing method at the SDL stage are equal and opposite to the lack-of-fit effects for the erected fit detailing method at the TDL stage.

This chapter uses 3D FEM analysis for calculating lack-of-fit effects. The 3D FEM analysis is generally avoided in the design office and therefore simplified analysis are required to develop the design provisions. Next chapter discuss the capability of simplified analyses to estimate lack-of-fit effects.

## **Chapter 3      METHODS OF ANALYSIS FOR DIFFERENT DETAILING METHODS**

Different methods of analysis that are commonly used for steel bridges with skewed supports include improved 2D grid analysis (GA), traditional 2D GA and 3D FEM analysis [2, 3, 4, 7, 8]. Currently, 2D GA can be used for the erected fit detailing method only, and a 3D FEM analysis with initial strains in the cross-frames is required for the final fit detailing method.

The objective of this chapter is to introduce different methods that can be used to calculate lack-of-fit effect for the erected fit detailing method at the TDL stage and final fit detailing method at the SDL stage. Comparison of different methods was done to recommend a single simplified method of analysis that can be used to calculate lack-of-fit effect for both erected fit and final fit detailing method with reasonable accuracy.

### **3.1 Erected Fit Detailing Method**

#### **3.1.1 Methods of Analysis**

Before discussing different structural responses of skewed steel girder bridges, it is important to discuss different methods of analysis that are used for calculation of these responses. These methods of analysis are discussed at length in NCHRP 725 [4]. A brief summary of these methods is provided here.

##### ***3.1.1.1 1D Line Girder Analysis***

In 1D line girder analysis (LGA) the girders are analyzed as line elements without any cross-frame attached to them. 1D LGA mentioned in this chapter refers to a line elements model of the bridge girders only.

##### ***3.1.1.2 2D Grid Analysis***

2D Grid Analysis (GA) mentioned in this chapter refers to a modeling technique in which each node has 6 degrees of freedom (3 translations and 3 rotations) but entire structural model of the bridge is in a single horizontal plane. This chapter uses two types of 2D GA, simplified methods that are used by some commercial programs, hereafter referred to as traditional 2D GA, and an improved 2D GA recommended in [4].

The torsional stiffness of the girders is estimated by the St. Venant term using the torsional constant ( $J$ ) in traditional 2D-grid analysis. In the improved 2D grid analysis, the torsional stiffness of the girder was modeled by using an equivalent torsional constant ( $J_{eq}$ ) that takes into account both the St. Venant and warping terms in the calculation of the torsional stiffness. A detailed expression for obtaining  $J_{eq}$  for I-sections is given in the literature [11] and presented here in Eqs. (3.1) and (3.2). Eq. (3.1) is based upon the assumption that both ends of the unbraced length,  $L_b$  are fixed, while Eq. (3.2) is based upon the assumption that one end of the unbraced length is fixed and the other is pinned.

$$J_{eq(fx-fx)} = J \left[ 1 - \frac{\sinh(pL_b)}{pL_b} + \frac{[\cosh(pL_b) - 1]^2}{pL_b \sinh(pL_b)} \right]^{-1} \quad (3.1)$$

$$J_{eq(fx-fx)} = J \left[ 1 - \frac{\sinh(pL_b)}{pL_b \cosh(pL_b)} \right]^{-1} \quad (3.2)$$

Where

$$p = \sqrt{\frac{GJ}{EC_w}}$$

$G$  is the modulus of rigidity and can be approximated by  $G = \frac{E}{2(1+\nu)}$ ,  $E$  is modulus of elasticity,  $\nu$  is

Poisson's ratio, and  $C_w$  is the warping constant.

Cross-frames are modeled using a beam element with a moment of inertia ( $I_{eq}$ ) that matches the flexural stiffness of the truss representation of the cross-frame. The beam also has a cross section area ( $A_{eq}$ ) that

matches the axial stiffness of the cross-frame system. The traditional 2D GA uses the Euler Bernoulli beam stiffness matrix whereas the improved 2D GA employed here uses an equivalent beam stiffness that matches the stiffness of a truss idealization of the cross-frames exactly within their plane. Detailed derivations and expressions for these stiffness matrices are provided in [3] and [4].

It should be noted that in the erected fit detailing method the lack-of-fit effects such as layovers, component of deflection due to lack-of-fit, cross-frame forces, component of reactions due to lack-of-fit, and flange lateral bending stress due to skew effects are of interest after placement of the wet concrete. Therefore, in order to carry out an erected fit analysis using the 2D GA, a complete model of the structure was constructed with cross-frames attached to the girders followed by activating the concrete dead load.

### ***3.1.1.3 3D FEM Analysis***

During conduct of research, numerous three-dimensional modeling was carried out using ANSYS [10]. Three-dimensional Finite Element Analysis (3D FEM) can be used with different levels of modeling techniques. For example, in a 3D FEM the flanges can be modeled using either beam elements or shell elements with or without bearing pads. 3D FEM analyses carried out as a part of NCHRP 725 modeled the flanges using beam elements without bearing pads. In this study, flanges are modeled using shell elements with a bearing pad model. The bearing pads were modeled with solid element of ANSYS [10] using an equivalent modulus of elasticity of 10 ksi.

3D FEM analysis for the erected fit detailing method can be accomplished by following the same steps used for 2D grid method of analysis.

### **3.1.2 Comparison of Different Methods of Analysis**

Different methods of analysis discussed in the above sections are used to evaluate lack-of-fit effects for the erected fit detailing method at the TDL stage. These lack-of-fit effects include, layovers, component of deflection due to lack-of-fit, component of reaction due to lack-of-fit, flange lateral bending stress, and cross-frame forces. In the following sections each lack-of-fit effect was obtained from different methods of analysis and compared to recommend a method of analysis for calculating the lack-of-fit effects.

### 3.1.2.1 Layovers

Layovers obtained from different methods of analysis, are compared for Bridge A in Figure 3.1 and for 'Bridge B' in Figure 3.2 for the erected fit detailing method at the TDL stage. For Bridge A traditional 2D grid analysis (2D GA Trd) does not give a good estimate of the layovers. The difference between the layovers obtained from different methods of analysis, was not significant for Bridge B.

It is recommended that the layovers should be calculated using the improved 2D-grid analysis (2D GA Imp) rather than the traditional 2D-grid method, since the improved method gives better estimates of the all responses both for contiguous cross-frame and staggered cross-frames.

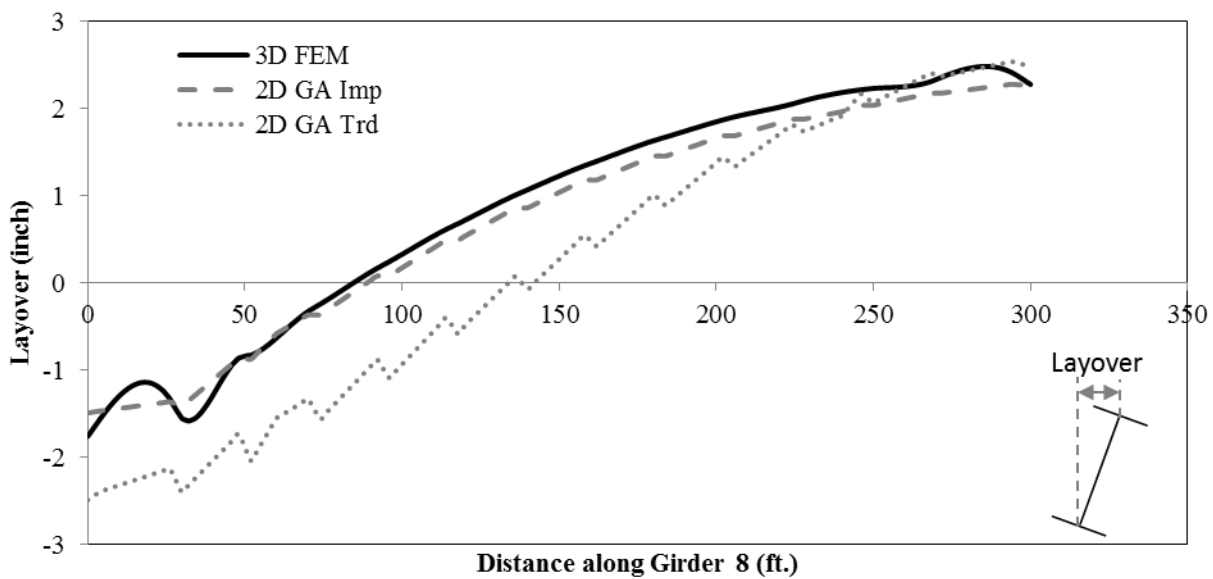


**Figure 3.1: Comparison of layovers calculated by different analysis method for Girder 8 of Bridge A**

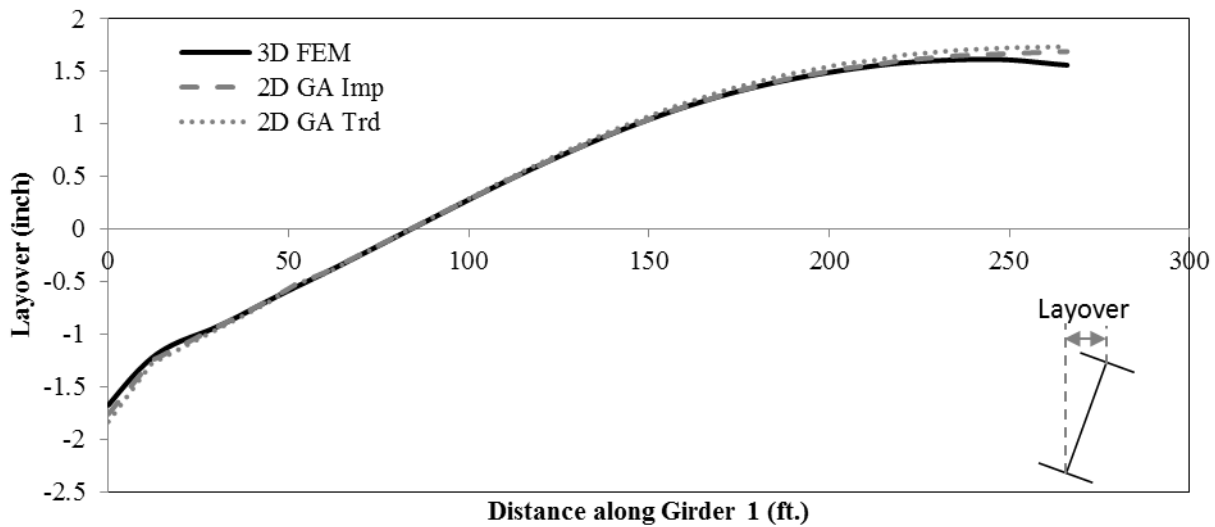


**Figure 3.2: Comparison of layovers calculated by different analysis method for Girder 8 of Bridge B**

Traditional 2D grid analysis method gives poor estimates of layovers for Bridge A and good estimates of layovers for Bridge B. This was also true for other structural responses such as reactions and cross-frame forces except for flange lateral bending stress,  $f_l$ . This is because of the staggered framing used in Bridge A, compared to straight framing used in Bridge B.

In staggered framing, a cross-frame connects only two girders, and forces in the cross-frames in the adjacent bays have to be transferred through the girders compared to contiguous framing in which forces can be directly transferred from cross-frames in adjacent bays. Therefore in staggered framing, lack-of-fit effects are dependent on the torsional stiffness of the independent girders. And since traditional 2D grid analysis method does not model the torsional stiffness of the independent girders, therefore, in staggered framing case (Bridge A), the lack-of-fit effects are not estimated correctly by traditional 2D grid analysis.

In contiguous framing, cross-frames are contiguous and can directly transfer the forces in the adjacent bays among each other without relying on torsional stiffness of the girders. Therefore lack-of-fit effects (except for flange lateral bending stress,  $f_l$ ) are not affected by torsional stiffness of the independent girders.

### 3.1.2.2 Component of Deflections due to Lack-of-fit

Deflections at a particular loading stage consists of two components as shown by the following equation

$$\text{Deflection} = D_{Y1} + D_{Y2} \quad (3)$$

$D_{Y1}$  is component of deflection from dead load and can be estimated from Line Girder Analysis (LGA) or an isolated girder analysis without attaching the cross-frames

$D_{Y2}$  is component of deflection due to lack-of-fit and can be estimated by rearranging Eq. (3) as follows

$$D_{Y2} = \text{Deflection} - D_{Y1}$$

Component of deflection due to lack-of-fit ( $D_{Y2}$ ) for the erected fit detailing method appears at the TDL stage. Generally  $D_{Y2}$  is highest in the interior girders and lowest in the fascia girders.  $D_{Y2}$  was obtained from different methods of analysis, are compared for Bridge A in Figure 3.3 and for 'Bridge B' in Figure 3.4 for the erected fit detailing method at the TDL stage.

For Bridge A traditional 2D grid analysis (2D GA Trd) does not give a good estimate of  $D_{Y2}$ . The difference between  $D_{Y2}$  obtained from different methods of analysis, was not significant for Bridge B. Improved 2D grid analysis (2D GA Imp) tends to give higher estimates of  $D_{Y2}$  for both bridges.

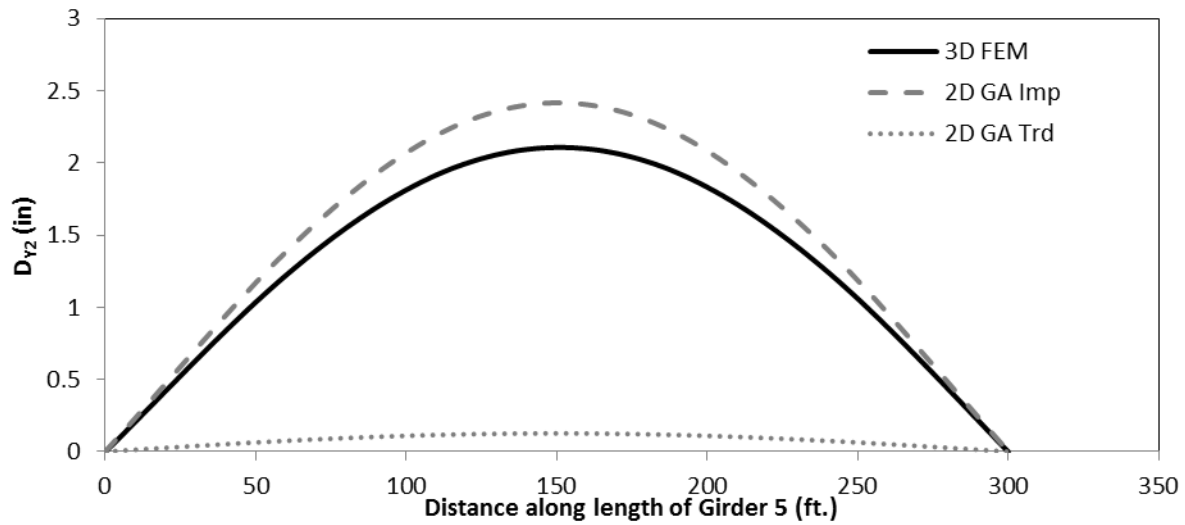


**Figure 3.3: Comparison of  $D_{Y2}$  calculated by different analysis method for Bridge A for erected fit at the TDL stage**

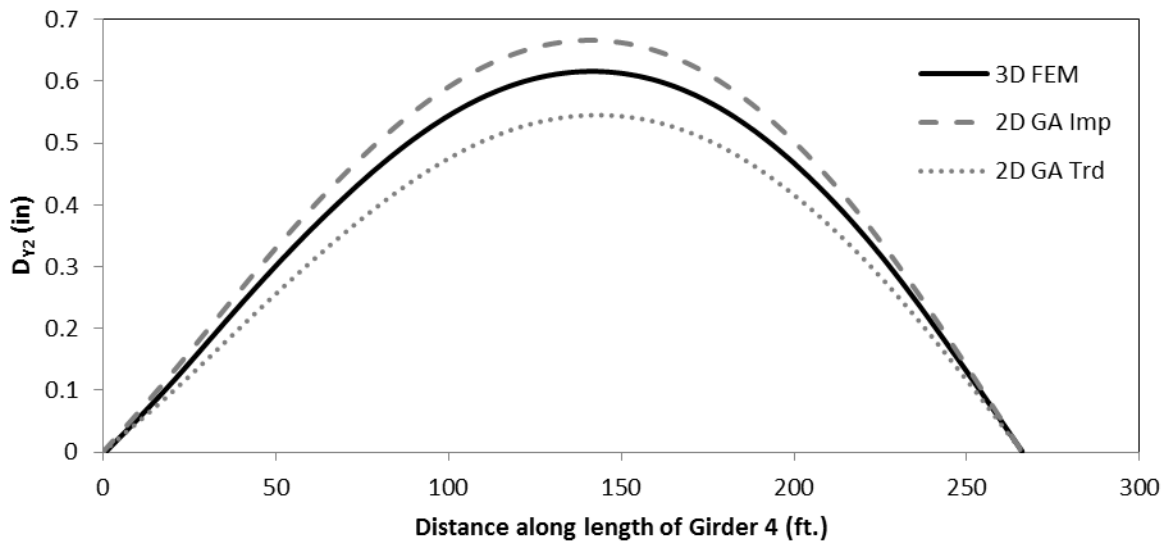


**Figure 3.4: Comparison of  $D_{Y2}$  calculated by different analysis method for Bridge B for erected fit at the TDL stage**

### 3.1.2.3 Component of Reactions due to Lack-of-fit

Similar to deflections reactions at a particular loading stage also consists of two components as shown by the following equation

$$\text{Reaction} = R_{Y1} + R_{Y2} \quad (4)$$

$R_{Y1}$  is component of reaction from dead load and can be estimated from Line Girder Analysis (LGA)

$R_{Y2}$  is component of reaction due to lack-of-fit and can be estimated by rearranging Eq. (4) as follows

$$R_{Y2} = \text{Reaction} - R_{Y1}$$

Component of reaction due to lack-of-fit ( $R_{Y2}$ ) for the erected fit detailing method appear at TDL loading stage.

$R_{Y2}$  obtained from different methods of analysis are compared for Bridge A in Figure 3.5 and for 'bridge B' in Figure 3.6 for the erected fit detailing method at the TDL stage.

As expected Traditional 2D grid analysis (2D GA Trd) gives very low estimates of  $R_{Y2}$  for Bridge A and reasonable estimates of  $R_{Y2}$  for Bridge B. Improved 2D grid analysis (2D GA Imp) gives the highest estimates of  $R_{Y2}$ . It can be concluded that the improved 2-D grid analysis is sufficient to calculate  $R_{Y2}$ .

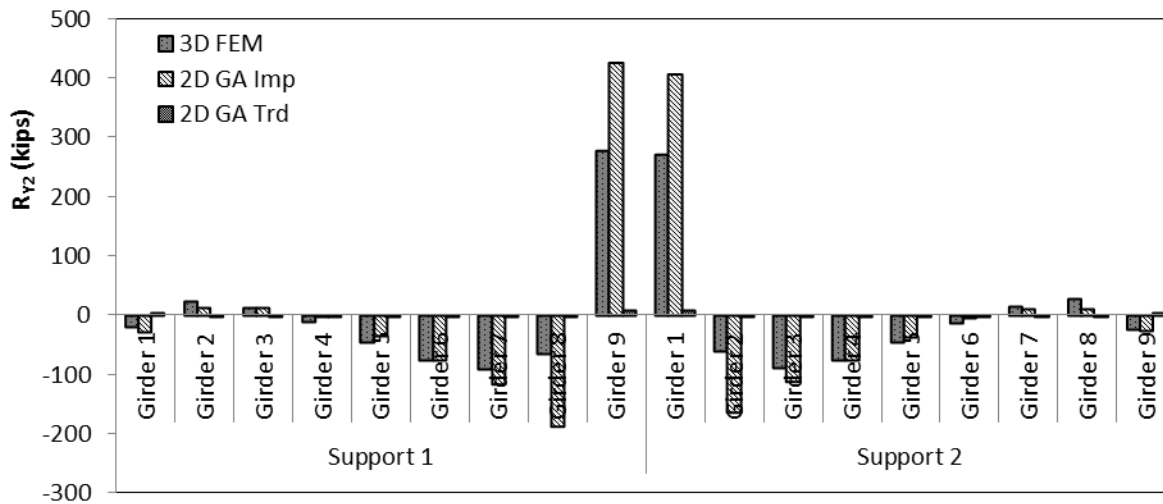


Figure 3.5: Comparison of  $R_{y2}$  calculated by different analysis method for Bridge A for erected fit at the TDL stage

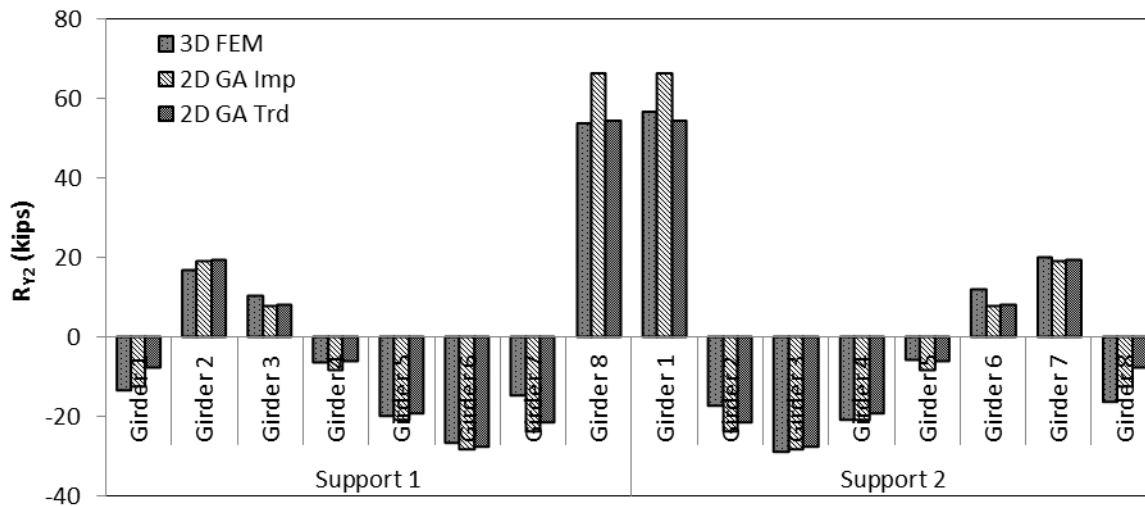


Figure 3.6: Comparison of  $R_{y2}$  calculated by different analysis method for Bridge B for erected fit at the TDL stage

#### 3.1.2.4 Flange Lateral Bending Stress ( $f_l$ )

A procedure to calculate flange lateral stress from 2D grid analysis for the erected fit detailing method has been specified in literature [3] and [4]. A brief summary of the procedure is provided here. The displacements corresponding to concrete dead load from 2D grid analysis are used to calculate forces in cross-frame members. These forces are then resolved into vertical and lateral components at the connection point of cross-frame and girder. Flange is assumed simply supported or fixed ended between the connections adjacent to the connection at which lateral force are obtained. Using lateral bending moment at the location of lateral load of this idealized beam model, lateral stress was calculated using flexural formula.

Flange lateral bending stresses obtained from different methods of analysis are compared for Bridge A in Figure 3.7 and for Bridge B in Figure 3.8 for the erected fit detailing method at the TDL stage. It can be noticed in both Figure 3.7 and Figure 3.8 that  $f_l$  is almost zero for traditional 2D grid analysis—does not include warping term in modeling the torsional stiffness of girders. More appropriate values of  $f_l$  are obtained by modeling the torsional stiffness of the girder correctly i.e. taking into account the warping torsional stiffness that will be there during twist of the girders. This warping torsional stiffness is incorporated into "improved" 2-D grid analysis. Increase in the torsional stiffness of the girder by incorporating the warping stiffness, makes the girder more "stiff". Stiffness attracts more force and therefore flange lateral bending stresses increase. The effect was more pronounced in  $f_l$  than in the deflections since small movement can have large effect in stress.

In improved 2D grid analysis two assumptions can be made for the segment of girder between three consecutive cross-frames for calculation of lateral moment as explained in NCHRP 725 [4]. Assuming simply supported (s-s) boundary condition for the segment gives more value of lateral moment and thereby calculates conservative estimates of  $f_l$  whereas assuming fix-fix boundary condition for the segment gives un-conservative estimates of  $f_l$ . The boundary condition in reality is somewhere between fix-fix and s-s, however such boundary condition was difficult to model. Results of this study indicate that average of  $f_l$  values obtained based on the two assumption constitutes an acceptable approach, which is in agreement with the recommendations of NCHRP 725 [4].

It could be concluded that improved 2-D grid analysis with an average value of  $f_l$  constitute an acceptable approach to approximate  $f_l$ .

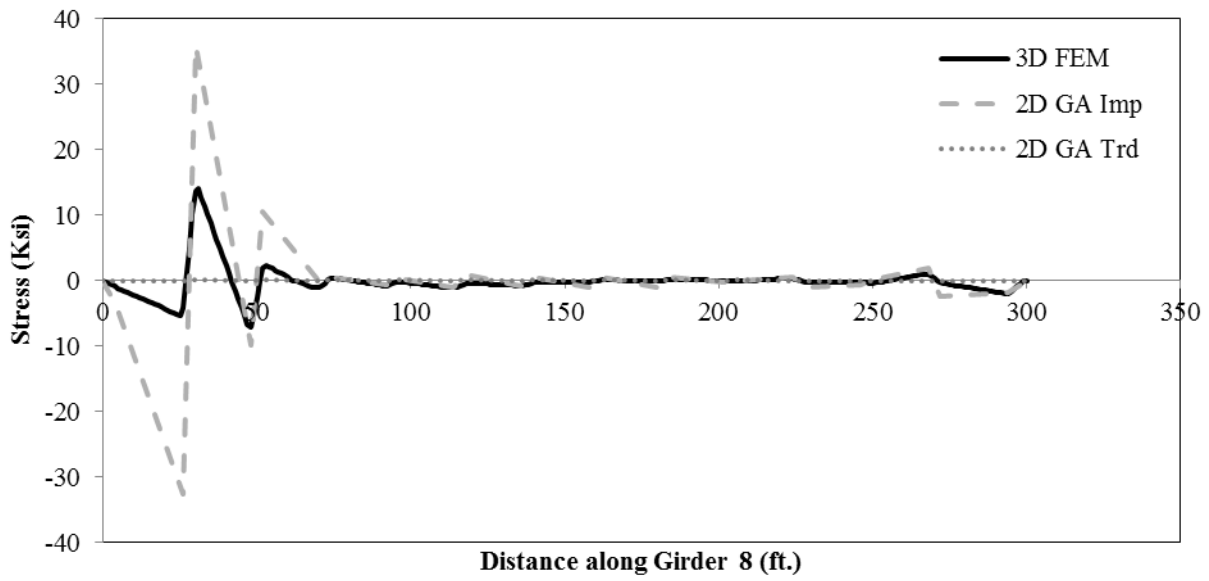


**Figure 3.7: Comparison of flange lateral bending stress calculated by different analysis method in Girder 8 of Bridge A for erected fit at the TDL stage**

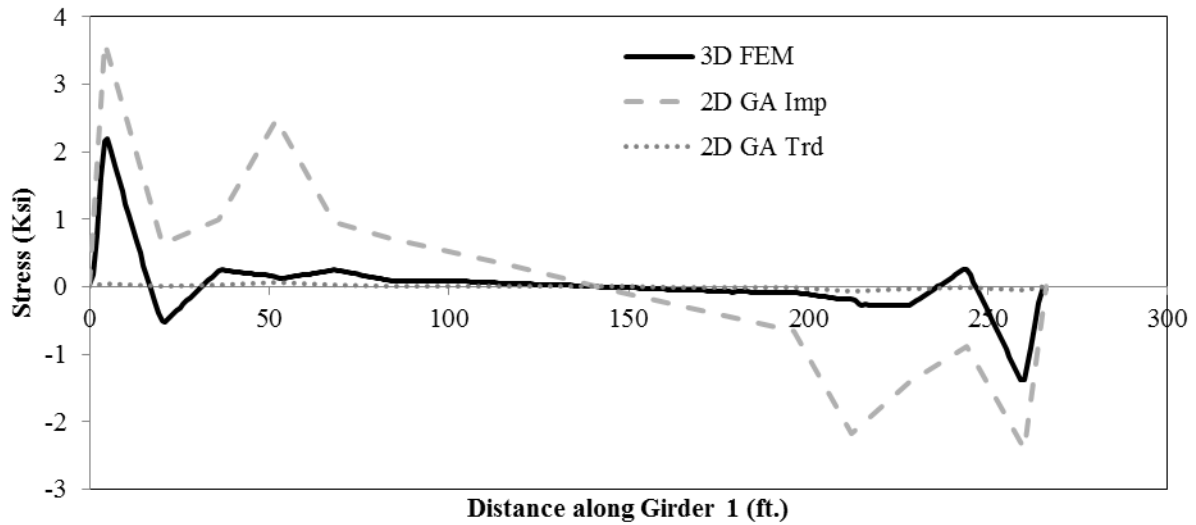


**Figure 3.8: Comparison of flange lateral bending stress calculated by different analysis methods in Girder 4 of Bridge B for erected fit at the TDL stage**

### 3.1.2.5 Cross-frame Forces

Comparison of cross-frame forces obtained from different methods of analysis is done for bridge A in Figure 3.9 and for bridge B in Figure 3.10 for the erected fit detailing method at the TDL stage. It can be observed that the difference between the cross-frame forces obtained from different methods of analysis was significant. Comparison also indicates that the cross-frame forces are highest for improved 2D grid analysis and lowest for 3D finite element analysis with bearing pads for Bridge A. The improved 2D-grid analysis significantly over-estimates the trend in the 3D FEA forces compared to the traditional 2D-grid analysis forces in a few of the bays. The traditional 2D-grid analysis forces are essentially zero, due to the gross underestimation of the girder torsional stiffness in the traditional 2D-grid methods. The difference in the cross-frame forces for Bridge B was not very significant. The results of a broad range of analyses on the different bridges demonstrate that in general the improved 2-D grid analysis is sufficient to calculate the cross-frame forces. The results from the improved 2D-grid analysis are generally accurate to conservative compared to 3D FEA.

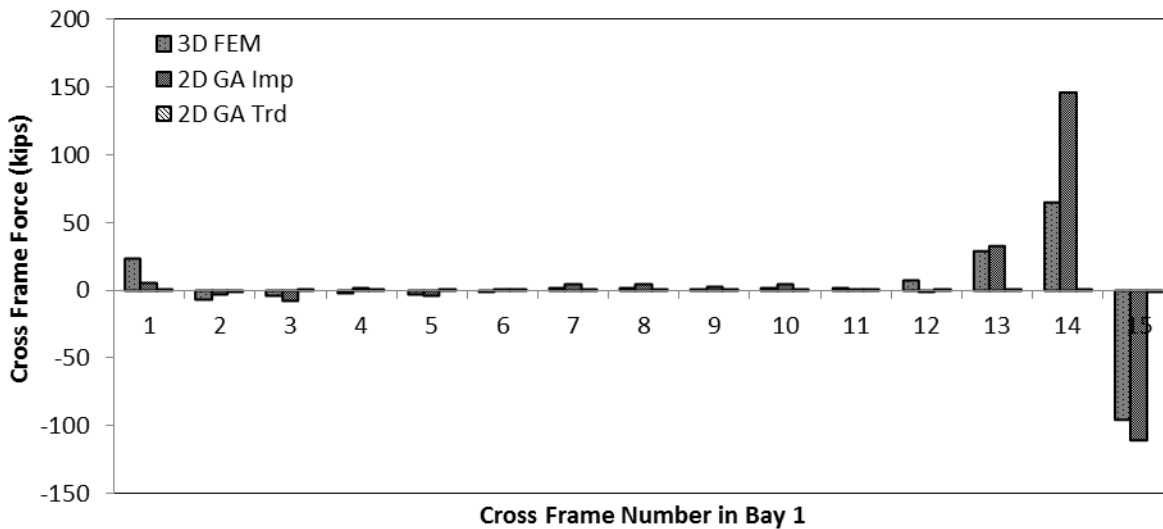


**Figure 3.9: Comparison of cross-frame forces calculated by different analysis method for Bridge A for erected fit at the TDL stage**

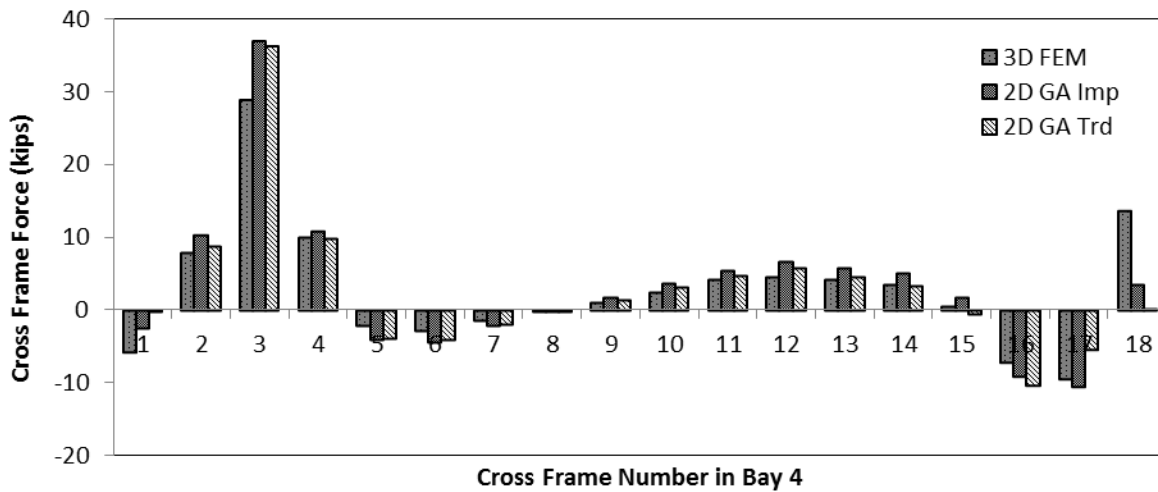


**Figure 3.10: Comparison of cross-frame forces calculated by different analysis method for Bridge B for erected fit at the TDL stage**

## 3.2 Final Fit Detailing Method

### 3.2.1 Methods of Analysis

Different methods analysis can be used to calculate lack-of-fit effects for the final fit detailing method at the SDL stage. These methods are

- Reversing 2D GA results for the erected fit
- 3D FEM using initial strains
- 3D FEM using Dead and Live cross-frames

The following sections shall provide a discussion on each one of them.

#### 3.2.1.1 Reversing 2D GA Results for the Erected Fit

Chapter 2 has shown that the lack-of-fit effects for the final fit detailing method at the SDL stage are equal and opposite to the lack-of-fit effects for the erected fit detailing method at the TDL stage. Lack-of-fit effects for the erected fit detailing method at the TDL stage can be obtained from grid analysis and reversing their sign shall give the lack-of-fit effects for the final fit detailing method at the SDL stage.

### 3.2.1.2 3D FEM Using Initial Strains

In this procedure initial strains are used to model lack-of-fit at the SDL stage for the final fit detailing method.

The configurations of cross-frames and girders to calculate the initial strain are shown in Figure 3.11 for the intermediate cross-frames perpendicular to web in Figure 3.12 for the cross-frame parallel to skew. The configuration 1 represents a real situation in which cross-frames do not fit between the girders at the SDL stage for the final fit detailing method. Configuration 2 represents an imaginary condition in which cross-frames are deformed to make the connections that were not established in the configuration 1. Configuration 2 is an imaginary high energy configuration of the system. Once the system was allowed to establish equilibrium it attains its lowest energy state. After equilibrium was established, the system has real configuration of steel framing after attaching the cross-frame for the final fit detailing method at the SDL stage.

The initial strain,  $\varepsilon_{Initial}$  in any cross-frame member can be calculated by the following formula.

$$\varepsilon_{Initial} = \frac{L_1 - L_2}{L_2}$$

Where,  $L_1$  is length of cross-frame member in configuration 1, and  $L_2$  is length of cross-frame member in configuration 2.

The two configurations of the cross-frames are shown in Figure 3.11, for the cross-frame that are perpendicular to web, and are shown in Figure 3.12, for the cross-frames parallel to skew.

Length of the cross-frame members that are perpendicular to girder web in configuration 1 as shown in Figure 3.11 can be calculated as follows.

$$L_{TC_1} = L_{BC_1} = S$$

$$L_{D1_1} = L_{D2_1} = \sqrt{S^2 + h_b^2}$$

Where  $L_{TC_1}, L_{BC_1}, L_{D1_1}, L_{D2_1}$  are lengths of Top Chord (TC), Bottom Chord (BC), Diagonal 1 (D1) and Diagonal 2 (D2) members of the cross-frame in configuration 1,  $S$  is spacing between the girders, and  $h_b$  is height of bracing.

Similarly length of the cross-frame members that are perpendicular to web in configuration 2 of Figure 3.11 can be calculated as follows.

$$L_{TC_2} = L_{BC_2} = \sqrt{S^2 + \Delta^2}$$

$$L_{D1_2} = \sqrt{S^2 + (h_b - \Delta)^2}$$

$$L_{D2_2} = \sqrt{S^2 + (h_b + \Delta)^2}$$

Where  $L_{TC_2}, L_{BC_2}, L_{D1_2}, L_{D2_2}$  are lengths of Top Chord (TC), Bottom Chord (BC), Diagonal 1 (D1) and Diagonal 2 (D2) members of the cross-frame in configuration 2.

$\Delta$  is the difference in elevation of the girders' section connected by the cross-frame and can be obtained from the concrete dead load camber calculated from line girder analysis (LGA) or isolated girder analysis (IGA). It was worth noting that  $\Delta$  was obtained from the concrete dead load camber calculated from deflection of system of girders and cross-frames attached together in NCHRP 725 [4]. This is wrong way of calculating  $\Delta$  for the final fit detailing method at the SDL stage as explained in chapter 2.

It should be noted that  $\Delta$  is difference in elevation of girders to calculate the initial strains that will simulate lack-of-fit due to concrete dead load and is different from the real value of  $\Delta$  that will exist between the girders at the SDL stage.

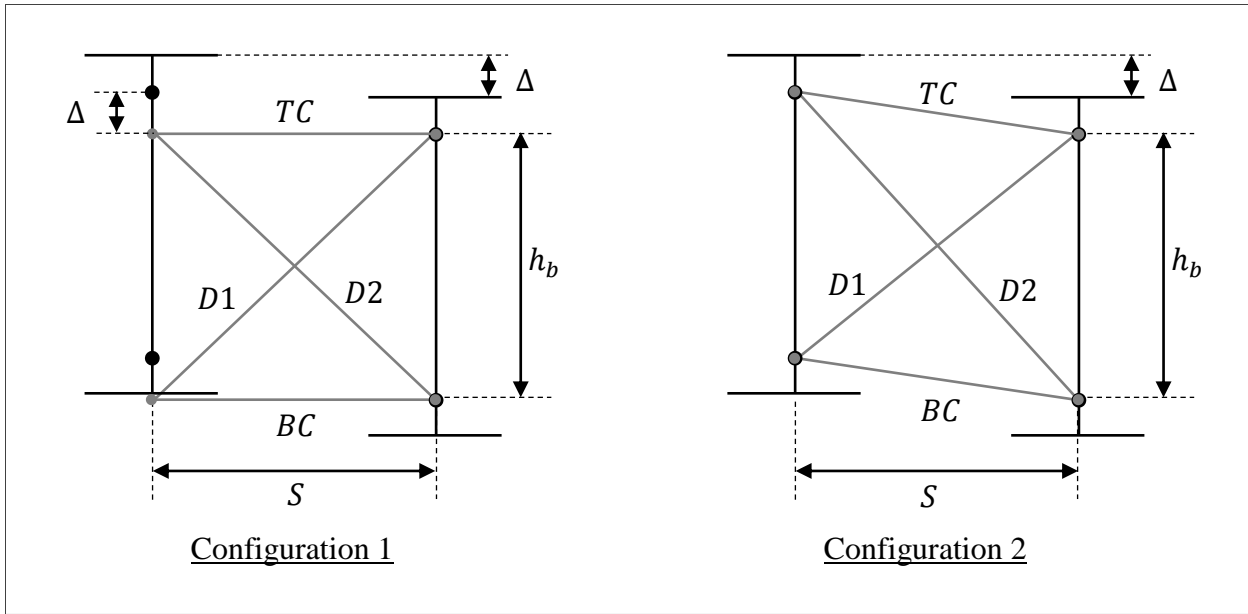


**Figure 3.11: Configurations to calculate initial strain in the cross-frames that are perpendicular to girder web**

Lack-of-fit in the cross-frames that are parallel to the skew supports, occurs due to major axis bending rotation of the girder section as shown in the Figure 3.12. Figure 3.12 illustrate the configuration of the cross-frames parallel to skewed support at the bearing lines, however the intermediate cross-frames parallel to skew shall have the similar configurations. Configuration 1 in Figure 3.12 shows that cross-frame does not fit between the girders due to major axis bending rotation,  $\phi$  of their ends. In configuration 2, the cross-frame is deformed to establish the connections as described previously for the cross-frames perpendicular to the girder web.

Length of the cross-frame members that are parallel to the skew supports in configuration 1 shown in Figure 3.12 can be calculated as follows.

$$L_{TC_1} = L_{BC_1} = \sqrt{\Delta_x^2 + S^2}$$

$$L_{D1_1} = L_{D2_1} = \sqrt{\Delta_x^2 + h_b^2 + S^2}$$

Neglecting the displacement in Y-direction of the connection points and taking  $\sin \theta \cong \theta$  it can be shown that length of the cross-frame members that are parallel to the skew supports in configuration 2 can be determined as follows.

$$L_{TC_2} = L_{BC_2} = \sqrt{\Delta_x^2 + S^2}$$

$$L_{D1_2} = \sqrt{(\Delta_x - \phi \cdot h_b)^2 + h_b^2 + S^2}$$

$$L_{D2_2} = \sqrt{(\Delta_x + \phi \cdot h_b)^2 + h_b^2 + S^2}$$

And

$$\Delta_x = S \times \tan \theta$$

Where,  $\theta$  is the skew angle, and  $\phi$  major axis bending rotation due to concrete dead load at the location of the cross-frame.  $\phi$  is positive (counter clockwise) for the bearing line having Girder 1 at the acute corner and is negative (clockwise) the bearing line having Girder 1 at the obtuse corner.

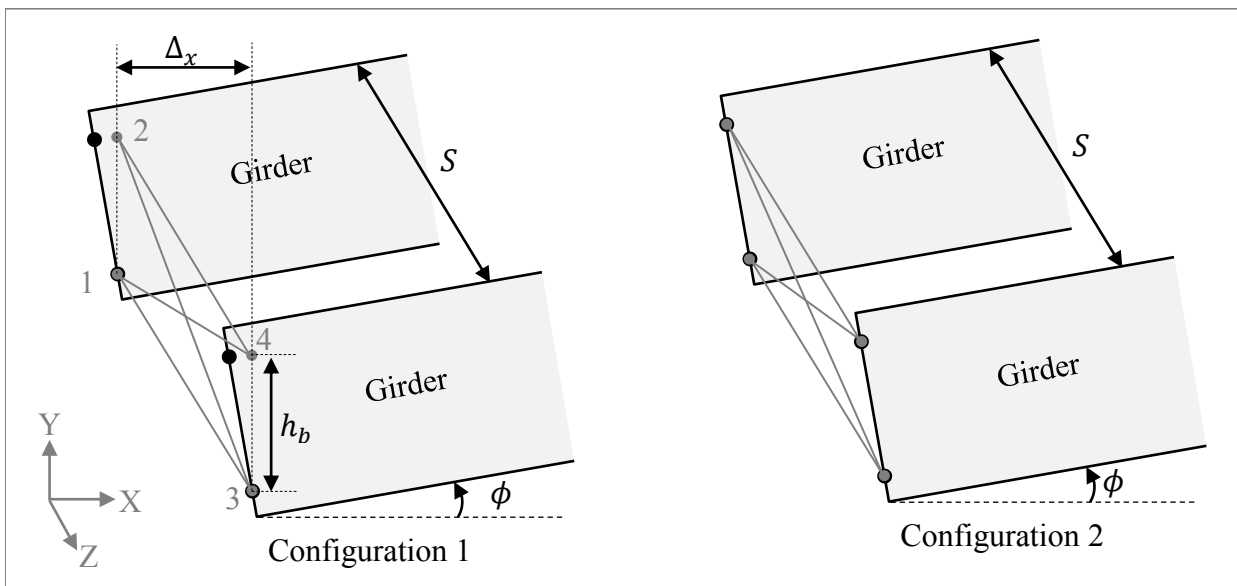


**Figure 3.12: Configurations to calculate initial strain in the cross-frames that are parallel to skew**

In order to get SDL configuration for the final fit detailing method, complete model of the bridge was built with cross-frames attached to the girders. A particular value of initial strain was assigned to each cross-frame member that can be calculated based on location and orientation of the cross-frame and type of the cross-frame member. Once initial strains were assigned to all the cross-frame members, static analysis was run without applying any external load. In the static analysis, the cross-frame members expand or contract depending on the initial strain value and establish equilibrium with the girders. Once equilibrium was established, the steel framing of the bridge achieves its stable lowest possible energy configuration. The geometry of the bridge obtained after the equilibrium was established represents the bridge geometry at the SDL stage for the final fit detailing method.

### ***3.2.1.3 3D FEM Using Dead and Live Cross-frames***

Lack-of-fit at steel dead load (SDL) stage for the final fit detailing method can also be simulated by using Birth and Death option for the cross-frame elements.

In final fit detailing method, cross-frames fit between the girders after application of the concrete dead load. Therefore, in this analysis, concrete dead load was applied to the girders to deflect the girders to a position where cross-frames fit between them. Once the girders were deflected by concrete dead load, the cross-frames were made alive. After that, concrete dead load was removed to get the SDL responses for the final fit detailing method.

It is a two-step FEM analysis after completing the bridge geometry with cross-frames attached.

**Step 1:** All the cross-frame elements were killed (using EKILL command in ANSYS), and concrete dead load was applied as shown in Figure 3.13.

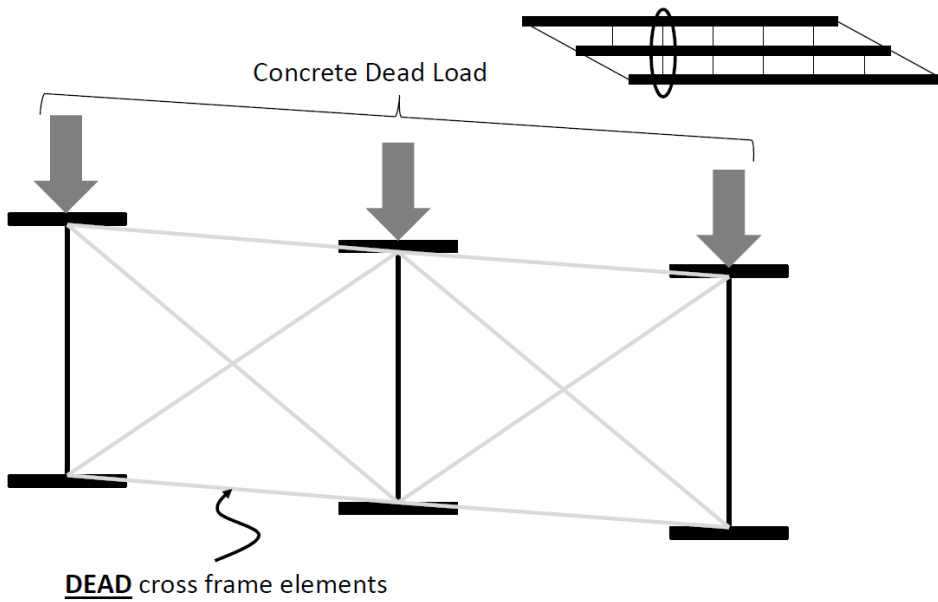


**Figure 3.13: Application of concrete dead load on girders after killing cross-frame elements**

**Step 2:** After the concrete dead load has deflected the girders, all the cross-frame elements were made alive (using EALIVE command in ANSYS), and concrete dead load was removed (made zero) as shown in Figure 3.14.

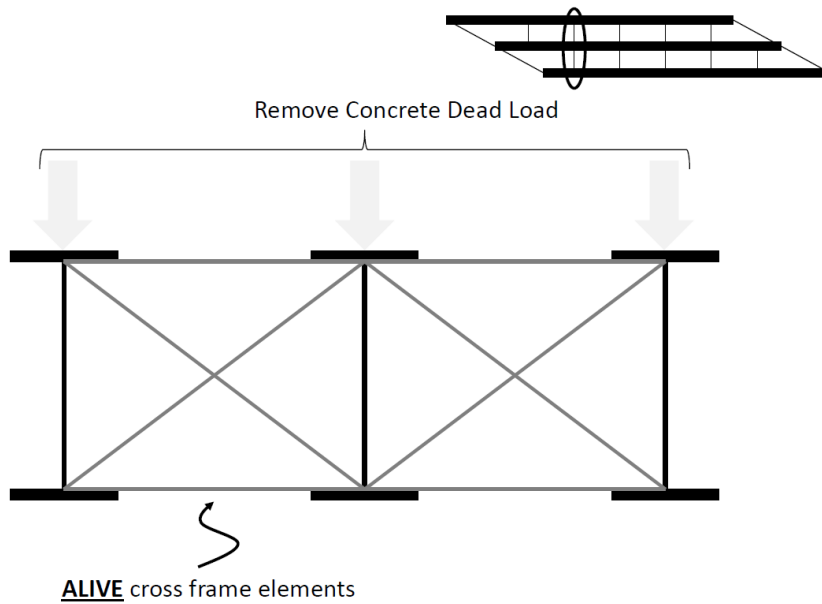


**Figure 3.14: Removal of concrete dead load from girders after making cross-frame elements alive**

At the completion of step 2, SDL configuration of bridge framing was obtained for the final fit detailing method.

It was worth noting that this method does not involve laborious calculation of initial strain for every single cross-frame member and gives the same results as the method of initial strains.

The detailed comparison of different responses obtained from different method of analysis was done in section 4.2.

### 3.2.2 Comparison of Different Methods of Analysis

Different lack-of-fit effect such as layovers, Component of deflection due to lack-of-fit ( $D_{Y2}$ ), Component of reaction due to lack-of-fit ( $R_{Y2}$ ), Flange lateral bending stress ( $f_l$ ), and cross-frame forces are compared for different methods of analysis Figure 3.15 to Figure 3.19 for the final fit detailing method at the SDL stage. 3D FEM analysis using initial strains (3D FEM Initial Strains) and 3D FEM analysis using dead and live cross-frame element (3D FEM Dead & Live) gives almost the same estimates of different lack-of-fit effect for Bridge A and Bridge B. Reasonable estimates of lack-of-fit effects are obtained by reversing improved 2D grid analysis (2D GA reversed) for both bridges.

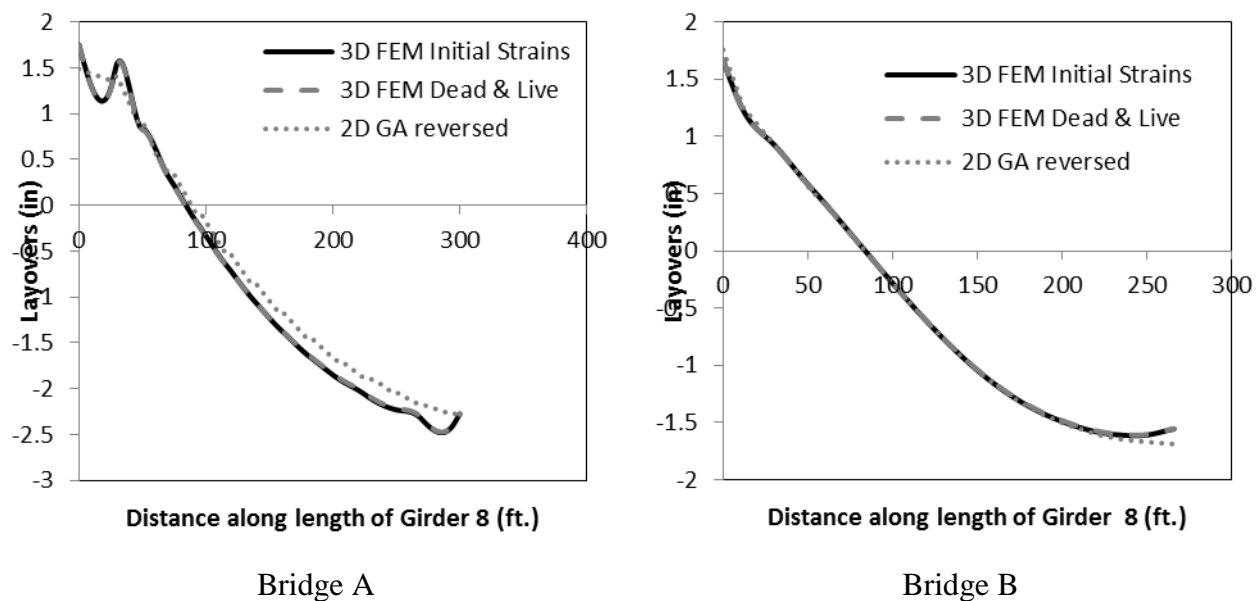
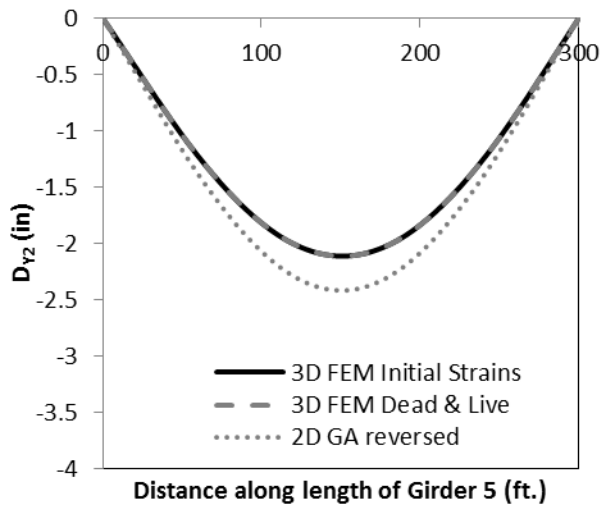
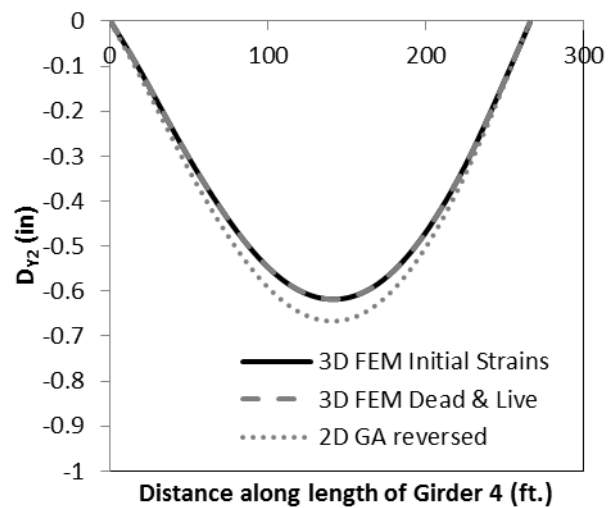


**Figure 3.15: Comparison of layovers calculated by different analysis methods—final fit at the SDL stage**

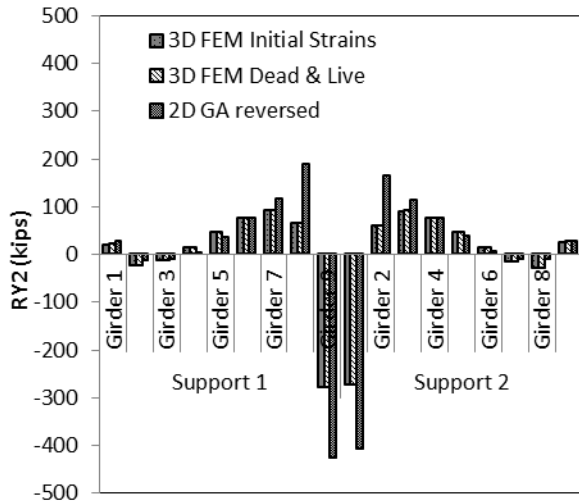


Bridge A

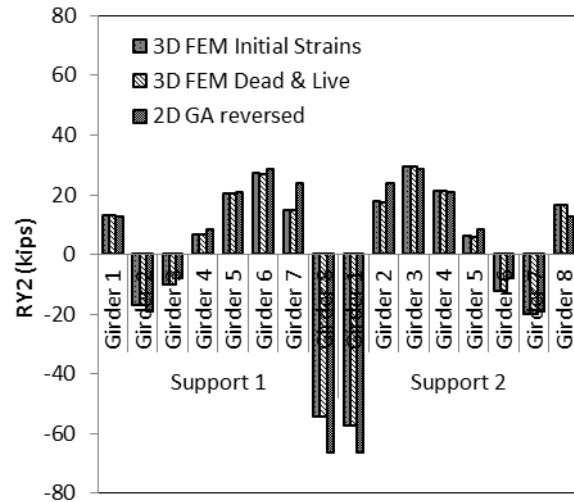


Bridge B

**Figure 3.16: Comparison of component of deflection due to lack-of-fit ( $D_{Y2}$ ) calculated by different analysis methods**

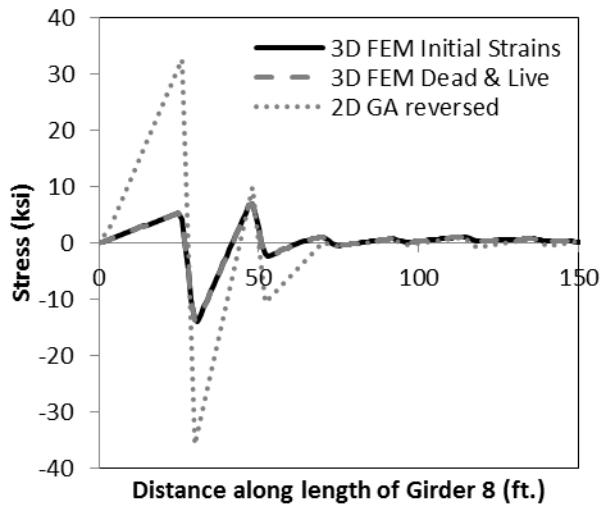


Bridge A

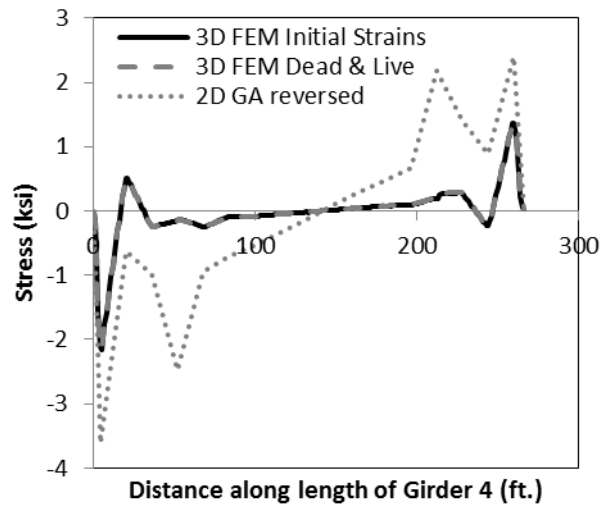


Bridge B

**Figure 3.17: Comparison of change in reactions due to lack-of-fit ( $R_{Y2}$ ) calculated by different analysis method for Bridge A**

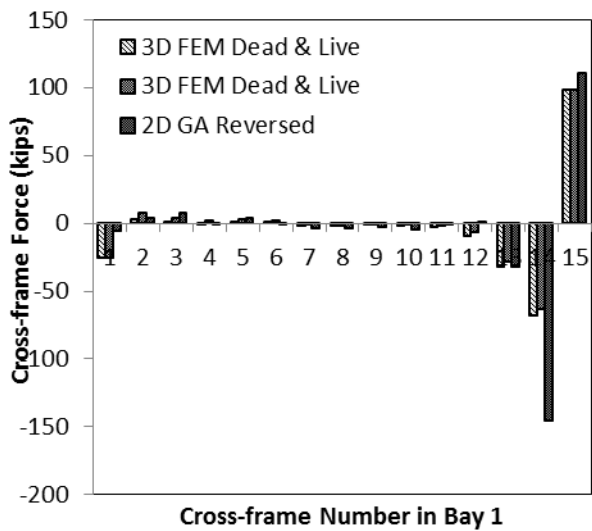


Bridge A

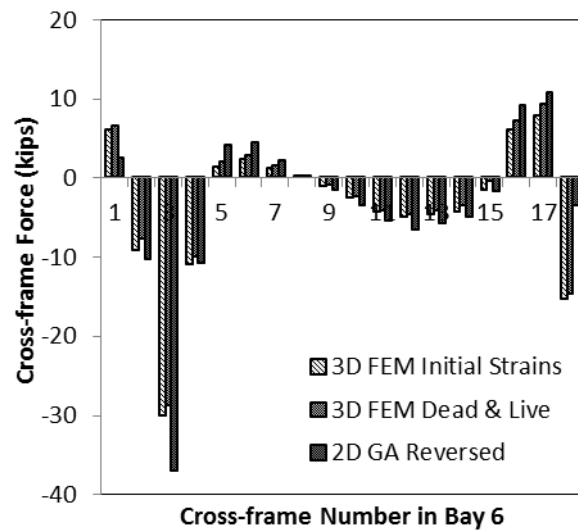


Bridge B

Figure 3.18: Comparison of flange lateral bending stress calculated by different analysis methods



Bridge A



Bridge B

Figure 3.19: Comparison of cross-frame forces calculated by different analysis methods

### 3.3 SUMMARY AND CONCLUSIONS

For the erected fit detailing method performance of improved and traditional 2D grid analysis is different for different framing options

- For bridges with contiguous cross-frames, traditional 2D GA gives reasonable estimates of all responses except for flange lateral bending stress and improved 2D GA gives reasonable estimates of all responses.
- For bridges with staggered cross-frame, traditional 2D GA gives erroneous estimates of all the responses and improved 2D GA gives reasonable estimates of all responses. However, when stagger distance is small,  $J_{eq}$  in improved 2D GA has very high value resulting in overestimation of lack-of-fit effects.

Lack-of-fit effects for the final fit detailing method at the SDL stage obtained from Method of initial strain shows a very good agreement with the lack-of-fit effects obtained from the method of Dead and Live cross-frames elements. Reversing improved 2D grid analysis results for the erected fit detailing method at the TDL stage also give reasonable estimates of the lack-of-fit effects for the final fit detailing method at the SDL stage.

The main conclusion is that improved 2D GA can be used to estimate the lack-of-fit effects both for the final fit and erected fit detailing methods for most of the straight skewed bridges.

This chapter discusses methods for estimating the lack-of-fit effects for the erected fit and final fit detailing methods. There is one more important issue related to final fit detailing method that is the fit-up force required to attach the cross-frames to the girders during erection. Next chapter discuss the methods to estimate these fit-up forces.

# Chapter 4 FIT-UP FORCES

## 4.1 Introduction

In final fit detailing method the webs of the girders are out-of-plumb at the completion of erection and before casting of concrete deck or steel dead load (SDL) stage and ideally deflect into plumb position after casting deck or total dead load (TDL) stage as shown in Figure 4.1. Some owners, erectors, fabricators and detailers prefer final fit detailing method because of the plumb girder at the final permanent loading stage (TDL stage). It should be noted that for the final fit, the webs may not be perfectly plumb at the TDL stage. The reason the web may not be plumb at the TDL stage is due to uncertainties in the actual restraints at bearings, differential curing of the concrete bridge deck, as well as several other factors.

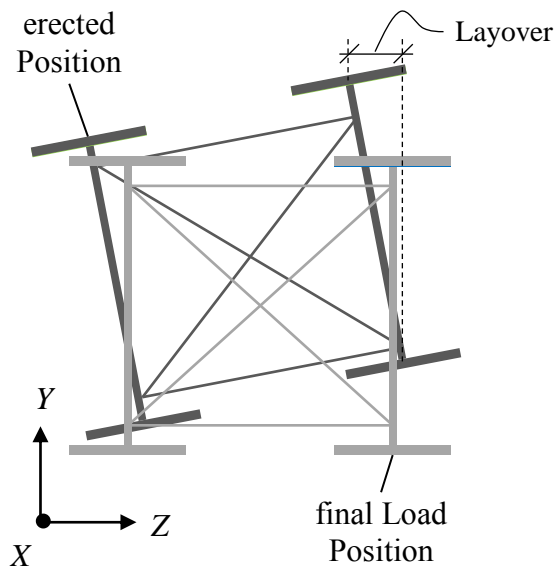


**Figure 4.1: Final fit detailing methods**

In final fit detailing method cross-frame are fabricated to fit between the girders at the TDL stage and therefore the cross-frame do not fit between the girders at the SDL stage. Therefore erector needs to apply a force generally referred as fit-up force to fit the cross-frame between the girders. It is important to know the magnitude of the fit-up force required to fit the cross-frame between the girders beforehand to make arrangements for the application of the fit-up force.

Before discussing the fit-up forces in detail, it is important to understand the lack-of-fit of cross-frame, detailed with final fit detailing method, between the girders during erection of skewed bridges.

#### **4.1.1 Lack-of-fit in Skewed Bridges**

Lack-of-fit refers to the fact that cross-frames do not fit between the girders at a particular loading stage in skew bridges. Lack-of-fit occurs at steel dead load (SDL) stage if final fit detailing method is used and at total dead load (TDL) stage if erected fit detailing method is used.

The lack-of-fit of cross-frames between girders for the final fit detailing method during the erection is explained by Figure 4.2. Figure 4.2 shows the framing plan of a skew bridge and concrete dead load cambers associated with each girder. The intermediate cross-frames in skewed bridges are typically perpendicular to the girder web, and connect the two adjacent girders at different elevations due to camber as shown in Figure 4.2.

It should be noted that the difference in elevation of girders can come from both cross-slope and girder cambers. However, the difference in elevation due to cross-slope remains the same at different loading stages and therefore does not contribute to lack-of-fit. However, the difference in girders' elevations due to camber does contribute to lack-of-fit and is illustrated in Figure 4.2. The figure shows some of the detailing complexities that the differential camber produces with respect to cross-frame detailing.

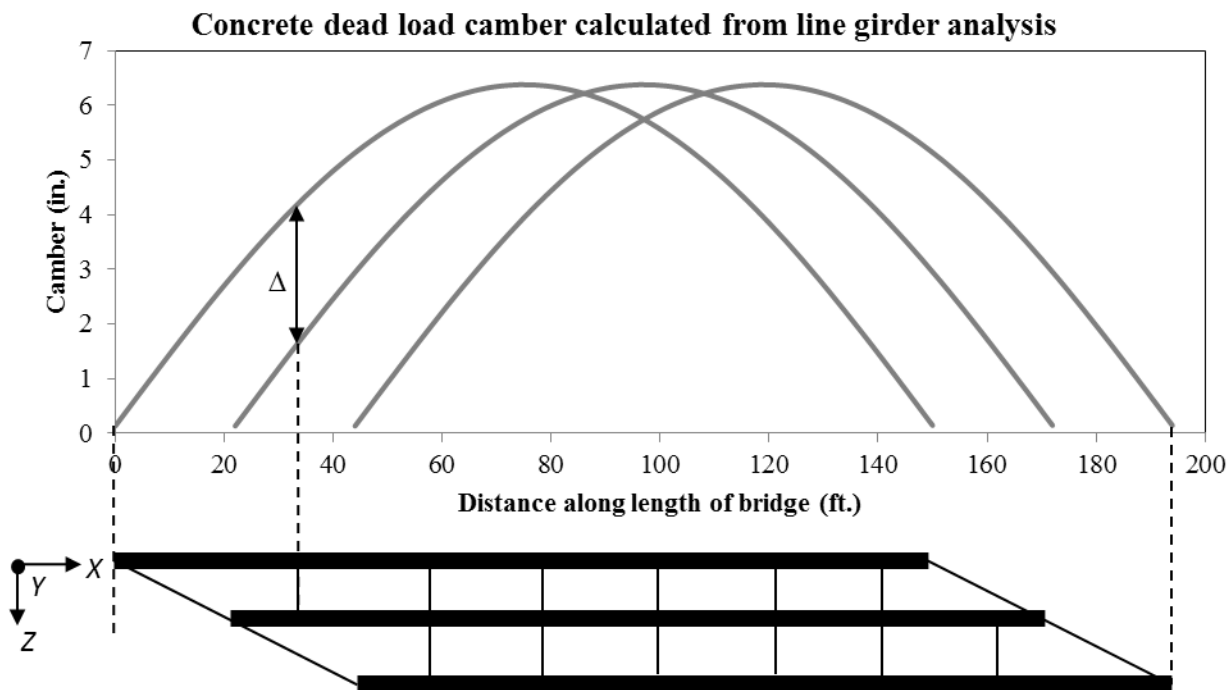


**Figure 4.2: Differential camber in a skew bridge**

#### 4.1.2 Fit-Up Forces

As explained earlier, in the final fit detailing method, the cross-frames are detailed to fit between the girders at total dead load (TDL) stage. These cross-frames therefore do not fit between the girders at steel dead load (SDL) stage or during the erection of steel framing. In order to fit the cross-frames detailed with final fit detailing method between the girders at the SDL stage or during the erection, a force is required to move the girders into a position where cross-frames can be attached. The girders are both twisted and moved in vertical direction to fit the cross-frames between the girders. This was accomplished by application of horizontal and vertical forces at top and bottom of the girders hence forth called as fit-up forces. In theory, four fit-up forces are required to move a girder for attaching cross-frame; two vertical forces acting on top and bottom of girder ( $F_y^T$  and  $F_y^B$ ) and two lateral forces acting on top and bottom of girder ( $F_z^T$  and  $F_z^B$ ) as shown in Figure 4.3.

Knowledge of the fit-up forces shall allow the bridge steel erector to make arrangements for application of the fit-up force. High fit-up forces are not desirable because these high forces can slow down construction of the skew bridges.

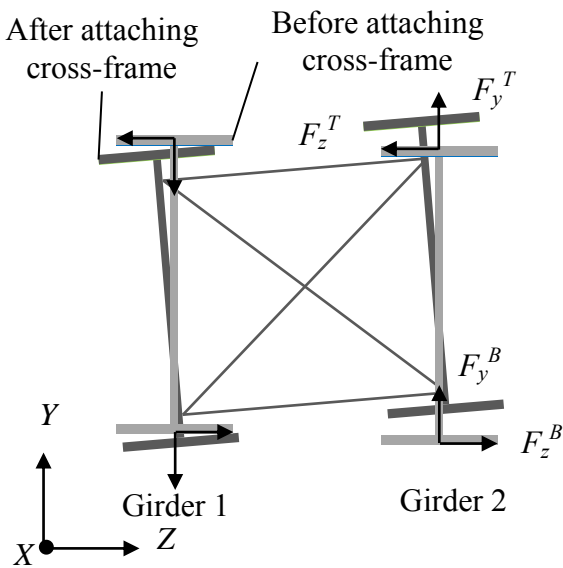


**Figure 4.3: Fit-up forces required to attach the cross-frames to the girders**

## 4.2 Proposed Methods of Calculating Fit-Up Forces

Two methods are proposed to calculate the fit-up forces required to fit the cross-frames detailed with final fit detailing method between the girders during the erection. The followings are the two methods proposed for estimating the fit-up forces.

- Cross-frame forces method
- 3D erection simulation method

Cross-frame forces method requires less effort and is less accurate compared to 3D erection simulation method that is more accurate but requires more effort.

The following section shall provide detail of each method.

### 4.2.1 Cross-frame Forces Method

Cross-frame forces at the SDL stage for the final fit detailing method are indicative of the fit-up forces. It is because of the facts that cross-frames are holding the girders into the twisted positions or are responsible for the lack-of-fit. Chapter 2 has shown that cross-frame forces for the final fit detailing method are equal and opposite to the cross-frame forces at the TDL stage for the erected fit detailing method. Therefore cross-frame forces for the final fit detailing method at the SDL stage can be obtained by reversing the sign of cross-frame forces for the erected fit detailing method at the TDL stage as shown in chapter 3. Cross-frame forces for the erected fit detailing method at the TDL stage can be obtained from improved 2D grid analysis thereby avoiding the use of 3D FEM analysis.

Once cross-frame forces are obtained they are resolved into vertical and lateral components at the connection points as shown in Figure 4.4. The fit-up forces in vertical direction,  $F_y$  and lateral direction,  $F_z$  at a connection point can be calculated by resolving the cross-frame forces into vertical and lateral components at the connection. For example, following equations can be used to calculate fit-up forces at top of Girder 2.

$$F_y^T = -F_{D1} \sin \theta$$

$$F_z^T = -F_{TC} - F_{D1} \cos \theta$$

Where,  $F_{BC}$ ,  $F_{TC}$ ,  $F_{D1}$  and  $F_{D2}$  are forces in Bottom Chord, Top Chord, Diagonal 1 and Diagonal 2 members of the cross-frames.

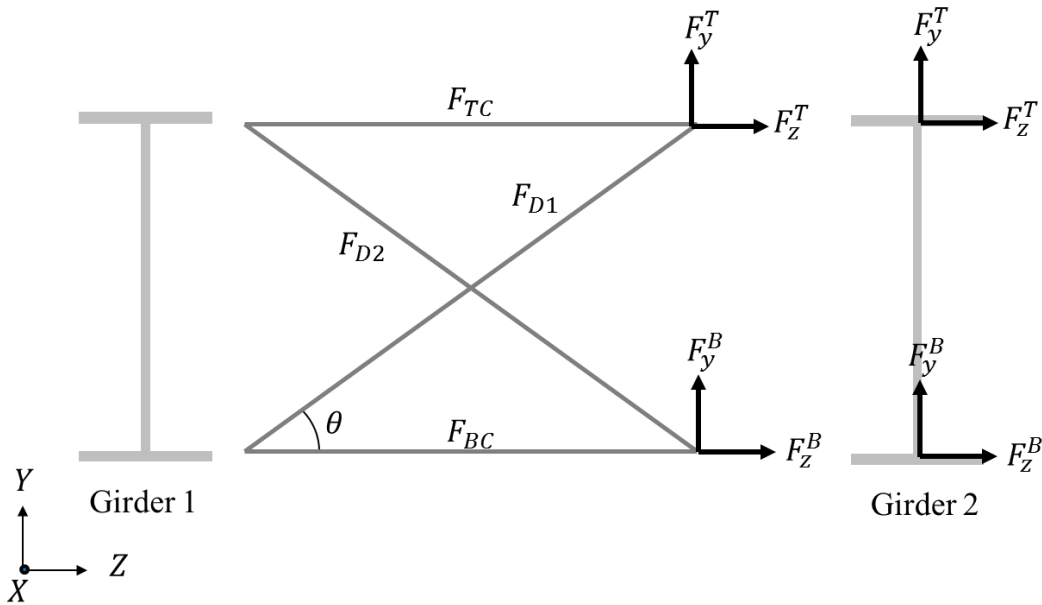


**Figure 4.4: Fit-up forces by resolving cross-frame forces at connection points**

#### 4.2.2 3D Erection Simulation Method

3D erection simulation attempts to mimic the erection of steel framing in the practice. In this simulation the cross-frames were erected one by one following a particular erection sequence similar the erection of real bridge in the practice. It is important to note that with the erection of cross-frames—detailed with final fit detailing method both stiffness and geometry of the bridge framing keep on changing. The change in bridge geometry is considered in erection simulation by updating the geometry after creating each cross-frame elements. The change in stiffness of the framing was automatically considered in the erection simulation by creation of cross-frame elements.

A step by step procedure for the erection simulation is described below.

Erection simulation consists of two steps for each cross-frame after completing FEM model of girder being cambered using line girder analysis/isolated girder analysis.

**Step 1.** In step 1, initial strains (INSTRN) were calculated based on the lengths of the cross-frame members detailed with final fit detailing method and the distance between the connection points of the girders. Each cross-frame member was assigned a value of initial strain as shown in Figure 4.5 (step 1). After assigning INSTRN to each cross-frame member, static

analysis was run to get the cross-frame forces in the cross-frame—detailed with final fit detailing method.

**Step 2.** From the cross-frame forces obtained in step 1, the fit-up forces were evaluated as explained earlier in section 4.2.1. Once the fit-up forces were obtained as shown in in Figure 4.5 (step 2), the geometry of the structure was updated and initial strains (INSTRN) were removed from the cross-frame being erected.

Step 1 and Step 2 were repeated for every single cross-frame in the bridge and the displacements are stored.

Different erection sequence can be used to erect the cross-frames in erection simulation. A detailed discussion on different erection sequences is provided in section 4.3.1.

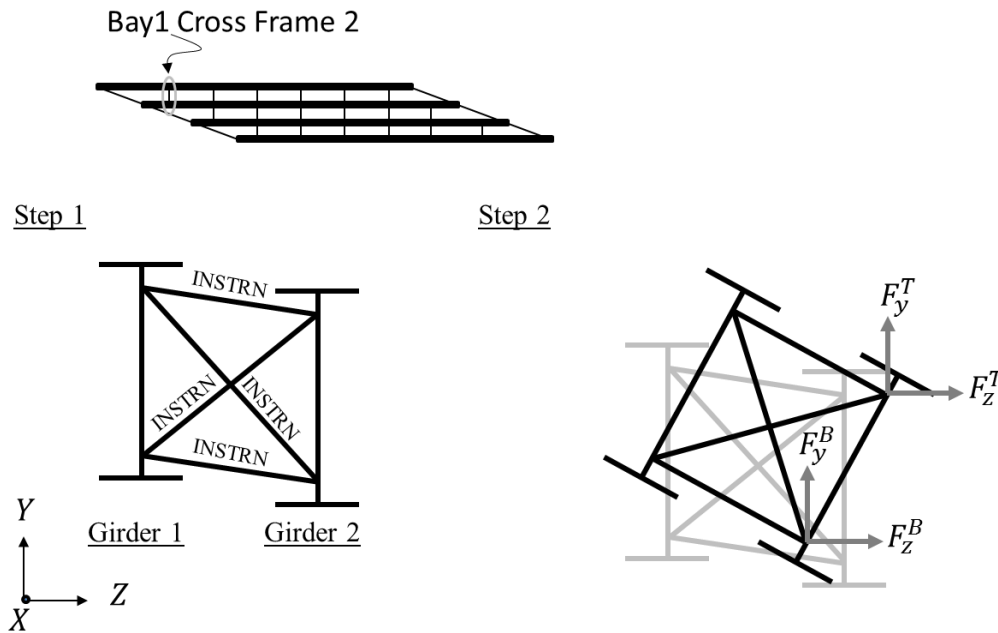


**Figure 4.5: Steps followed to calculate fit-up forces in erection simulation**

Bridge girders are generally elastic during the erection of steel framing. The final deflected geometry of elastic girders is not affected by attaching cross-frames (CFs) one by one or attaching all cross-frames at once. Therefore, geometry of girders at the end of erection simulation (attaching CFs one by one) should be same as geometry of girders attaching CFs all at once. Comparison of geometry of girders (layovers and girder elevations) at the end of erection simulation (attaching CFs one by one) to geometry of

girders attaching CFs all at once is done in Figure 4.6 for Girder 4 of Bridge C. As indicated by the Figure 4.6 both attaching the cross-frames all at once or attaching them one by one results in identical final geometry (layovers and girder elevations) of Girder 4 of Bridge C. Results shown in Figure 4.6 provide evidence that erection simulation was working properly. Similar results were obtained for other girders of the Bridge C as well as Bridge A and Bridge B.

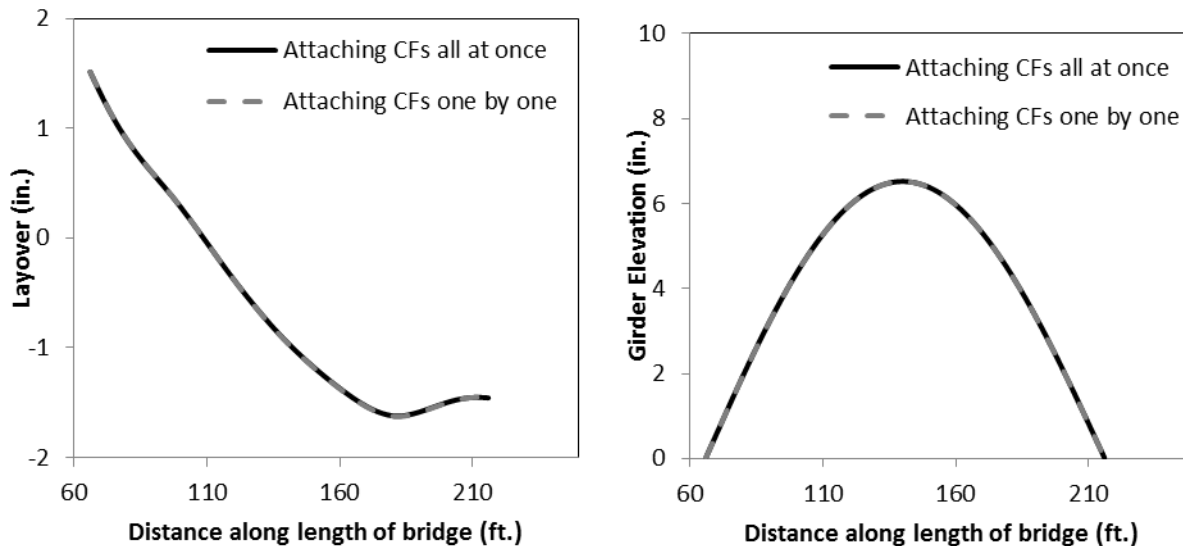


**Figure 4.6: Geometry of Girder 4 of Bridge C after completion of erection**

An alternative approach to 3D erection simulation can be to use Dead and Live option with cross-frame elements and evaluate cross-frame forces for the final fit detailing method at steel dead load (SDL) stage. The details for carrying out analysis using Dead and Live option with cross-frame elements is provided in chapter 3. Once the cross-frame forces are obtained, the fit-up forces can be calculated by resolving the cross-frame forces in horizontal and vertical direction as explained in section 4.2.1. However, in this case all the cross-frames are erected at once and an erection sequence cannot be followed for erecting cross-frames one by one.

### 4.2.3 Discussion and Comparison of Fit-Up Forces

As discussed earlier, erection of a cross-frame require both lateral and vertical forces at the top and bottom ( $F_{zT}$ ,  $F_{zB}$ ,  $F_{yT}$ ,  $F_{yB}$ ) to move the girders into a position where connections can be made between the cross-frame and girders. Comparison of these fit-up forces obtained from Cross-frame

Force Method (CF Force Method) and erection simulation method (Erect. Simul. Method) is shown in Figure 4.7 and Figure 4.8 for Girder 3 of Bridge C for erecting cross-frames in Bay 3. The results of erection simulation method discussed in this section are obtained following erection sequence 1. Following observation can be made from by inspecting the data presented in Figure 4.7 and Figure 4.8.

- Lateral fit-up forces at the top and bottom are in opposite direction indicating that girder is required to be twisted to make the connections between a cross-frame and girders.
- Vertical fit-up forces for top and bottom are generally in the same direction indicating that girder needs to be moved up or down to make connection between a cross-frame and girders.
- Both lateral and vertical fit-up forces are relatively high for the first intermediate cross-frame because; a) the distance between the cross-frame and connection point is highest for this cross-frame and b) girders have large stiffness near the supports and require more force for deflection and twisting.
- The highest fit-up force calculated from Cross-frame Force Method is in good agreement with the highest fit-up force calculated from Erection Simulation Method.

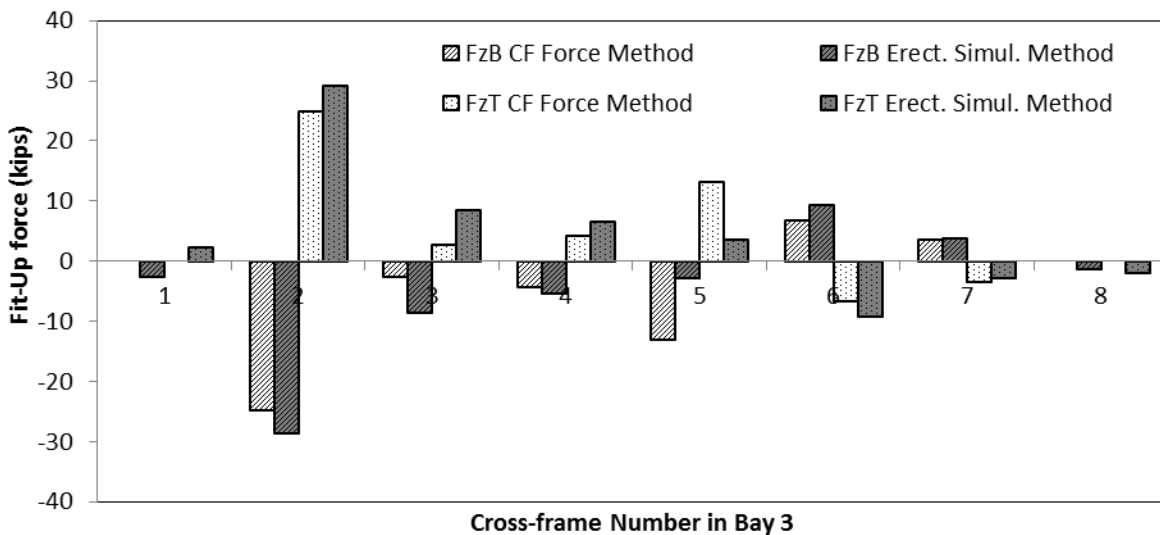


**Figure 4.7: Lateral fit-up forces applied to Girder 3 of Bridge C for erecting cross-frames in Bay 3**

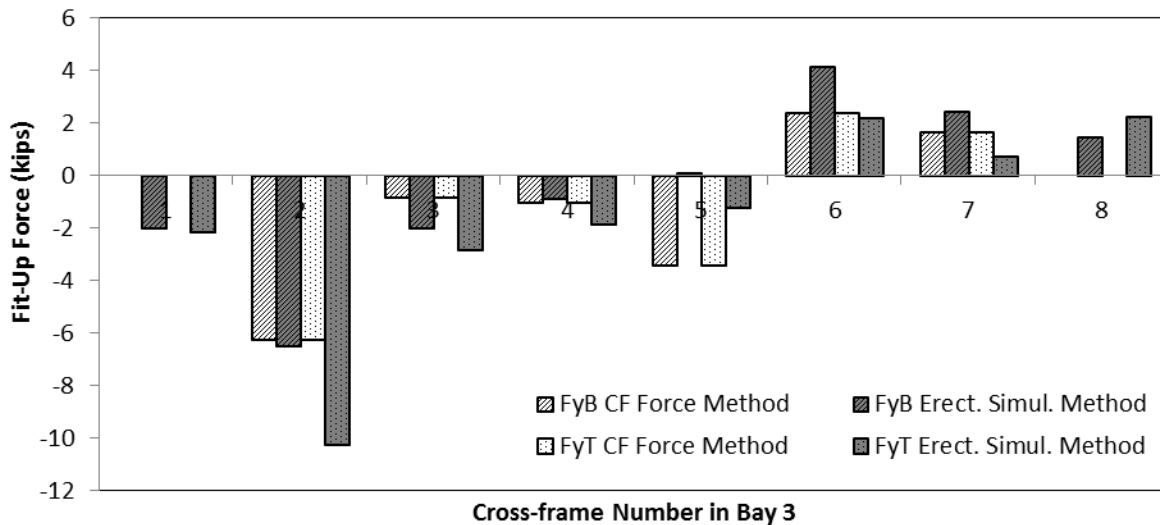


**Figure 4.8: Vertical fit-up forces applied to Girder 3 of Bridge C for erecting cross-frames in Bay 3**

Generally, erector is interested in knowing the maximum level of fit-up force required to fit the cross-frames—detailed with final fit detailing method, between the girders during the erection of steel bridge. Therefore absolute maximum fit-up force in both vertical and lateral direction was obtained from different methods of analysis for Bridge A, Bridge B and Bridge C as shown in Table 4.1. It can be noticed that fit-up forces calculated from cross-frame forces (obtained from improved 2D grid analysis) are in close agreement with the fit-up forces obtained from erection simulation except for Bridge A. For Bridge A, Cross-frame Forces Method overestimates the fit-up forces because the cross-frame forces are overestimated by improved 2D grid analysis for this bridge. The overestimation of cross-frame forces by improved 2D grid analysis for Bridge A is discussed in detail in chapter 3. In summary, cross-frame forces obtained from improved 2D grid analysis can be used to estimate fit-up forces required for the final fit detailing method at erection stage.

**Table 4.1: Absolute Maximum fit-up force from different methods**

|          | Absolute Maximum Fit-Up force (kips) |               |           |               |
|----------|--------------------------------------|---------------|-----------|---------------|
|          | Lateral                              |               | Vertical  |               |
|          | CF Forces                            | Erect. Simul. | CF Forces | Erect. Simul. |
| Bridge A | 230                                  | 180           | 104       | 131           |
| Bridge B | 41                                   | 38            | 28        | 30            |
| Bridge C | 25                                   | 29            | 7         | 10            |

### 4.3 Effect of Different Practices on Fit-Up Forces

Different construction and detailing practices also affect the fit-up forces. These construction and detailing practices include the following:

- Erection sequence
- Distance of first intermediate cross-frame from the support

These effects are evaluated by carrying out the erections simulation and 3D FEM analysis. Detailed discussion on the effect of each construction practice on the fit-up forces is provided in the following sections.

#### 4.3.1 Different erection sequences

Three different erection sequences that can be followed for attaching the cross-frame to the girders are shown in Figure 4.9. In erection sequence 1, cross-frame are attached starting from one end of a bay and moving toward the other end of the bay. In erection sequence 2, the cross-frames are attached starting from the two ends of a bay and moving toward the middle of the bay. In erection sequence 3, cross-frames are attached starting from the middle of the bay and moving outward toward the ends of the bay.

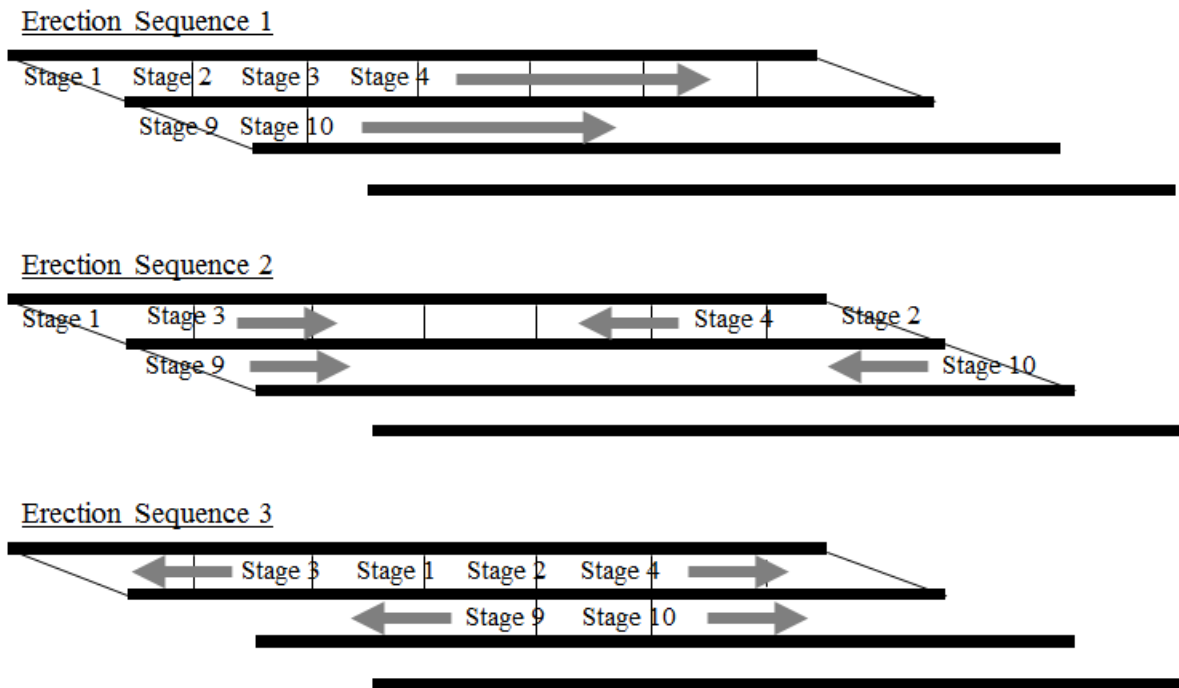


**Figure 4.9: Erection sequences for attaching cross-frames to girders in final fit detailing method**

Fit-up forces are evaluated from 3D erection simulation following the three erection sequences to find out the erection sequence that requires minimum fit-up force. These fit-up forces for Girder 8 of Bridge A for erection of cross-frame in Bay 8 are compared in Figure 4.10. Following observations can be made by inspecting data presented in Figure 4.10.

- Large fit-up forces are required to erect the cross the cross-frames near the obtuse corner of the bridge.
- Less fit-up force is required if erection sequence 3 is followed compared to fit-up forces required by following erections sequence 1 and 2.
- Fit-up forces are more evenly distributed for erection sequence 3 compared to the distribution of fit-up forces in erections sequence 1 and 2.

These observations can be partly explained by the following discussion.

Fit-up forces for the erection of a particular cross-frame depends on the distance between the cross-frames and their connection points and the vertical and torsional stiffness of the girders in a bay. As shown in Figure 4.2, the distance between the cross-frames and their connection points is small for the cross-frames in the middle of a bay compared to the cross-frames at the ends of the bay. This distance between cross-frame and their connection points change during the erection of cross-frames because erection of each cross-frame deflects the girders into a new position. Generally, this distance between the cross-frames and their connection points decreases with increase in number of cross-frames attached to the girder during the erection. The torsional and vertical stiffness of the girders does not change significantly during the erection of cross-frames in a bay.

In erection sequence 3, the cross-frame that has less displacement between its connection points is attached first and thereby gradually deflects the girders and decreases the distance between the connection points for the end cross-frames. Therefore, the maximum fit-up force is less in erection sequence 3 compared to the maximum fit-up force in erection sequence 1 and 2. In erection sequence 1 and 2, the cross-frame near the end of the bay are erected first and girders need to be displaced through a large distance to make the connections, thereby requiring relatively larger forces.

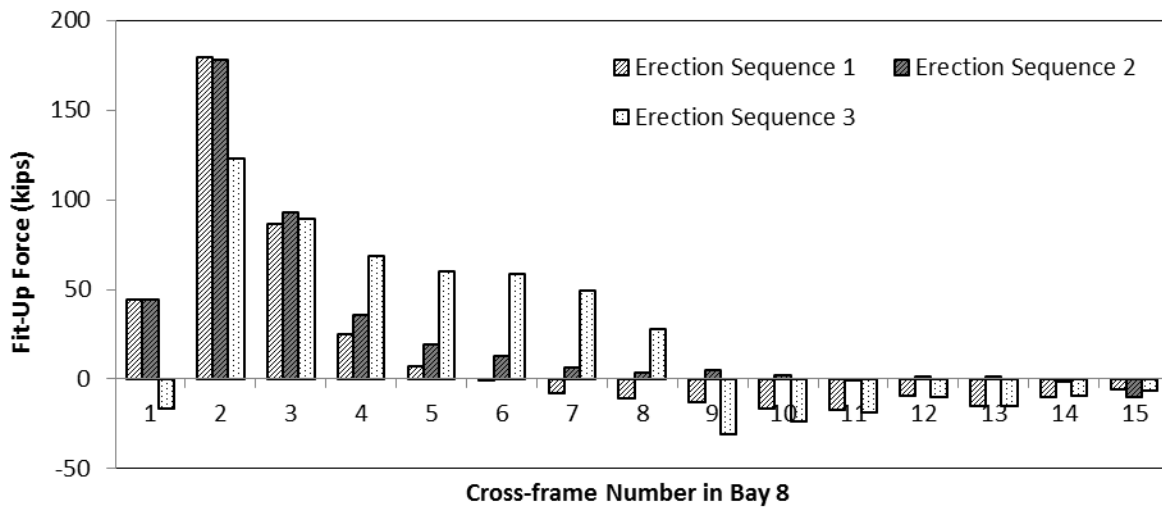


**Figure 4.10: Fit-up force at the top of Girder 8 of Bridge A for erecting the cross-frames in Bay 8**

Also note that the stiffness of the bridge frame is large near the obtuse corners compared to acute corners and therefore the cross-frame near the obtuse end of a bay require more fit-up force compared to fit-up force required to erect cross-frame on the acute end as shown in Figure 4.10.

In summary less fit-up force is required if cross-frames are attached using erection sequence 3 that is attaching the cross-frames in the middle of a bay first and proceeding toward the end of the bay.

In order to verify the conclusion drawn for Figure 4.10 the maximum fit-up force was calculated for Bridge A, Bridge B and Bridge C following the three different erections sequence as shown in Table 4.2. As shown in Table 4.2 fit-up force is less following erection sequence 3 (ES3) for the three bridges in both vertical and lateral direction.

**Table 4.2: Absolute Maximum fit-up force from different erection sequences**

|          | Absolute Maximum Fit-Up force (kips) |     |     |          |     |     |
|----------|--------------------------------------|-----|-----|----------|-----|-----|
|          | Lateral                              |     |     | Vertical |     |     |
|          | ES1                                  | ES2 | ES3 | ES1      | ES2 | ES3 |
| Bridge A | 180                                  | 178 | 123 | 131      | 131 | 89  |
| Bridge B | 38                                   | 40  | 32  | 31       | 32  | 25  |
| Bridge C | 29                                   | 30  | 20  | 10       | 11  | 8   |

### 4.3.2 Distance of the First Intermediate Cross-frame from Support

Distance of first intermediate cross-frame from the support also affects the fit-up forces. In this chapter it has been shown that fit-up forces can be calculated from the cross-frame forces. Effect of distance of first intermediate cross-frame from the support on the cross-frame forces was evaluated in a parametric study shown in chapter 3. The cross-frame forces decreases with the increase in distance from the support however, the decrease in the cross-frame forces is not very significant. Therefore, it was expected that maximum fit-up forces decrease with the increase in the distance of first intermediate cross-frame from the support.

## 4.4 Summary and Conclusions

The knowledge of fit-up forces required for attaching the cross-frames in the case of final fit, will provide the erector with an estimate of level of forces required and allow mobilization of the appropriate equipment on site and avoiding job delays.

Two different methods are introduced to evaluate the fit-up forces that are required to erect the framing of a skew bridge. These methods are cross-frame forces method and 3D erection simulation method.

It has been shown that cross-frame forces evaluated from improved 2D grid analysis can be used to estimate the fit-up forces required to fit the cross-frames—detailed with final fit detailing method between the girders during the erection of steel bridge.

Three different erection sequences have been used in erection simulation method to find out the most efficient sequence of erection. It has been found that the maximum fit-up force required to erect the cross-frames is relatively less if cross-frames are erected starting from the middle of a bay going toward the ends of the bay (erection sequence 3).

This chapter provides methods to estimate the fit-up forces required for attaching the cross-frames, detailed with final fit detailing method, to girders during erection. Chapter 2, 3 and 4 provide elements and foundation to develop complete and simplified design approach for the skewed bridges. The next chapter develops this design approach for the skewed bridges.

## **Chapter 5      DESIGN PROVISIONS**

Chapters 2 through 4 discuss different issues related to straight skew I-girder bridges in detail. These chapters identify the structural responses associated with different detailing methods and provide simplified methods to estimate the responses. Knowing the structural responses related with skew bridges and methods of analysis to estimate them provide elements and foundation to develop complete and simplified design approach for the skewed bridges. The design of steel bridges is already perceived to be difficult, as compared to concrete bridges, and there is no need to strengthen this perception.

Therefore, objective of this chapter is to simplify the design and construction of steel bridges with skewed supports by introducing a complete and coherent design approach. The focus of this chapter is on straight bridges; however, some of the information is also applicable to horizontally curved girder systems. This objective is achieved by the following:

- 1) Recommending method of analysis for calculation of camber for different detailing methods.
- 2) Identification of important structural responses and recommendation of methods of analyses for obtaining these responses.
- 3) Evaluation of the effect of different framing options on different structural responses of the bridges.
- 4) Development of a flow chart that can help designers to choose the appropriate detailing of the cross-frames for straight skewed I-girder bridges.

### **5.1 Recommendation on Calculation Of Cambers**

The cambers need to be estimated correctly in skew bridges as there is no conservative side in estimation of cambers. Incorrect estimation of cambers either above or below the correct values results in potential lack-of-fit effects, and change in bridge cross-slopes. These problems can potentially lead to expensive retrofit, delays in construction, and litigation.

Different methods of analysis can result in different calculation of cambers in skew bridges. For example cambers calculated from line girder analysis are different from the cambers calculated from the grid analysis. This is because in skew bridges, girders' deflections at different loading stages are affected by the lack-of-fit depending on the detailing method. Lack-of-fit effects include a component of vertical deflection due to lack-of-fit of cross-frames between girders as discussed in detail chapter 3.

This component of deflection due to the lack-of-fit might be permanent or temporary depending on the detailing method used. Therefore depending on the detailing method used cambers can be correctly estimated by either line girder analysis or a combination of line girder and grid analysis.

For the erected fit detailing method, SDL cambers should be estimated by line girder analysis because there is no component of deflection due to lack-of-fit in girders at the SDL stage. The concrete dead load (CDL) cambers should be calculated by 2D grid analysis or 3D FEM analysis modeling all the girders and cross-frames connected together. This is because the CDL move the girders into a position where cross-frame don't fit between the girders and result in lack-of-fit. This lack-of-fit and accompanied component of vertical deflection is permanent and therefore should be included into the camber calculation.

For the final fit detailing method both SDL and CDL cambers need to be calculated by line girder analysis. This is because in the final fit detailing method cross-frames are detailed to fit between the girders at the TDL stage. Therefore there is no lack-of-fit and associated component of vertical deflection in the girders at the TDL stage. It should be noted that in final fit detailing method lack-of-fit and component of vertical deflection appears at the SDL stage. However, this lack-of-fit and accompanied component of vertical deflection is temporary and goes away once CDL was applied. Further, if cambers from the grid analysis are used for the final fit detailing method the cross-frame shall not fit between the girders at the TDL stage and therefore result in lack-of-fit at the TDL stage.

**Table 5.1: Method of calculation of camber for different detailing methods**

| Detailing Method | Method of calculation of camber for |                      |
|------------------|-------------------------------------|----------------------|
|                  | Steel dead load                     | Concrete dead load   |
| Erected fit      | Line girder analysis                | 2D grid analysis     |
| Final fit        | Line girder analysis                | Line girder analysis |

**5.1.1 Verification of Recommendation Using Numerical Models**

In order to verify the recommendation, the cambers calculated from the recommended analyses are incorporated in 3D FEM analysis and proceeded with the construction sequence—placing girders on supports, attaching the cross-frame, and applying the dead loads. For the final fit detailing method there

is lack-of-fit between the cross-frame and girders at SDL simulated by initial strains calculated from the camber diagram see chapter 3 for details, whereas for the erected fit detailing method cross-frames are attached to the girders without initial strains at the SDL stage.

Three straight skewed, simply supported I-girder bridges, having different levels of skew, are selected for consideration in this study. All three bridges have their girders and cross-frames designed with Grade 50 steel having a modulus of elasticity of 29,000 ksi.

Bridge A is an extreme case of straight skew bridges and was used to show extreme skew effects in previous studies [2, 3, 4]. Bridge A has 300 ft. long 144 inches deep girders simply supported on 70.4° skewed supports. The girders of Bridge A are braced with X-type cross-frames containing L6 x 6 x 1 angles. The bridge uses staggered cross-frames at spacing of 22 ft. between 9 girders at 9.25 ft. c/c spacing. Framing planes and sizes of the web and flanges of the bridges studied are shown in Figure 5.1.

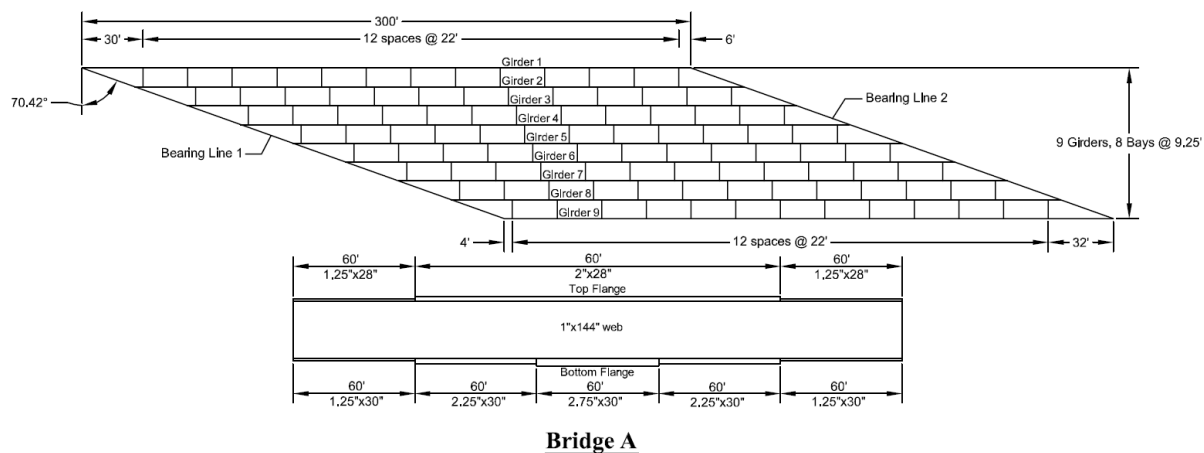


**Figure 5.1: Framing plans and girder sizes of the Bridge A**

Bridge B is another highly skewed bridge, however skewed effect in Bridge B are smaller compared to Bridge A. Bridge B has 266 ft. long 120.5 inches deep girders simply supported on 62.6° skewed supports. The girders of the Bridge B are braced with X-type cross-frames containing L6 x 6 x 1/2 angles. The bridge uses cross-frames at spacing of 16 ft. between 8 girders@7.26 ft. c/c spacing. Framing planes and sizes of the web and flanges of the bridges studied are shown in Figure 5.2.

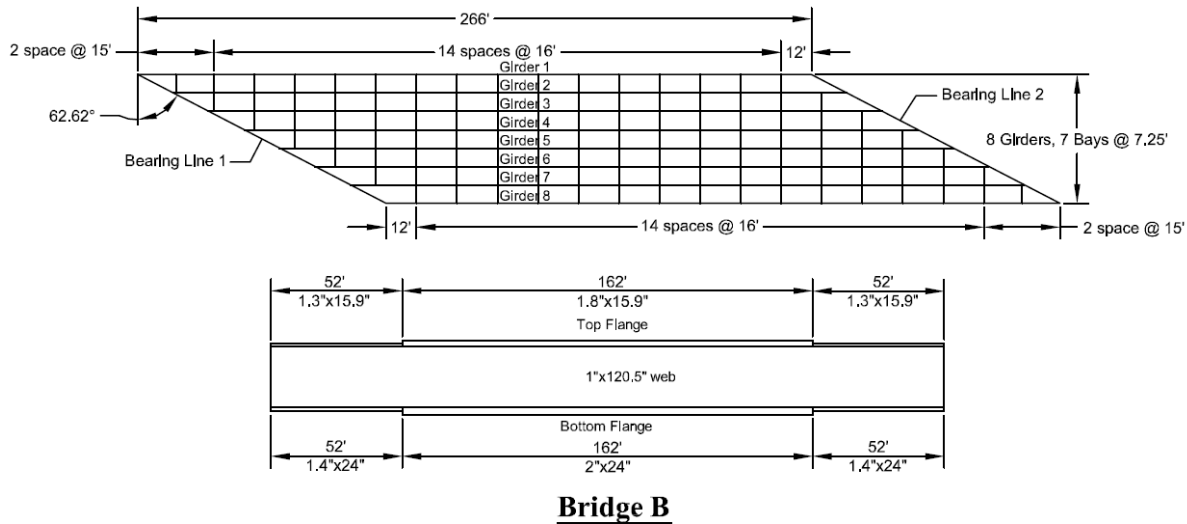


**Figure 5.2: Framing plans and girder sizes of the Bridge B**

Bridge C has 150 ft. long 56.1 inches deep girders simply supported on 70.0° skewed supports. The girders of the Bridge C are braced with X-type cross-frames containing L6 x 3 1/2 x 5/16 angles. The bridge uses cross-frames at spacing of 21 ft. between 4 girders@8 ft. c/c spacing. Framing planes and sizes of the web and flanges of the bridges studied are shown in Figure 5.3.

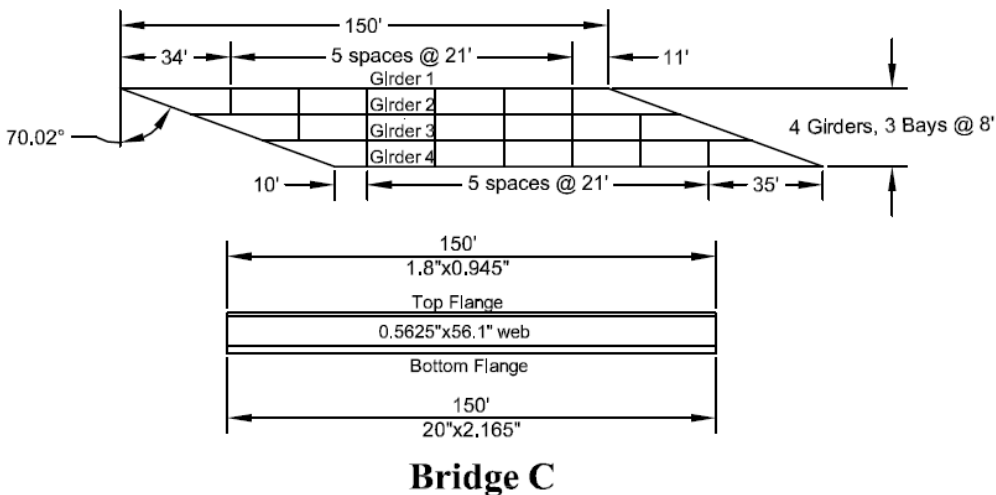
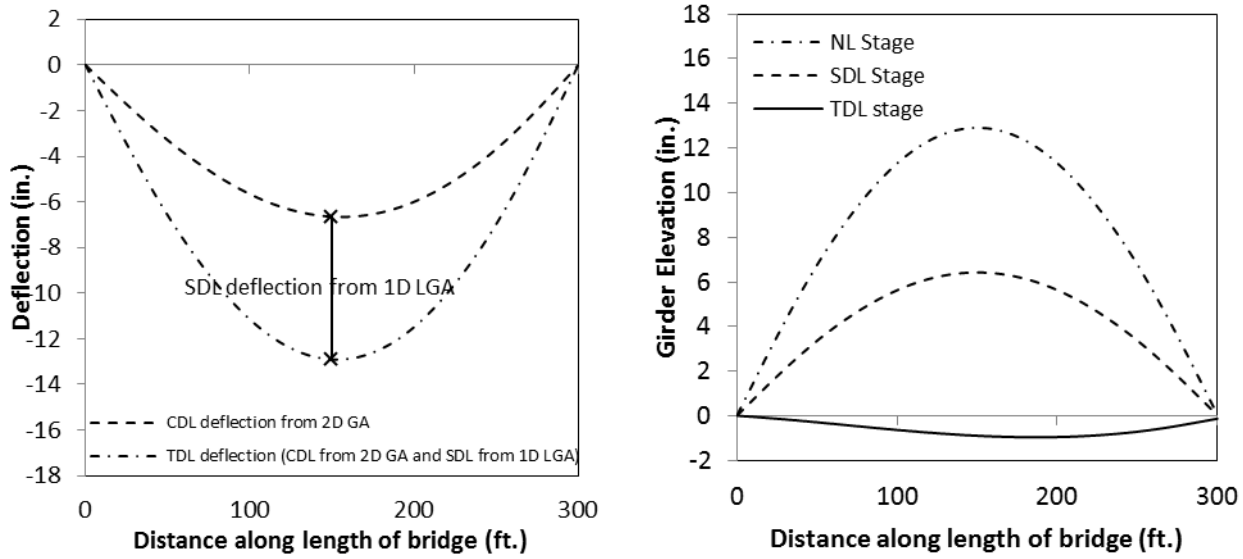


**Figure 5.3: Framing plans and girder sizes of the Bridge C**

Following discussion explains the numerical analysis results of the bridges described above and provide evidence that recommendations regarding camber calculation shown in Table 5.1 are correct. Figure 5.4 to Figure 5.9 show the deflections calculated from the recommended method of analysis and the verification of camber recommendation by the 3D FEM analysis for Bridge A, Bridge B and Bridge C. For example Figure 5.4a shows TDL deflection of the girder 1 of 'Bridge A' calculated by combination of line girder analysis (1D LGA) and 2D grid analysis (2D GA) as per the recommendation for the erected fit detailing method. Figure 5.4b shows the camber in the girder 1 in 3D FEM model of Bridge A at different loading stages. At No Load (NL) Stage the camber in the girder is equal to the TDL deflection calculated as per recommendation. Line corresponding to SDL stage in Figure 5.4b shows the camber in girder 1 after application of the steel dead load (SDL). Since for the erected fit detailing method cross-frames are detailed to fit between the girders at the SDL stage, attaching the cross-frame to the girder at the SDL stage does not cause a component of deflection due to lack-of-fit. Therefore cambers at the SDL stage for the erected fit detailing method are same before and after attaching the cross-frame. Line corresponding to TDL stage in Figure 5.4b shows the remaining cambers in girder 1 of bridge's 3D FEM model after application of TDL. If the camber recommendations are correct the girder should be flat with zero camber at the TDL stage.

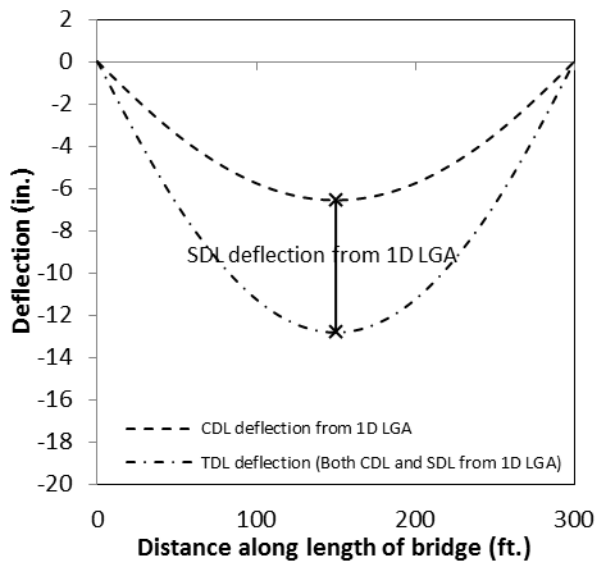
Similarly Figure 5.5a shows TDL deflection of girder 1 of the bridge calculated by line girder analysis (1D LGA) only as per recommendation for the final fit detailing method. Figure 5.5b shows the camber in the girder 1 of bridge's 3D FEM model at different loading stages. At No Load (NL) Stage the camber in the girder is equal to the TDL deflection calculated as per recommendation. There are two lines for SDL stage in Figure 5.5b. The dashed line shows the camber in girder 1 after application of the steel dead load (SDL) but before attaching the cross-frames. The dotted line shows the camber in girder 1 after application of the steel dead load (SDL) after attaching the cross-frames. This is because the cross-frames in final fit detailing method do not fit between the girders at the SDL stage. Therefore attaching the cross-frames detailed with final fit detailing method at the SDL stage was accompanied by a component of deflection due lack-of-fit of cross-frames between girders. Due to this component of deflection, cambers are different before and after attaching the cross-frame for the final fit detailing method as shown in Figure 5.5b. Line corresponding to TDL stage in Figure 5.5b shows the remaining cambers in girder 1 of bridge's 3D FEM model after application of TDL. If the camber recommendations are correct the girder should be flat with zero camber at the TDL stage.

It is worth mentioning that in the case of Bridge A and B the deflection due to weight of steel girder is close to deflection due to concrete dead weight, because of the girder sizes and girder spacing. In most usual cases, one would expect to have a SDL deflection to be about 30% of the total camber. This is the case for bridge C.

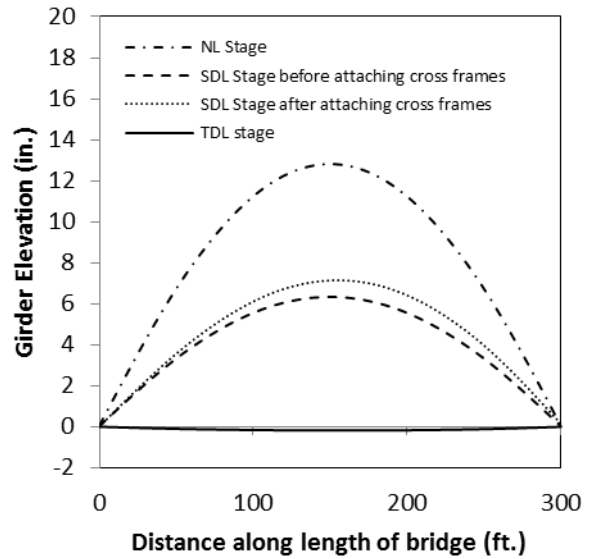


- a) Calculation of camber from 1D LGA and 2D GA as per recommendation      b) Verification of recommendation by 3D FEM analysis

**Figure 5.4: Verification of camber recommendation for the erected fit detailing method-Bridge A Girder 1**

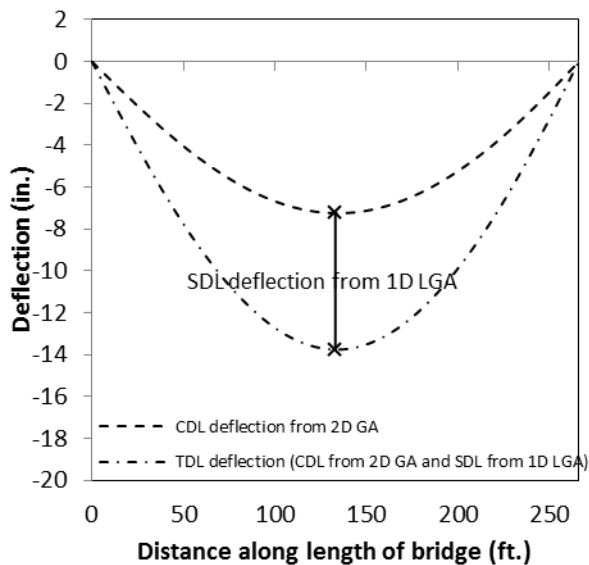


a) Calculation of camber from 1D LGA as per recommendation

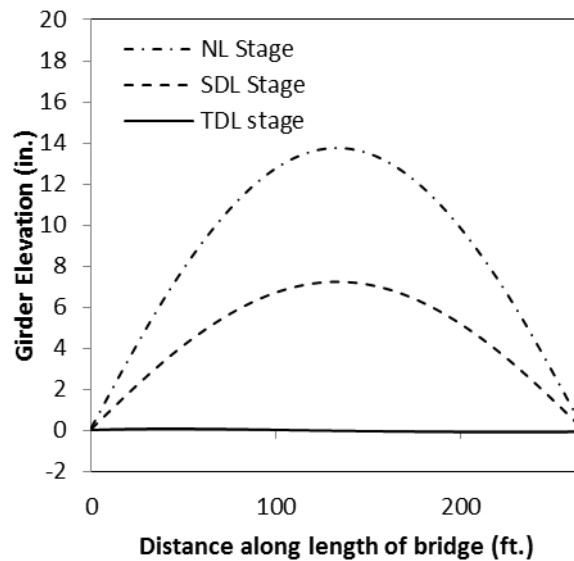


b) Verification of recommendation by 3D FEM analysis

**Figure 5.5: Verification of camber recommendation for the final fit detailing method-Bridge A Girder 1**

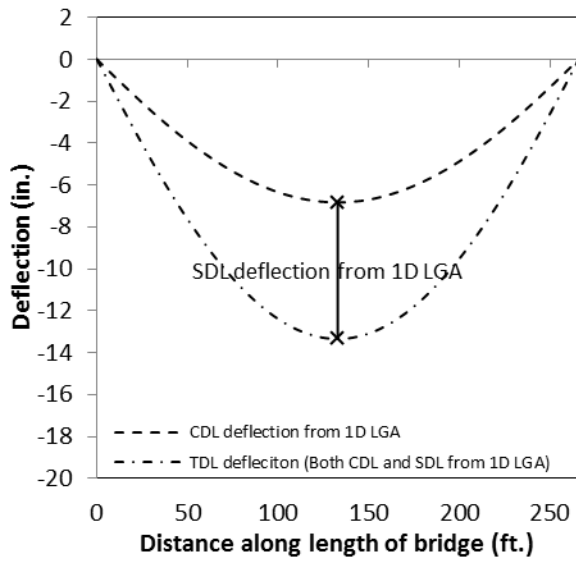


a) Calculation of camber from 1D LGA and 2D GA as per recommendation

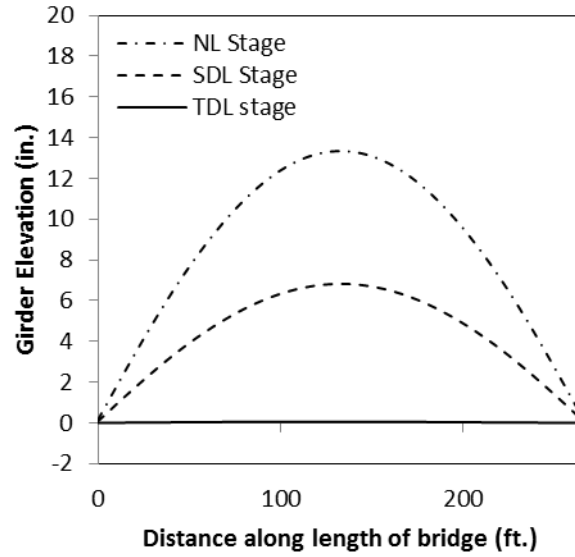


b) Verification of recommendation by 3D FEM analysis

**Figure 5.6: Verification of camber recommendation for the erected fit detailing method-Bridge B Girder 1**

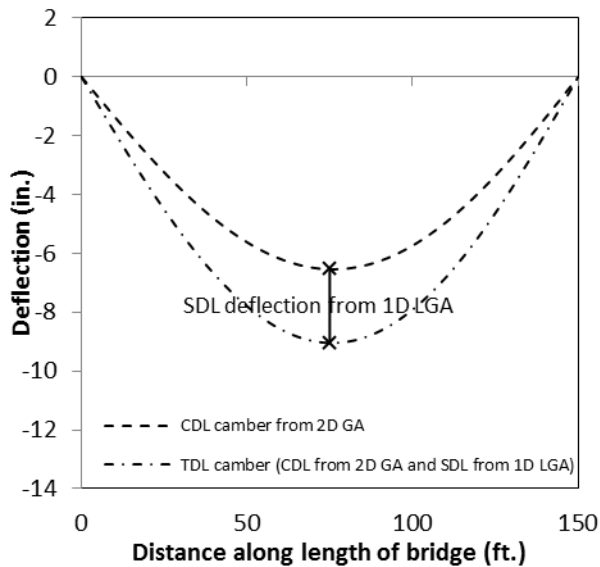


a) Calculation of camber from 1D LGA as per recommendation

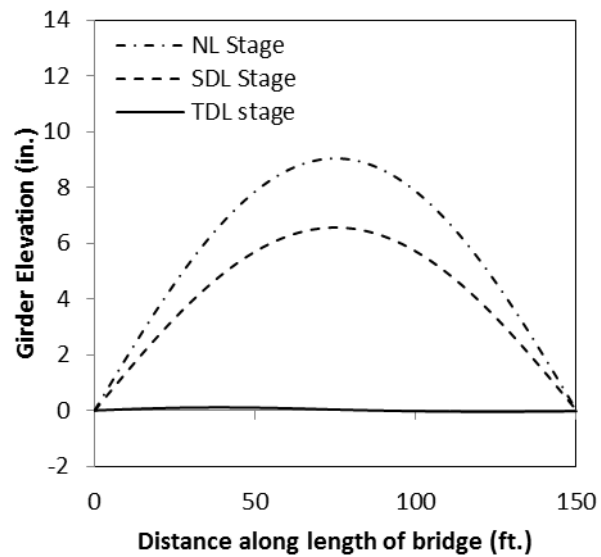


b) Verification of recommendation by 3D FEM analysis

**Figure 5.7: Verification of camber recommendation for the final fit detailing method-Bridge B Girder 1**

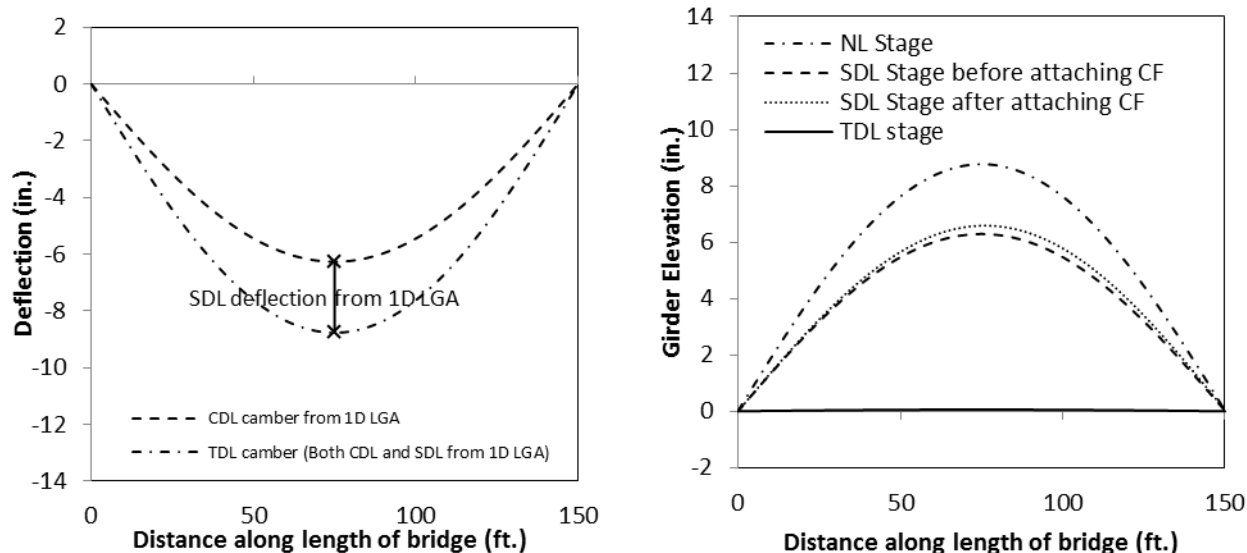


a) Calculation of camber from 1D LGA and 2D GA as per recommendation



b) Verification of recommendation by 3D FEM analysis

**Figure 5.8: Verification of camber recommendation for the erected fit detailing method-Bridge C Girder 1**



a) Calculation of camber from 1D LGA as per recommendation  
 b) Verification of recommendation by 3D FEM analysis

**Figure 5.9: Verification of camber recommendation for the final fit detailing method-Bridge C Girder 1**

### 5.1.2 Summary and Discussion on Numerical Analysis

Summary of results obtained from the numerical analysis done in section 5.1.1 is shown in Table 5.2 for the three bridges. Table 5.2 shows the maximum difference from flat or zero line at the TDL stage considering all the girders in the bridge for both erected fit and final fit detailing method. It can be observed from Table 5.2 that maximum difference from zero line at the TDL stage is less than 2% for all the bridges for both erected fit and final fit detailing method except for the erected fit detailing method for Bridge A. It is also worth noting that magnitude of error (different from zero line at the TDL stage) is less in final fit detailing method compared to erected fit detailing method. This is because 2D grid analysis was used in calculation of concrete dead load deflections in case of erected fit detailing. In the 2D grid analysis, the torsional stiffness of the girders was estimated by using an equivalent torsional constant ( $J_{eq}$ ). This torsional constant approximates the torsional stiffness of the girders and has an effect on concrete dead load (CDL) deflections of the girders. In most of the bridges,  $J_{eq}$  does a good job in approximating the torsional stiffness of the girder; however, when a bridge has staggered cross-frames with very small staggered distance (Bridge A), the unbraced length ( $L$ ) gets very small, and  $J_{eq}$  gets very large. High  $J_{eq}$  value gives an artificially high torsional stiffness to the girders, decreasing their

deflection. Therefore, the CDL deflections obtained from 2D grid analysis are relatively low compared to CDL deflection obtained from 3D FEM analysis.

Other sources of errors correspond to differences in boundary conditions (3D FEM Vs. 1D LGA and 2D GA) and difficulty in building exact cambers in 3D FEM models.

**Table 5.2: Summary of camber analysis**

|          | Maximum difference from zero line at the TDL stage |                    |           |                    |
|----------|--|--------------------|-----------|--------------------|
|          | erected fit  |                    | final fit |                    |
|          | inches   | %age of TDL camber | inches    | %age of TDL camber |
| Bridge A | -1.01  | -9.4%              | -0.21     | -1.6%              |
| Bridge B | -0.09  | -0.7%              | 0.06      | 0.5%               |
| Bridge C | 0.14   | 1.8%               | 0.06      | 0.7%               |

NOTE: A negative difference shows that girders are deflected below the zero line at the TDL stage.

## 5.2 Structural Responses of The Skewed Bridges Affected By Detailing Methods

Different structural responses of skewed bridges affected by detailing methods are referred as lack-of-fit effects and are discussed at length in chapter 2. Table 5.3 summarizes the lack-of-fit effects associated with erected fit and final fit detailing methods presented chapter 2.

As indicated in Table 5.3, different lack-of-fit effects associated with erected and final fit methods appear at different stages of the construction. Lack-of-fit effects for the erected fit detailing method are zero at the SDL stage and are significant at the TDL stage. Converse is true for the final fit detailing method. In the discussion to follow importance of each lack-of-fit effect is discussed to make design recommendations.

Layover are not of any structural consequence, as long as the load levels are less than a small fraction of the critical elastic buckling load at the factored strength load levels, i.e., they do not have any significant impact on the strength of the structural system .

Component of reaction due to lack-of-fit ( $R_{Y2}$ ) can be downward (positive) or upward (negative) depending on the location of support in the bridge. If magnitude of upward  $R_{Y2}$  at a particular support exceeds the magnitude of downward dead load reaction at the support, uplift is observed at that support. This uplift is more common in case of final fit detailing method as  $R_{Y2}$  appear at SDL loading stage when downward dead load reaction is only from the SDL. However, SDL stage is temporary stage and  $R_{Y2}$  is zero at the TDL stage. For the erected fit  $R_{Y2}$  appear at the TDL stage, however negative reaction is not observed because high positive dead load reaction at the TDL stage.

Component of deflection due to lack-of-fit ( $D_{Y2}$ ) for the final fit detailing method appear at temporary SDL stage and is zero at the TDL stage and therefore should not be included in calculation of cambers. For the erected fit detailing method  $D_{Y2}$  appear at permanent TDL stage and therefore should be included in the camber.

Flange lateral bending stress ( $f_l$ ) is important for stability of the flanges. For the final fit detailing method  $f_l$  appears at the SDL stage due to lack-of-fit of cross-frames between girders. At the SDL stage  $f_l$  can also appear from the wind load regardless of the detailing method. However, at the SDL stage, girder's major axis bending stress at low level being caused by only SDL. For the erected fit detailing method  $f_l$  appear at the TDL stage. Other sources of  $f_l$  at the TDL stage include lateral load from knee brace. At the TDL stage girder's major axis bending stresses are high due to presence of both SDL and CDL on the structure. Therefore,  $f_l$  can be critical for both erected fit and final fit detailing methods and needs to be checked to satisfy AASHTO requirements.

Excessive cross-frame forces during construction of steel bridge might result in buckling of cross-frames members, however, to authors' knowledge no such problems has been reported.

For the final fit detailing method, lack-of-fit between the cross-frames and girders appear at the erection stage. Therefore fit-up forces are required to fit the cross-frames between the girders. Calculation of the fit-up forces is explained in detail in chapter 4. Knowledge of fit-up force is helpful regarding making arrangements for its application and selection of detailing of detailing method.

**Table 5.3: Structural issues related to Erected fit and Final fit detailing method**

|   | <b>erected fit</b>   | <b>final fit</b>   | <b>Comments</b>  |
|---|--|--|--|
| <b>Layovers</b>   | Close to zero at erection,<br><br>Can be significant at the TDL stage                                    | Can be significant at the erection,<br><br>Close to zero at the TDL stage  | Layovers do not have significant impact on strength of the structural system   |
| <b>Component of reaction due to lack-of-fit (<math>R_{Y2}</math>)</b>   | Close to zero at erection,<br><br>Can be significant at the TDL stage and can result in potential uplift | Can be significant at the erection,<br><br>Close to zero at the TDL stage  | Uplift observed for the final fit at the SDL stage.<br><br>No uplift observed for the erected fit at the TDL stage.                            |
| <b>Component of deflection due to lack-of-fit (<math>D_{Y2}</math>)</b> | Close to zero at erection,<br><br>Can be significant at the TDL stage                                    | Can be significant at the erection,<br><br>Close to zero at the TDL stage  | $D_{Y2}$ should be included in camber calculation for the erected fit. $D_{Y2}$ should not be included in camber calculation for the final fit |
| <b>Flange lateral bending stress (<math>f_l</math>)</b>                 | Small at erection,<br><br>Can be significant when wet concrete is placed over girders                    | Can be significant at the erection due to pull and push of flanges and before casting deck,<br><br>Close to zero after completing casting the deck                             | Need calculation and comparison to AASHTO limits   |
| <b>Cross-frame Forces</b>   | Small at erection, Can be significant when wet concrete is placed over girders                           | Can be significant at the erection due to lack-of-fit of cross-frames between the girders,<br><br>Small after completing casting the deck                                      | No field problems reported for the cross-frames during construction of skew bridges.   |
| <b>Applied Fit-Up Forces</b>  | Close to zero for cases when girders are under their own weight (SDL stage)                              | Can be significant at the SDL stage because cross-frames are detailed to fit the connection at the TDL stage and therefore do not fit between the connections at the SDL stage | See chapter 4 for more detail description  |

### 5.3 Other Considerations

There are other considerations that must be taken into account, when selecting the detailing methods for skewed steel bridges. These considerations include erection, detailing and fabrication work required, and inspection during construction.

The choice of detailing method could affect different fabricators in different ways. In the erected fit method the cross-frames are detailed to fit between the girders, before casting the deck and when steel dead loads are applied. In this case there are two alternatives. A) detail and fabricate each cross-frame differently and b) vary the location of bolt holes within the stiffeners used to attach the cross-frames to the girder. Some fabricators choose to fabricate each cross-frames differently and mark them appropriately for identification and installation in the field. At a first glance, this appears to increase the amount of work significantly. However, some fabricators feel this is not the case. On the other hand for the final fit, the cross-frames are detailed to fit between the girders at the TDL stage and therefore many of them are the same if cross-slope is constant along the length of bridge. Therefore in final fit method the amount of detailing and fabrication it appears to be lower. However, the significance of these issues, considering the automation processes in place, depends largely to detailers and fabricator's capabilities.

With respect to erection, erected fit method is simpler as compared to final fit method. This is because of the fact that in erected fit method, cross-frames are detailed to fit between the girder at the SDL stage, while fit-up forces are required to fit the cross-frames between the girders in the case of final fit method. In extreme cases, the level of fit-up forces could be significant for the final fit method [2, 4].

Another consideration that deserves attention is the sequence of deck casting. There are two separate "deck casting" sequence considerations. First related to phased construction, where each half of the bridge is constructed in "stages" and then connected together using closure pour and cross-frames. The choice of detailing method in this case requires specific analysis and no general statement can be made. The second case is when deck casting sequence is used to minimize the cracking of the deck during casting. In multi-span bridges in general the positive moment sections need to be cast simultaneously, followed by casting the remaining negative moment sections, which are near supports. The recommendation is to ensure that all cross-frames are first attached, prior to doing any deck casting, which is the practice norm.

Some contractors have raised a concern about inspection. The webs of the girders are out of plumb for the final fit method during SDL stage and TDL stage for the erected fit. This behavior needs to be communicated with owner, erector and contractor and could avoid any miss communications and some of the issues reported by erectors and contractors. It should also be noted that even in the case of final fit the web could be somewhat out of plumb during TDL stage and should not be a point of concern, as web out of plumbness does not affect the structural response of skewed steel bridges, significantly.

## 5.4 Parametric Studies

Parametric studies were carried out to evaluate options a designer might consider for framing of straight skewed I girder bridges. These parametric studies include the following:

- Effect of cross-frame stiffness
- Effect of distance of first intermediate cross-frame from the support
- Effect of cross-frame orientation

### 5.4.1 Effect of Cross-frame Stiffness

Cross-frame forces are also affected by the equivalent areas of the cross-frame members,  $A_b$ , considered in modeling of the bridge. Typical single-angle or structural tee cross-frames members are subjected to additional bending deformations due to the eccentricity of their end connections normal to the connection and/or gusset plates. The corresponding bending deformations reduce the stiffness of the cross-frame members and, hence, the overall stiffness of the cross-frames [12]. In this research, the effect of reducing the equivalent area of the cross-frame members on cross-frame forces was studied. Cross-frame forces in top chord of cross-frames in Bay 7 of Bridge A for different areas of cross-frame members for the erected fit detailing method at the TDL stage are shown in Figure 5.10. The results shown in Figure 5.10 are obtained from 3D finite element analysis with flanges modeled with beam elements; however, similar results are obtained from other methods of analysis. From Figure 5.10, the following observations are made:

- The cross-frame forces are reduced by reducing the area of cross-frame members.
- The reduction in force varies significantly between different cross-frame members because redistribution of force occurs by reducing the cross-frame area.

Similar observations were observed for other bridges analyzed as part of this study.

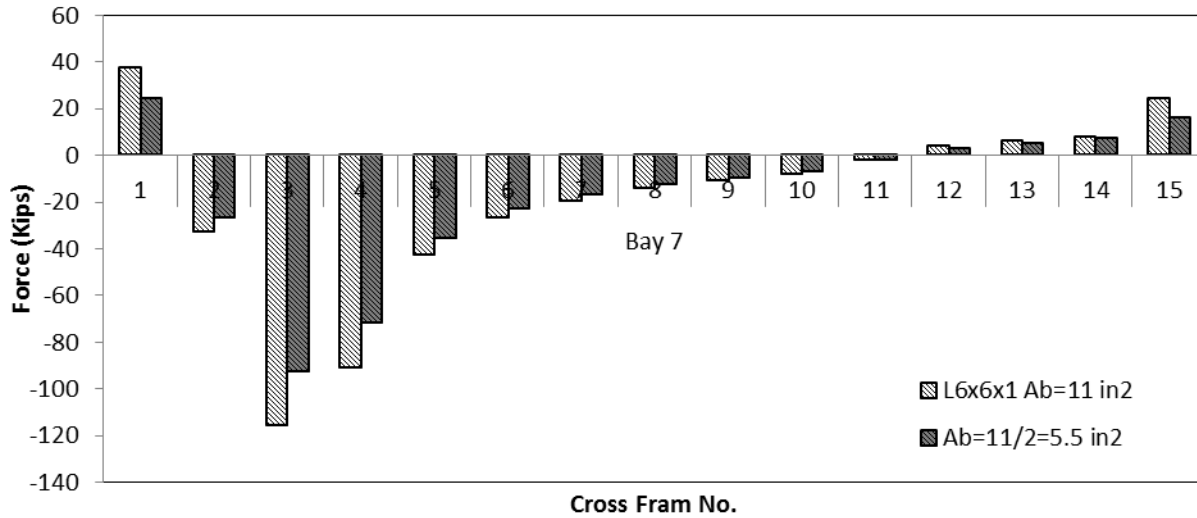


**Figure 5.10: Effect of reducing the area of cross member on cross-frame forces in Bridge A for erected fit at the TDL stage**

Table 5.4 provides summary of reduction in maximum cross-frame force by reducing the area of cross-frame members by half for Bridge A, Bridge B and Bridge C. As shown in Table 5.4 the maximum cross-frame force does not reduce significantly by reducing the area of cross-frame member to half for bridges studied.

**Table 5.4: Summary of effect area of cross-frame members on cross-frame forces**

|  | Bridge A |      | Bridge B |       | Bridge C |       |
|--|----------|------|----------|-------|----------|-------|
| Area of cross-frame members (in <sup>2</sup> ) | 11       | 5.5  | 5.75     | 2.875 | 2.87     | 1.435 |
| Maximum Absolute cross-frame force (kips)      | 115.6    | 92.9 | 38.5     | 24.4  | 20.3     | 14.5  |

#### 5.4.2 Effect of Distance of the First Intermediate Cross-frame from Support

Field observations indicate that distance between support and first intermediate cross-frame has significant influence during erection of skewed steel girder bridges. To study the this parameter, framing plan of Bridge A was changed to create several framing plan that are identical, except the distance

between the support and first intermediate cross-frame, as shown in Figure 5.11. This objective, as shown in Figure 5.11, was achieved by varying the distance between support and first cross-frame by 6 ft. increment, while keeping the spacing between other cross-frames at constant 26 ft.

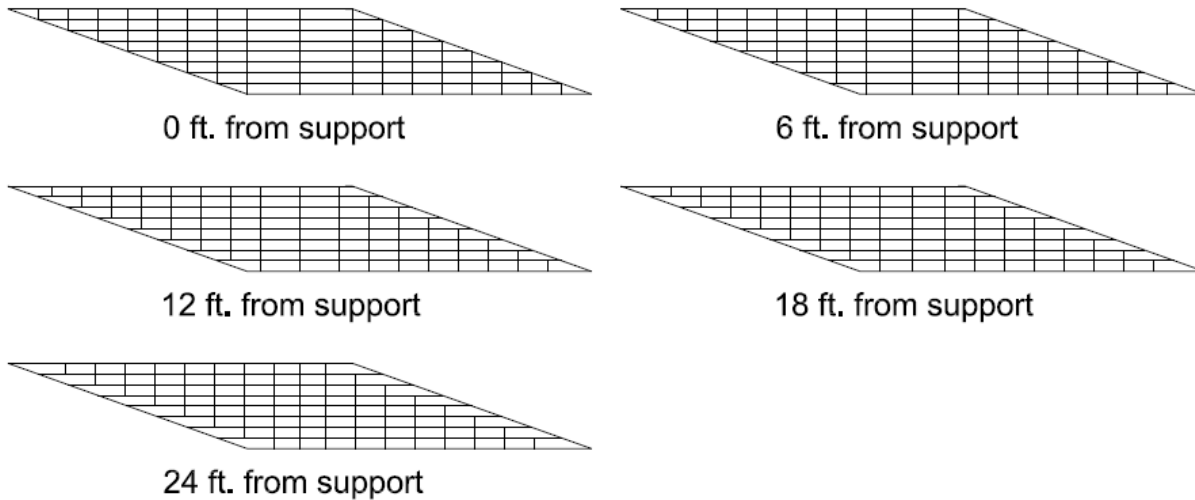


**Figure 5.11: Framing planes to study effects of location of first intermediate cross-frame from the support in bridge A**

Different structural responses, such as layovers, cross-frame forces, reactions were then evaluated through 3D FEM analysis for the erected fit detailing method at the TDL stage for the framing plans shown in Figure 5.11. Out of different structural responses, cross-frame forces appear to be most affected by varying the distance between the support and first cross-frame, as shown in Figure 5.12. Cross-frame forces decrease with increase in distance of first intermediate cross-frame from the support. However, the total change in cross-frame force is about 25% for changing the location of first intermediate cross-frame from the support from 0 ft. to 24 ft. The influence of distance between support and first cross-frame does not appear to significantly influence the reactions, as shown in Figure 5.12. Similarly the results of this study also show that layovers are not affected significantly by distance between support and first cross-frame.

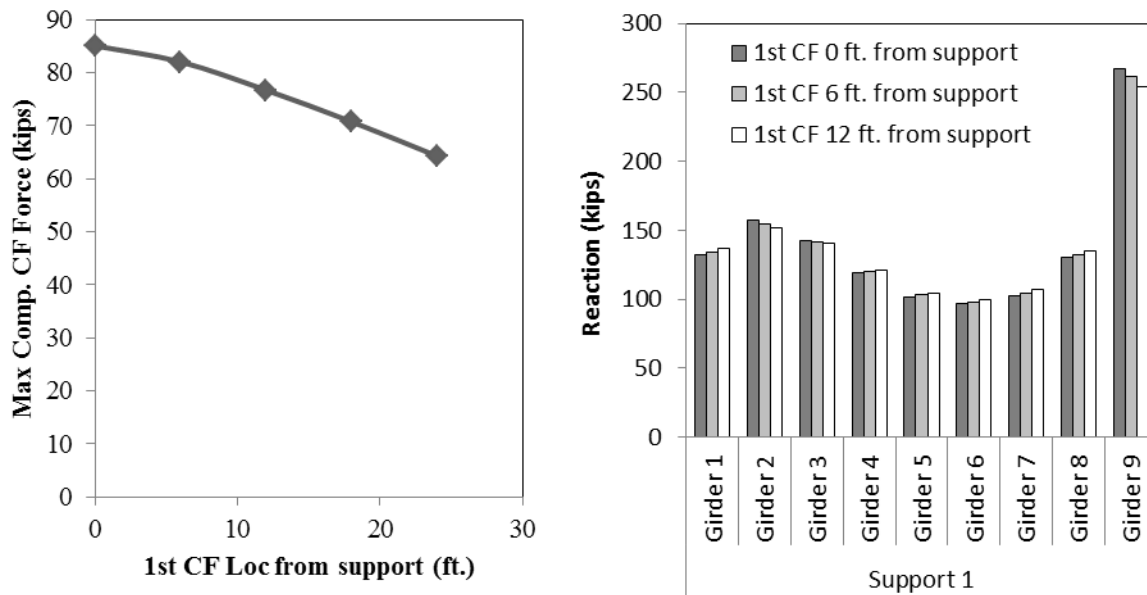


**Figure 5.12: Variation of structural responses by changing location of first intermediate cross-frame from the support in bridge A with erected fit detailing under TDL**

Effects of distance between support and first intermediate cross-frame need to be evaluated for a continuous bridge because the cross-frames on the opposite sides of the continuous support in the continuous bridge twist the girders in opposite directions and that can magnify certain structural responses.

A typical two-span (150 ft. and 140 ft.) continuous bridge with a skew of 60.0° at all supports was selected to study the effects of distance between support and first intermediate cross-frame. The bridge has six 54-inch-deep girders spaced at 8.2 ft. c/c. Top and bottom flanges are 18 inch wide with varying thickness along the length of the girder (1 inch thick from 0 ft. to 88 ft., 1.75 inch thick from 89 ft. to 118 ft., 2.75 inch thick from 119 ft. to 176 ft., 1.75 inch thick from 177 ft. to 206 ft., and 1 inch thick from 207 ft. to 290 ft.). The girders of the bridge are braced with X-type cross-frames containing 4 x 4 x 3/8 angles. The bridge uses cross-frames at spacing of 14 ft. near the support. Framing planes of the bridge used for this study are shown in Figure 5.13

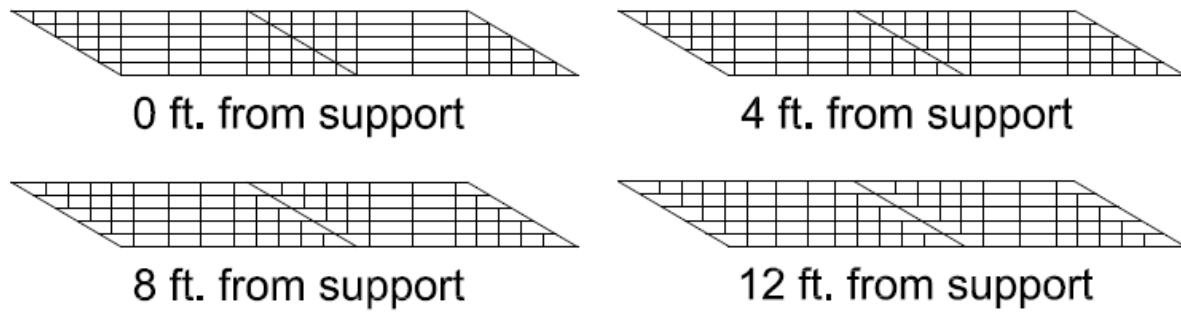


**Figure 5.13: Framing planes to study effects of location of first intermediate cross-frame from the support in a continuous bridge**

Different structural responses, such as layovers, cross-frame forces, reactions were then evaluated through 3D FEM analysis for the erected fit detailing method at the TDL stage for the framing plans shown in Figure 5.13.

Out of different structural responses, cross-frame forces appear to be most affected by varying the distance between the support and first cross-frame, as shown in Figure 5.14. Cross-frame forces decrease with increase in distance of first intermediate cross-frame from the support. However, total change in cross-frame force is about 30% for changing the location of first intermediate cross-frame from the support from 0 ft. to 12 ft. The influence of distance between support and first cross-frame, does not appear to significantly influence the reactions, as shown in Figure 5.15. Similarly results of this study also shows that layovers are not affected significantly by distance between support and first cross-frame.

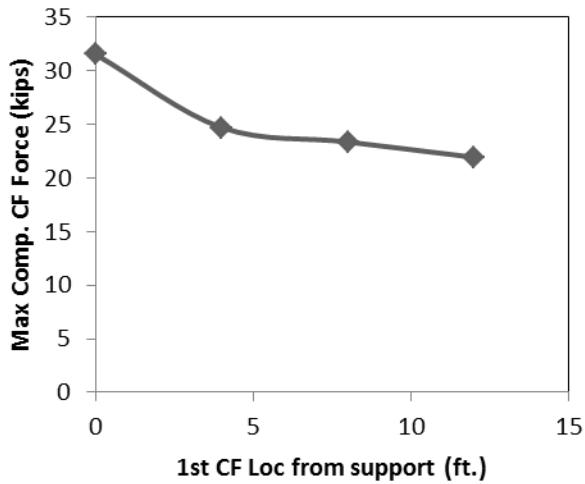


**Figure 5.14: Variation of cross-frame forces by changing location of first intermediate cross-frame from the support for erected fit at the TDL stage**

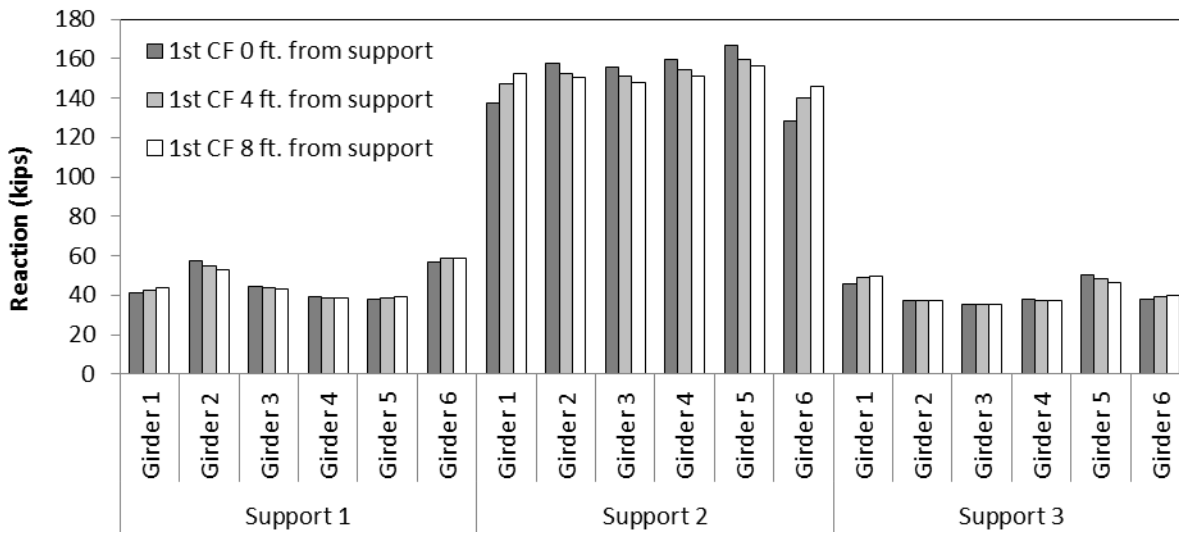


**Figure 5.15: Variation of reactions by changing location of first intermediate cross-frame from the support for erected fit at the TDL stage**

### 5.4.3 Effect of Cross-frame Orientation

Different cross-frame orientations are normally used to mitigate the layovers in the girders. Comparison of two such framing options is done here for Bridge A. In framing plan 1 cross-frame are attached perpendicular to girder and are staggered along the length of the bridge as shown in Figure 5.16a. The framing plane 2 has cross-frames place parallel to skewed supports with typical cross-frame spacing of 20ft as shown in Figure 5.16b.

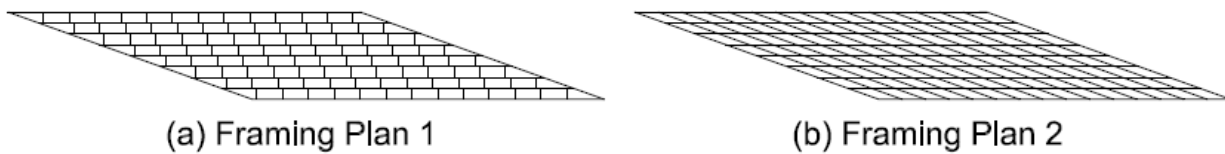
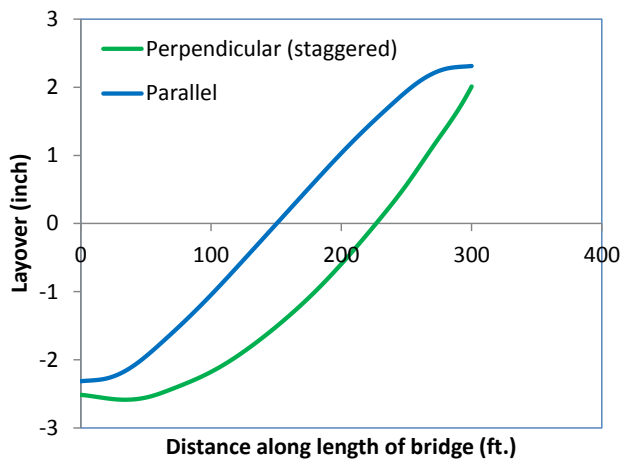


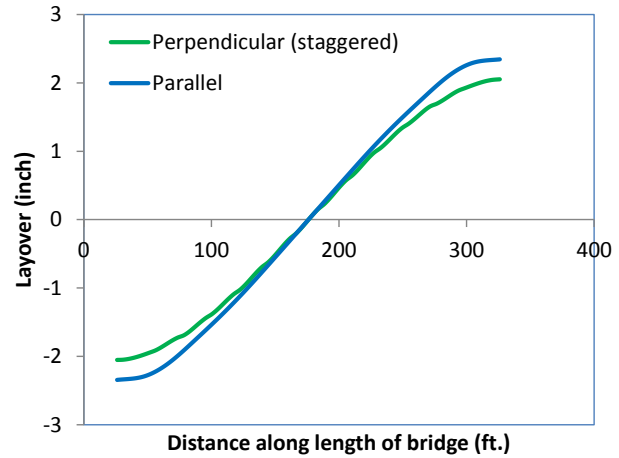
**Figure 5.16: Different cross-frame orientations**

As discussed in chapter 2 there are two major sources of twist in the straight skewed bridges and these are differential deflection of the points attached by cross-frames perpendicular to web and rotation of the cross-frame parallel to the skew. In framing plan 1, layovers appear due to both differential deflection and rotation of cross-frames parallel to skew, whereas in framing plan 2, layovers appear from rotation of the cross-frames parallel to skew only. For these cases the layovers are compared for the erected fit detailing method at the TDL stage.

Comparison of layovers obtained for different framing options are shown for Girder 1 and Girder 5 of Bridge A in Figure 5.17. In Girder 1 layovers are higher for framing plan 1 compared to the layovers obtained for framing plan 2. For Girder 5 layovers are less for framing plane 1 compared to framing plane 2. In both case the difference in layovers is not that significant. Results of the study indicate that having the cross-frame parallel to skew does not significantly reduce the layovers. When cross-frames are parallel to skew, they still cause twist of the girder, because axis of rotation of these cross-frames is not parallel to the major axis bending axis of rotation of girders.



(a) Girder 1

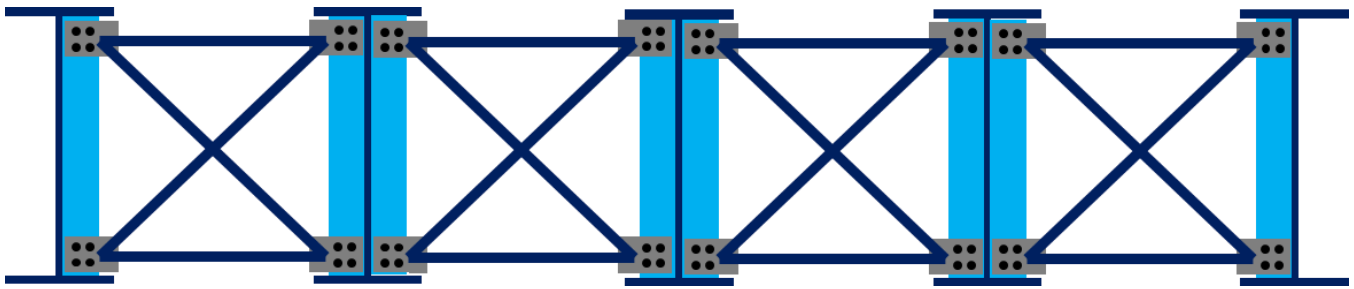


(b) Girder 5

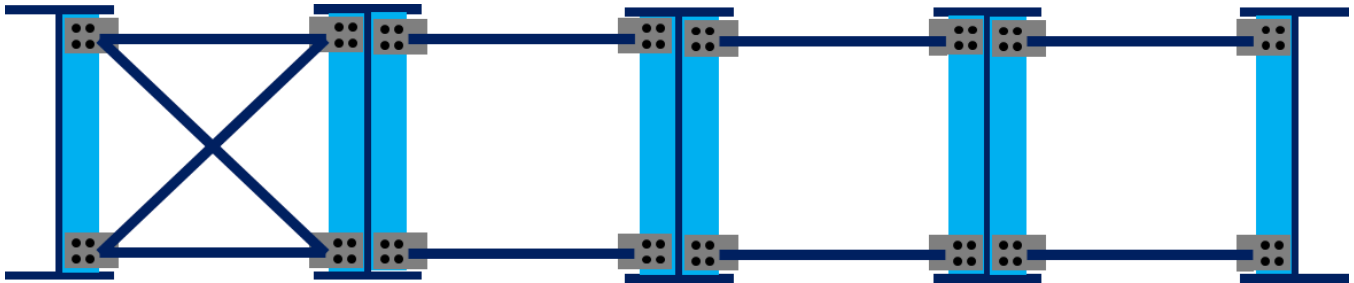
**Figure 5.17: Layover for different cross-frame orientations for erected fit at the TDL stage**

## 5.5 Cross-frame Configuration

The lean on bracing system is developed by eliminating the diagonal cross-frame members from a conventional bracing system. In traditional bracing layouts for steel bridges, a bracing line typically has a full line of cross-frames across the bridge. The cross frames are typically comprised of two struts and two diagonal members. In a lean-on system, full cross frames are positioned in some of the bays within a bracing line while select cross frames are replaced with systems that only have top and bottom struts. Such a system is shown in Figure 5.18. In the lean-on bracing system the girders attached to cross-frames with only top and bottom chord “lean” on the girders attached with full cross-frames. Elimination of diagonal members from the cross-frames results in the reduction of cross-frame forces due to differential deflection in skew bridges. A potential framing plan of a skew bridge using lean-on bracing system is shown in Figure 5.19. The cross-frames marked with X have full cross-frames while other cross-frames have only top and bottom chord members. The full cross-frames are arranged along the longer diagonal of skew bridge, between the acute corners, instead of the shorter diagonal, between the obtuse corner, that has large stiffness. It is important to have a few intermediate within at least every bay so that differential displacement of the girder is controlled. The detailed design of cross-frames is provided elsewhere [13].



(a) Conventional Bracing



(b) Lean-On Bracing

**Figure 5.18: Conventional and lean-on bracing line.**

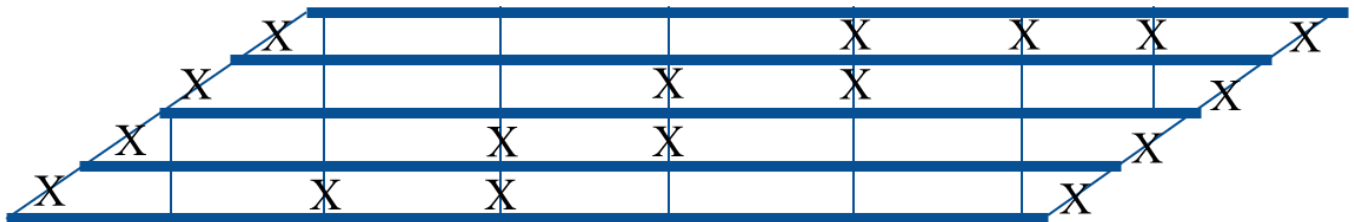


**Figure 5.19: A skew bridge with lean-on bracing system**

The lean on bracing system was implemented in three skewed bridges in Lubbock, Texas. One of the bridge was the 19<sup>th</sup> Street Bridge in Lubbock, Texas (shown in Figure 5.20). The bridge is two spans continuous with 60° skew at supports consisting of six girders that are 300 ft long and 54 inches deep. The bridge was instrumented to get the cross-frame forces, deflection and layovers during deck casting. The instrumented cross-frame had 14.5 kips tension and 2.7 kip compression during deck casting. Due

to use of stiff bearing pads in the bridge, field measured rotation was less than predicted by the ANSYS 3D model that assumed flexible supports. The maximum measured rotation was around  $0.51^\circ$ .



**Figure 5.20: Lean-on bracing system in 19<sup>th</sup> street Bridge**

Lean-on bracing might reduce fabrication costs due to fewer bracing members. It might also provide advantages in maintenance over the life of the bridges due to fewer cross-frames to inspect. The most significant advantage of using lean-on cross-frame concepts in skewed bridges is the reduction in cross-frame forces under truck traffic in the completed bridge, compared to cross-frame force in a conventional cross-frame layout.

Lean-on cross-frame configuration is not available in most the commercial 2D grid analysis software. There are no studies on the effect of lean on bracing on the redundancy bridge. Using lean on bracing is not a well-established common practice in steel bridge. Lean-on bracing is designed based on stability; however AASHTO LRFD code does not include the design of braces based on stability.

## 5.6 Flow Chart for Design

Ultimate choice of detailing method is left to owner and designer. The selection of the detailing method depends on many factors and the final choice that could be influenced by several factor, such as, local practices and owner, designer, fabricator and erector preferences. However, a flow chart was developed for each detailing method, as shown in Figure 5.21 to facilitate the selection of detailing method.

Flange lateral bending stress,  $f_l$  needs to be checked for both final fit and erected fit detailing methods to satisfy the AASHTO bridge design requirements. For the final fit detailing method  $f_l$  at the SDL stage comes from lack-of-fit and wind load. For the erected fit detailing method  $f_l$  at the TDL stage comes from lack-of-fit and knee braces. AASHTO LRFD Bridge Design Specifications should be used to check the level of flange lateral bending stresses,  $f_l$ . There may be a need to increase the flange sizes, which may dictate the choice of detailing method.

In final-Fit method the additional structural response that needs to be checked is the fit-up forces required for fitting the cross-frames between the adjacent girders during erection. The knowledge of fit-up forces will allow erector to assess the need for having special equipment to fit the cross-frames between the adjacent girders.

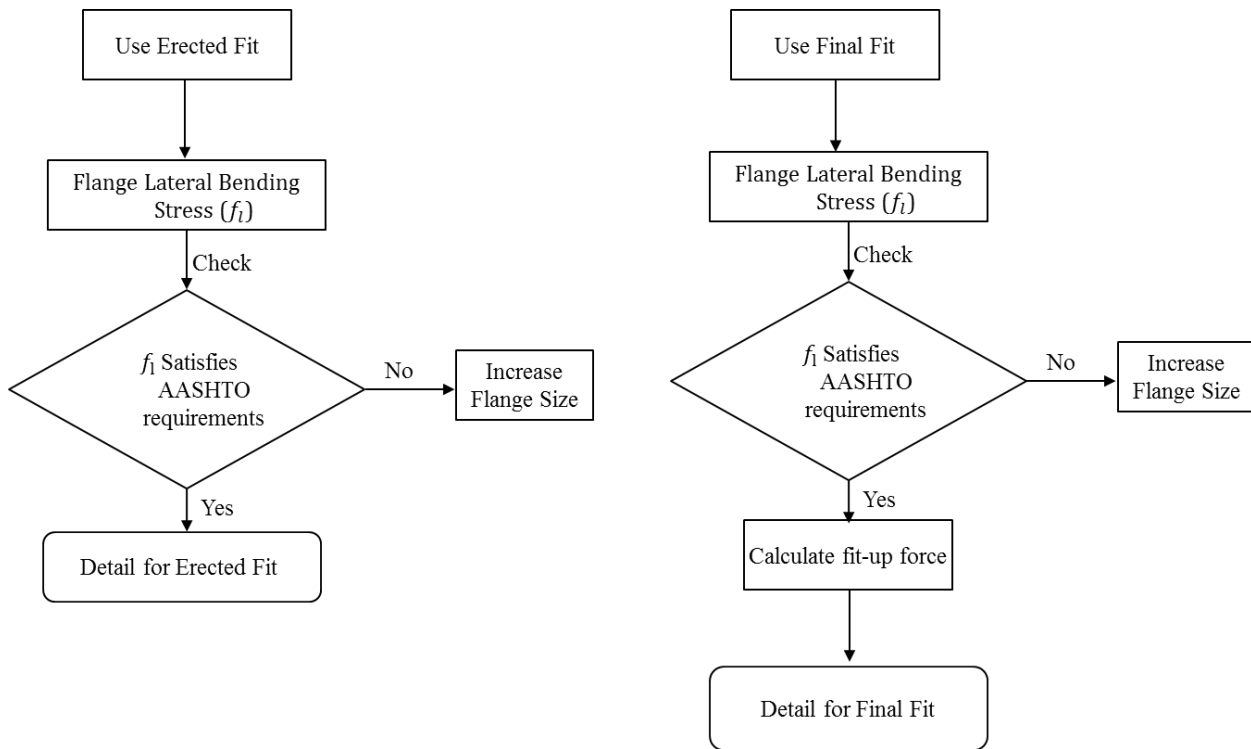


**Figure 5.21: Flow chart to guide designer to deal with skew bridges**

## 5.7 Summary and Conclusions

This chapter provides recommendation to calculate the cambers for the erected fit and final fit detailing methods. For the erected fit detailing method, SDL cambers should be estimated by line girder analysis and concrete dead load (CDL) cambers should be calculated by 2D grid analysis or 3D FEM analysis modeling all the girders and cross-frames connected together. For the final fit detailing method both SDL and CDL cambers need to be calculated by line girder analysis.

From these limited analysis following conclusions could be made:

- 1- The recommended procedure does a good job of predicting the camber for the final fit detailing method.
- 2- When cross-frames are staggered or for odd cases, where one would be suspicious about accuracy of 2D grid analysis, camber needs to be calculated using refined methods of analysis.

This chapter also provides summary of lack-of-fit effects in skewed and straight steel girder bridges and related field challenges. Important lack-of-fit effects that need to be checked for a particular detailing method are identified. Summary of other construction issues, such as detailing and fabrication, deck casting sequence, and inspection during erection is also provided. Parametric studies have shown that distance of first intermediate cross-frame from the support and reducing the cross section area of cross-frame members do not have significant effect on cross-frame forces and other lack-of-fit effects. Further arranging the cross-frames parallel to skewed supports or perpendicular to the girders do not change the maximum value of layover significantly. Finally, a flowchart was developed for each detailing method to facilitate the selection of detailing method and carrying the necessary design calculations.

## Chapter 6 CONCLUSIONS AND RECOMMENDATIONS

Summary of main conclusion are provided at the end of every chapter. This chapter lists the main conclusions the project.

- Lack-of-fit effects for the final fit detailing method at the steel dead load stage are equal and opposite to the lack-of-fit effects for the erected fit detailing method at the total dead load stage. The lack-of-fit effect include the following
  - Girder layovers
  - Cross-frame forces
  - Flange lateral bending stress
  - Component of vertical deflection due to lack-of-fit
  - Component of vertical reaction due to lack-of-fit
  - Lateral reaction/movement
- Improved 2D GA can be used to estimate the lack-of-fit effects for both the final fit and the erected fit detailing method. However, for bridges with staggered bracing improved 2D grid analysis overestimates some lack-of-fit effect especially when staggered distance is very small.
- A relatively simple 3D FEM analysis using dead and live cross-frames can be used in lieu of 3D FEM analysis using initial strains to get steel dead load state of the bridge frame detailed with final fit detailing method.
- Maximum level of fit-up force required during the erection can be estimated by the cross-frame forces evaluated from improved 2D grid analysis.
- Attaching the cross-frame starting from the middle of the bay and moving toward the ends might help in reducing the fit-up forces
- The recommendation on calculation of camber for straight skewed bridges is given in Table 5.1.
- The ultimate choice is left to owner, designer, and contractor to select the detailing method of their choice. However, a flow char is developed for each detailing method to facilitate the selection and carryout the necessary checks as shown in Figure 5.21.
- Flange lateral bending stress needs to be checked for both detailing methods to satisfy the AASHTO LRFD specification requirements.

- For the final fit detailing method fit-up forces are also required to be calculated and communicated to erector. The magnitude of the fit-up forces and erector's capability to apply the fit-up force might dictate the selection of the detailing method.

## References

- [1] AASHTO. (2010). American Association of State Highway and Transportation Officials. *AASHTO LRFD Bridge Construction Specifications, 5th Ed.*, AASHTO. Washington, DC.
- [2] Ozgur, C. (2011). *Influence of Cross frame detailing on curved and skewed steel I-Girder Bridges*. PhD Thesis . Georgia Institute of Technology.
- [3] Grunauer, T. A. (2011). *Influence of bracing systems on the behaviour of curved and skewed steel I-Girder Bridges during construction*. PhD thesis . Georgia Institute of Technology.
- [4] White, D. W., Coletti, D., Chavel, B. W., Sanchez, A., Ozgur, C., Chong, J. M., et al. (2012). *NCHRP 725: Guidelines for Analysis Methods and Construction Engineering of Curved and Skewed Steel Girder Bridges*. NCHRP and NSBA.
- [5] Norton, E., Linzell, D., & Laman, J. (2003). Examination of the Response of a Skewed Steel Bridge Superstructure During Deck Placement. *Journal of the Transportation Research Board No. 1845* , 66-75.
- [6] Ahmadi, A. K., & Henney, R. (2005). Lessons Learned from the Construction of a Sharply Skewed, Two-span, Steel Multi-girder Bridge. *22nd Annual International Bridge Conference June 13-15, 2005* (pp. 520-527). Pittsburgh, PA: Engineers Society of Western Pennsylvania.
- [7] AASHTO/NSBA, C. S. (2011). *G 13.1 Guidelines for steel girder bridge analysis*. AASHTO/NSBA Steel Bridge Collaboration.
- [8] Linzell, D., Chen, C., Sharafbayani, M., Seo, J., Nevling, D., Jaissa-Ard, T., et al. (2010). *Guidelines for Analyzing Curved and Skewed Bridges and Designing them for Construction*. Harrisburg, PA: Pennsylvania Department of Transportation.
- [9] Chavel, B. W., & Earls, C. J. (2006). Construction of a horizontally curved steel I-girder bridge: Inconsistent detailing. *Journal of Bridge Engineering, Vol. 11, No. 1* , 91-98.
- [10] ANSYS. (2009). ANSYS Release 12.1 UP20091102. *Analysis Software* . Copyright 2009 SAS IP, ANSYS Inc.

- [11] Ahmed, M., & Weisberger, F. (1996). Torsion Constant for Matrix Analysis of Structures Including Warping Effect. *International Journal of Solids and Structures, Elsevier* 33(3) , 361-374.
- [12] Wang, W. H., Battistini, A. D., Helwig, T. A., Engelhardt, M. D., & Frank, K. H. (2012). Cross Frame Stiffness Study by Using Full Size Laboratory Test and Computer Models. *Proceedings of Structural Stability Research Council/North American Steel Construction Conference, Grapevine, TX, April 17-21, 2012.*
- [13] Wang, W. (2013). A Study of Stiffness of Steel Bridge Cross Frames. *Doctoral Dissertation* . The University of Texas at Austin.

## Appendix A: Description of Bridges

Three straight skewed, simply supported I-girder bridges, having different levels of skew, are selected for consideration in this study. All three bridges have their girders and cross-frames designed with Grade 50 steel having a modulus of elasticity of 29,000 ksi.

Bridge ‘A’ is an extreme case of straight skew bridges and is used to show extreme skew effects in previous studies [1, 2, 3][1][2][3]. Bridge ‘A’ has 300 ft. long 144 inches deep girders simply supported on 70.4° skewed supports. The girders of Bridge ‘A’ are braced with X-type cross-frames containing 6 x 6 x 1 angles. The bridge uses staggered cross-frames at spacing of 22 ft. between 9 girders at 9.25 ft. c/c spacing. Framing planes and sizes of the web and flanges of the bridges studied are shown in Figure 2.4.

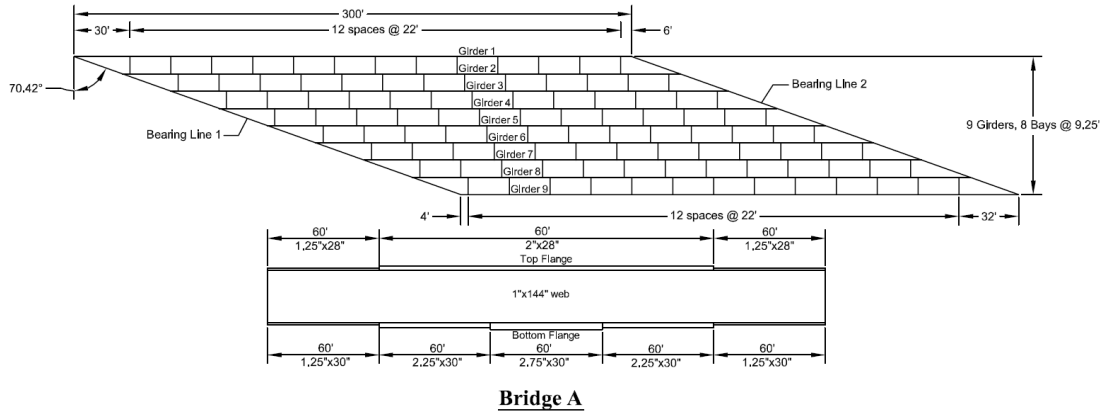


**Figure A.1: Framing plans and girder sizes of the Bridge A**

Bridge ‘B’ is another highly skewed bridge, however skewed effect in Bridge ‘B’ are smaller compared to Bridge ‘A’. Bridge ‘B’ has 266 ft. long 120.5 inches deep girders simply supported on 62.6° skewed supports. The girders of the Bridge ‘B’ are braced with X-type cross-frames containing 6 x 6 x 1/2 angles. The bridge uses cross-frames at spacing of 16 ft. between 8 girders@7.26 ft. c/c spacing. Framing planes and sizes of the web and flanges of the bridges studied are shown in Figure 2.5.

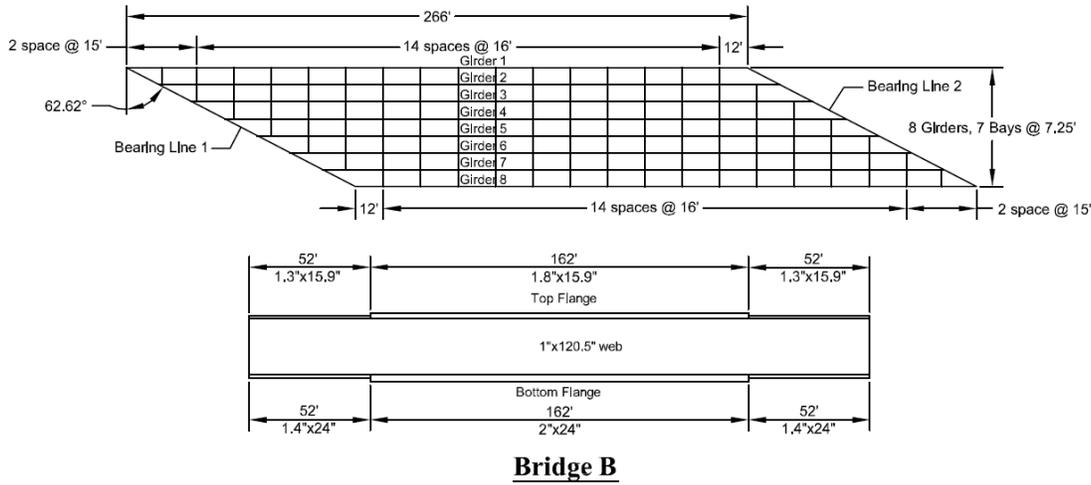


**Figure A.2: Framing plans and girder sizes of the Bridge B**

Bridge 'C' has 150 ft. long 56.1 inches deep girders simply supported on 70.0° skewed supports. The girders of the Bridge 'C' are braced with X-type cross-frames containing 6 x 3 1/2 x 5/16 angles. The bridge uses cross-frames at spacing of 21 ft. between 4 girders@8ft. c/c spacing. Framing planes and sizes of the web and flanges of the bridges studied are shown in Figure 2.6.

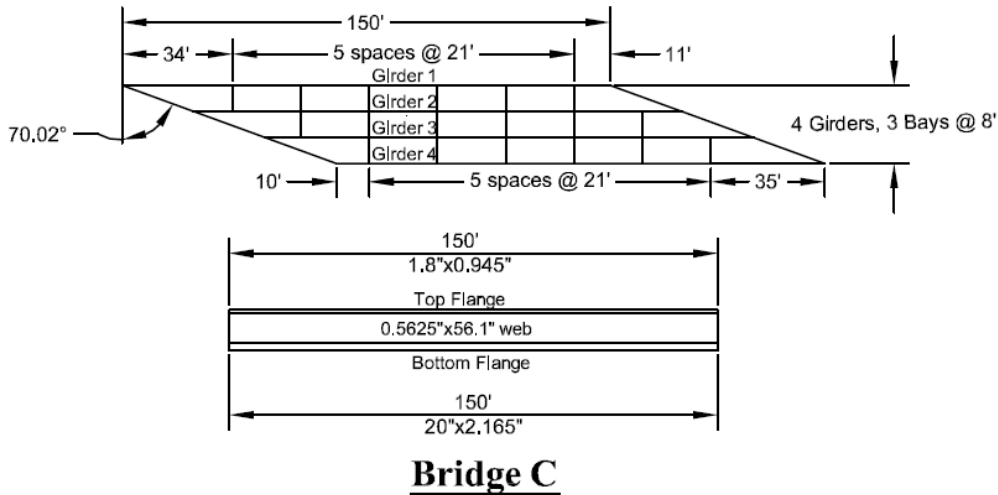
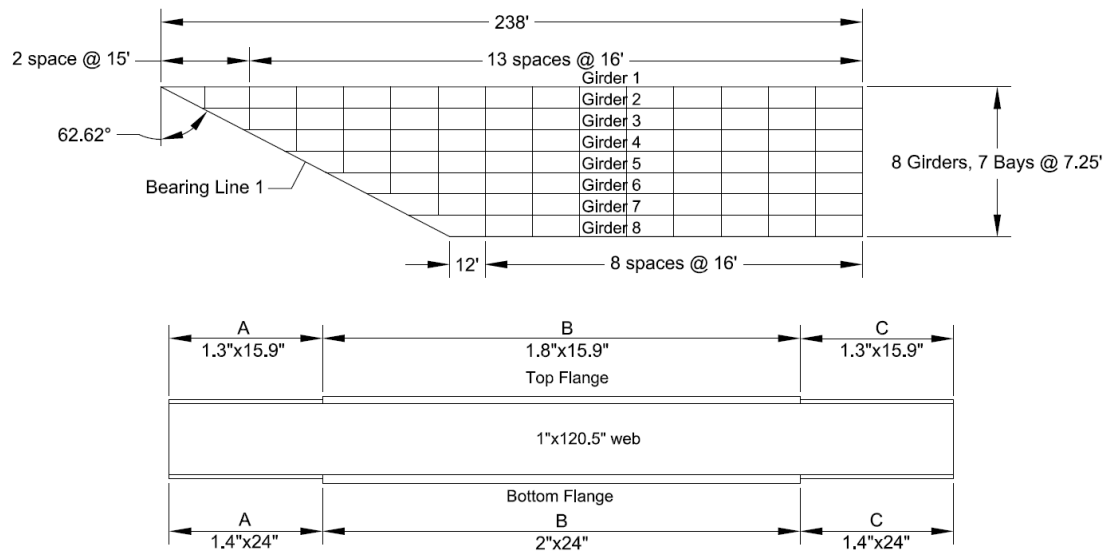


**Figure A.3: Framing plans and girder sizes of the Bridge C**



### **Bridge B2**

**Figure A.4: Framing plans and girder sizes of the Bridge B2**

|          | A (ft.) | B (ft.) | C (ft.) | L (ft.) |
|----------|---------|---------|---------|---------|
| Girder 1 | 79      | 79      | 80      | 238     |
| Girder 2 | 75      | 75      | 74      | 224     |
| Girder 3 | 70      | 70      | 70      | 210     |
| Girder 4 | 65      | 65      | 66      | 196     |
| Girder 5 | 61      | 61      | 60      | 182     |
| Girder 6 | 56      | 56      | 56      | 168     |
| Girder 7 | 51      | 51      | 52      | 154     |
| Girder 8 | 47      | 47      | 46      | 140     |

# Appendix B: Comparison of Detailing Methods

## B.1 Concrete Dead Load Deflections

### B.1.1 Bridge A

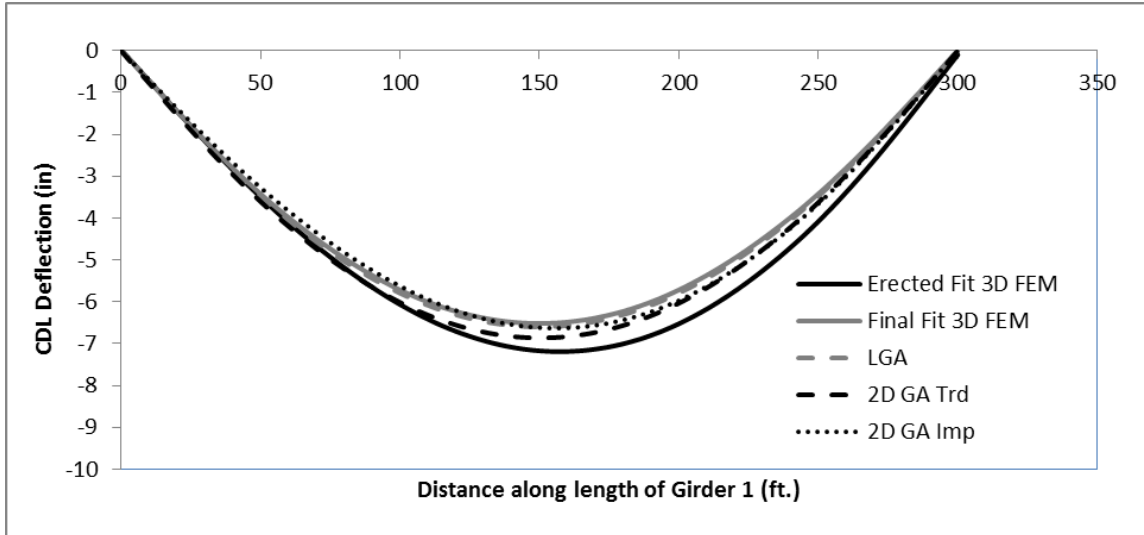


Figure B.1: Concrete dead load (CDL) deflection in Girder 1 of Bridge A

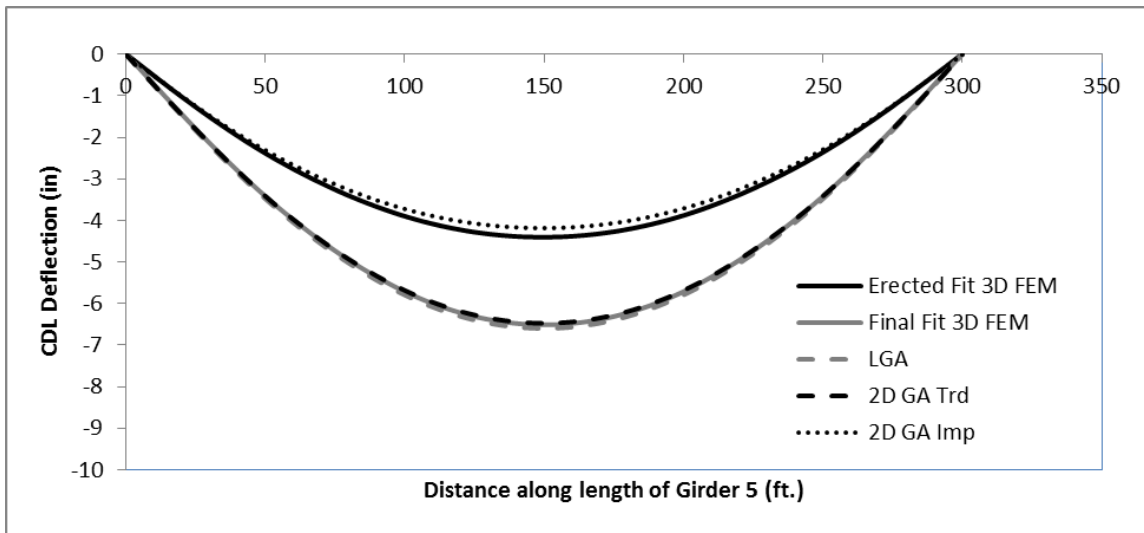


Figure B.2: Concrete dead load (CDL) deflection in Girder 5 of Bridge A

### B.1.2 Bridge B

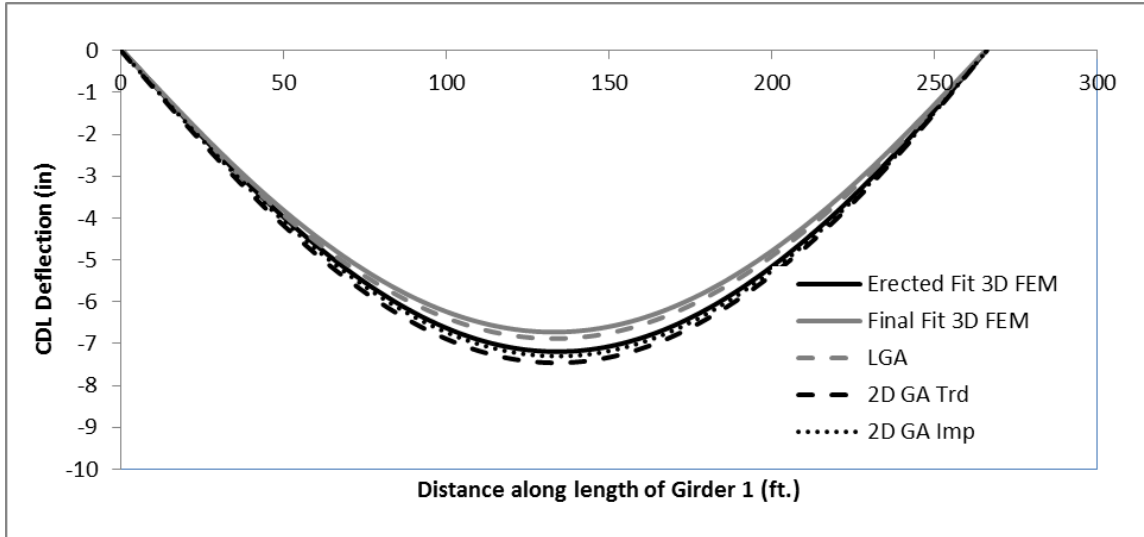


Figure B.3: Concrete dead load (CDL) deflection in Girder 1 of Bridge B

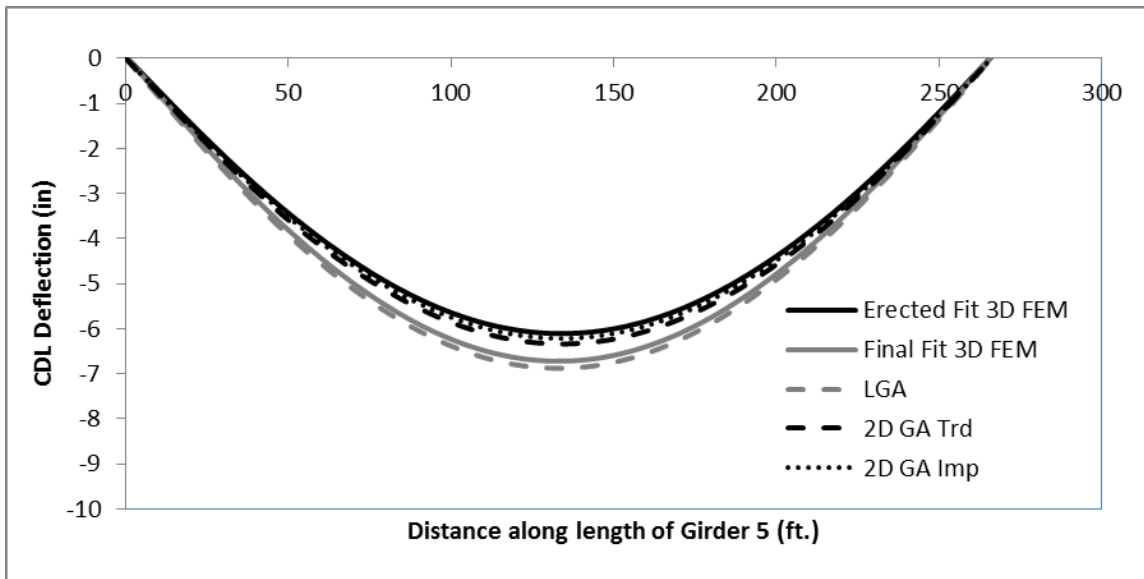


Figure B.4: Concrete dead load (CDL) deflection in Girder 5 of Bridge B

### B.1.3 Bridge C

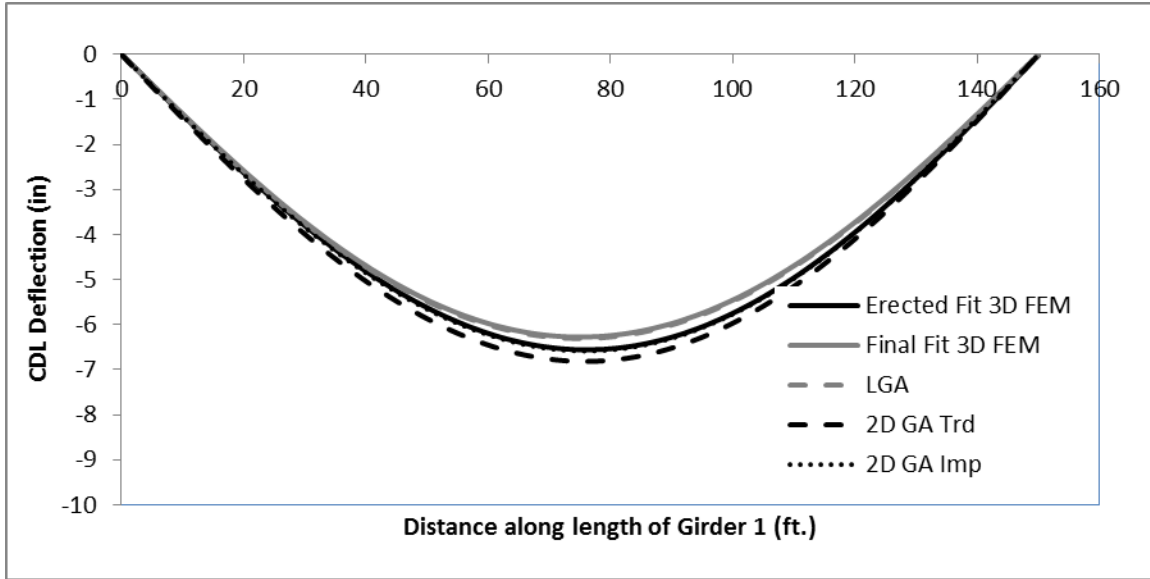


Figure B.5: Concrete dead load (CDL) deflection in Girder 1 of Bridge C

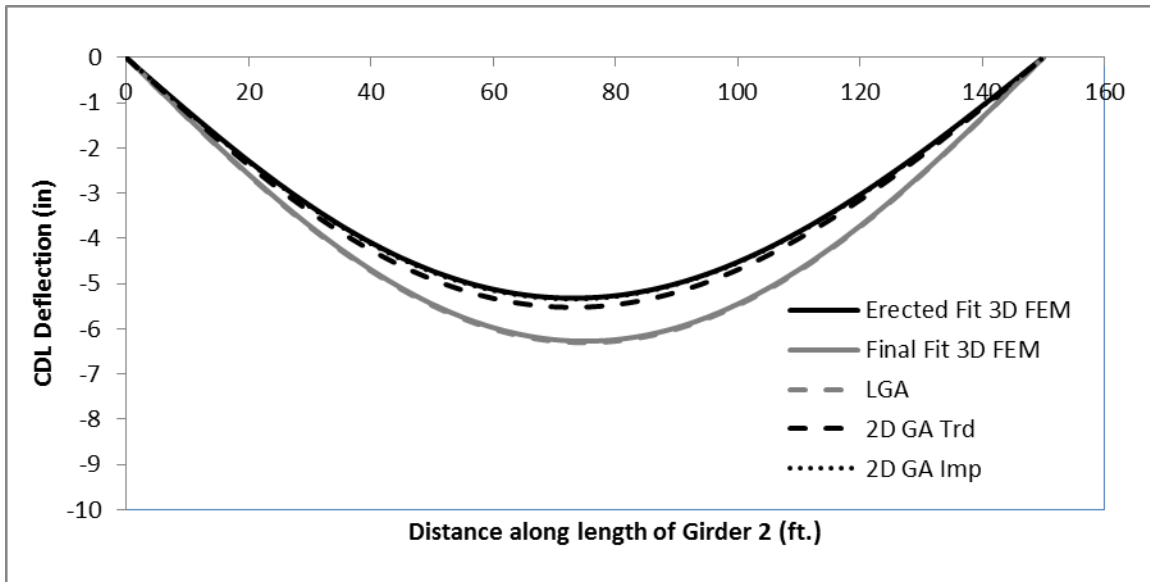
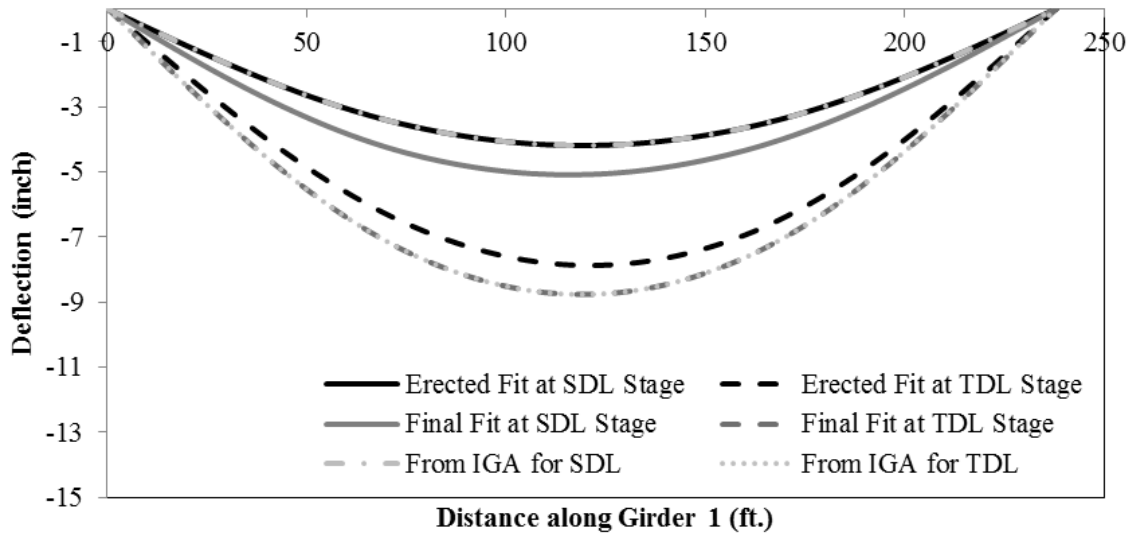
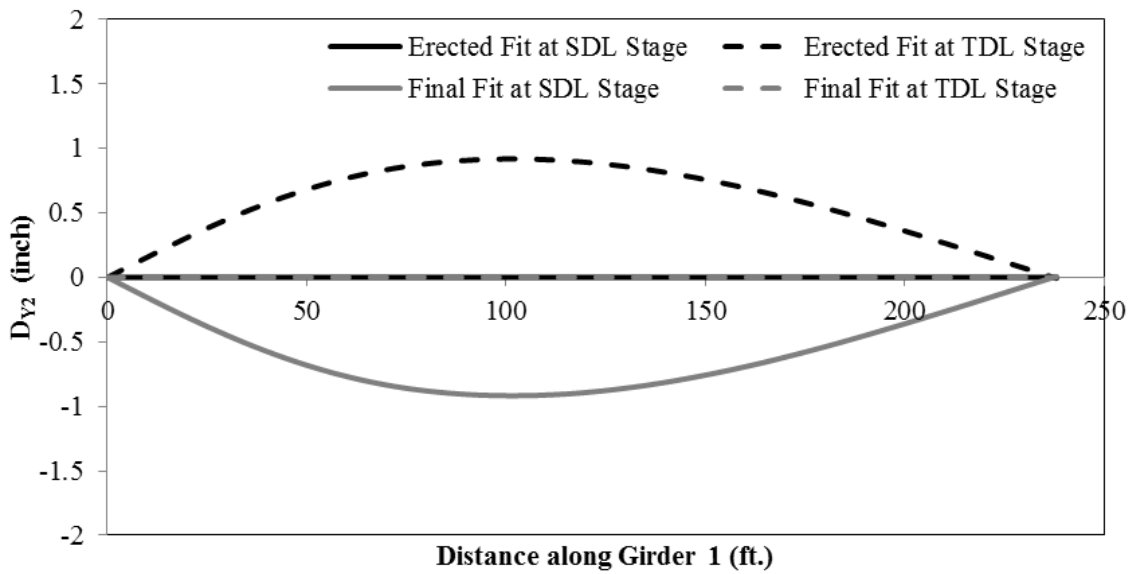


Figure B.6: Concrete dead load (CDL) deflection in Girder 2 of Bridge C

### B.1.4 Bridge B2



**Figure B.7: Deflection in Girder 1 of Bridge B2 for different detailing methods at different loading stages of construction**



**Figure B.8: Component of deflection due lack-of-fit in Girder 1 of Bridge B2 for different detailing methods at different loading stages of construction**

## B.2 Layovers

### B.2.1 Bridge A

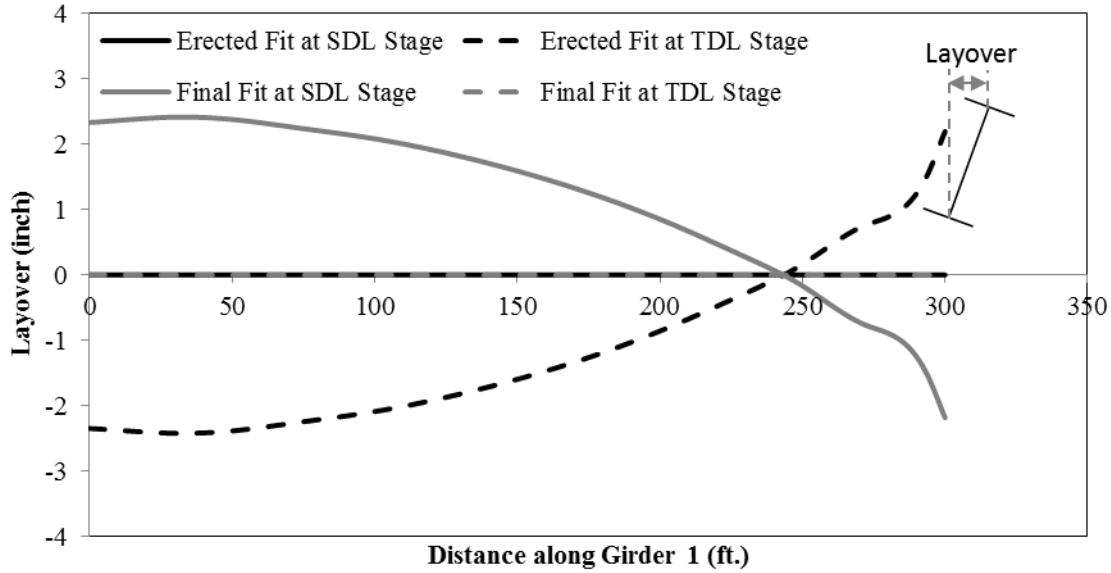


**Figure B.9: Layovers in Girder 1 of Bridge A for different detailing methods at different loading stages of construction**

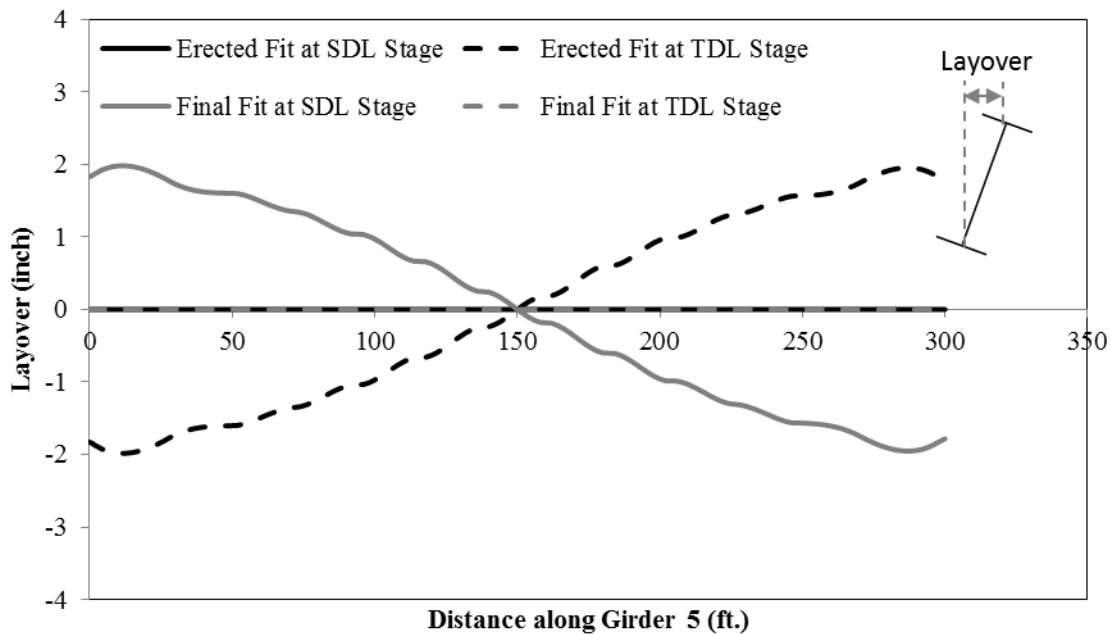


**Figure B.10: Layovers in Girder 5 of Bridge A for different detailing methods at different loading stages of construction**

### B.2.2 Bridge B

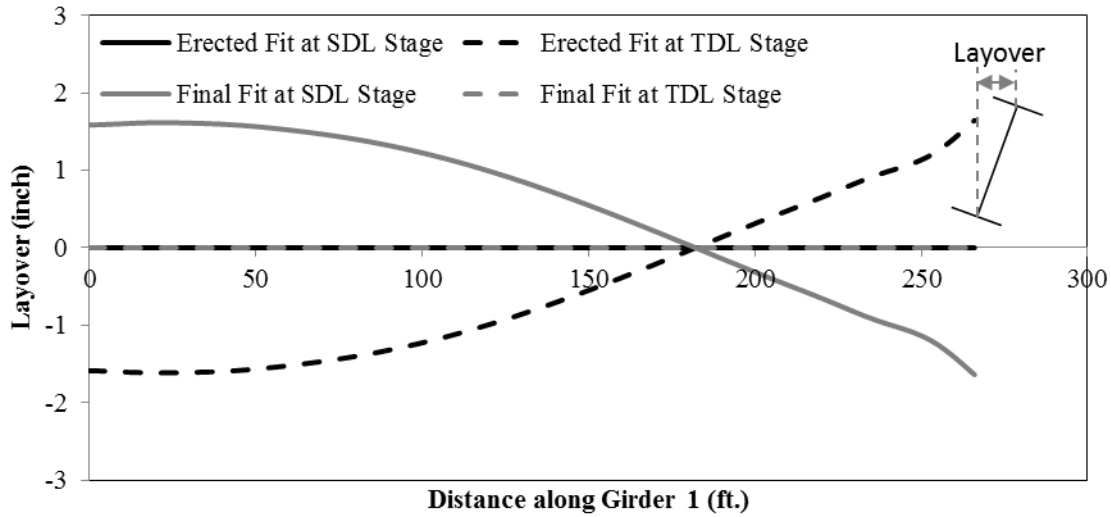


**Figure B.11: Layovers in Girder 1 of Bridge B for different detailing methods at different loading stages of construction**

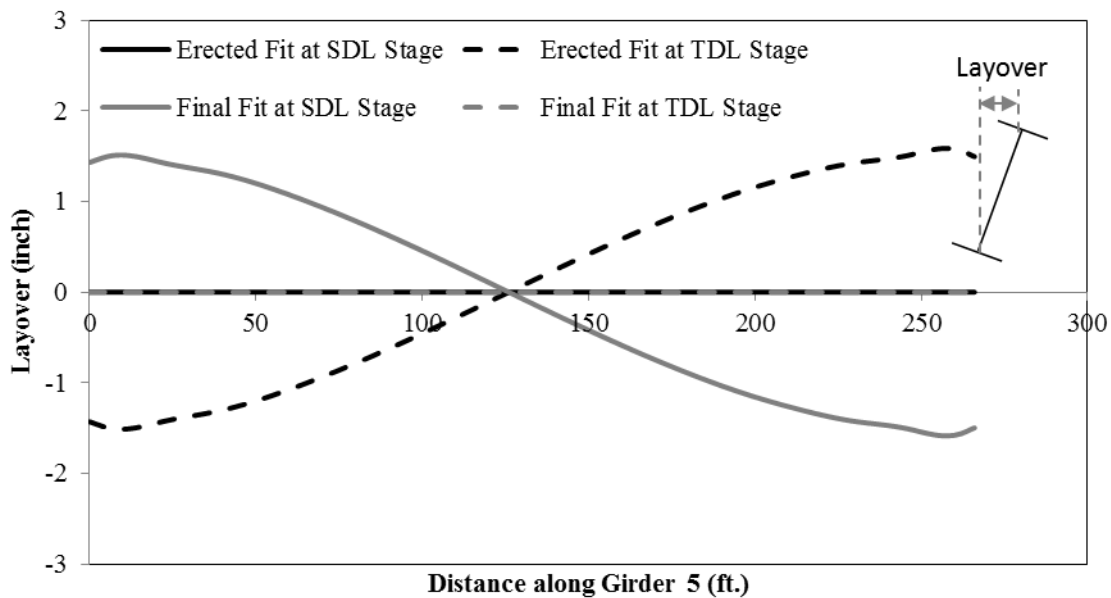


**Figure B.12: Layovers in Girder 5 of Bridge B for different detailing methods at different loading stages of construction**

### B.2.3 Bridge C

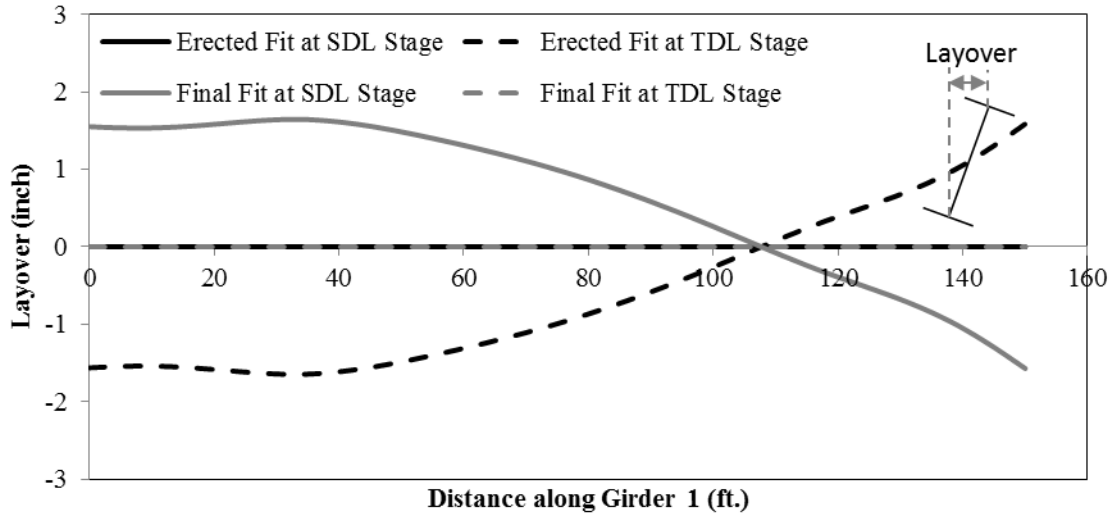


**Figure B.13: Layovers in Girder 1 of Bridge C for different detailing methods at different loading stages of construction**

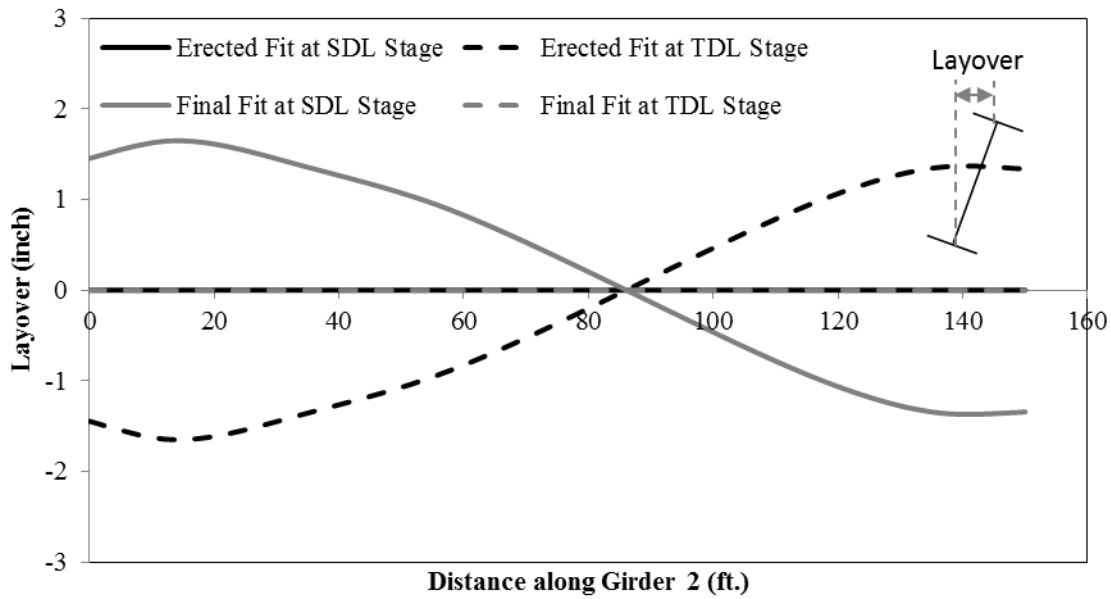


**Figure B.14: Layovers in Girder 2 of Bridge C for different detailing methods at different loading stages of construction**

### B.2.4 Bridge B2

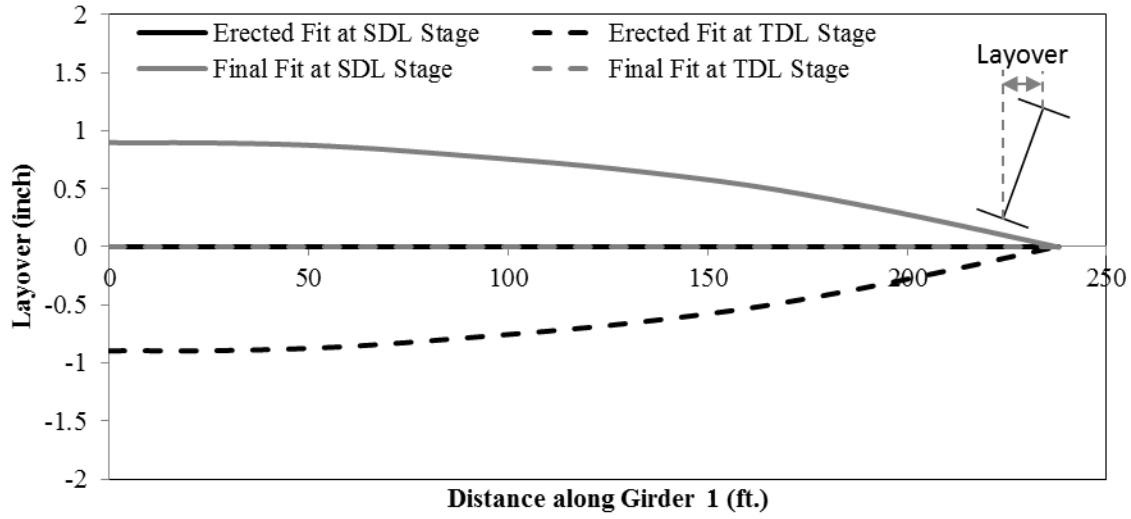


Figure B.15: Layovers in Girder1 of Bridge B2 for different detailing methods at different loading stages of construction

### B.3 Flange Lateral Bending Stress

#### B.3.1 Bridge A

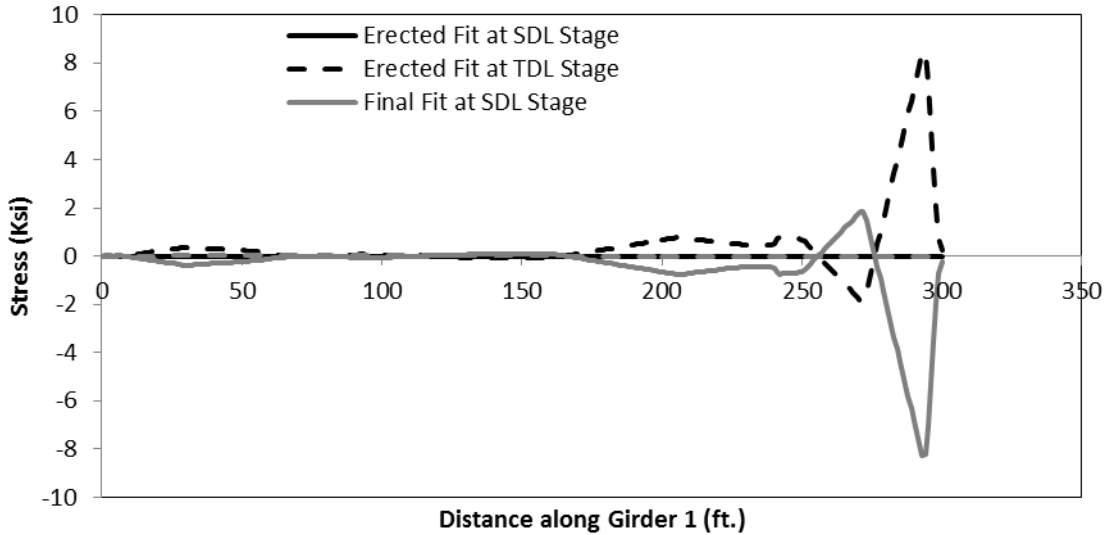


Figure B.16: Flange lateral bending stress in top flange of Girder 1 of Bridge A for different detailing methods at different loading stages of construction

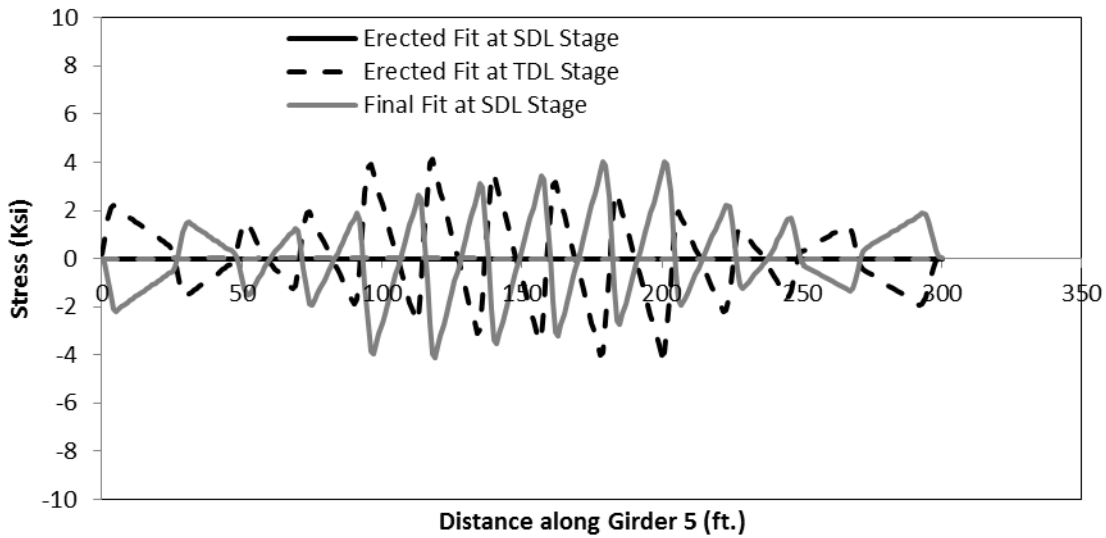


Figure B.17: Flange lateral bending stress in top flange of Girder 5 of Bridge A for different detailing methods at different loading stages of construction

### B.3.2 Bridge B

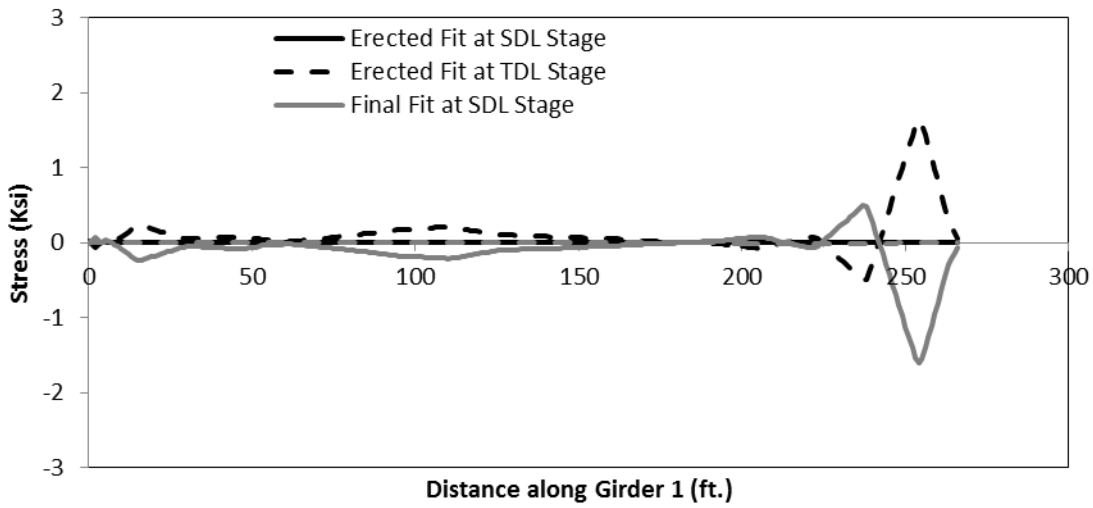


Figure B.18: Flange lateral bending stress in top flange of Girder 1 of Bridge B for different detailing methods at different loading stages of construction

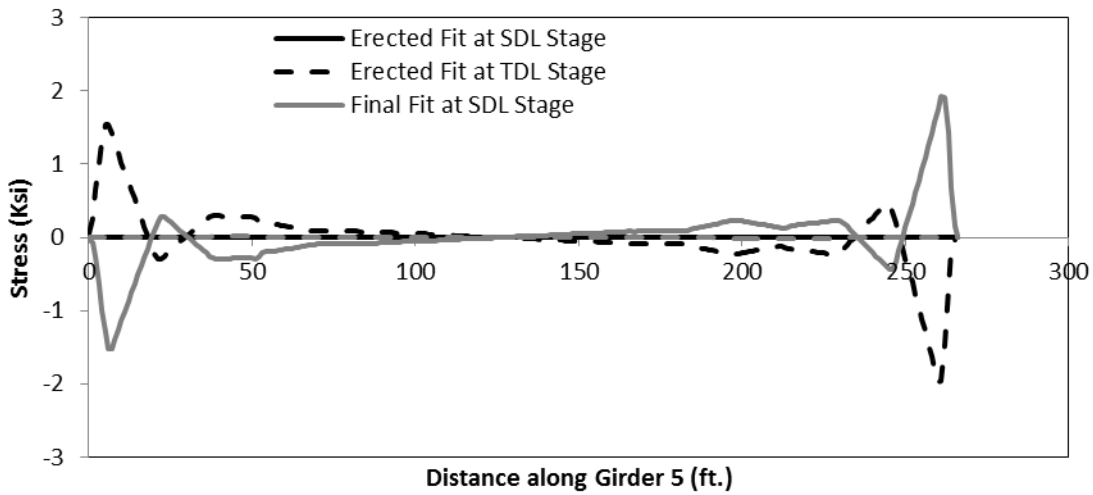


Figure B.19: Flange lateral bending stress in top flange of Girder 5 of Bridge B for different detailing methods at different loading stages of construction

### B.3.3 Bridge C

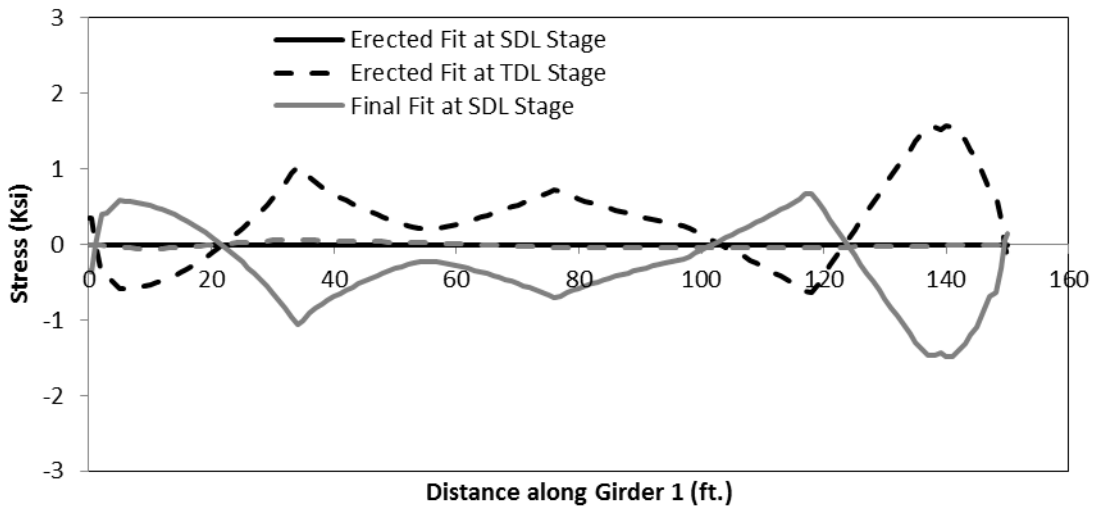


Figure B.20: Flange lateral bending stress in top flange of Girder 1 of Bridge C for different detailing methods at different loading stages of construction

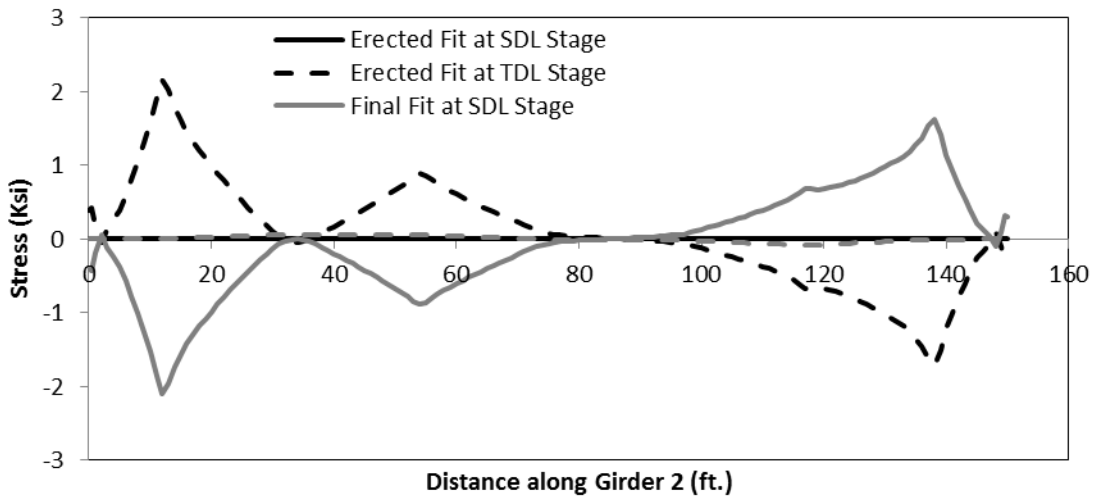
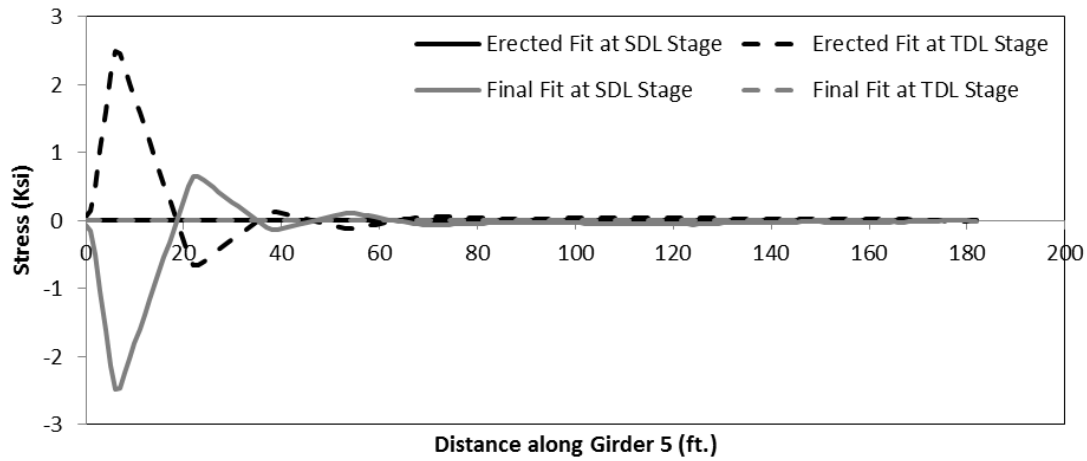


Figure B.21: Flange lateral bending stress in top flange of Girder 2 of Bridge C for different detailing methods at different loading stages of construction

### B.3.4 Bridge B2



**Figure B.22: Flange lateral bending stress in top flange of Girder 5 of Bridge B2 for different detailing methods at different loading stages of construction**

## B.4 Reactions

### B.4.1 Bridge A

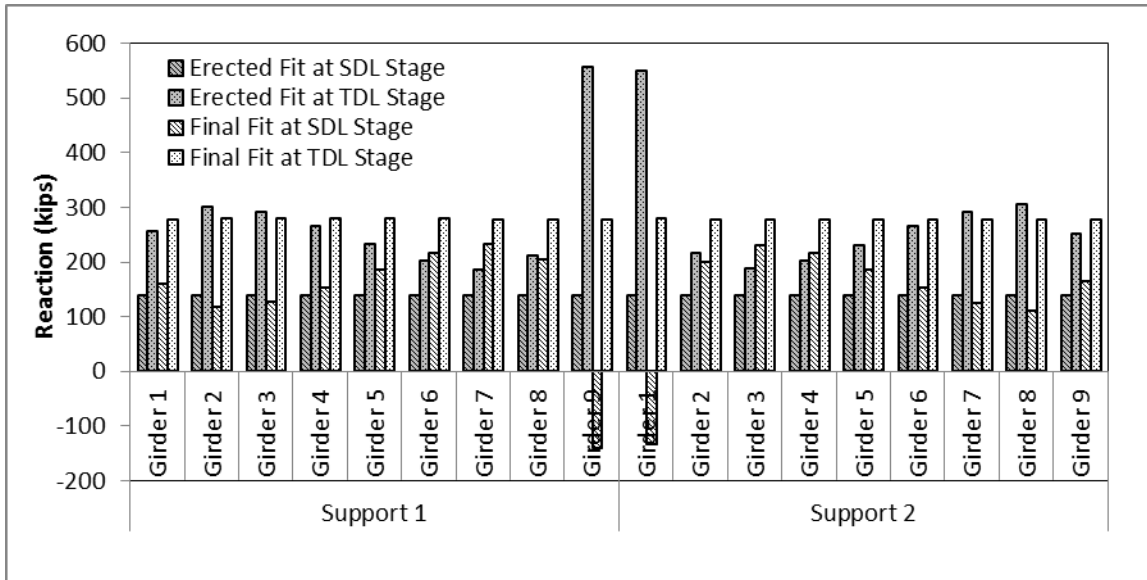


Figure B.23: Reactions of Bridge A for different detailing methods at different loading stages of construction

### B.4.2 Bridge B

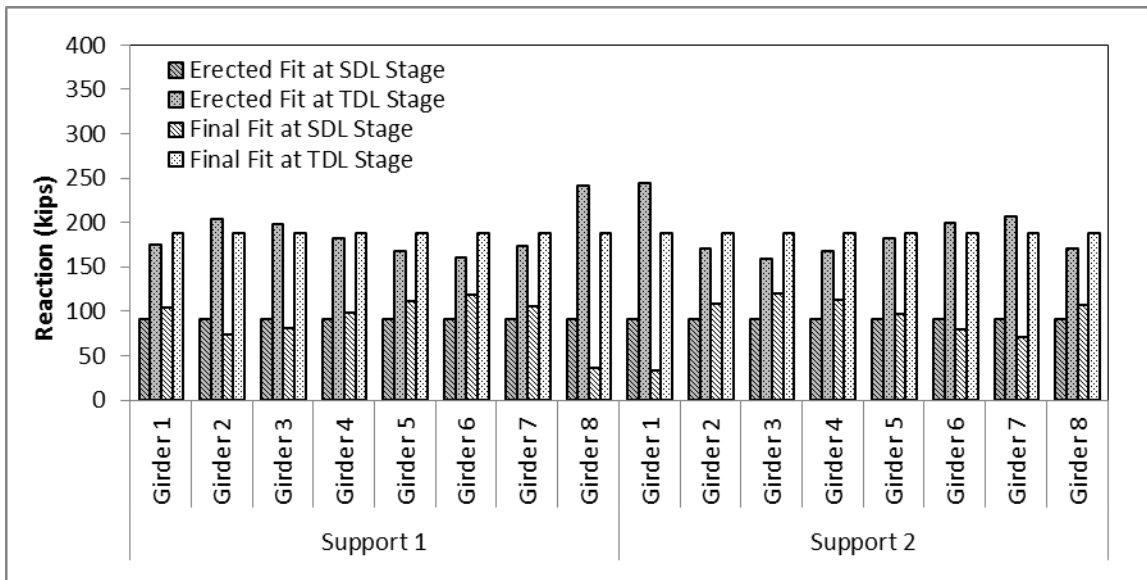


Figure B.24: Reactions of Bridge B for different detailing methods at different loading stages of construction

### B.4.3 Bridge C

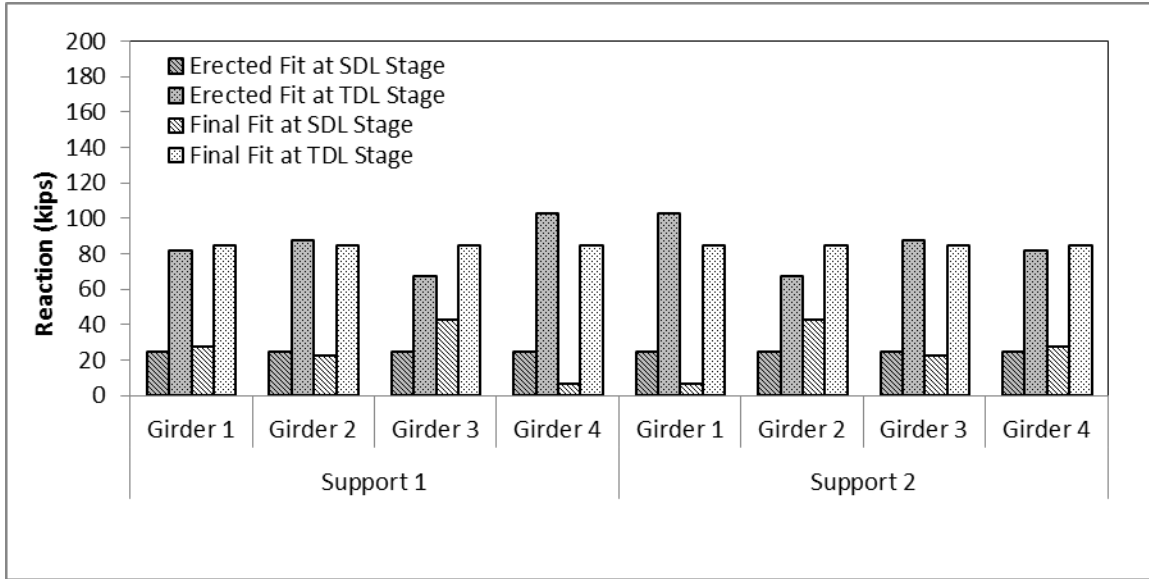


Figure B.25: Reactions of Bridge C for different detailing methods at different loading stages of construction

### B.4.4 Bridge B2

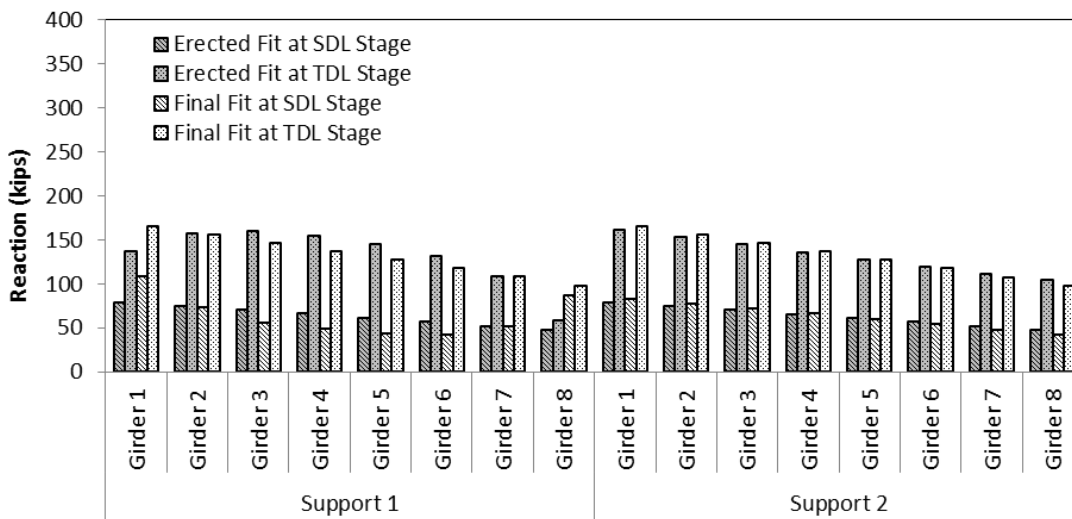
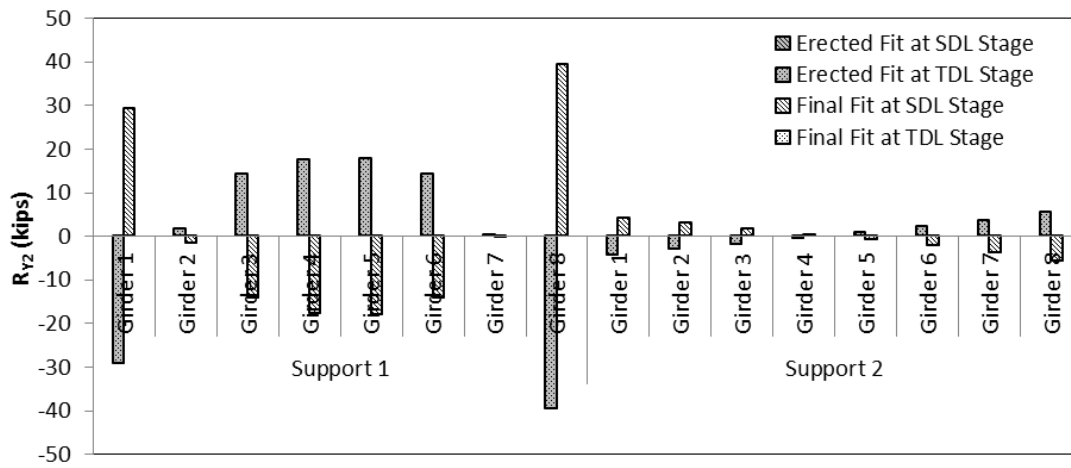


Figure B.26: Reactions of Bridge B2 for different detailing methods at different loading stages of construction



**Figure B.27: Component of reaction due to lack-of-fit ( $R_{Y2}$ ) for Bridge B2 for different detailing methods at different loading stages of construction**

## B.5 Cross-frame Forces

### B.5.1 Bridge A

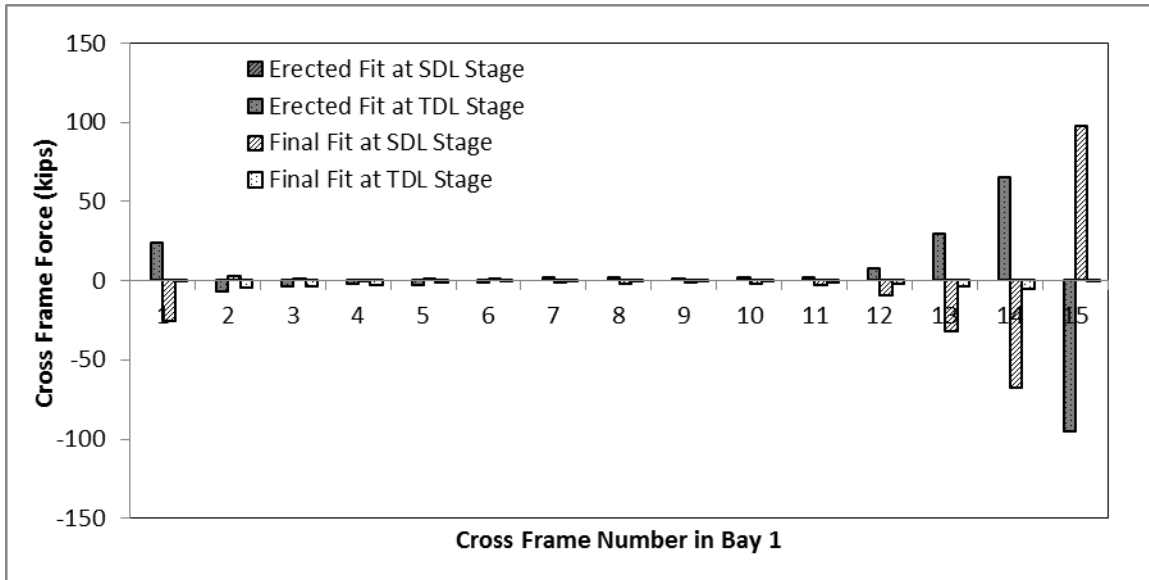


Figure B.28: Cross-frame forces in top chord of cross-frames in Bay 1 of Bridge A for different detailing methods at different loading stages of construction

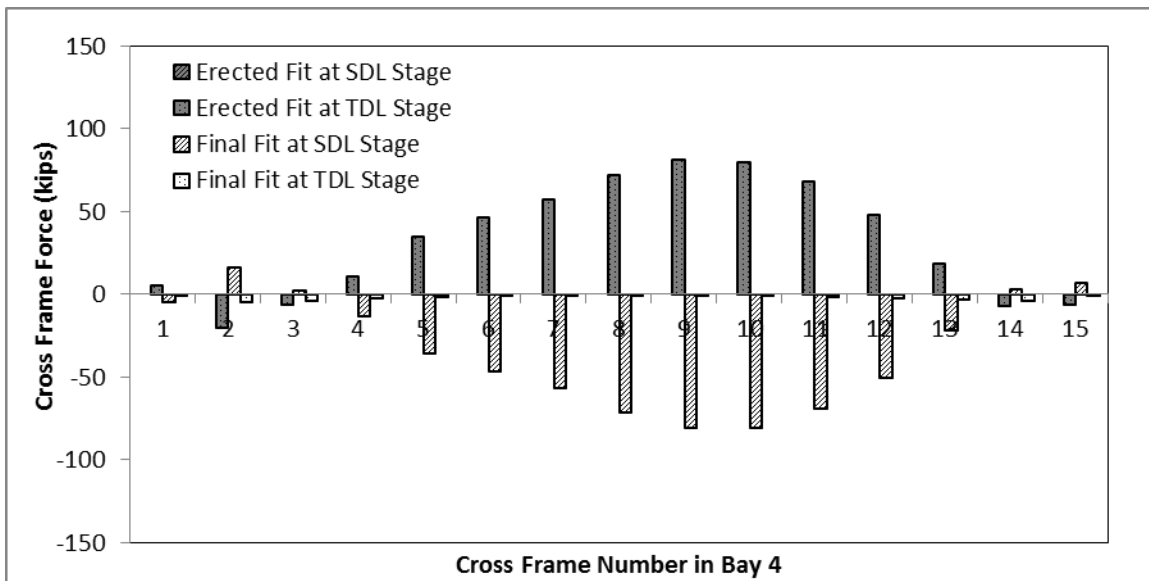
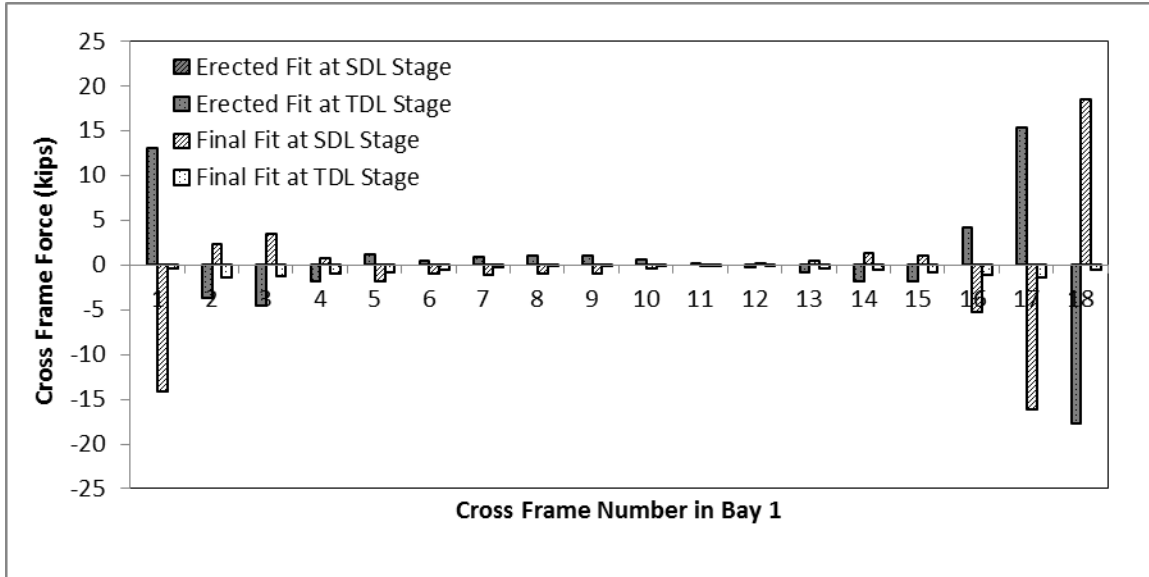
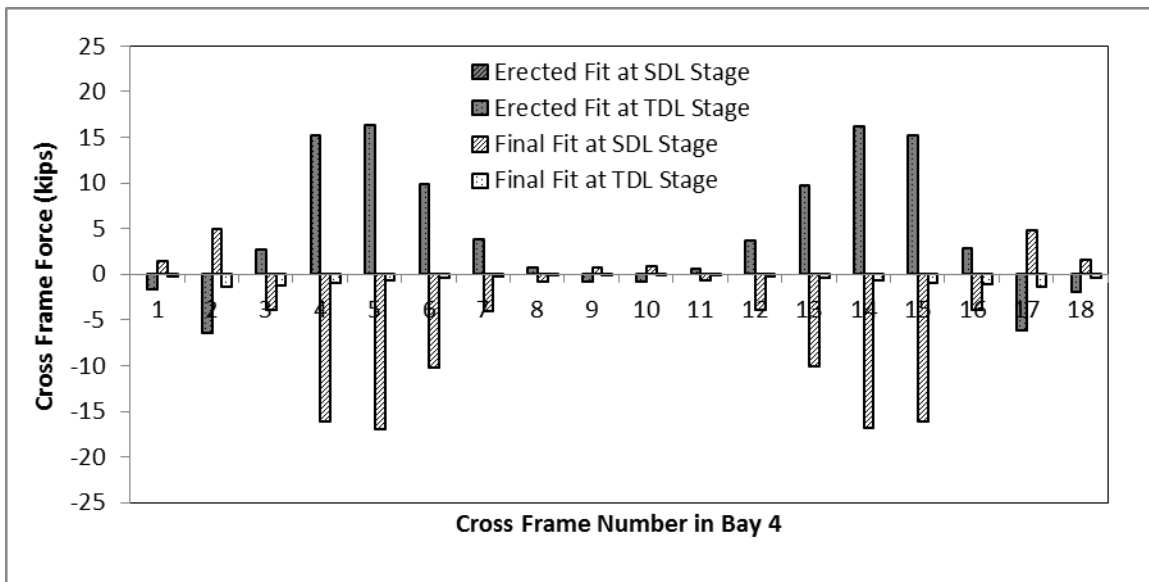


Figure B.29: Cross-frame forces in top chord of cross-frames in Bay 4 of Bridge A for different detailing methods at different loading stages of construction

### B.5.2 Bridge B



**Figure B.30: Cross-frame forces in top chord of cross-frames in Bay 1 of Bridge B for different detailing methods at different loading stages of construction**



**Figure B.31: Cross-frame forces in top chord of cross-frames in Bay 4 of Bridge B for different detailing methods at different loading stages of construction**

### B.5.3 Bridge C

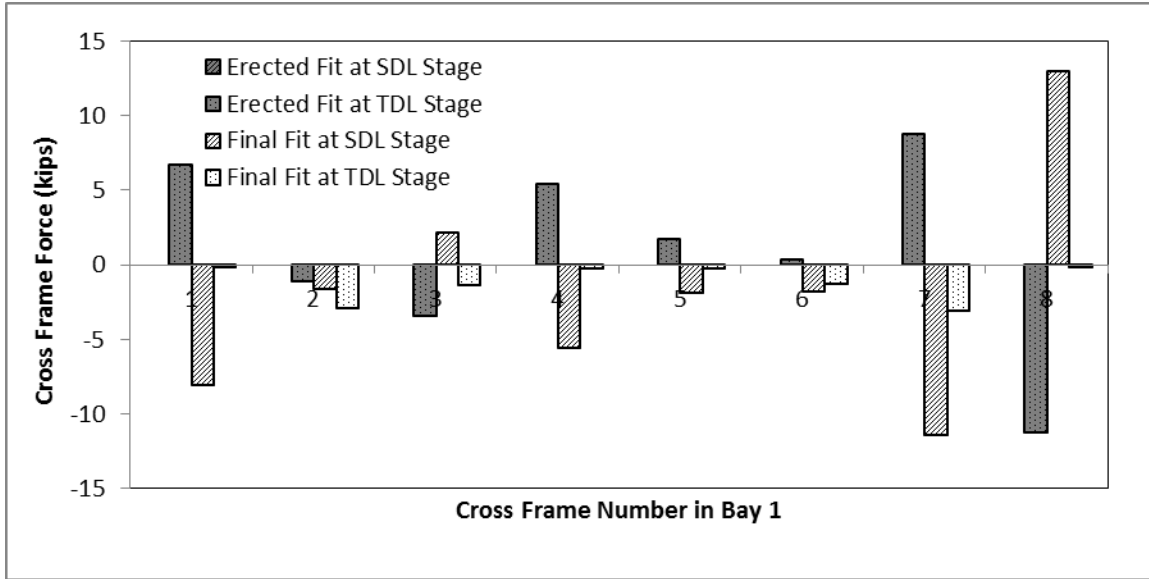


Figure B.32: Cross-frame forces in top chord of cross-frames in Bay 1 of Bridge C for different detailing methods at different loading stages of construction

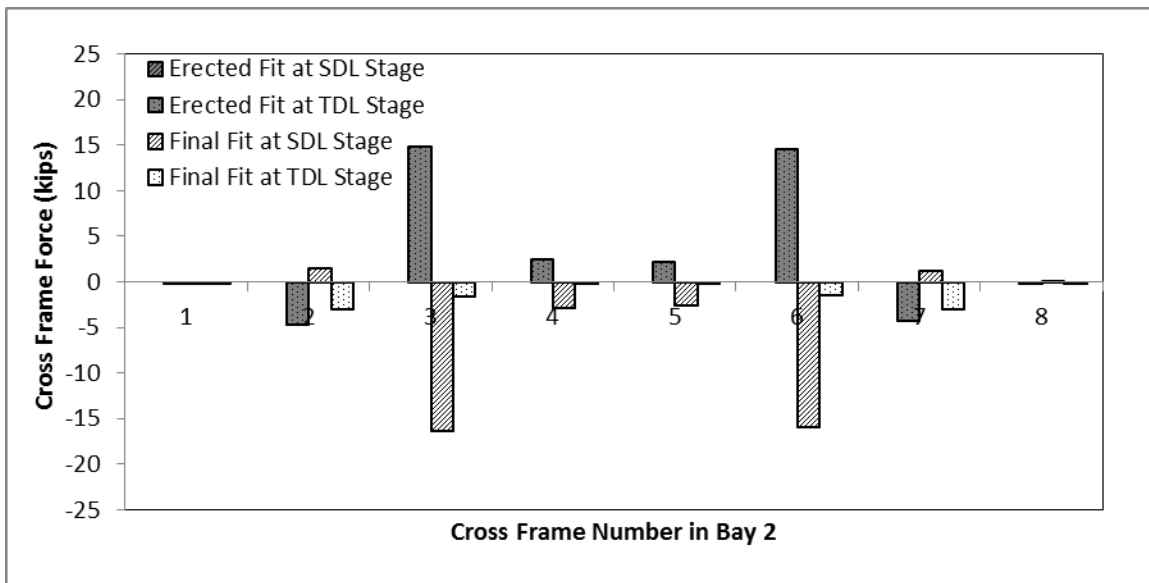
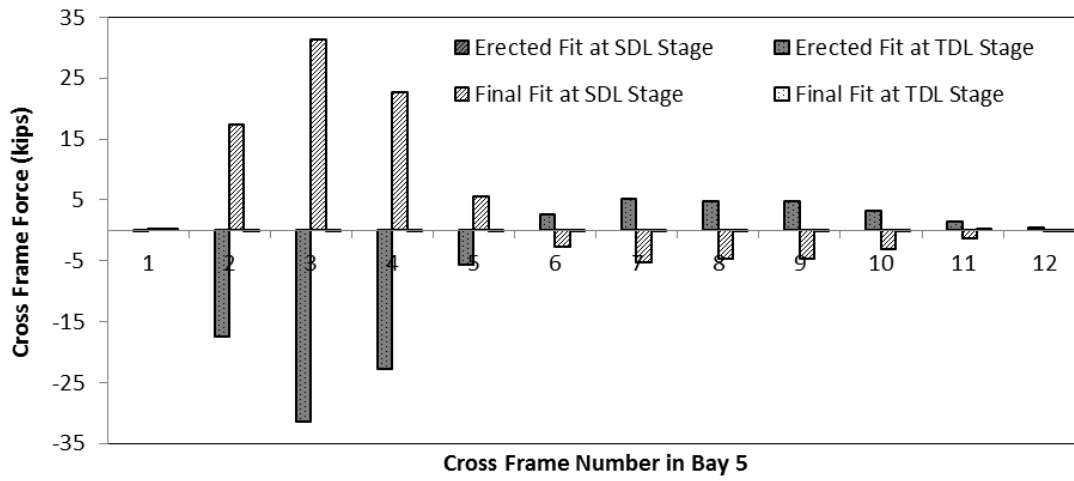


Figure B.33: Cross-frame forces in top chord of cross-frames in Bay 2 of Bridge C for different detailing methods at different loading stages of construction

### B.5.4 Bridge B2



**Figure B.34: Cross-frame forces in top chord of cross-frames in Bay 5 of Bridge B2 for different detailing methods at different loading stages of construction**

# Appendix C: Methods of Analysis: Erected Fit

## C.1 Concrete Dead Load Deflections

### C.1.1 Bridge A

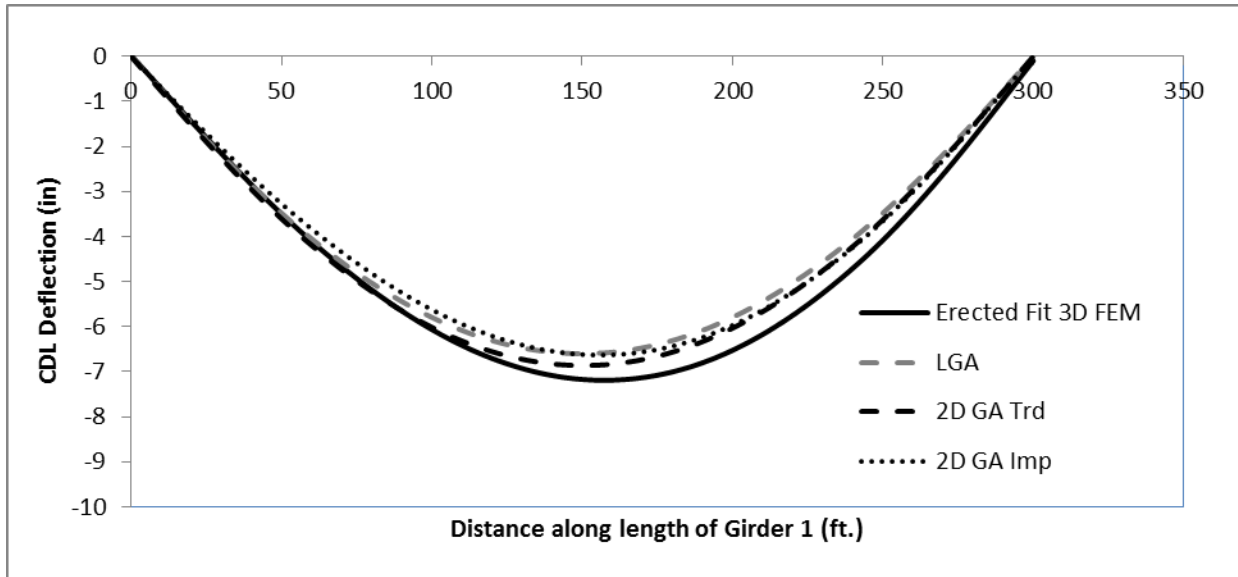


Figure C.1: Concrete dead load (CDL) deflection in Girder 1 of Bridge A by different methods of analysis

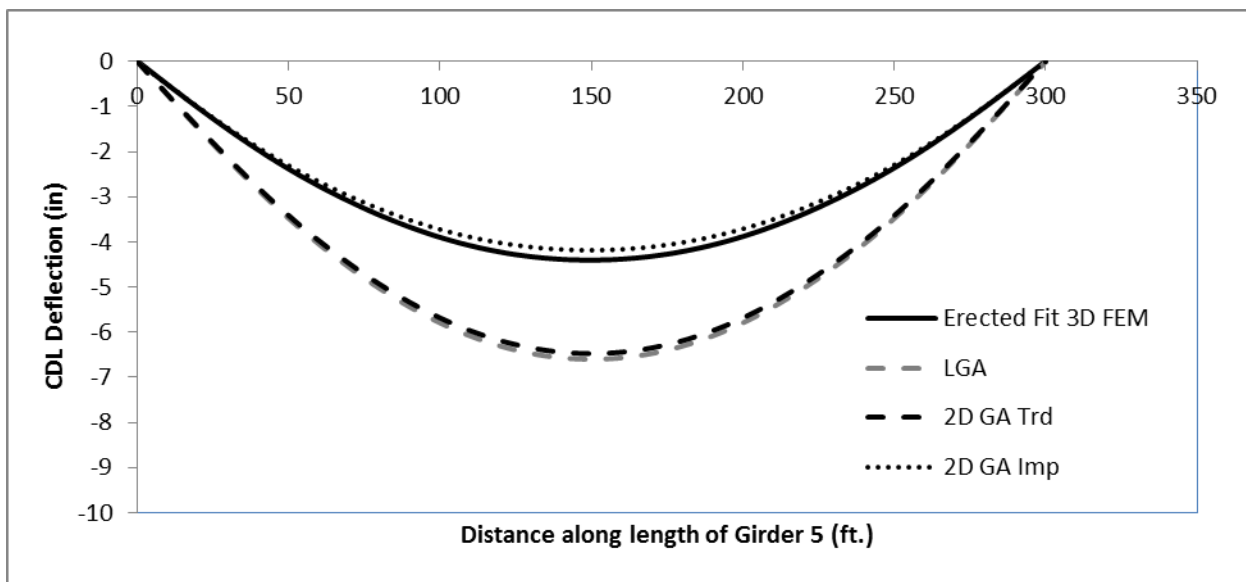


Figure C.2: Concrete dead load (CDL) deflection in Girder 5 of Bridge A by different methods of analysis

### C.1.2 Bridge B

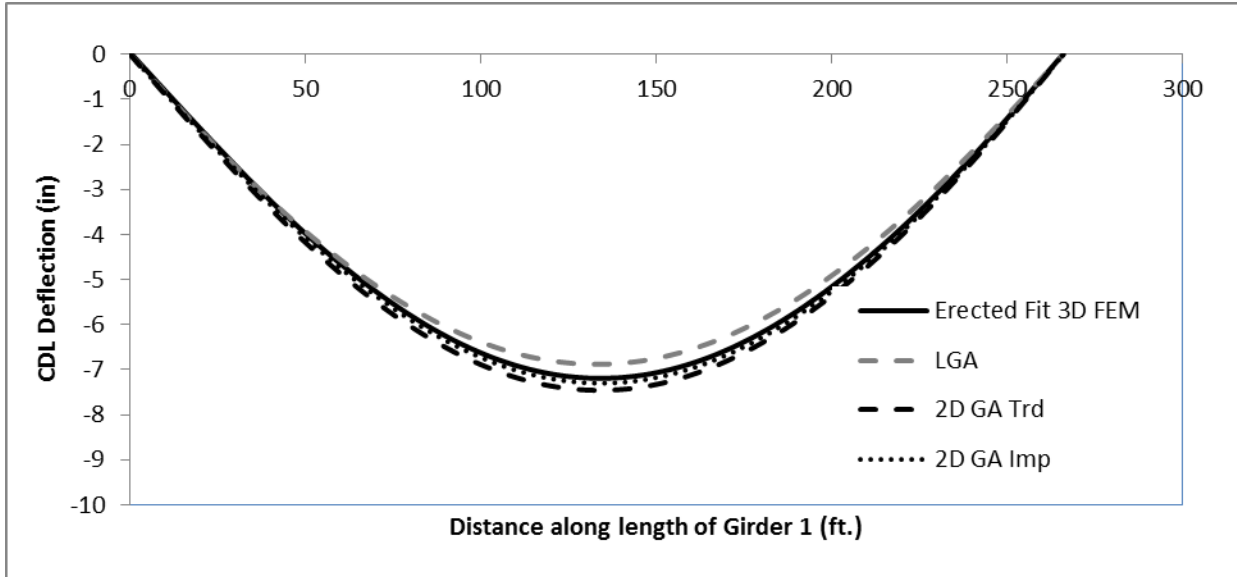


Figure C.3: Concrete dead load (CDL) deflection in Girder 1 of Bridge B by different methods of analysis

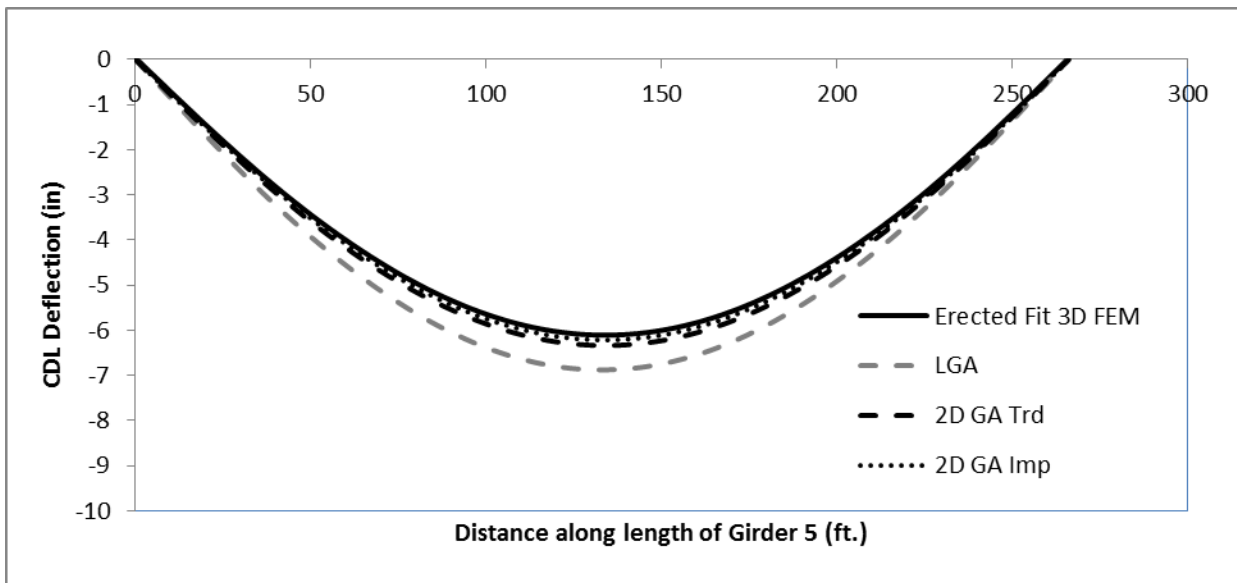


Figure C.4: Concrete dead load (CDL) deflection in Girder 5 of Bridge B by different methods of analysis

### C.1.3 Bridge C

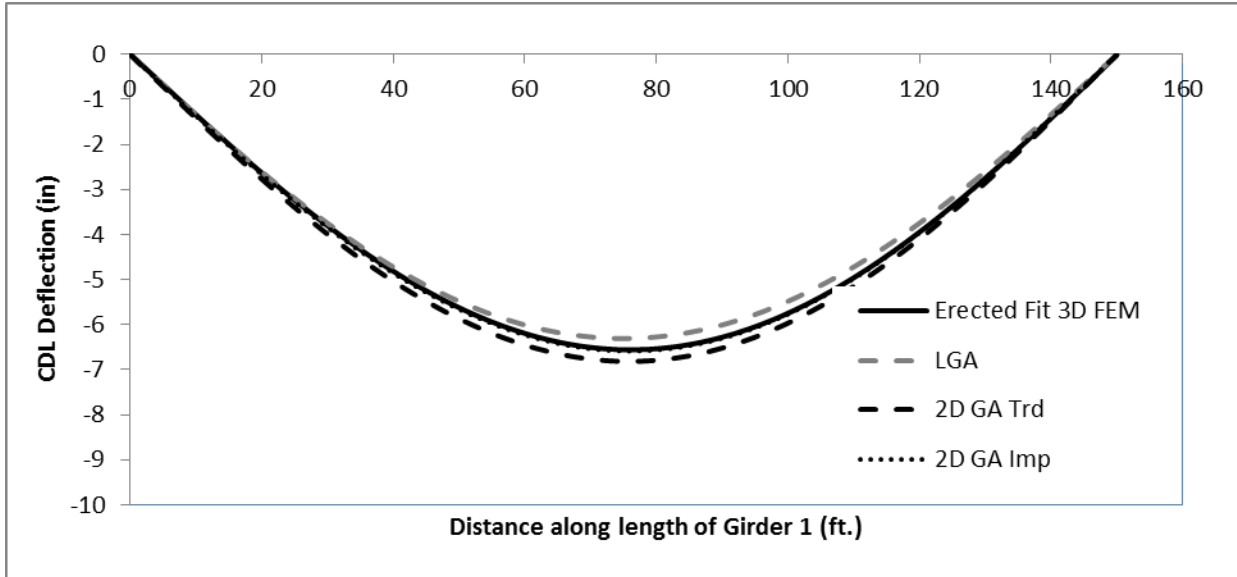


Figure C.5: Concrete dead load (CDL) deflection in Girder 1 of Bridge C by different methods of analysis

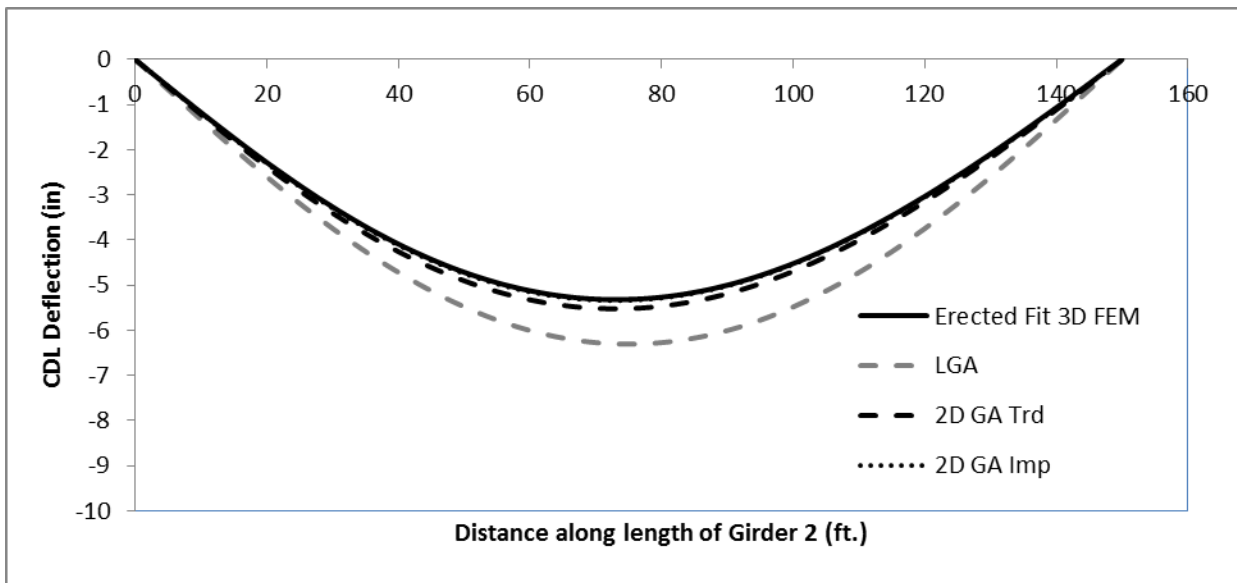


Figure C.6: Concrete dead load (CDL) deflection in Girder 1 of Bridge C by different methods of analysis

## C.2 Layovers

### C.2.1 Bridge A

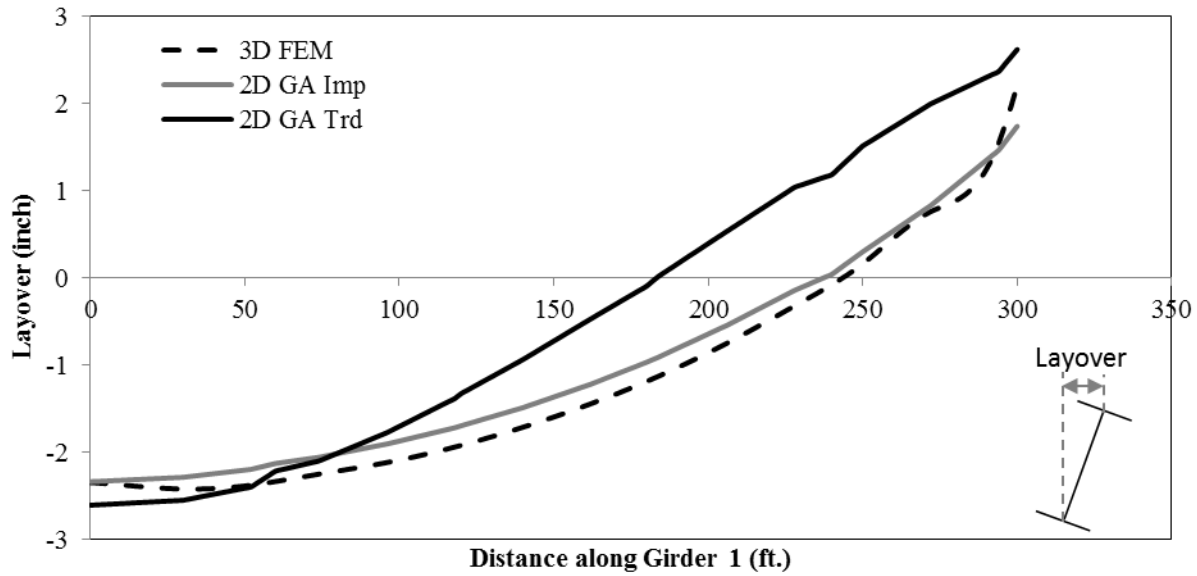


Figure C.7: Comparison of layovers calculated by different analysis method for Girder 1 of Bridge A

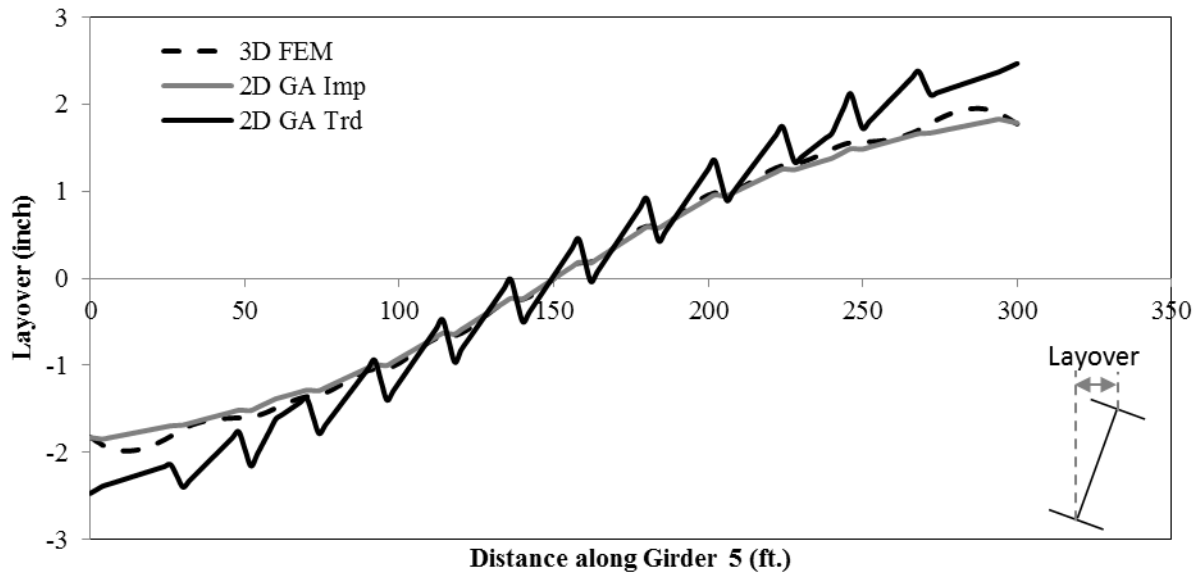


Figure C.8: Comparison of layovers calculated by different analysis method for Girder 5 of Bridge A

### C.2.2 Bridge B

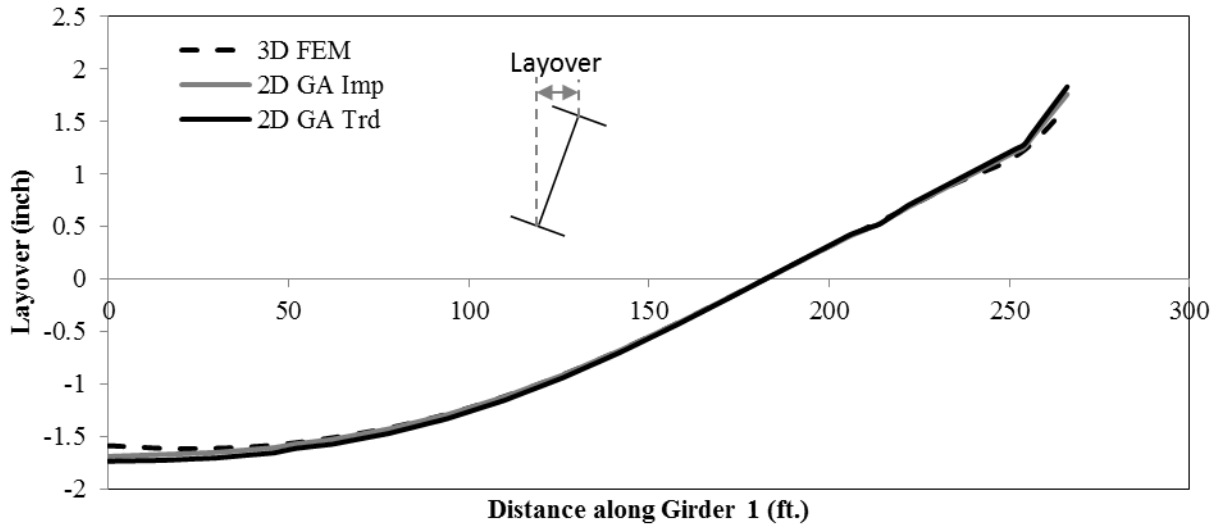


Figure C.9: Comparison of layovers calculated by different analysis method for Girder 1 of Bridge B

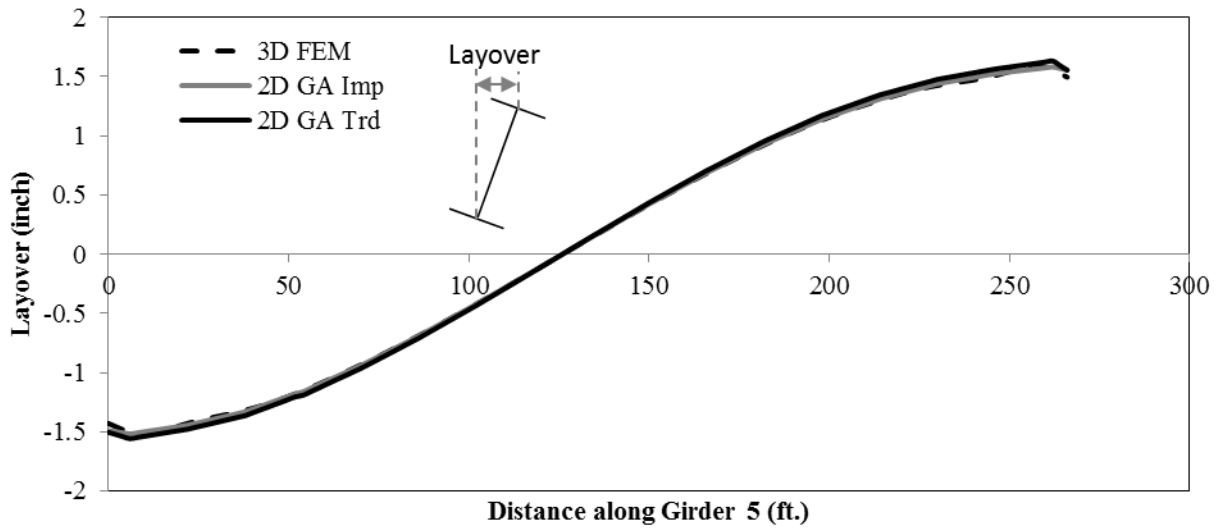


Figure C.10: Comparison of layovers calculated by different analysis method for Girder 5 of Bridge B

### C.2.3 Bridge C

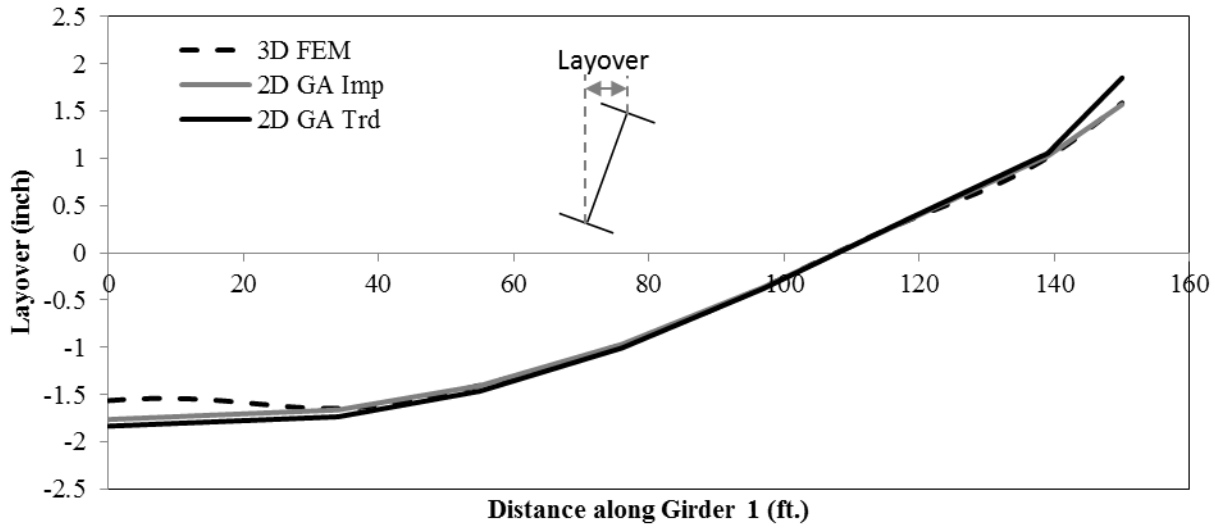


Figure C.11: Comparison of layovers calculated by different analysis method for Girder 1 of Bridge C

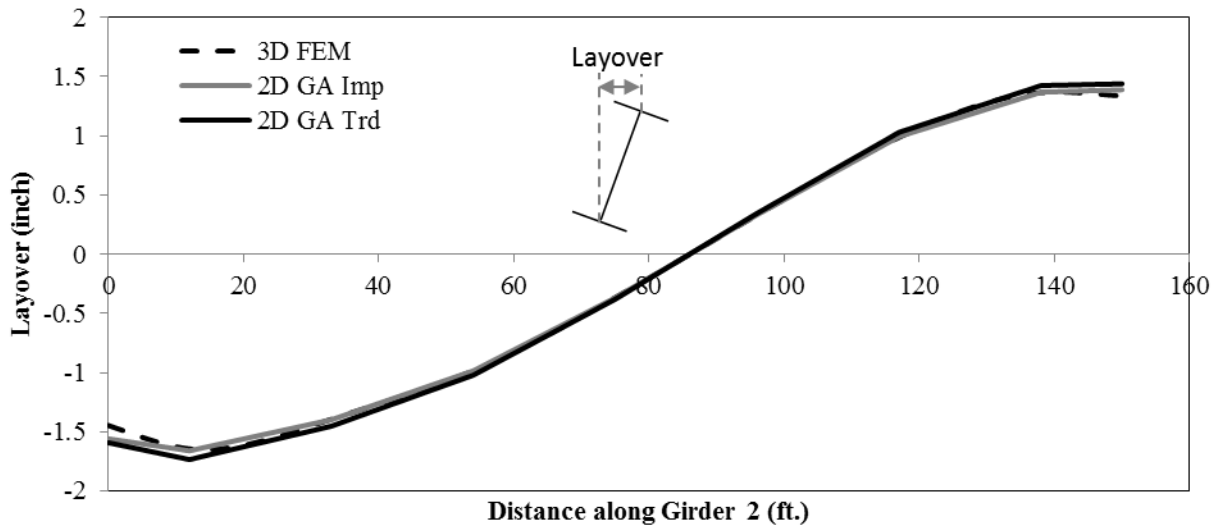


Figure C.12: Comparison of layovers calculated by different analysis method for Girder 2 of Bridge C

### C.3 Flange Lateral Bending Stress

#### C.3.1 Bridge A

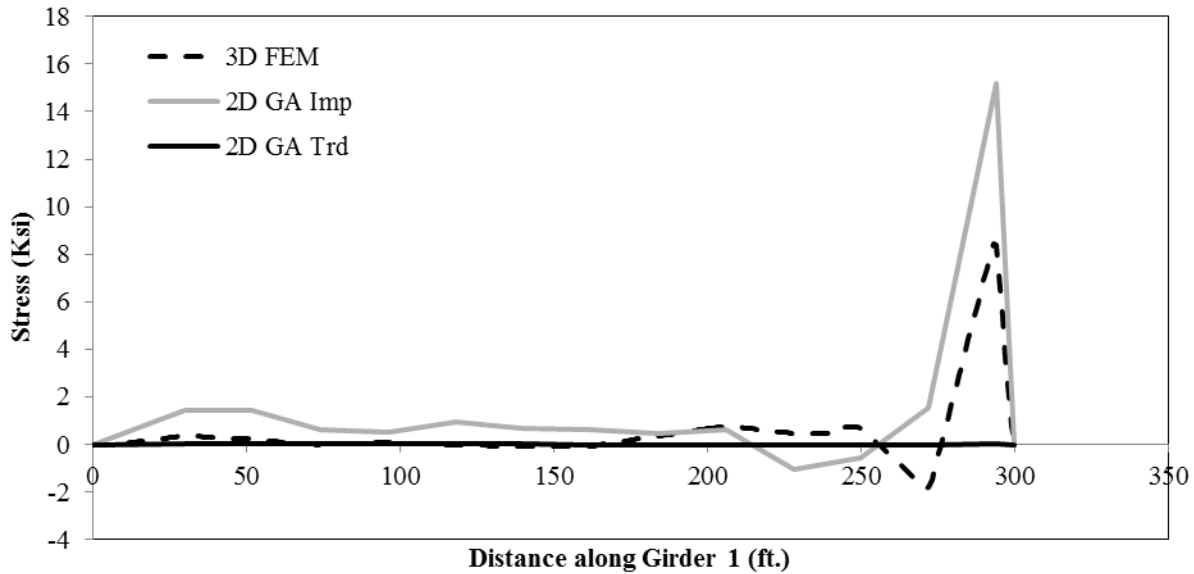


Figure C.13: Comparison of flange lateral bending stress calculated by different analysis method in Girder 1 of Bridge A for erected fit at the TDL stage

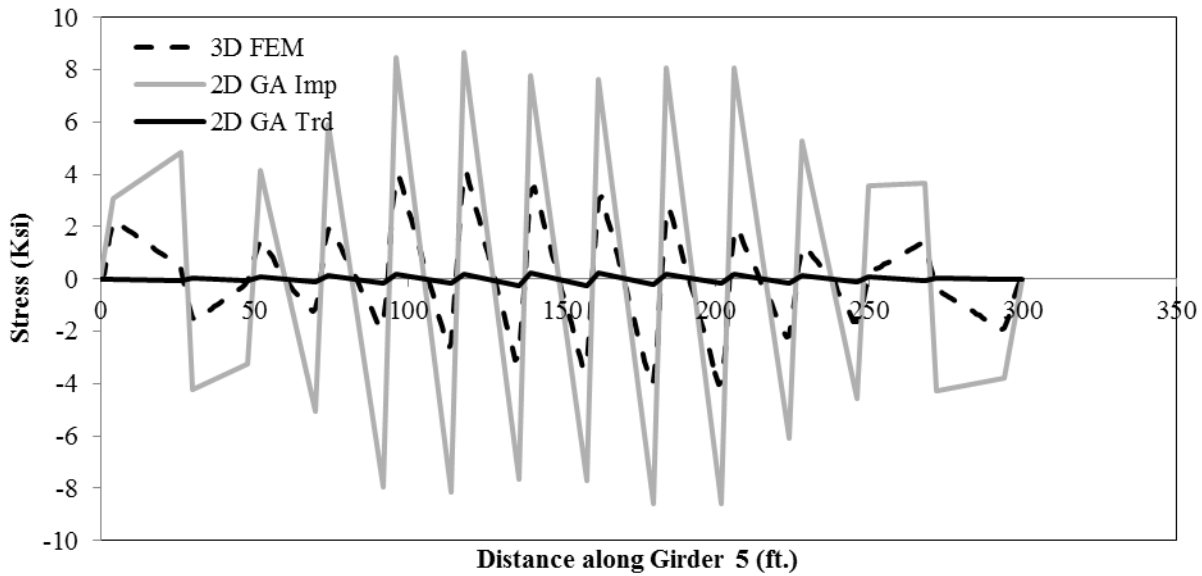


Figure C.14: Comparison of flange lateral bending stress calculated by different analysis method in Girder 5 of Bridge A for erected fit at the TDL stage

### C.3.2 Bridge B

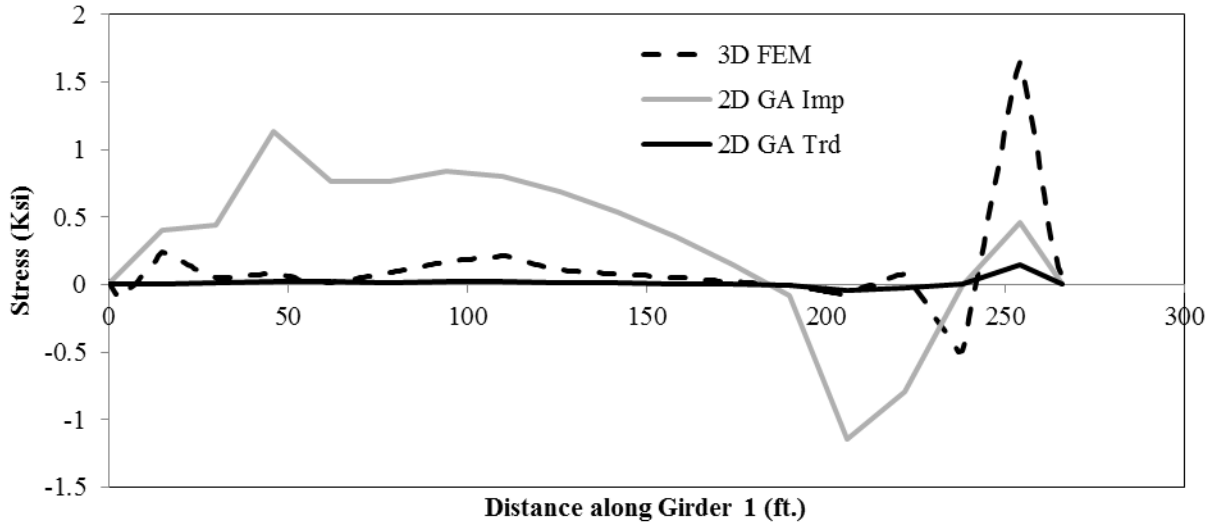


Figure C.15: Comparison of flange lateral bending stress calculated by different analysis method in Girder 1 of Bridge B for erected fit at the TDL stage

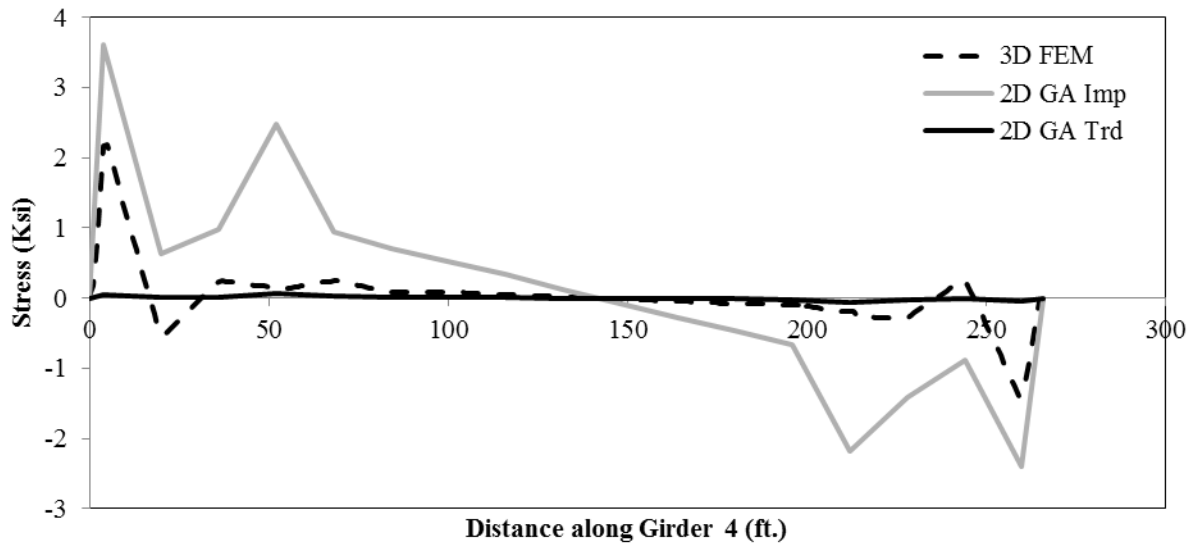


Figure C.16: Comparison of flange lateral bending stress calculated by different analysis method in Girder 4 of Bridge B for erected fit at the TDL stage

### C.3.3 Bridge C

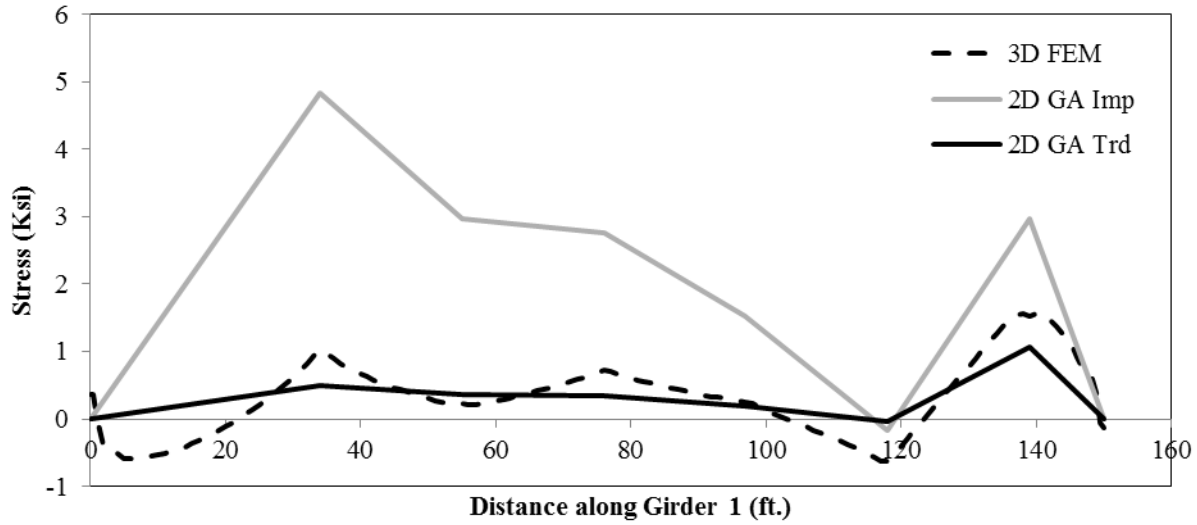


Figure C.17: Comparison of flange lateral bending stress calculated by different analysis method in Girder 1 of Bridge C for erected fit at the TDL stage

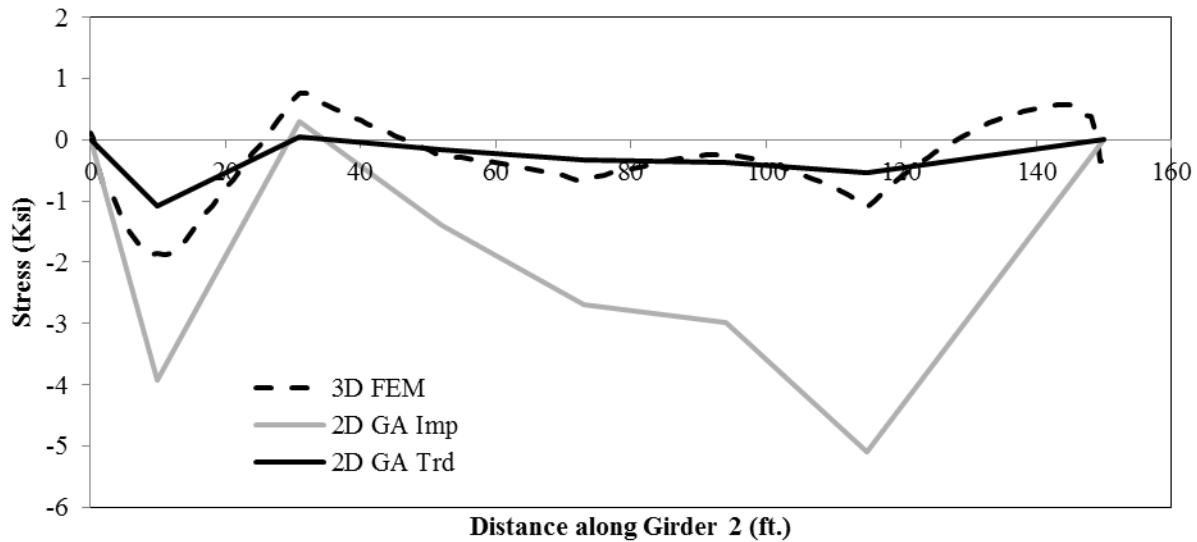


Figure C.18: Comparison of flange lateral bending stress calculated by different analysis method in Girder 2 of Bridge C for erected fit at the TDL stage

## C.4 Reactions

### C.4.1 Bridge A

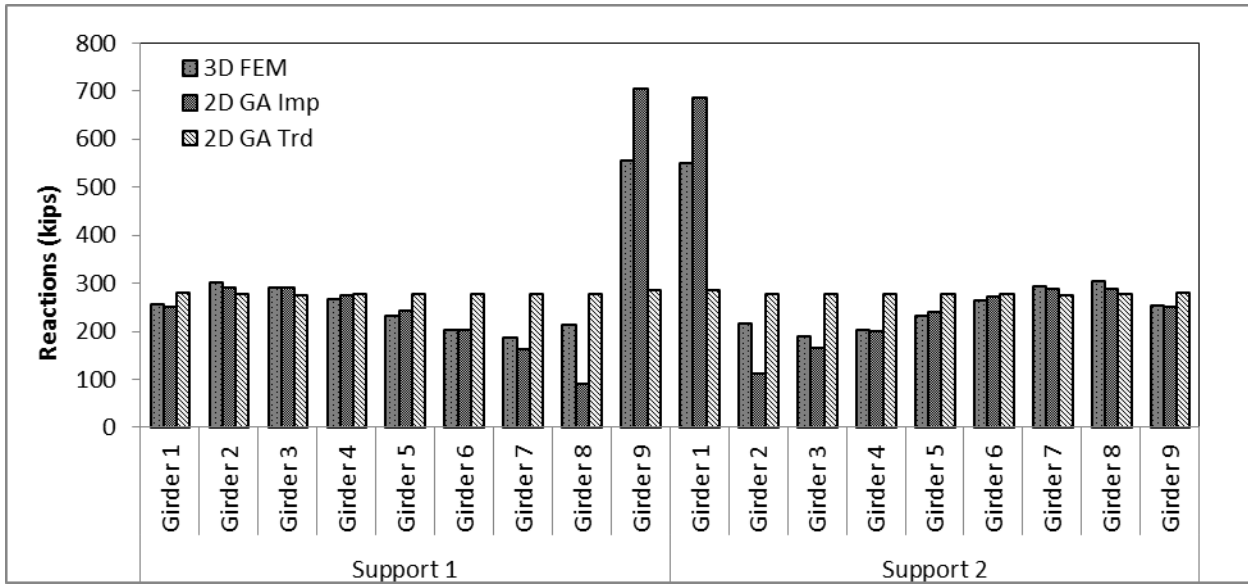


Figure C.19: Comparison of vertical reactions calculated by different analysis method for Bridge A for erected fit at the TDL stage

### C.4.2 Bridge B

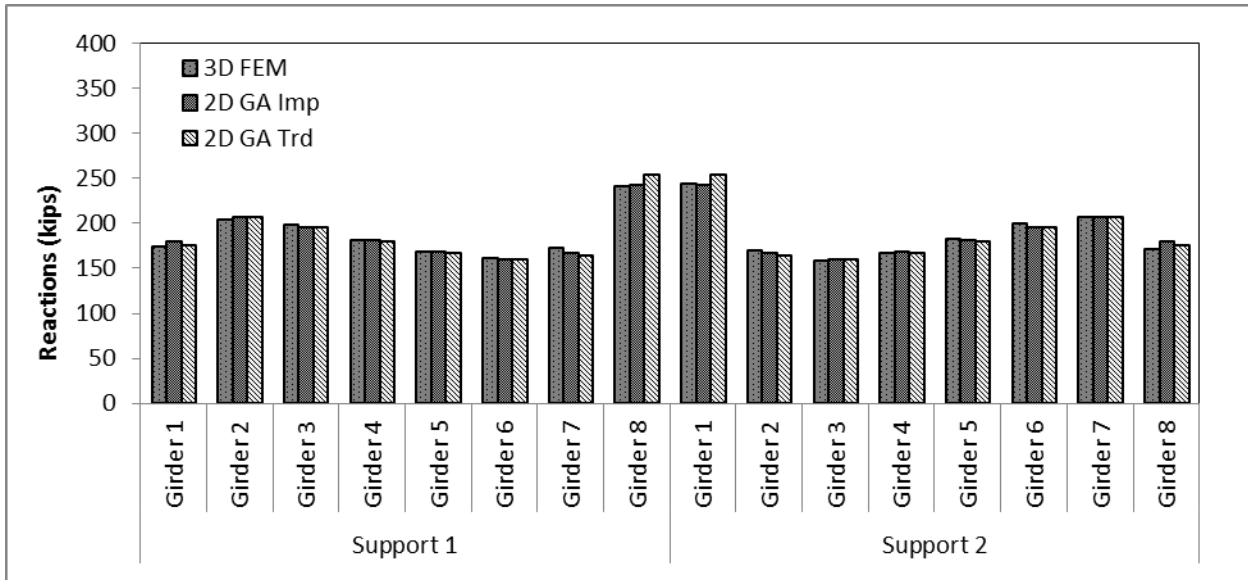
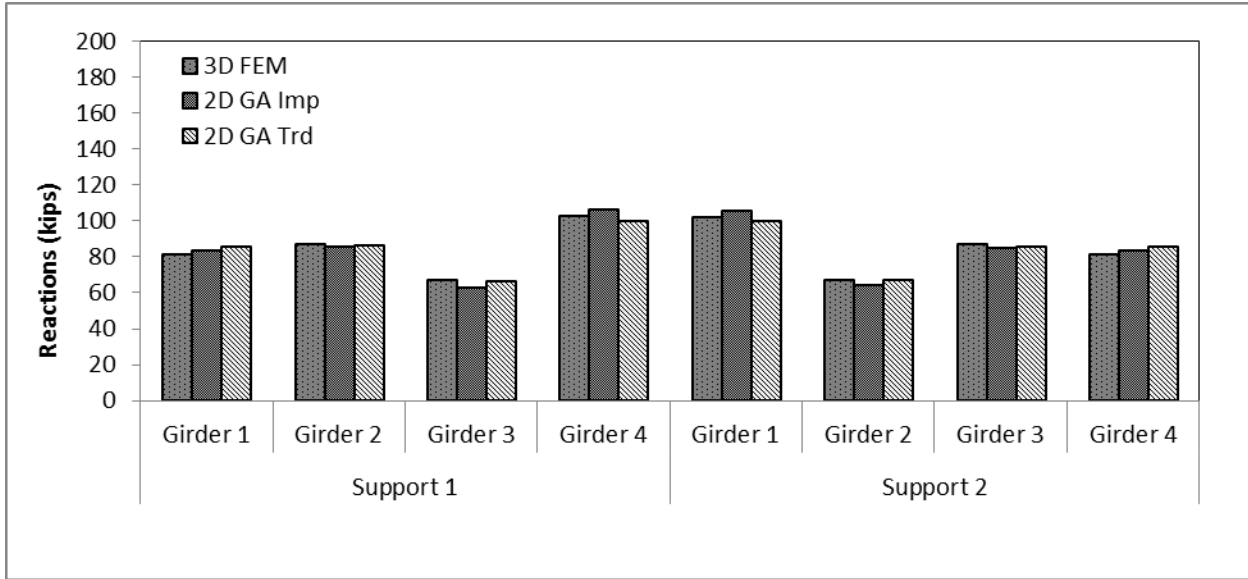


Figure C.20: Comparison of vertical reactions calculated by different analysis method for Bridge B for erected fit at the TDL stage

### C.4.3 Bridge C



**Figure C.21: Comparison of vertical reactions calculated by different analysis method for Bridge C for erected fit at the TDL stage**

## C.5 Cross-frame Forces

### C.5.1 Bridge A

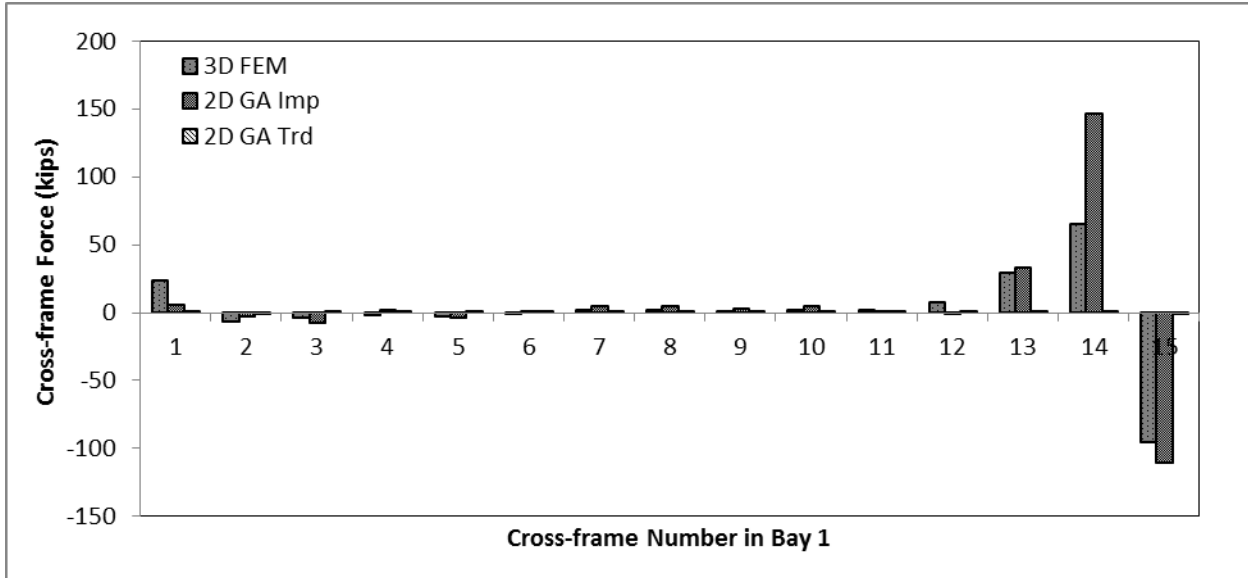


Figure C.22: Comparison of cross-frame forces calculated by different analysis method for Bridge A for erected fit at the TDL stage

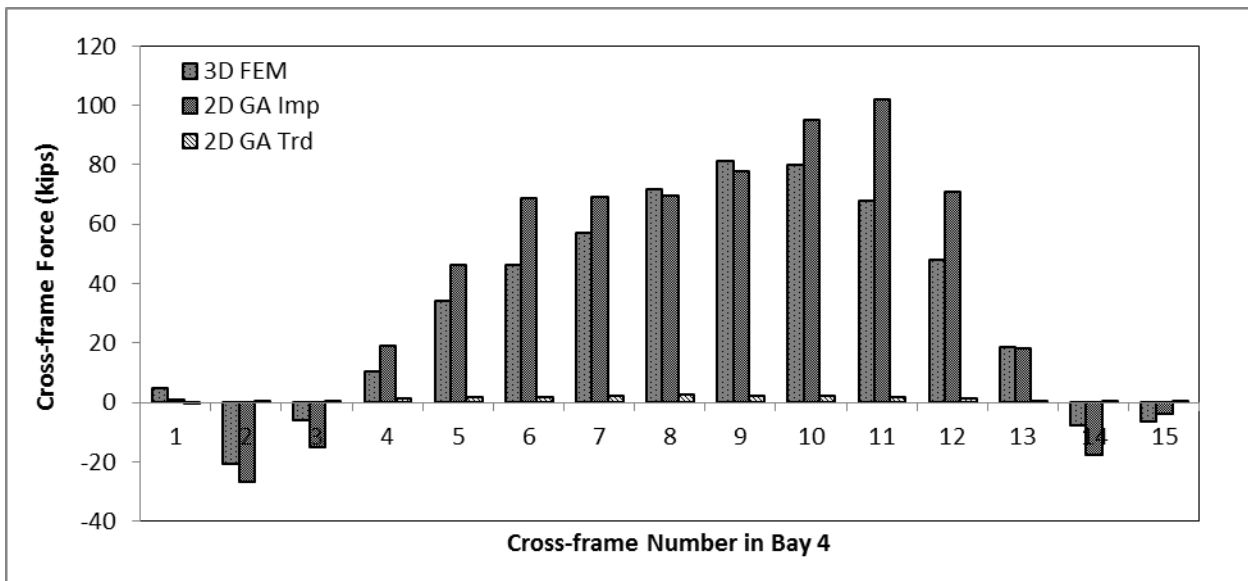


Figure C.23: Comparison of cross-frame forces calculated by different analysis method for Bridge A for erected fit at the TDL stage

### C.5.2 Bridge B

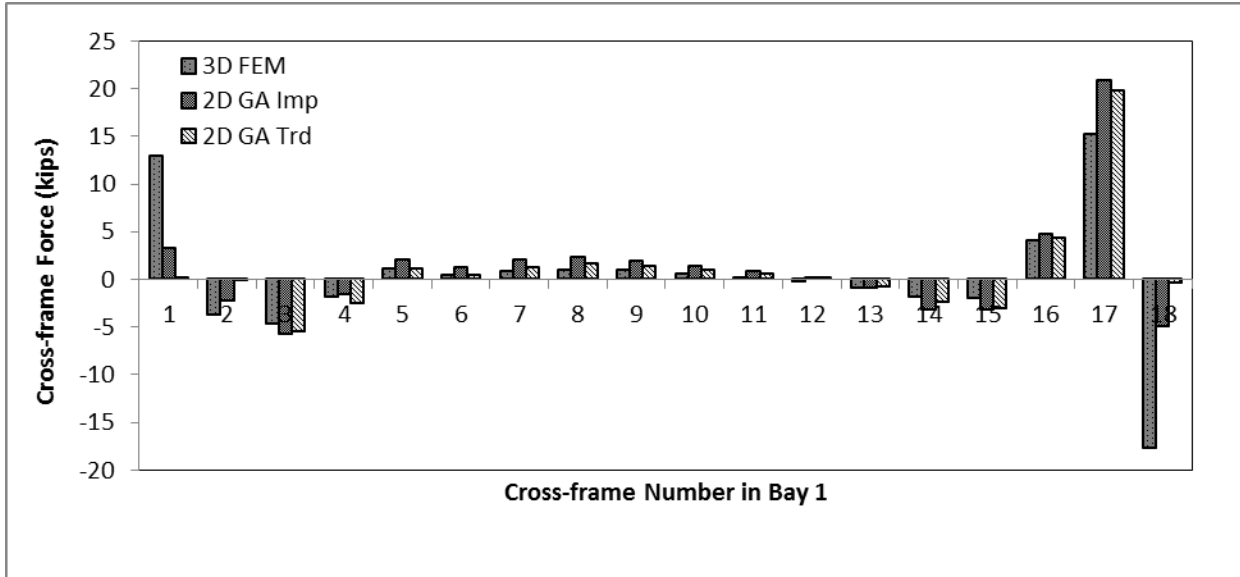


Figure C.24: Comparison of cross-frame forces calculated by different analysis method for Bridge B for erected fit at the TDL stage

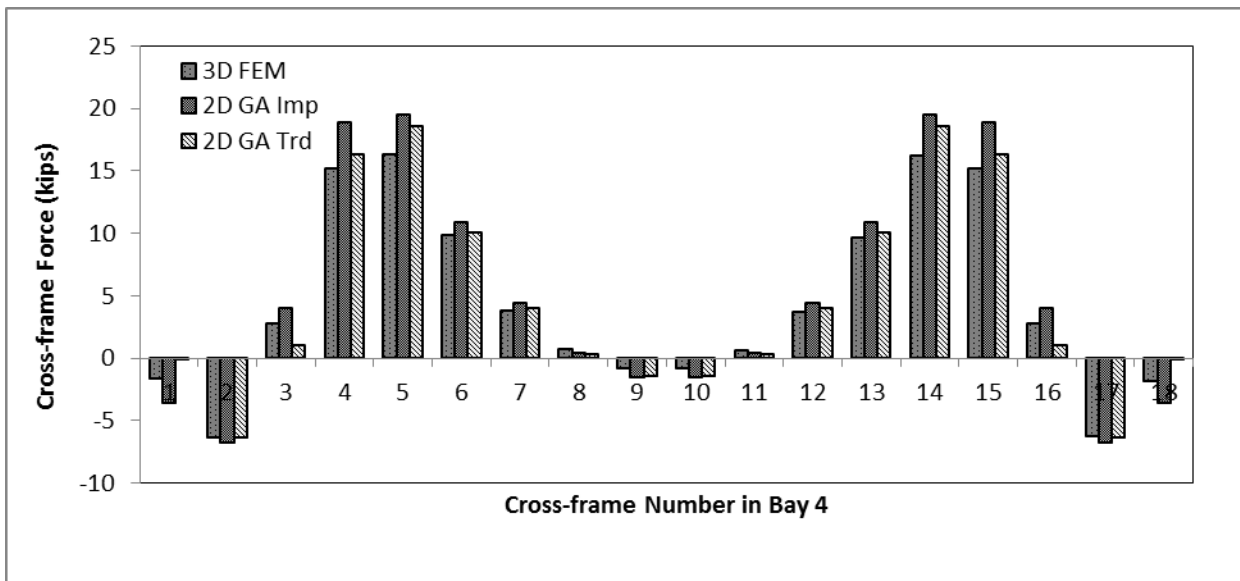


Figure C.25: Comparison of cross-frame forces calculated by different analysis method for Bridge B for erected fit at the TDL stage

### C.5.3 Bridge C

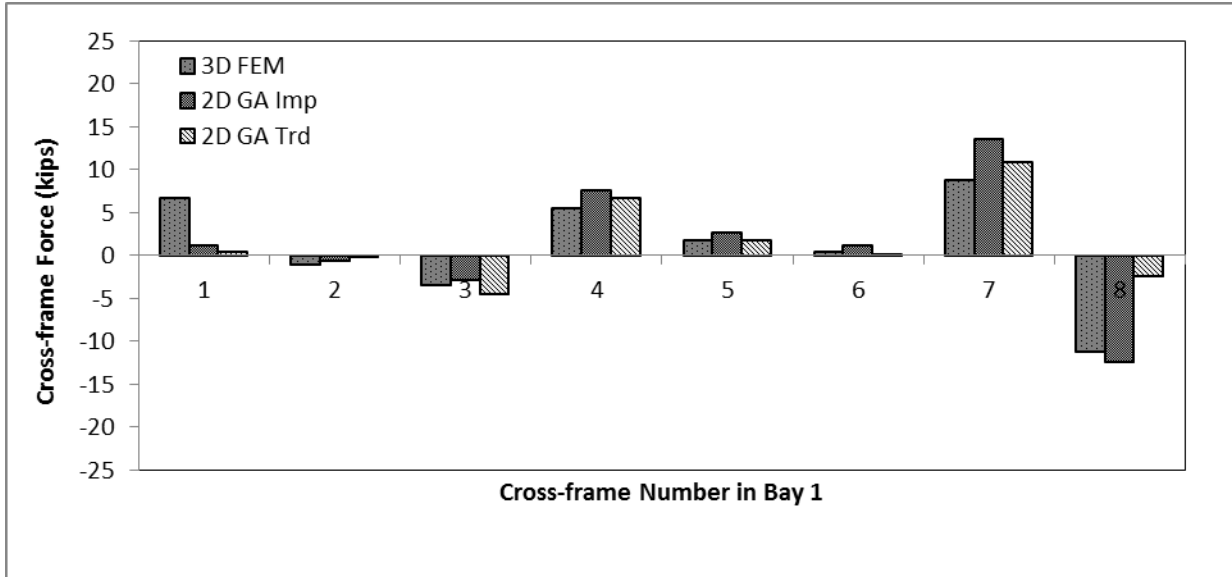


Figure C.26: Comparison of cross-frame forces calculated by different analysis method for Bridge C for erected fit at the TDL stage

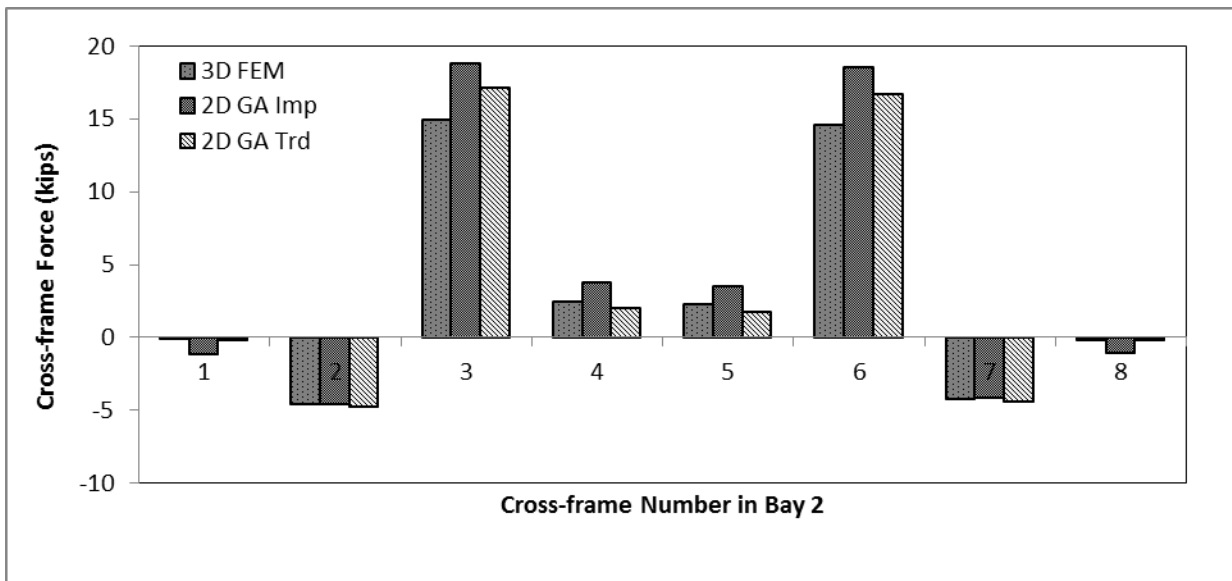


Figure C.27: Comparison of cross-frame forces calculated by different analysis method for Bridge C for erected fit at the TDL stage

# Appendix D: Methods of Analysis: Final Fit

## D.1 Change in Elevation Due to Lack of Fit

### D.1.1 Bridge C

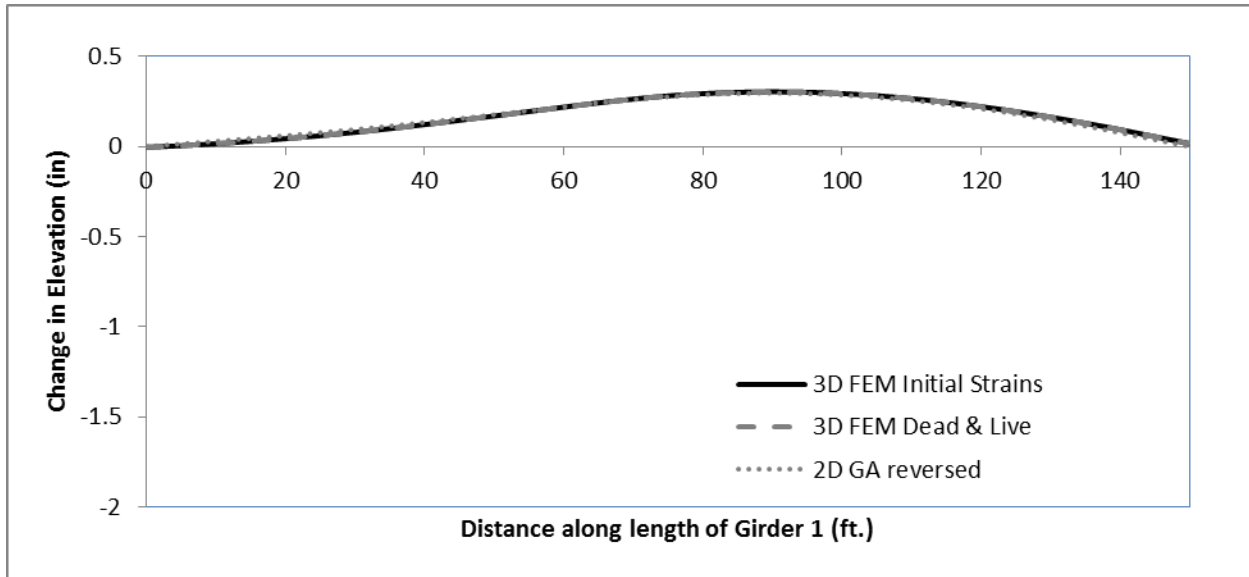


Figure D.1: Change in elevation due to lack of fit calculated by different analysis method for Bridge C for final fit at the SDL stage

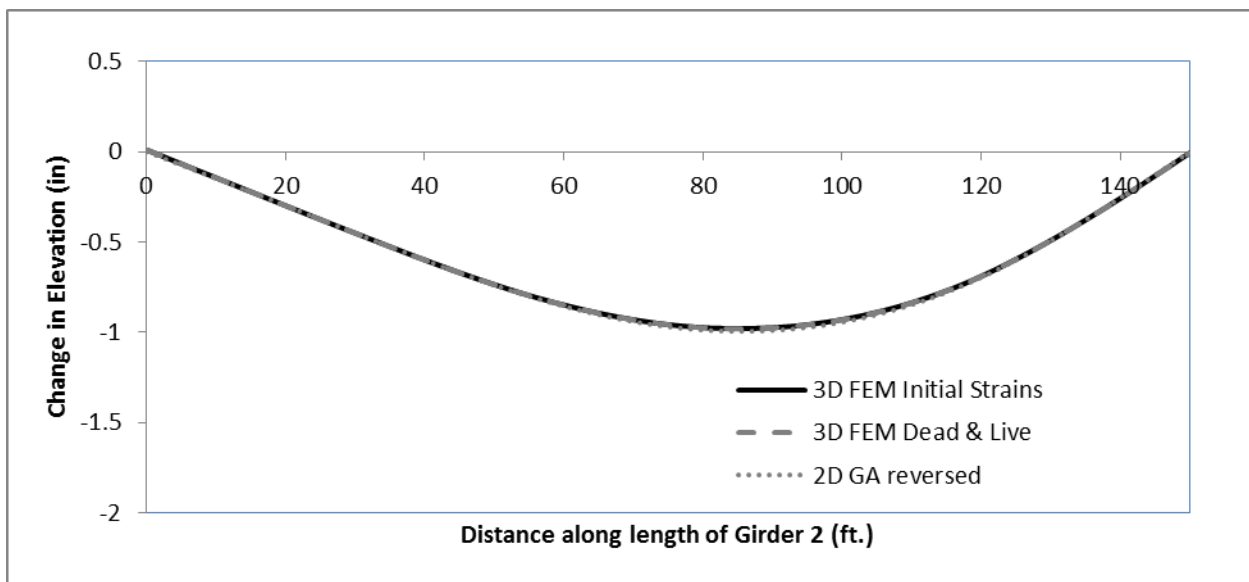


Figure D.2: Change in elevation due to lack of fit calculated by different analysis method for Bridge C for final fit at the SDL stage

## D.2 Layovers

### D.2.1 Bridge C

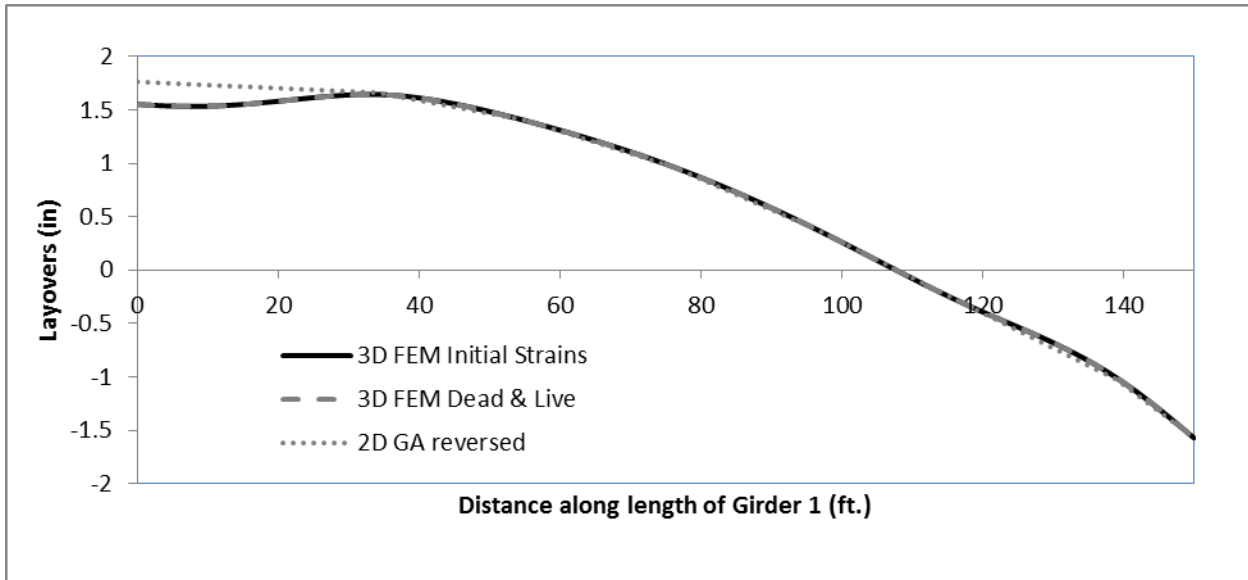


Figure D.3: Comparison of layovers obtained by different analysis method for Bridge C for final fit at the SDL stage

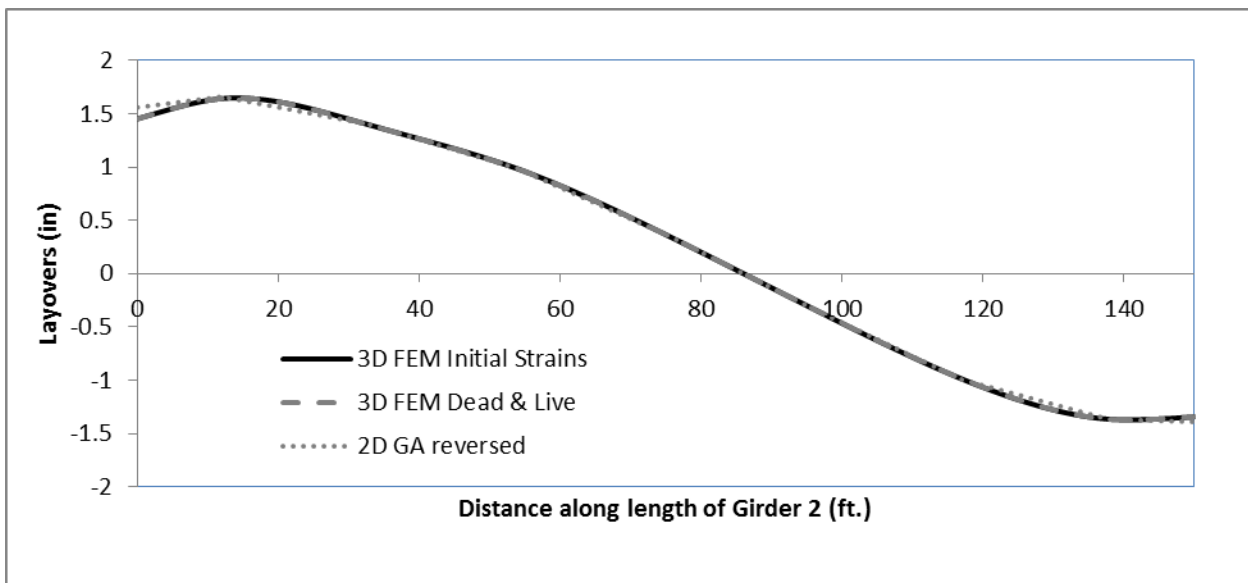


Figure D.4: Comparison of layovers obtained by different analysis method for Bridge C for final fit at the SDL stage

### D.3 Flange Lateral Bending Stress

#### D.3.1 Bridge C

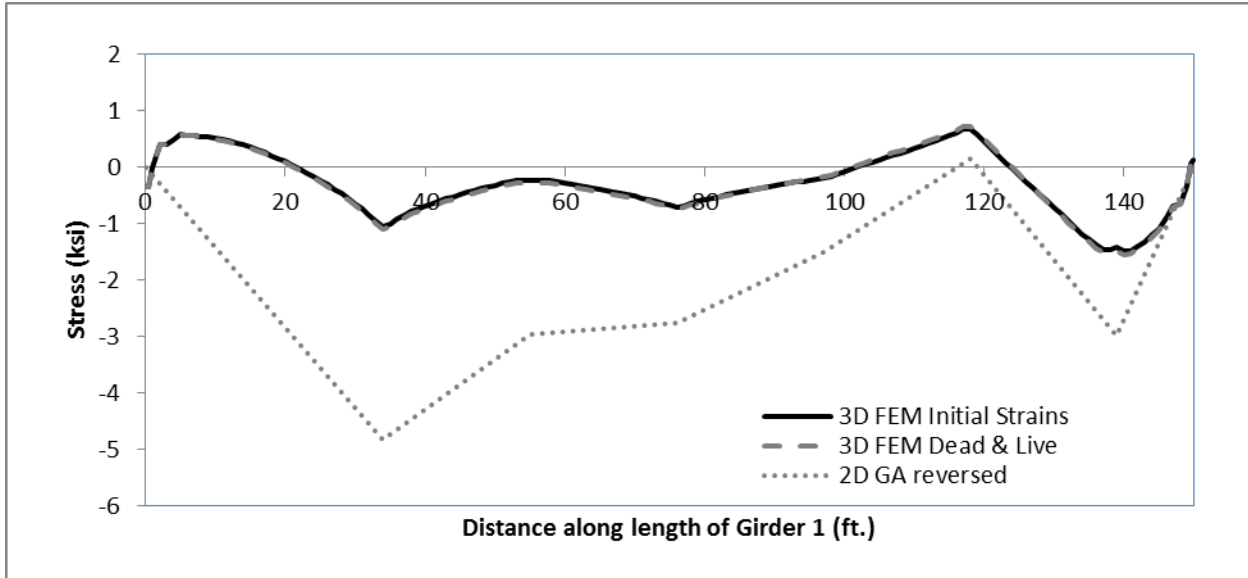


Figure D.5: Comparison of flange lateral bending stress obtained by different analysis method for Bridge C for final fit at the SDL stage

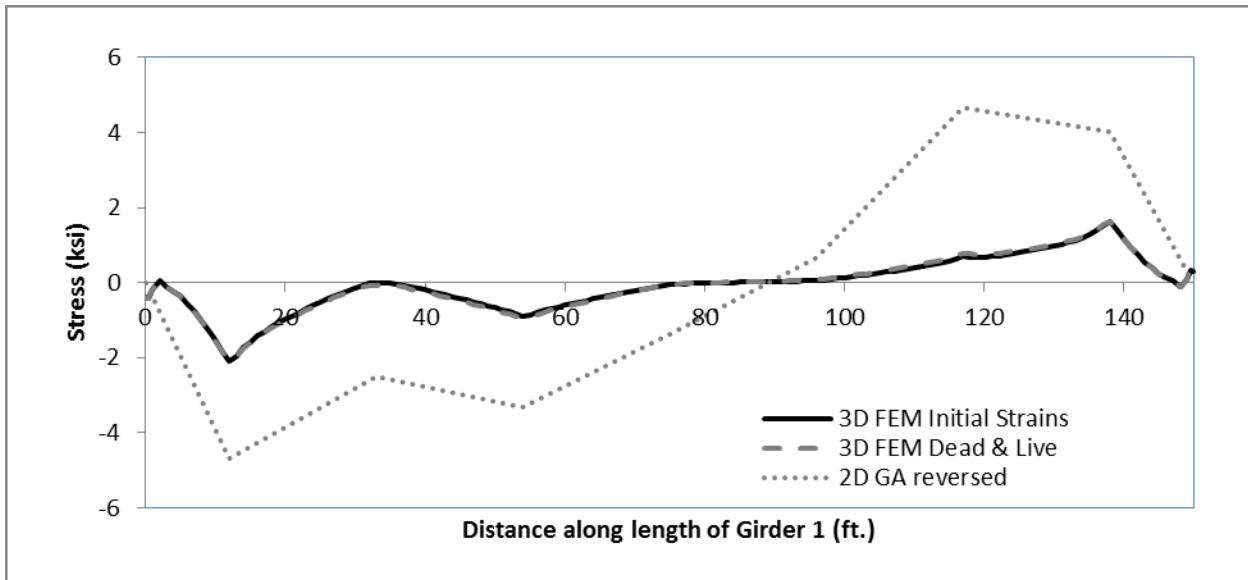
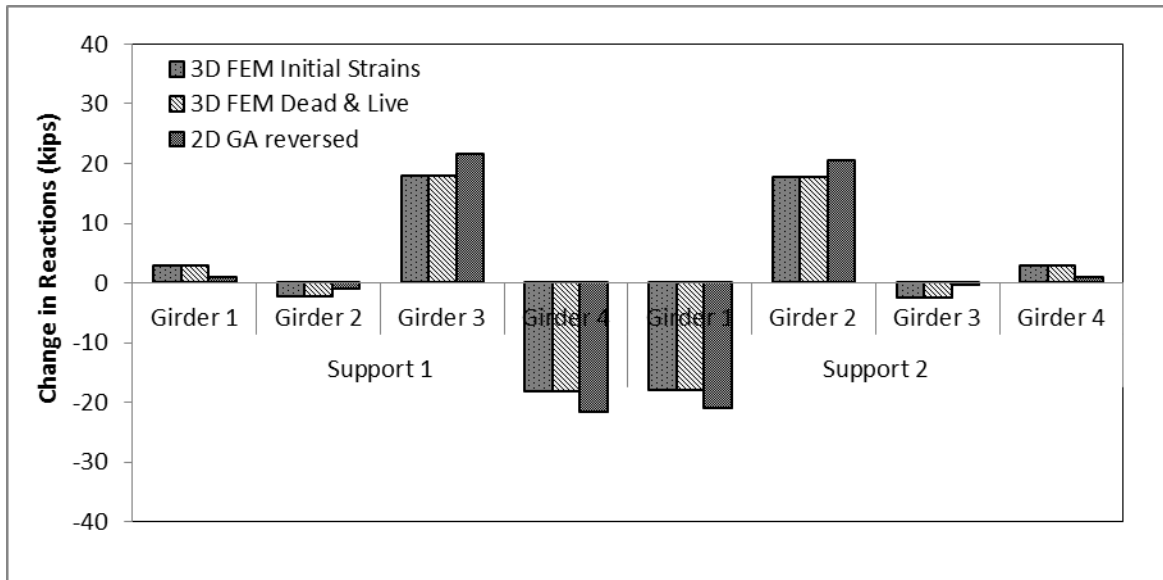


Figure D.6: Comparison of flange lateral bending stress obtained by different analysis method for Bridge C for final fit at the SDL stage

## D.4 Change in Reactions

### D.4.1 Bridge C



**Figure D.7: Comparison of vertical reaction obtained by different analysis method for Bridge C for final fit at the SDL stage**

## D.5 Cross-frame Forces

### D.5.1 Bridge C

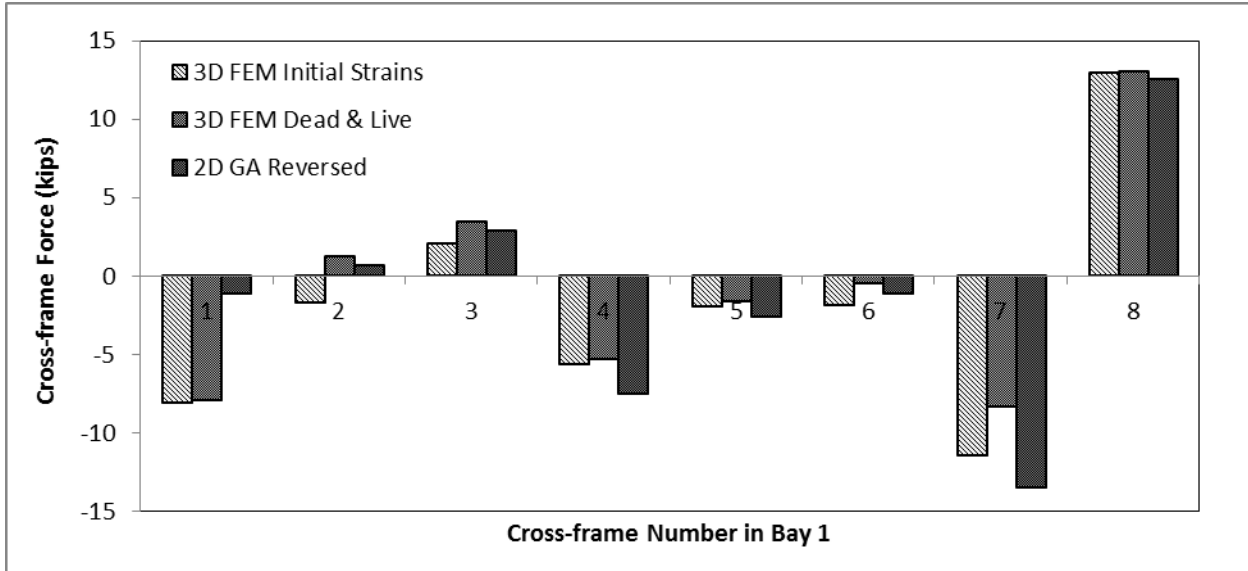


Figure D.8: Comparison of cross frame forces obtained by different analysis method for Bridge C for final fit at the SDL stage

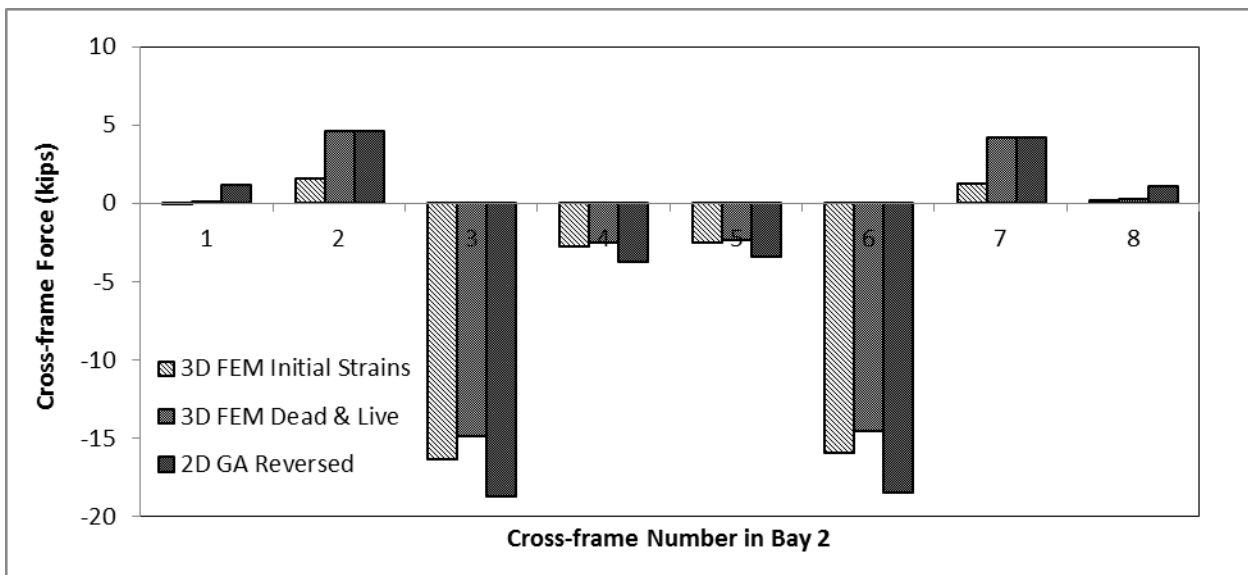


Figure D.9: Comparison of cross frame forces obtained by different analysis method for Bridge C for final fit at the SDL stage

## Appendix E: Examples

This appendix shows the examples of calculating following:

- Initial strains
- Equivalent torsional constant ( $J_{eq}$ )
- Different structural responses of a bridge from 2D grid analyses

Initial strains are required in a 3D FEM analysis of a bridge, detailed with dead load fit detailing methods, to simulate the lack-of-fit at different construction stages. Equivalent torsional constant is used in improved 2D grid analysis to have better estimate of torsional stiffness of the girders by taking into account the warping stiffness. 2D grid analyses results do not have different structural responses of a bridge and some post processing of the analysis results is required to get different structural responses. Examples for calculating the structural responses from 2D grid analysis results are given in section E.3 of this appendix.

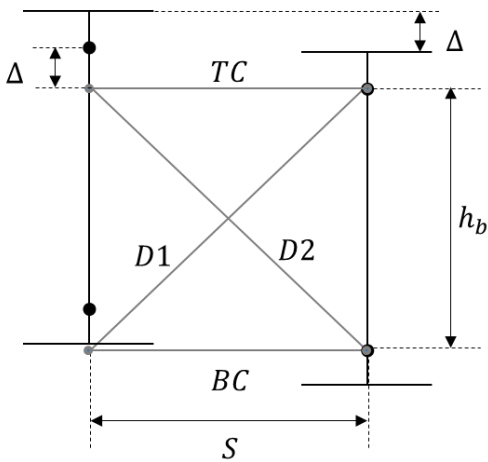
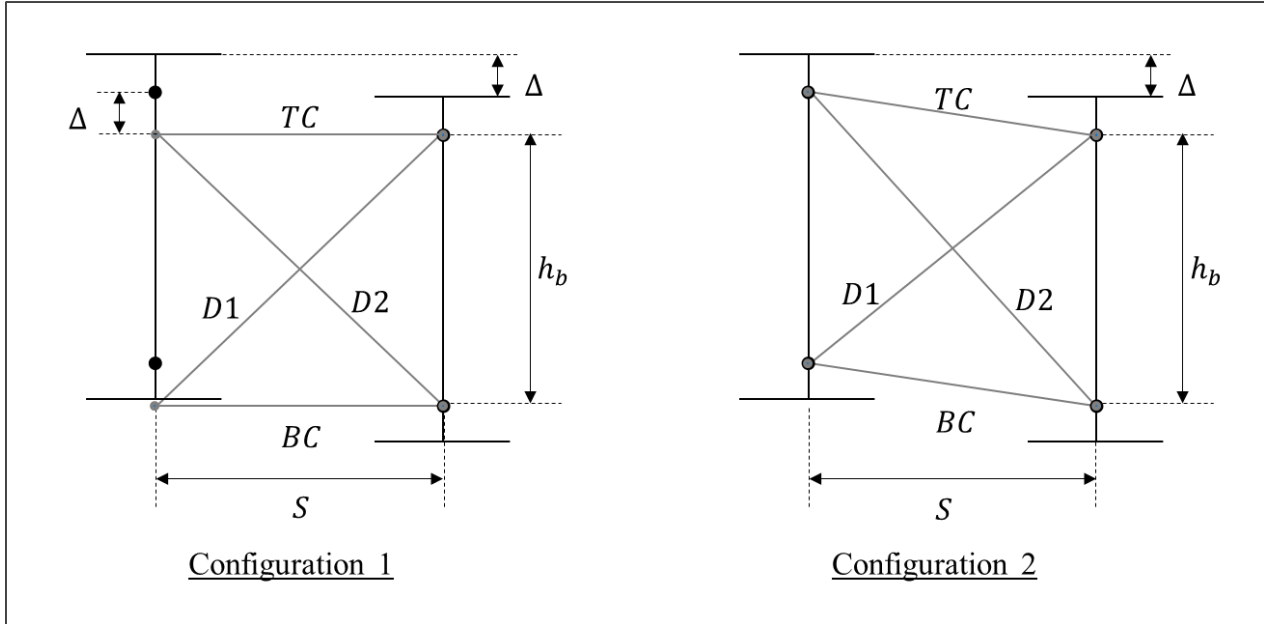
### E.1 Calculation of Initial Strains

### E.1.1 Intermediate Cross-frame

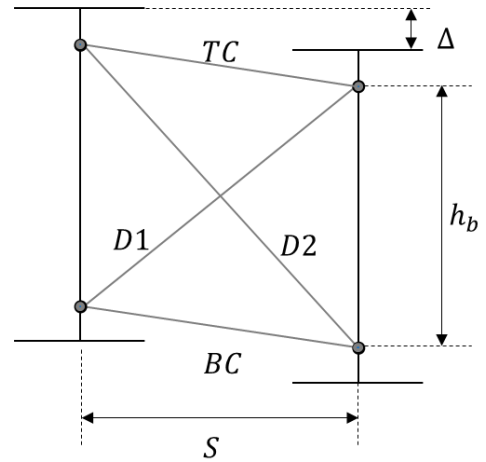
$$\epsilon_{initial} = \frac{L_1 - L_2}{L_2}$$

$L_1$  is length of a cross frame member in configuration 1

$L_2$  is length of a cross frame member in configuration 2



Configuration 1



Configuration 2

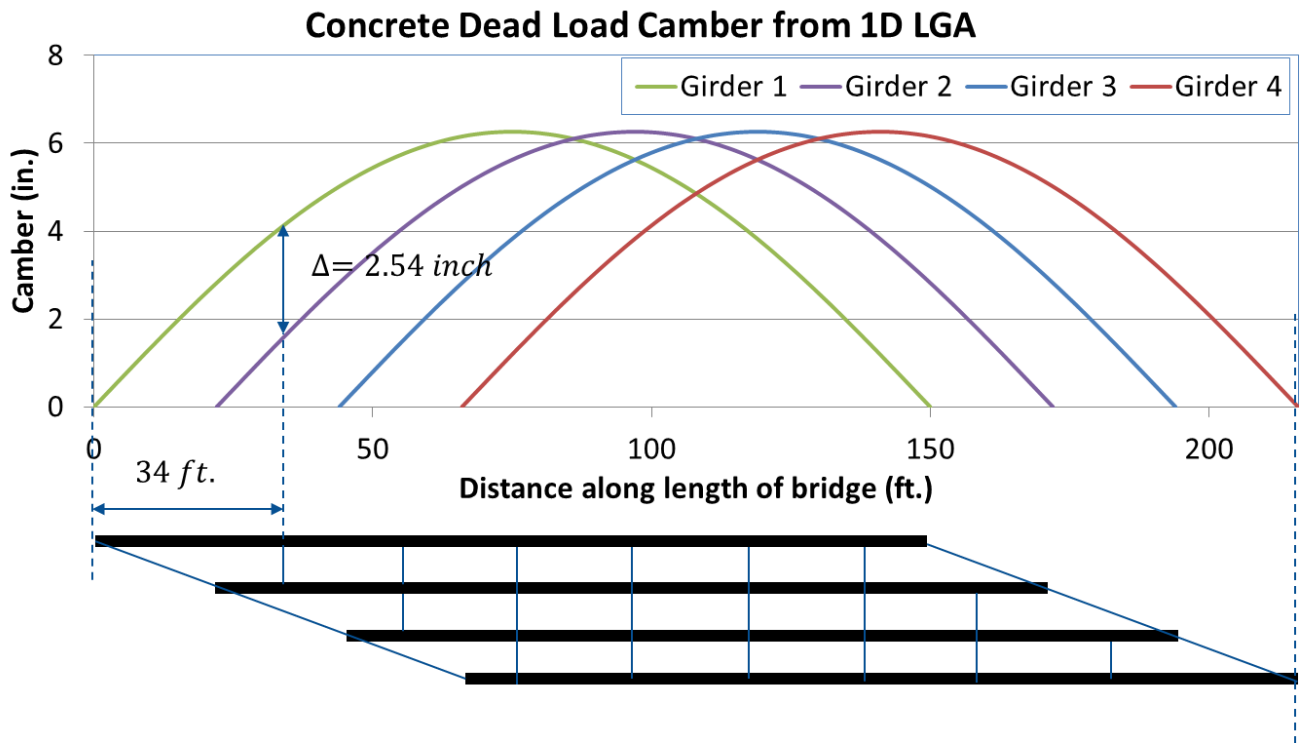
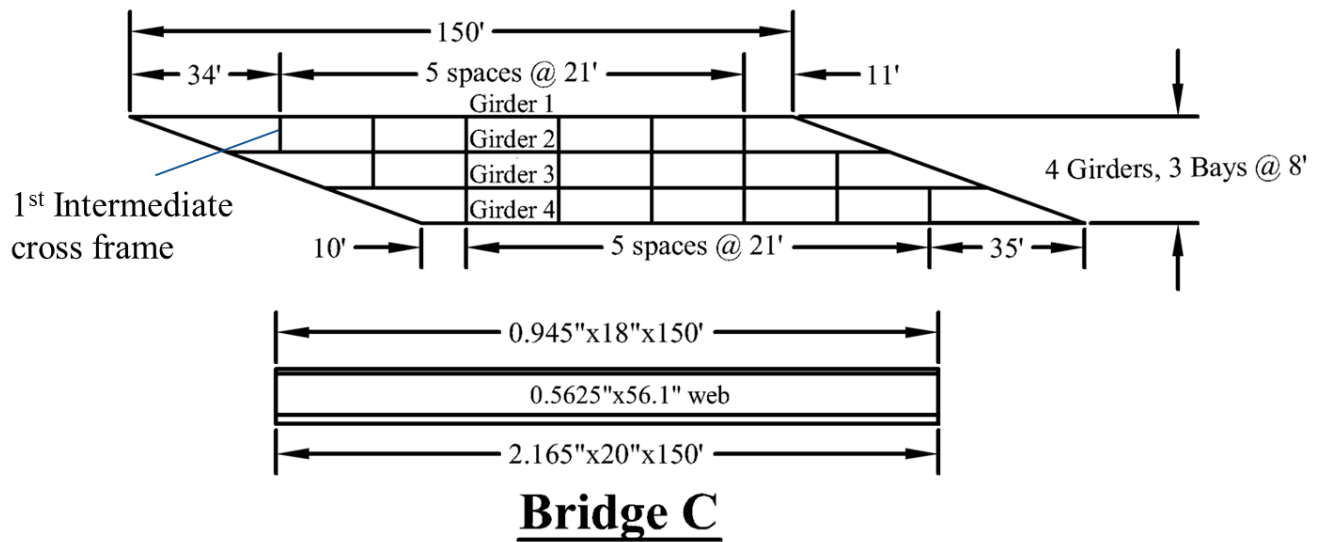
$$L_{TC_1} = L_{BC_1} = S$$

$$L_{D1_1} = L_{D2_1} = \sqrt{S^2 + h_b^2}$$

$$L_{TC_2} = L_{BC_2} = \sqrt{S^2 + \Delta^2}$$

$$L_{D1_2} = \sqrt{S^2 + (h_b - \Delta)^2}$$

$$L_{D2_2} = \sqrt{S^2 + (h_b + \Delta)^2}$$



$S =$  Spacing between girders = 8 ft. = 96 in.

$h_b =$  Height of bracing = 44.88 in.

$\Delta =$  Difference in elevation due to camber = 2.54 in. (from figure above)

$$L_{TC_1} = L_{BC_1} = S = 96 \text{ in.}$$

$$L_{D1_1} = L_{D2_1} = \sqrt{S^2 + h_b^2}$$

$$L_{D1_1} = L_{D2_1} = \sqrt{96^2 + 44.88^2}$$

$$L_{D1_1} = L_{D2_1} = 105.973 \text{ in.}$$

$$L_{TC_2} = L_{BC_2} = \sqrt{S^2 + \Delta^2}$$

$$\begin{aligned} L_{TC_2} = L_{BC_2} &= \sqrt{96^2 + 2.54^2} \\ &= 96.034 \text{ in.} \end{aligned}$$

$$L_{D1_2} = \sqrt{S^2 + (h_b - \Delta)^2}$$

$$\begin{aligned} L_{D1_2} &= \sqrt{96^2 + (44.88 - 2.54)^2} \\ &= 104.922 \text{ in.} \end{aligned}$$

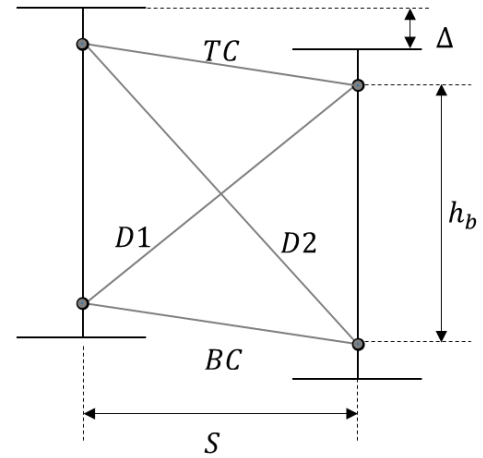
$$L_{D2_2} = \sqrt{S^2 + (h_b + \Delta)^2}$$

$$\begin{aligned} L_{D2_2} &= \sqrt{96^2 + (44.88 + 2.54)^2} \\ &= 107.073 \text{ in} \end{aligned}$$

$$\begin{aligned} \epsilon_{initial_{TC}} = \epsilon_{initial_{BC}} &= \frac{L_{TC_2} - L_{TC_1}}{L_{TC_1}} = \frac{L_{BC_2} - L_{BC_1}}{L_{BC_1}} \\ &= \frac{96 - 96.034}{96} = 0.00035 \end{aligned}$$

$$\begin{aligned} \epsilon_{initial_{D1}} &= \frac{L_{D1_2} - L_{D1_1}}{L_{D1_1}} = \frac{104.922 - 105.973}{105.973} \\ &= -0.0099 \end{aligned}$$

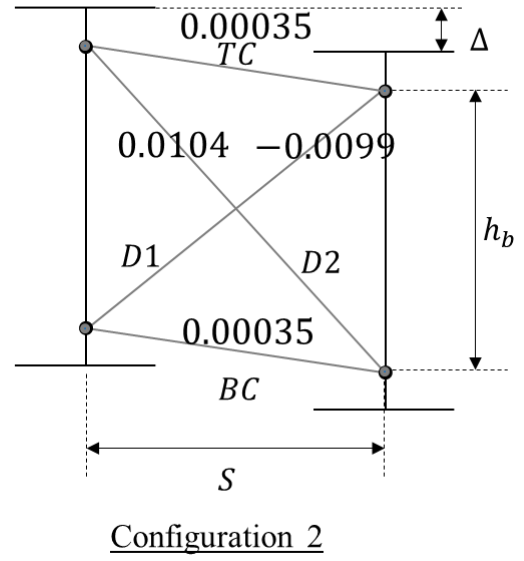
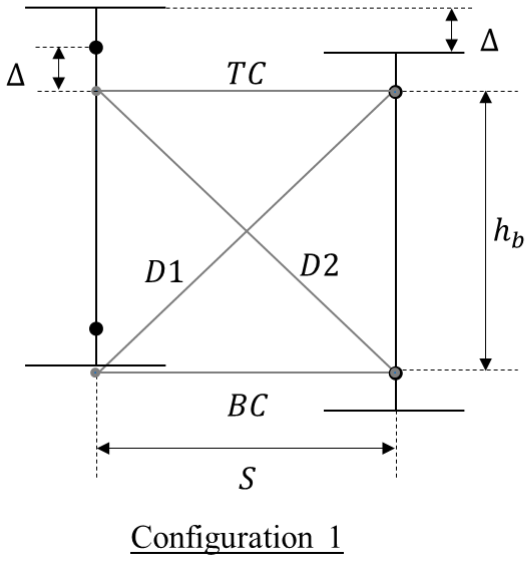
$$\begin{aligned} \epsilon_{initial_{D2}} &= \frac{L_{D2_2} - L_{D2_1}}{L_{D2_1}} = \frac{107.073 - 105.973}{105.973} \\ &= 0.0104 \end{aligned}$$



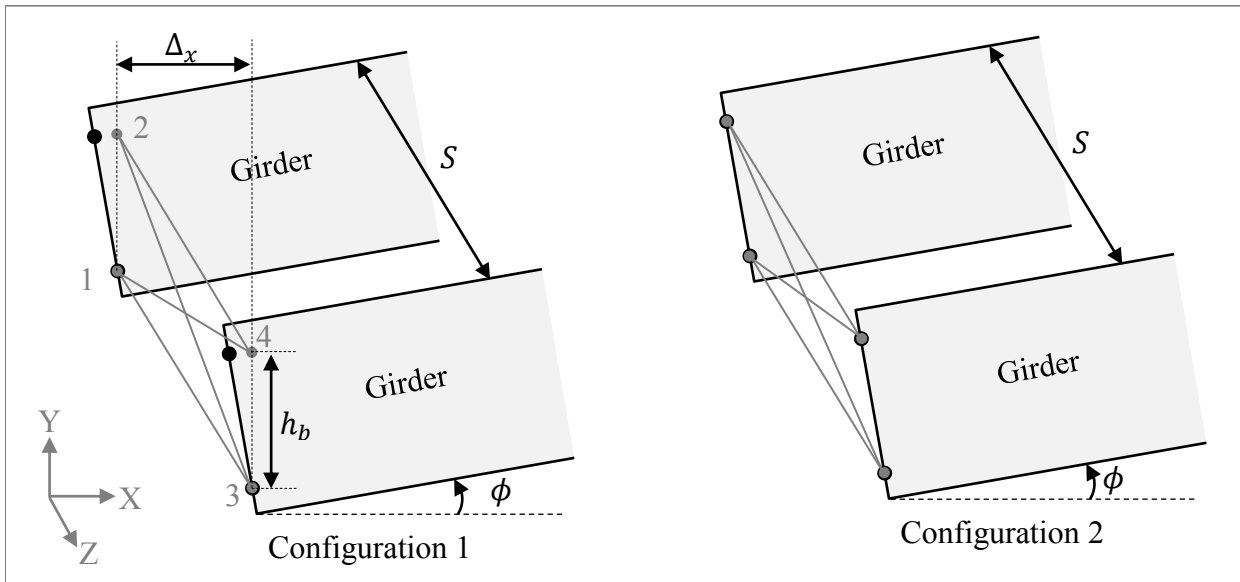
+ive = member stretched

-ive = member compressed

+ive = member stretched  
 -ive = member compressed



**E.1.2 End cross-frame**



$$L_{TC_1} = L_{BC_1} = \sqrt{\Delta_x^2 + S^2}$$

$$L_{D1_1} = L_{D2_1} = \sqrt{\Delta_x^2 + h_b^2 + S^2}$$

$$L_{TC_2} = L_{BC_2} = \sqrt{\Delta_x^2 + S^2}$$

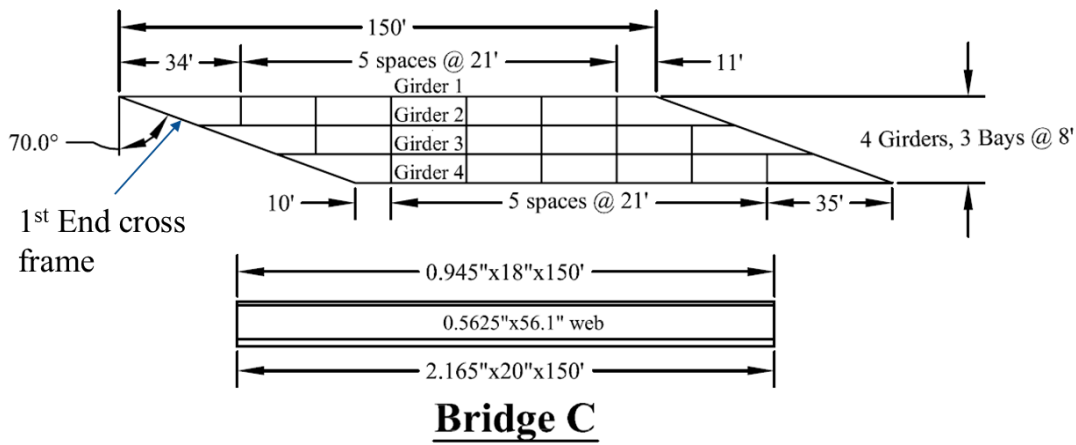
$$L_{D1_2} = \sqrt{(\Delta_x - \phi h_b)^2 + h_b^2 + S^2}$$

$$L_{D2_2} = \sqrt{(\Delta_x + \phi h_b)^2 + h_b^2 + S^2}$$

$$\Delta_x = S \times \tan \theta$$

$\theta = \text{Skew angle}$

$\phi = \text{End rotation of girder}$



$$\Delta_x = S \times \tan \theta = 96 \times \tan 70.01 = 264 \text{ in.}$$

$$L_{TC_1} = L_{BC_1} = \sqrt{\Delta_x^2 + S^2}$$

$$L_{D1_1} = L_{D2_1} = \sqrt{\Delta_x^2 + h_b^2 + S^2}$$

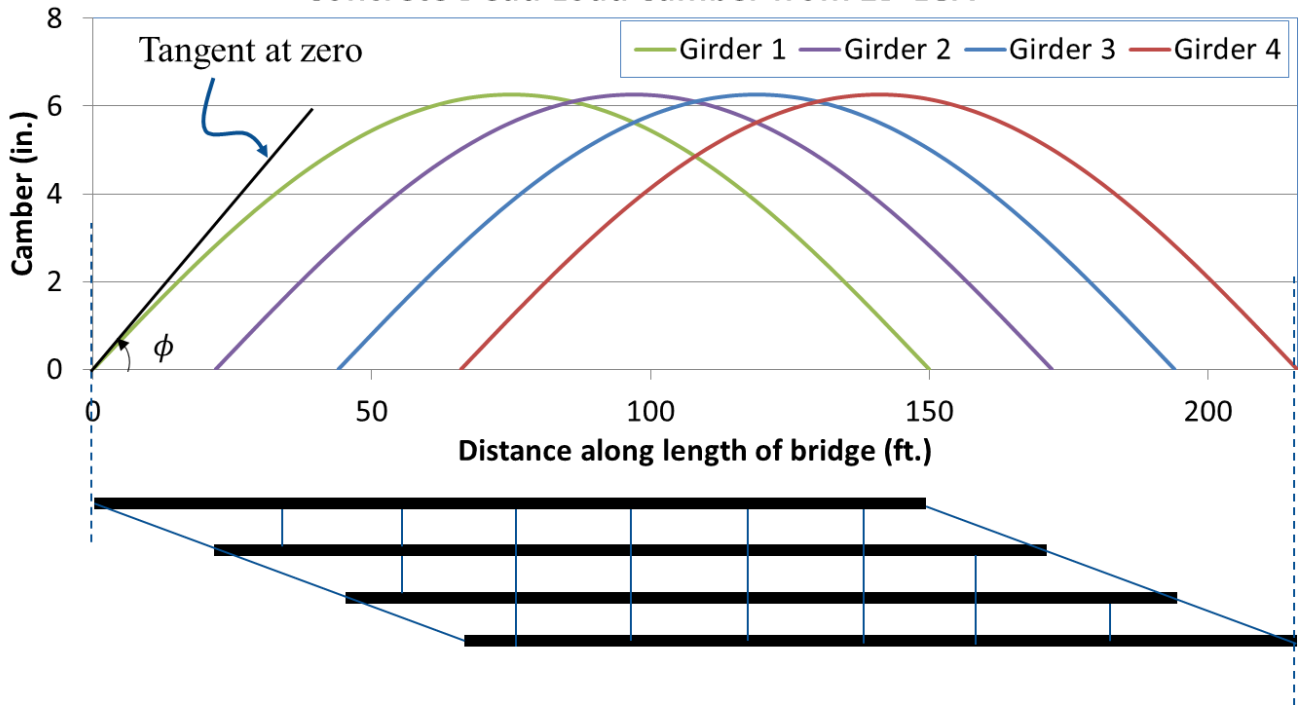
$$L_{TC_1} = L_{BC_1} = \sqrt{264^2 + 96^2}$$

$$= 280.913 \text{ in.}$$

$$L_{D1_1} = L_{D2_1} = \sqrt{264^2 + 44.88^2 + 96^2}$$

$$= 284.475 \text{ in.}$$

### Concrete Dead Load Camber from 1D LGA



From CDL camber 1D LGA

$$\phi = \frac{\Delta y}{\Delta x} = \frac{0.1336}{12} = 0.01114 \text{ rad.}$$

$$L_{TC_2} = L_{BC_2} = \sqrt{\Delta_x^2 + S^2} = 280.913 \text{ in.}$$

$$L_{D1_2} = \sqrt{(\Delta_x - \phi h_b)^2 + h_b^2 + S^2}$$

$$L_{D1_2} = \sqrt{(264 - 0.01114 \times 44.88)^2 + 44.88^2 + 96^2} = 284.012 \text{ in.}$$

$$L_{D2_2} = \sqrt{(\Delta_x + \phi h_b)^2 + h_b^2 + S^2}$$

$$L_{D1_2} = \sqrt{(264 - 0.01114 \times 44.88)^2 + 44.88^2 + 96^2} = 284.939 \text{ in.}$$

+ive = member stretched

-ive = member compressed

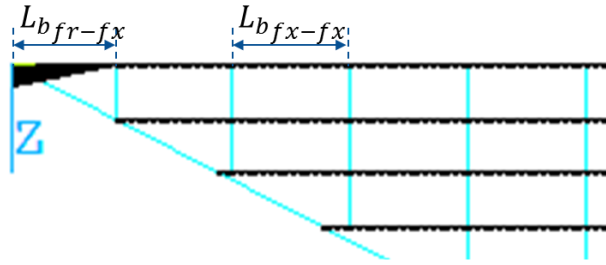
$$\begin{aligned}\epsilon_{initial_{TC}} = \epsilon_{initial_{BC}} &= \frac{L_{TC_2} - L_{TC_1}}{L_{TC_1}} = \frac{L_{BC_2} - L_{BC_1}}{L_{BC_1}} \\ &= \frac{280.913 - 280.913}{280.913} = 0\end{aligned}$$

$$\begin{aligned}\epsilon_{initial_{D1}} &= \frac{L_{D1_2} - L_{D1_1}}{L_{D1_1}} = \frac{284.012 - 284.475}{284.475} \\ &= -0.00163\end{aligned}$$

$$\begin{aligned}\epsilon_{initial_{D1}} &= \frac{L_{D2_2} - L_{D2_1}}{L_{D2_1}} = \frac{284.939 - 284.475}{284.475} \\ &= 0.00163\end{aligned}$$

## E.2 Calculation of $J_{eq}$ for Improved 2D Grid Analysis

- $J_{eq}$  calculation input
  - Unbraced length ( $L_b$ )
  - Boundary condition



$$J_{eq}(fx-fx) = J \left[ 1 - \frac{\sinh(pL)}{pL} + \frac{[\cosh(pL) - 1]^2}{pL \sinh(pL)} \right]^{-1}$$

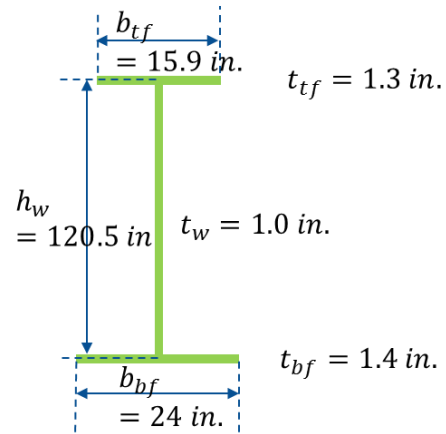
$$J_{eq}(fr-fx) = J \left[ 1 - \frac{\sinh(pL)}{pL \cosh(pL)} \right]^{-1} \quad p = \sqrt{\frac{GJ}{EC_w}} \quad G = \frac{E}{2 \times (1 + 0.3)}$$

$$J = \frac{1}{3} (b_{tf} t_{tf}^3 + h_w t_w^3 + b_{bf} t_{bf}^3) \quad C_w = \frac{h_w^2 b_{bf}^3 t_{bf}}{12 \left( 1 + \left( \frac{b_{bf}}{b_{tf}} \right)^3 \left( \frac{t_{bf}}{t_{tf}} \right) \right)}$$

$$J = \frac{1}{3}(b_{tf}t_{tf}^3 + h_w t_w^3 + b_{bf}t_{bf}^3)$$

$$J = \frac{1}{3}(15.9 \times 1.3^3 + 120.5 \times 1^3 + 24 \times 1.4^3)$$

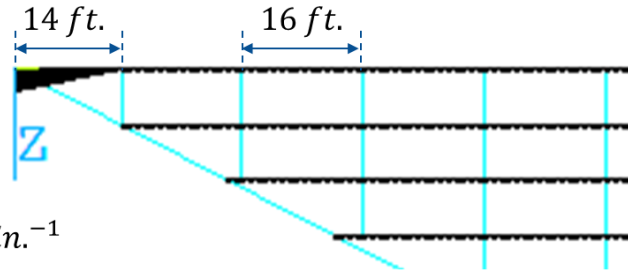
$$J = 73.76 \text{ in}^4$$



$$C_w = \frac{h_w^2 b_{bf}^3 t_{bf}}{12 \left( 1 + \left( \frac{b_{bf}}{b_{tf}} \right)^3 \left( \frac{t_{bf}}{t_{tf}} \right) \right)} = \frac{120.5^2 \times 24^3 \times 1.4}{12 \left( 1 + \left( \frac{24}{15.9} \right)^3 \left( \frac{1.4}{1.3} \right) \right)} = 4.98 \times 10^6 \text{ in}^6$$

$$G = \frac{E}{2 \times (1 + \nu)} = \frac{29 \times 10^6}{2 \times (1 + 0.3)} = 11.15 \times 10^6$$

$$p = \sqrt{\frac{GJ}{EC_w}} = \sqrt{\frac{11.15 \times 73.76}{29 \times 4.98 \times 10^6}} = 0.0024 \text{ in.}^{-1}$$

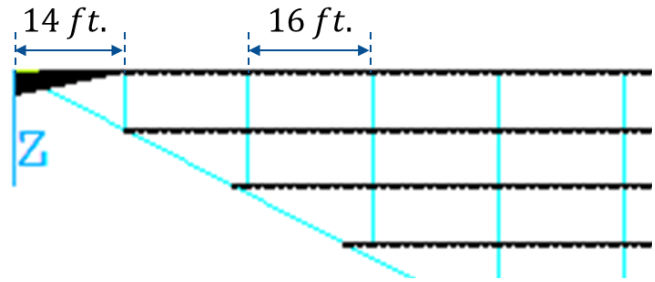


$$pL_{fr-fx} = 0.0024 \times (14 \times 12) = 0.403 \text{ rad}$$

$$J_{eq(fr-fx)} = J \left[ 1 - \frac{\sinh(pL)}{pL \cosh(pL)} \right]^{-1} = 73.76 \left[ 1 - \frac{\sinh(0.403)}{0.403 \cosh(0.403)} \right]^{-1}$$

$$J_{eq(fr-fx)} = 1451 \text{ in}^4$$

$J_{eq}$  is about 20 times greater than  $J$



$$pL_{fx-fx} = 0.0024 \times (16 \times 12) = 0.461 \text{ rad}$$

$$J_{eq}(fx-fx) = J \left[ 1 - \frac{\sinh(pL)}{pL} + \frac{[\cosh(pL) - 1]^2}{pL \sinh(pL)} \right]^{-1}$$

$$J_{eq}(fx-fx) = 73.76 \left[ 1 - \frac{\sinh(0.461)}{0.461} + \frac{[\cosh(0.461) - 1]^2}{0.461 \sinh(0.461)} \right]^{-1}$$

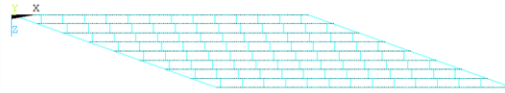
$$J_{eq}(fr-fx) = 4251 \text{ in}^4$$

$J_{eq}$  is about 58 times greater than  $J$

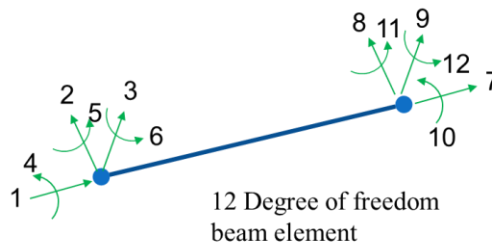
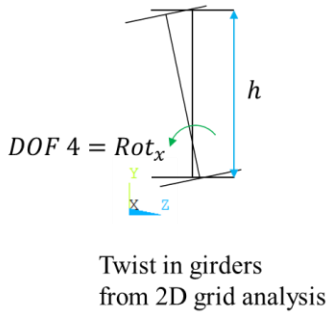
### E.3 Calculation of Responses from 2D Grid Analysis

#### E.3.1 Layovers

$$\text{Layover} = Rot_x \times h$$

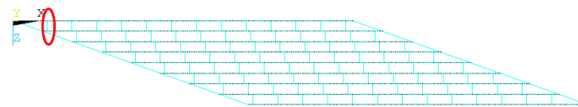


2D Grid Model



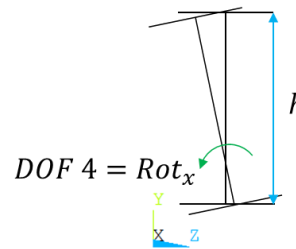
| Girder Length | Skew | Girder Depth | Girder Spacing |
|---------------|------|--------------|----------------|
| 300 ft.       | 70°  | 144 inch     | 9.25 ft.       |

$Rot_x = 0.01654$  rad  
From 2D grid analysis



2D Grid Model

$$\begin{aligned} \text{Layover} &= Rot_x \times h \\ &= 0.01654 \times 144 \\ &= 2.38 \text{ in.} \end{aligned}$$

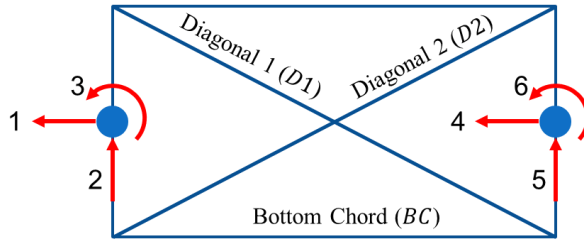


### E.3.2 Cross-frame Forces

**Step 1:** Build the complete model of girders with cross-frames attached

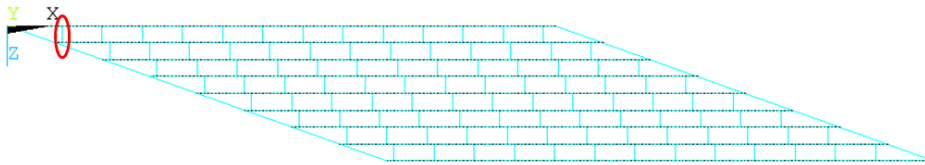
**Step 2:** Activate concrete dead load

**Step 3:** Calculate cross-frame forces from the nodal displacements



For top chord

$$F_{TC} = \frac{E \cdot A_{TC}}{L_{TC}} \left[ (u_4 - u_1) + \frac{h_b}{2} (u_3 - u_6) \right]$$



$$A_{TC} = 2.87 \text{ in}^2$$

$$L_{TC} = 9.25 \text{ ft.}$$

From grid analysis

$$u_1 = 0 \text{ in.}$$

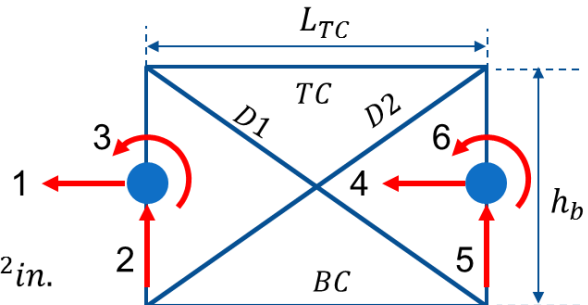
$$u_4 = 0 \text{ in.}$$

$$u_2 = -2.1239 \text{ in.}$$

$$u_5 = -0.2737 \text{ in.}$$

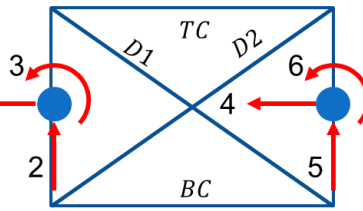
$$u_3 = 1.65396 \times 10^{-2} \text{ in.}$$

$$u_6 = 1.65052 \times 10^{-2} \text{ in.}$$



For top chord

$$F_{TC} = \frac{E \cdot A_{TC}}{L_{TC}} \left[ (u_4 - u_1) + \frac{h_b}{2} (u_3 - u_6) \right]^1$$



$$F_{TC} = \frac{29 \times 10^6 \times 2.87}{9.25 \times 12} \left[ (0 - 0) + \frac{115.2}{2} (1.65396 \times 10^{-2} - 1.65052 \times 10^{-2}) \right]$$

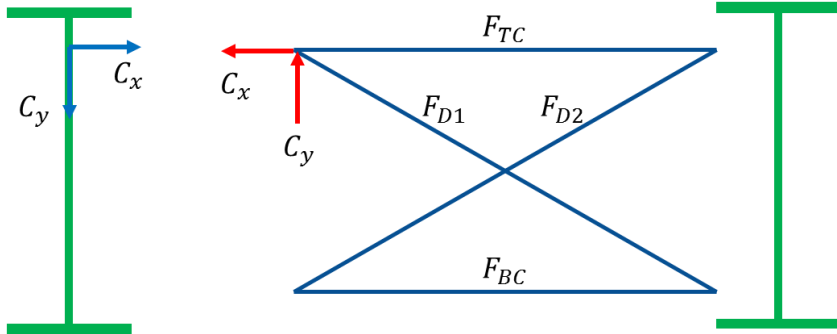
$$F_{TC} = 1485 \text{ lbs} = 1.485 \text{ kips}$$

### E.3.3 Flange Lateral Bending Stress

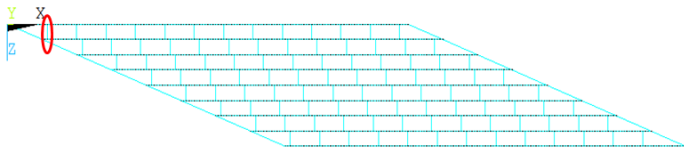
Bridge A

| Girder Length | Skew | Brace height ( $h_b$ ) | Girder Spacing |
|---------------|------|------------------------|----------------|
| 300 ft.       | 70°  | 115.2 inch             | 9.25 ft.       |

**Step 1:** Calculate lateral force on girders from cross-frame forces



$$C_x = F_{TC} - F_{D1} \cos(\theta)$$

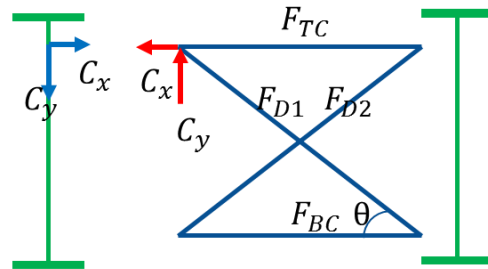


$$\theta = \tan^{-1}\left(\frac{h_b}{S}\right) = \tan^{-1}\left(\frac{115.2}{9.25 \times 12}\right) = 46 \text{ deg.}$$

$$C_x = F_{TC} - F_{D1} \cos(\theta)$$

$$C_x = 1.487 - (-6.093) \cos(46^\circ)$$

$$C_x = 5.71 \text{ kips}$$

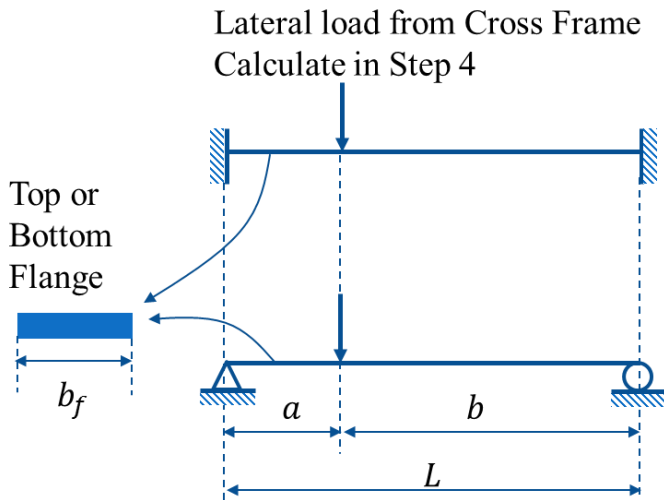


From Step 3

$$F_{TC} = 1.487 \text{ kips} \quad F_{BC} = -1.483 \text{ kips}$$

$$F_{D1} = -6.093 \text{ kips} \quad F_{D2} = 6.093 \text{ kips}$$

**Step 2:** Calculate lateral moment and stress



$$M_{l(Fix-Fix)} = \frac{2Pa^2b^2}{L^3}$$

$$M_{l(Pin-Pin)} = \frac{Pab}{L^3}$$

$$f_l = \frac{M_l}{S_f}$$

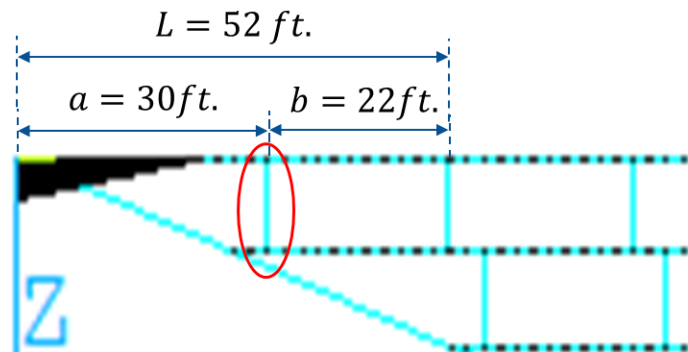
$$M_{l(Fix-Fix)} = \frac{2Pa^2b^2}{L^3}$$

$$M_{l(Fix-Fix)} = \frac{2 \times 5.71 \times 30^2 \times 22^2}{52^3}$$

$$M_{l(Fix-Fix)} = 35.4 \text{ kip} - \text{ft}$$

$$f_l = \frac{35.4 \times 12}{163.33} = 2.6 \text{ ksi}$$

$$P = C_x = 5.71 \text{ kips}$$



$$S_{tf} = \frac{t_{tf}b_{tf}^2}{6} = \frac{1.25 \times 28^2}{6} = 163.33 \text{ in.}^4$$